Identification of Novel Regulators of TNF-α Signaling using Genome-wide RNAi Screens

Dissertation

by

Dorothee Nickles

2009

Dissertation

submitted to the
Combined Faculties for the Natural Sciences and for Mathematics
of the Ruperto-Carola University of Heidelberg, Germany
for the degree of
Doctor of Natural Sciences

presented by
Dipl.-Biol. Dorothee Nickles
born in Landau/Pfalz, Germany

date of oral examination: 22.01.2010

Identification of Novel Regulators of TNF-α Signaling using Genome-wide RNAi Screens

Dissertation

by

Dorothee Nickles

Referees:

Prof. Dr. Lutz Gissmann

Prof. Dr. Herbert Steinbeisser

Acknowledgments

First of all I want to thank my supervisor Michael Boutros for giving me this interesting and challenging project. I am especially thankful that he gave me the opportunity to visit several international conferences and courses from which I benefited a lot.

I acknowledge my referees, Lutz Gissmann and Herbert Steinbeisser, for taking over the correctorship of this thesis and their advice during PhD committee meetings. I am also grateful to Anne Regnier-Vigouroux for her constant support ever since I worked with her as a student.

My thank goes to all - former and current - members of the "Heidelberg branch" of the Boutros group for providing a nice working atmosphere. Even though I think almost everyone in the lab helped me at some point with either reagents, protocols or advice, I am especially indebted to Nadege Pelte, who was a great teacher, Anan Ragab, with whom I had critical as well as reassuring discussions, Dierk Ingelfinger and Sandra Steinbrink, who introduced me to RNAi screening in human cells, David Kuttenkeuler, who had lots of good advice concerning assay design and data analysis, as well as Thomas Sandmann who supported me greatly in finalizing my thesis.

I also want to thank Tobias Haas and Markus Brechmann for fruitful discussions.

I owe many thanks to Wolfgang Huber as he agreed on taking a me as a guest for a week in his group and contributed a lot to raising my interest into R. I also want to thank the whole Huber group who was always very friendly and helpful whenever I turned with questions towards them. Special thanks go to Florian Hahne for his patience with my limited programming skills and for sharing insights into the Bioconductor world.

I would like to thank Sheena Pinto for unforgettable lunch breaks. I am extraordinarily grateful to my family and friends for their support, cheering-up words and interest in my work. I especially thank Patrick König for always being there.

Abstract

Signaling pathways are crucial for multicellular organisms: they are necessary for cell communication and development, they enable cells to specialize and act together. TNF-α signaling is one such pathway crucial for orchestrating the body's response to cellular stress or invasion by pathogens. TNF-α signaling mediates inflammation, a key event for an efficient innate immune response. As inflammation has to be tightly controlled in order to avoid damage to the host, deregulation of TNF-α signaling has been implicated in the pathogenesis of many inflammatory diseases and cancer.

TNF-α exerts inflammatory effects by binding to its receptor, TNFR1. Upon binding, several proteins including DD (death domain) proteins are recruited to TNFR1 to form the TNFR complex, resulting in the activation of the IκB kinase complex (IKK). Subsequently, inhibitor of κB (IκB) proteins are phosphorylated and degraded, releasing transcription factors of the NF-κB family. NF-κB then controls the expression of hundreds of different genes required for inflammation and innate immunity.

The aim of my PhD project was to identify new factors required for TNF-α signaling. In order to monitor NF-κB transcriptional activity upon stimulation with TNF-α, I established a cell-based dual luciferase assay. This assay was suited to measure TNF-α signaling activity in miniaturized format necessary for large-scale experiments. For finding novel regulators of TNF-α signaling, I used the cell-based dual luciferase assay in two genome-wide RNAi screens. These screens identified several candidates potentially implicated in NF-κB activation by TNF-α. I next established secondary assays for confirming the requirement of these candidates in TNF-α signaling. On the basis of the results of these secondary assays, I selected three candidates, SPP1, GAB3 and CASP4, for further characterization.

Epistasis experiments revealed that SPP1, GAB3 and CASP4 are required for the activation of the IκB kinase complex. Further experiments demonstrated that the candidates are not essential for proper TNFR1 cell surface expression. SPP1, a multifunctional protein, has been described to interact with the DD protein MyD88 during Toll-like receptor signaling. It could thus interact with DD proteins present in the TNFR complex. GAB3 belongs to a family of scaffold proteins of which one member, GAB2, has been shown to interact with RANK, a TNFR family member. Analogously, GAB3 could act as a scaffold at TNFR1 supporting the recruitment of signaling molecules. CASP4 is an inflammatory caspase. My results indicate that CASP4 catalytical activity is dispensable for its role in TNF-α signaling. CASP4 could thus serve as another scaffold protein in the TNFR complex as described for other caspases. Future experiments will identify the interaction partners of SPP1, GAB3 and CASP4, clarifying the molecular details of their mode of action in TNF-α-induced activation of NF-κB.

Zusammenfassung

Signalwege sind zur Kommunikation zwischen den Zellen komplexer Organismen unentbehrlich. Sie steuern Prozesse wie Zelldifferenzierung und Entwicklung. Inflammatorische Signalwege spielen bei Immunantworten und der Reaktion auf Zellstress eine Rolle. Ein zentraler Mediator von Entzündungsreaktionen ist das inflammatorische Cytokin TNF-α. Aufgrund seiner Schlüsselfunktion sind Missregulierungen des TNF-α Signalwegs an vielen inflammatorischen Krankheiten und Krebs beteiligt.

TNF-α vermittelt Entzündungsreaktionen durch seine Bindung an den TNF-α-Rezeptor (TNFR) 1. Die Aktivierung des Rezeptors induziert die Ausbildung des TNFR-Komplexes, in den z.B. Proteine mit "death domains" (DD) rekrutiert werden. Der TNFR-Komplex aktiviert den "inhibitor of κB" (IκB) Kinasekomplex (IKK), der IκB phosphoryliert und zum Abbau markiert. Durch den Abbau von IκB werden Transkriptionsfaktoren der NF-κB-Familie freigesetzt. Diese aktivieren daraufhin die Expression vieler verschiedener Gene, die für Entzündungsreaktionen und angeborene Immunantworten benötigt werden.

Ziel dieser Doktorarbeit war es, neue Komponenten des TNF-α Signalweges zu identifizieren. Es wurde ein so genannter "dual luciferase assay" in HEK293T Zellen etabliert, um die Aktivierung des Transkriptionsfaktors NF-κB nach Stimulation mit TNF-α zu messen. Dieser Assay ermöglichte es, in genomweiten RNA-Interferenz Screens nach Regulatoren des TNF-α Signalweges zu "fahnden". Mithilfe zweier Screens wurden mehrere solche mögliche Regulatoren identifiziert. Sekundärassays wurden etabliert, mit deren Hilfe die Phänotypen der Screening-Kandidaten überprüft und schließlich die drei Kandidaten SPP1, GAB3 und CASP4 zur weiteren Charakterisierung ausgewählt wurden.

Durch Epistaseexperimente wurde gezeigt, dass alle drei Proteine an der Aktivierung des IKK beteiligt sind. Ihre Expression wurde nicht für die Lokalisation des TNFR1 an der Zelloberfläche benötigt. Diese Arbeit stellt Modelle vor, welche Rolle die drei identifierten Proteine im TNF-α Signalweg einnehmen könnten. SPP1 erfüllt viele diverse Funktionen. Unter anderem interagiert es am TLR9 mit dem DD-Protein MyD88. Es könnte also mit DD-Proteinen im TNFR-Komplex interagieren. GAB3 gehört einer Familie von Adaptorproteinen an, deren Mitglieder mit der Aktivierung von NF-κB in Verbindung gebracht wurden. So wurde von GAB2 berichtet, dass es mit dem TNFR Familienmitglied RANK interagieren kann. Analog dazu wäre es denkbar, dass GAB3 an TNFR1 bindet. CASP4 gehört zu den inflammatorischen Caspasen, einer Familie von Cysteinpeptidasen. Experimente weisen jedoch darauf hin, dass CASP4 unabhängig von seiner Enzymaktivität NF-κB aktiviert. Auch für andere Caspasen wurde eine nicht-enzymatische Adaptorfunktion beschrieben. Um die vorgestellten Modelle zu testen, müssen nun die Interaktionspartner der drei Kandidaten identifiziert werden.

Contents

1 Introduction **1**

1.1 Innate Immunity 1

1.1.1 Inflammation in innate immunity 1

1.1.2 TNF-α in innate immunity 2

1.1.3 TNF-α receptor 1 signaling - an overview 4

1.1.4 NF-κB signaling downstream of TNFR1 5

1.1.5 Termination of TNFR1 signaling 10

1.2 RNA Interference 13

1.3 Using RNAi to Study Gene Function 14

1.3.1 Cell-based assays employed in RNAi screening 17

1.3.2 RNAi reagents and cell-based screening formats 17

1.3.3 Assay design 18

1.4 Aim of This Thesis 20

2 Results **21**

2.1 Genome-wide RNAi Screens for Identifying Novel Regulators of TNF-α Signaling 21

2.1.1 Design and development of a cell-based assay to study NF-κB transcriptional activity 21

2.1.2 Genome-wide RNAi screening 29

2.1.3 Hit definition and screen comparison 30

2.1.4 First candidate selection 36

2.1.5 Secondary validation of candidate genes 36

2.2 SPP1, CASP4, GAB3 45

2.2.1 Knockdown of SPP1, GAB3 and CASP4 interferes with NF-κB transcriptional activity 45

2.2.2 Epistasis assays map novel regulators in the pathway 53

2.2.3 Knockdown of SPP1, GAB3 and CASP4 does not affect TNFR1 cell surface expression . . . 56
2.3 Caspase 4 As a Novel Regulator of TNF-α Signaling . . . 59
2.3.1 CASP4 primarily localizes to the cytoplasm . . . 59
2.3.2 CASP4 is not cleaved after TNF-α stimulation . . . 61

3 Discussion **63**
3.1 RNAi Screening Design and Analysis . . . 64
3.1.1 Selection of a suitable cell line for RNAi screening . . . 64
3.1.2 Designing a dual luciferase assay for monitoring NF-κB activity . . . 64
3.1.3 Defining criteria for screening hit selection . . . 66
3.1.4 Comparison to other RNAi screens for TNF-α signaling . . . 69
3.1.5 Various assays are required to place candidates into the pathway . . . 71
3.2 Potential Novel Regulators of TNF-α Signaling Identified by Genome-wide RNAi Screening . . . 73
3.2.1 GAB3 in TNF-α signaling . . . 74
3.2.2 SPP1 in TNF-α signaling . . . 76
3.2.3 CASP4 as a novel regulator of TNF-α signaling . . . 78
3.3 Outlook . . . 82

4 Material and Methods **83**
4.1 Material . . . 83
4.1.1 Cell lines . . . 83
4.1.2 Chemicals, media, buffers and solutions . . . 83
4.1.3 siRNAs, plasmids and transfection reagents . . . 85
4.1.4 Antibodies . . . 89
4.1.5 Enzymes and kits . . . 90
4.1.6 Oligos . . . 90
4.1.7 Miscellanous . . . 92
4.2 Methods . . . 92
4.2.1 Cell culture and cell maintenance . . . 92
4.2.2 Transfection protocols . . . 93
4.2.3 Measuring cell viability using the CellTiterGlo assay . . . 95
4.2.4 ELISA . . . 95
4.2.5 Handling bacteria . . . 95
4.2.6 Cloning . . . 96
4.2.7 RNA extraction, cDNA synthesis and quantitative real time PCR . . . 97

4.2.8 Expression profiling 98
4.2.9 Cell lysis, measurement of protein concentration, SDS page and Western Blotting 98
4.2.10 Confocal immunofluorescence microscopy 99
4.2.11 FACS staining 100
4.2.12 Computational analyses 100

A Supplement **103**

Nomenclature **125**

Chapter 1

Introduction

1.1 Innate Immunity

The body is protected from intrusion of pathogens by its skin and mucosal surfaces. However, if pathogens penetrate these barriers, the body has to be able to detect and fight the intruders. The immune system confers these abilities. It can be divided into two branches: innate immunity acting as a first line of defense; and adaptive immunity, comprising the activation and proliferation of B and T lymphocytes. In contrast to adaptive immunity, innate immune responses are fast and target pathogens unspecifically, e.g. by mediating their lysis or phagocytosis. Additionally, innate immune responses can also activate the adaptive immune system when innate immunity is not sufficient to fight the pathogen.

1.1.1 Inflammation in innate immunity

Signaling pathways involved in innate immune responses are evolutionarily conserved. There are two main types of receptors that are important for an efficient innate immune response: receptors that recognize pathogens and receptors that facilitate to alert the body to the threat.

(i) Pattern recognition receptors (PRRs), such as Toll-like receptors (TLRs), recognize pathogen-associated molecular patterns (PAMPs) on the surface of pathogens, e.g. bacterial proteoglycans or lipids like lipopolysaccharide (LPS). There are many different receptors belonging to the PRRs; they can be transmembrane receptors (TLR4, scavenger receptors), secreted into the plasma (complement system) or intracellular [e.g. nucleotide oligomerization domain protein-like receptors (NLRs)]. As diverse as the make-up and function of PRRs is their expression in different tissues. However, they all share the ability to sense pathogens directly (for more information see [5] and references therein).

(ii) Cytokine and chemokine receptors bind to inflammatory molecules that are secreted

by cells activated by PRRs. Main source of inflammatory cytokines and chemokines are activated tissue macrophages [167]. These inflammatory molecules help to alert the body to potential intruders and mediate an inflammatory response that is characterized by heat, pain, redness and swelling. During inflammation, blood vessels become dilated and permeabilized, thus enabling leukocytes to enter the tissue at the site of an infection. Additionally, inflammatory cytokines induce the expression of adhesion molecules on endothelial cells, further facilitating extravasation of cells of the immune system. Inflammatory chemokines serve as chemoattractants to guide leukocytes to the site of infection or damaged tissue. Inflammation is hence key to mount an efficient immune response or to promote healing after tissue injury (Figure 1.1). However, if inflammatory processes become chronic or systemic, tissue damage and diseases entail (e.g. Crohn's disease, psoriasis) [126, 31].

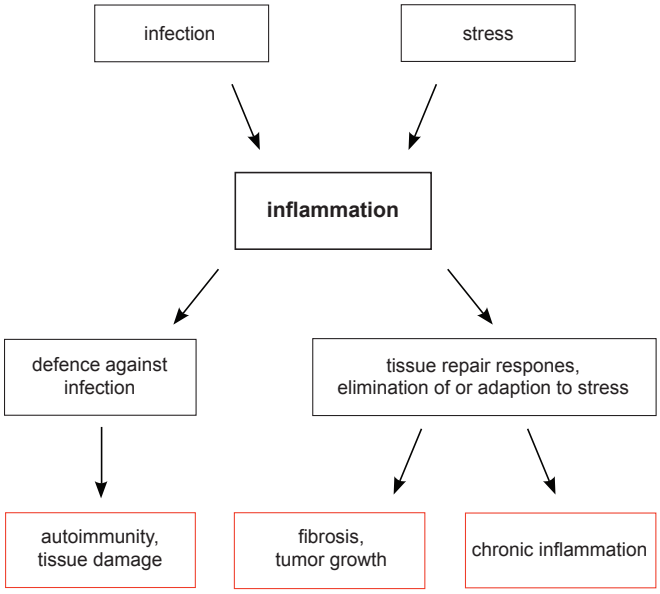

Figure 1.1: The role of inflammation in health and disease. Inflammatory responses are induced by different triggers such as infection and cell stress due to disturbances of tissue homeostasis. If the physiological purpose of inflammation is met, e.g. clearance of infection or restoration of the homeostatic state, the transient inflammatory response is terminated. Under pathological circumstances (marked in red), prolonged inflammation causes diseases.

1.1.2 TNF-α in innate immunity

Cytokines and their receptors can be classified into the following groups: (i) hematopoietins [e.g. interleukin (IL) 6] whose receptors signal through receptor-associated kinases, (ii) chemokines (e.g. IL-8) that bind to seven-transmembrane-domain receptors interacting with intracellular trimeric GTP-binding proteins, and (iii) the tumor necrosis factor (TNF)

family (e.g. TNF-α) [152].

19 proteins have been classified according to their structure to belong to the TNF-α family [22]. This family includes mediators of immune responses [such as lymphotoxin-α (LT-α) and CD40 Ligand (CD40L)] as well as death-inducers [like CD95 Ligand/Fas ligand (FasL) and TNF-related apoptosis-inducing ligand (TRAIL)] and factors involved in organogenesis [such as receptor activator of NF-κB ligand (RANKL)] [12, 152]. All family members initiate similar pathways (Figure 1.2). These pathways ultimately induce apoptosis and activation of nuclear factor κB (NF-κB) [243, 90]. Signaling by the founding member of the TNF family, TNF-α, is subject of this thesis.

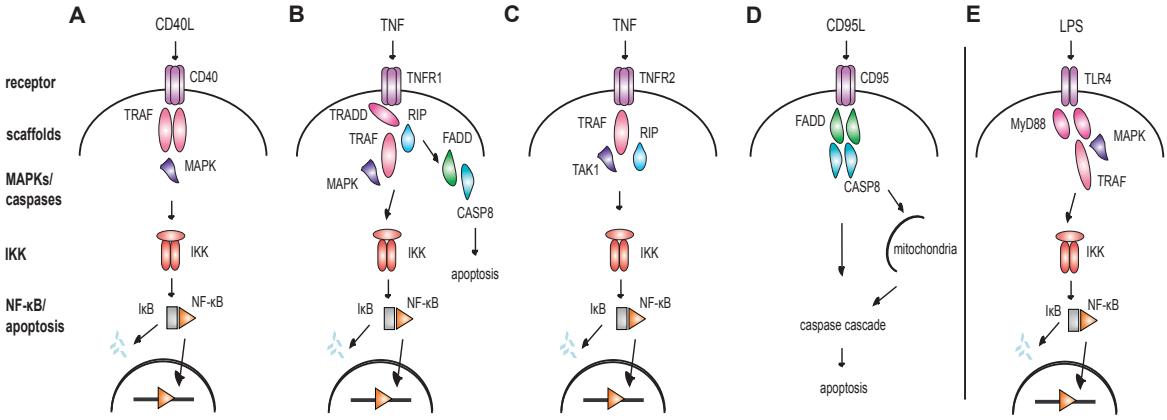

Figure 1.2: Signaling pathways initiated by members of the TNF-α family share similarities with each other as well as other immune signaling pathways such as TLR (Toll like receptor) signaling. They involve scaffold proteins bearing death domains (such TRADD, FADD, RIP) and/or TRAF proteins as well as MAPKs (mitogen-activated kinases). Pathways ultimately either activate NF-κB transcriptional activity or initiate the caspase cascade and apoptosis.

TNF-α was first identified as a soluble factor that is able to induce necrosis in tumor cells [36]. Later it was realized that, depending on the cellular context and the duration of the signal, TNF-α induces either apoptotic or anti-apoptotic proteins in target cells. However, TNF-α's main effect is not its cytotoxicity but its ability to mediate inflammation [12]. TNF-α can be produced by all cell types, including non-immune cells such as fibroblasts and endothelial cells as well as immune cells like monocytes, lymphocytes and macrophages. TNF-α is made as a transmembrane protein in response to activation of PRRs and has to be cleaved in order to be secreted into the extracellular space [20]. The secreted cytokine is active as a homotrimer [233]. It induces the expression of cell surface proteins like integrins that facilitate the extravasation of leukocytes, chemotactic proteins and cytokines further promoting inflammation. Secreted systemically (e.g. during septic

shock), TNF-α is toxic for the body, causing for example wasting syndrome and liver failure. Observed cytotoxicity is probably caused by TNF-α-induced production of mediators of tissue destruction like nitric oxide (NO) and reactive oxygen species (ROS) [247].

There are two TNF-α receptors, TNFRSF1A (TNFR1) and TNFRSF1B (TNFR2). While TNFR1 is constitutively expressed in most tissues, TNFR2 expression is typical for immune cells [247]. TNFR2 fulfills functions in lymhoid organ development. It cannot be fully activated by secreted TNF-α, having a higher affinity for the membrane-bound cytokine. Thus, TNFR1 is the main mediator of the effects of soluble TNF-α [88].

1.1.3 TNF-α receptor 1 signaling - an overview

Binding of TNF-α to its receptor mainly causes either activation of NF-κB or apoptosis by activation of caspases. TNFR1 mediates responses by recruitment of different adaptor and signaling molecules to the intracellular tail of the receptor, which contains death domains (DDs). These domains are important for homotypic protein-protein interactions (table 1.1) [234, 39]. Triggering of TNFR1 induces the interaction of the DDs of the receptor with the DD protein TNFR1-associated death domain protein (TRADD), initiating formation of TNFR complex I (TNFR-C). This in turn activates a signaling cascade that leads via mitogen-activated protein kinases (MAPKs) to the activation of the inhibitors of NF-κB kinase (IKK) complex. The activated IKK then phosphorylates inhibitors of NF-κB (IκB). Subsequently, IκB proteins are degraded and release NF-κB transcription factors into the nucleus (Figure 1.3).

In addition to initiating inflammatory and proliferative responses via the activation of NF-κB, DD interactions are also important for the induction of the caspase cascade by TNF-α ultimately resulting in apoptosis. Upon receptor internalization [204], TRADD recruits Fas-associated death domain protein (FADD) to the TNFR [109] inducing the formation of the TNFR complex II [171]. FADD associates with caspase (CASP) 8, an initiator caspase activating a signaling cascade which results in apoptosis (Figure 1.3) [207, 258].

Even though the DDs of TNFR1 are main mediators of signaling events, TNFR1 can also interact with non-DD proteins. For example, the intracellular domain of TNFR1 interacts with the scaffold protein growth factor receptor-bound protein (GRB) 2, thereby initiating Rat sarcoma (Ras) signaling upon receptor ligation [100]. In addition, signaling through TNFR1 activates the MAPK cascade, including MAP3Ks, Jun N-terminal kinases (JNKs), p38 and extracellular signal-regulated kinases (ERKs), either promoting cell survival or cell death by activating the transcription factor AP-1 [212]. TNF-α also induces

the production of ROS, promoting DNA damage [40]. Stress responses are additionally induced by the production of the second messenger ceramide via activation of acidic and neutral sphingomyelinases (SMases) [2, 27]. Furthermore, PI(3)Ks, PKCs and PKB become activated upon TNFR1 ligation, all having influence on NF-κB as well [247].

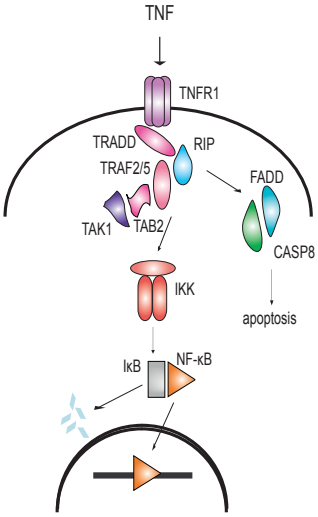

molecule	function
TNF (trimeric)	ligand
TNFR1 (trimeric)	receptor
TRADD	scaffold protein
TRAF2/5	scaffold and E3 ligase function
RIP1	scaffold protein
FADD	scaffold protein
CASP8	cysteine-aspartic acid protease
TAB2	scaffold protein
TAK1	kinase
IKK	γ: scaffold and regulatory function; α+β: kinase
IκB	inhibitory proteins, retaining NF-kB in cytoplasm
NF-κB	transcription factor

Figure 1.3: Schematic presentation of human TNF-α signaling. Activated TNFR1 recruits death domain containing proteins. These serve as adaptors for further protein binding resulting in the activation of MAP kinases that activate the IκB kinase (IKK) complex. IKK in turn phosphorylates IκB, thus releasing NF-κB. Once released, the transcription factor can translocate into the nucleus and induce the expression of target genes like cytokines. In parallel, signaling through TNFR1 can also lead to induction of apoptosis by activation of caspase 8.

1.1.4 NF-κB signaling downstream of TNFR1

The TNFR1 complex When trimeric TNF-α binds to the extracellular domains of its trimeric receptor, TNFR1 translocates to lipid rafts [146] and TRADD associates with the DDs in the intracellular part of TNFR1 [117]. TRADD serves as a scaffold for the binding of TNFR-associated factor (TRAF) 2 [108] and receptor interacting protein (RIP1) [224, 237], initiating the formation of the TNFR-C.

Regulation of TNF-α signaling is strongly dependent on reversible modifications of signaling components (see box 1). Ubiquitination is such a modification that either targets a protein for destruction or enhances its interaction with other signaling molecules. It is mediated by three enzymes, a ubiquitin-activating enzyme (E1), a ubiquitin-conjugating enzyme (E2) and finally a ubiquitin-ligating enzyme (E3) which confers specificity to the process as it recognizes the substrate [13]. Ubiquitination at the TNFR-C is mediated by

a "team" of proteins: the E2 complex Ubc13/Uev1A (Ubiquitin conjugating enzyme/Ubc-like factor ubiquitin conjugating enzyme variant) and TRAF-2 [78]. Nearly all members of the TRAF protein family carry Really Interesting New Gene (RING) domains that confer ubiquitin ligase (E3) activity (table 1.1) [246]. TRAF2 does not only mediate ubiquitination, it is also ubiquitinated itself. Both processes are needed for TNF-α-induced NF-κB activation [58].

TRAF2 mediates binding of the inhibitor of apoptosis (IAP) family members cIAP-1 and cIAP-2 [196, 217], two proteins bearing RING domains as well [265, 111]. cIAP-1 can ubiquitinate TRAF2, causing its degradation and interfering with TNF-α-induced NF-κB activation [148]. Besides, cIAP-1 and cIAP-2 inhibit the activation of the apoptotic caspase cascade via CASP8 [248].

The IKK - the link between receptor and NF-κB activation - is recruited by two processes to the TNFR-C. Firstly, TRAF2 cooperates with TRAF5 in incorporating the IKK complex into the TNFR-C [232]. Secondly, TRAF2 ubiquitinates RIP1 with the help of Ubc13/Uev1A [108, 65]. Subsequently, RIP1 interacts with the ubiquitin-binding domain (UBD) of IKK-γ [260, 65], the regulatory subunit of the IKK that is crucial for IKK function [60]. IKK-γ thereby helps to recruit the IKK to the TNFR-C [262].

Table 1.1: Protein domains important in TNF-α signaling. TNFR1: TNF receptor superfamily member 1A, TNFR2: TNF receptor superfamily member 1B, TRADD: TNFR1-associated death domain protein, FADD: Fas-associated death domain, RIP: receptor interacting protein, IAP: inhibitor of apoptosis

domain	**examples**	**function**
death domain (DD)	TNFR1, TRADD, FADD, RIP1	protein-protein interactions
TNFR-associated factor (TRAF)	TNFR2, TRAF proteins	protein-protein interactions
really interesting new gene (RING)	TRAF proteins cIAP1, cIAP2	E3 ligase activity

The IκB kinase complex The activation of the IKK is the key event leading to NF-κB activation. In addition to IKK-γ, the IKK consists of two catalytically active subunits, IKK-α and IKK-β [90]. IKK activation is achieved by phosphorylation of the catalytical subunits in their activation loops [57, 150]. Activated IKK phosphorylates proteins of the

IκB family [227, 13], marking them for degradation by the proteasome [61] and thereby releasing NF-κB. Subsequently, the transcription factor NF-κB can translocate into the nucleus to interact with other transcriptional regulators and DNA. Two general pathways lead to the activation of the IKK: the non-canonical and the canonical pathway. The non-canonical pathway is mediated by MAP3K14 and IKK-α (for review see [23], also see Figure 1.4). The canonical pathway, e.g. activated by TNF-α, leads to phosphorylation of IKK-β [90]. The kinase activating IKK-β still awaits identification. Even though RIP1 is required for TNF-α-induced activation of the IKK [130], its kinase activity is dispensable [108, 237]. Hence, RIP1 does not activate the IKK directly. Two possibilities remain how the IKK is catalytically activated: (i) the IKK complex, brought together in close proximity with the help of RIP1, autophosphorylates itself or (ii) the IKK complex is phosphorylated by a kinase that is recruited to the TNFR-C by RIP1 [125]. Several candidate kinases have been proposed, most of them MAPKs, e.g. MEKK3 [264] or transforming growth factor-β-activated kinase (TAK) 1 [202].

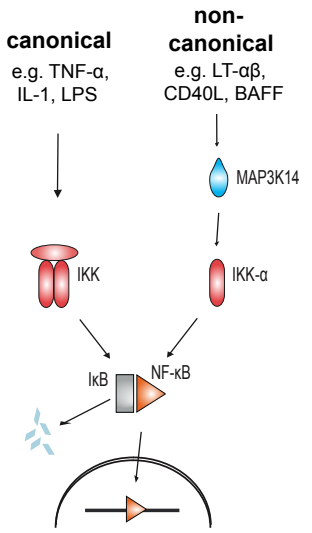

domain	examples	function
Rel homology domain (RHD)	NF-κB	interaction with other NF-κBs or proteins of IκB family, DNA binding
transactivation domain (TAD)	NF-κB	activation of gene transcription
ubiquitin binding domain (UBD)	IKK-γ	binding of lysine 63-linked ubiquitin

Figure 1.4: Inducers and regulators of NF-κB signaling. NF-κB transcriptional activity can be stimulated by either canonical signaling, as described in the text, or by non-canonical signaling via activation of MAP3K14. The table lists domains important in the activation and regulation of NF-κB transcriptional activity.

Activation of NF-κB Transcription factors of the NF-κB family regulate diverse gene expression programs mediating inflammatory responses as well as anti-apoptotic and developmental processes [96]. In mammals, there are five NF-κB family members that all share

a common Rel homology domain (RHD): (i) NF-κB1/p50, (ii) NF-κB2/p52, (iii) c-Rel, (iv) RelA/p65 as well as (v) RelB. NF-κB proteins form homo- and heterodimers via interaction through their RHD. Only c-Rel, RelA and RelB can activate gene transcription due to a C-terminal transcription activation domain (TAD); p50 and p52 do not contain a TAD and act as repressors unless they form dimers with TAD-containing family members [96].

A wide range of signaling pathways results in the activation of NF-κB. Among these are pathways induced by receptors recognizing extracellular danger [166] in innate and adaptive immunity (such as TLR4 or T cell and B cell receptor, respectively). NF-κB can also be activated via intracellular signaling pathways responding to intruders (e.g. the inflammasome) or physical stress such as UV radiation and ROS [188]. Activation of NF-κB is regulated by proteins of the IκB family. IκB proteins bind to NF-κB and retain them in the cytoplasm [257]. Different IκB proteins fulfill different functions which are determined by the kinetics of their degradation upon phosphorylation by the IKK [104] and their binding affinity for specific NF-κB dimers [84]. IκB-α, the target of TNF-α-induced NF-κB activation, binds to and regulates the activity of RelA:p50 dimers which are to date the best studied NF-κB dimers.

Upon TNF-α-induced activation of IKK and degradation of IκB-α, NF-κB is released to translocate into the nucleus and induce target gene expression. However, NF-κB is only fully activated after phosphorylation and acetylation [176]. These modifications enhance DNA binding and mediate the interaction with additional transactivators such as CREB binding protein (CPB)/p300 and histone acetyl transferases (HATs) [44]. Many proteins have been shown to modify NF-κB [179, 249, 103], including nuclear IKK-α [218, 44, 263, 7]. However, IKK-α also plays a role in the termination of the NF-κB response (see below). For a comprehensive review on modifications of NF-κB see [187].

Fully activated NF-κB then drives the expression of target genes. The induced target gene expression profile is not only dependent on which NF-κB proteins were activated but also on NF-κB nuclear oscillations [177, 105] (see box 1). Among TNF-α-induced target genes are cytokines such TNF-α itself [211, 51], chemokines like CCL20/MIP-3α (CC-motif chemokine ligand 20) [139, 238], and IL-8 [138] as well as TNF-α pathway components such as IκB-α [95, 230, 56] and c-IAP2 [248].

BOX 1: Principles of signaling mechanisms

Discoveries in TNF-α signaling often have identified principles of signaling regulation that have later been shown to be also valid for other signaling pathways. These findings argue for a more complex view on signaling pathways than just mere induced interaction between different proteins. One such principle of regulation has been established for a while: reversible modifications such as ubiquitination and phosphorylation. These modifications are involved in the regulation of many components of TNF-α signaling, but also play a role in regulating other immune signaling pathways (e.g. [45, 229, 16]). A recently emerged principle of regulation of signaling is compartmentalization. At the plasma membrane, TNFR complex I consisting of TRADD, TRAF2/5 and RIP1, signals to anti-apoptotic NF-κB. Upon endocytosis the apoptotic TNFR complex II is formed comprising FADD and caspase 8 which induces apoptosis [205]. CD40-induced MAPK and IKK signaling is regulated in a similar manner [165, 206]. TLR signaling has recently been reported to be regulated by compartmentalization as well [70, 11]. Lastly, kinetics is another principle of regulation. Signaling to NF-κB is a fast reponse, and only if activation of the pathway is sustained, apoptosis induction can occur (see also Figure 1.5). Moreover, kinetics determine the gene expression program induced by activated NF-κB [177, 105].

BOX 1 continued

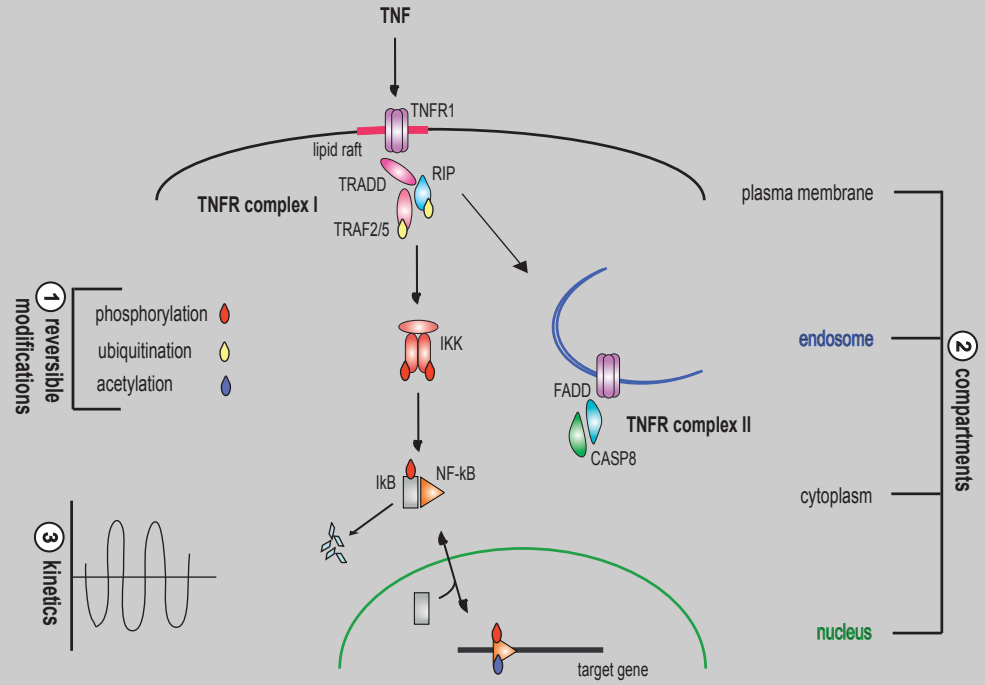

Figure 1.5: The outcome of TNF-α-induced signaling events is not merely dependent on interacting proteins. (1) Modifications such as phosphorylation and ubiquitination either act as binding sites for interaction partners and activators of enzymes or signal proteasomal degradation. (2) Compartmentalization is fundamental in the decision between life and death (e.g. TNFR complex I at the plasma membrane vs. endocytosed TNFR complex II). (3) Kinetics is another important factor: fast reponses usually entail NF-κB activation which is shut down again with a time lag (e.g. the fast ubiquitination of RIP1 enables interaction with signaling molecules, whereas its delayed poly-ubiquitination causes its degradation). Kinetics also determine the transcriptional outcome of induced signaling events (e.g. NF-κB nuclear oscillations).

1.1.5 Termination of TNFR1 signaling

The termination of TNF-α-induced NF-κB activation is still poorly understood (Figure 1.6) [84]. There are several negative feedback loops involved in this process. One is affecting TNF-α mRNA stability (and interferes thereby with a positive feedback loop consisting in TNF-α-induced TNF-α production). TNF-α mRNA bears an AU-rich element (ARE) sequence in the 3' untranslated region (UTR) [34]. Tristetraprolin (TTP) is an ARE sequence-binding protein mediating deadenylation and destabilization of bound mRNAs. TTP is induced by TNF-α, promoting the decay of TNF-α mRNA [235]. Another TNF-α target

gene is IκB-α which can bind to RelA:p50 in the nucleus and shuttle it back to the cytoplasm [230, 195, 112]. IKK-α can terminate NF-κB activation by promoting RelA nuclear degradation [142].

TNF-α-induced protein (TNFAIP) 3 is involved in a negative feedback loop further upstream at the level of RIP1 activation. This protein possesses both de-ubiquitinating (DUB) enzyme as well as ubiquitin ligase activities [256]. TNFAIP3 removes activating lysine 63-linked ubiquitin from RIP1 and adds lysine 48-linked poly-ubiquitin, thus marking RIP1 for destruction [256]. Cylindromatosis (CYLD) is another negative regulator of TNF-α signaling, detaching lysine 63-linked ubiquitin from IKK-γ and TRAF2 [136, 239].

Even further upstream acts the so-called receptor shedding, consisting in the secretion of TNFR1 from the plasma membrane [99]. Receptor shedding has two consequences. Firstly, the cell cannot respond to TNF-α because of lost excitability. Secondly, soluble TNFR1 scavenges extracellular TNF-α so that less cytokine is available for stimulation. Defects in proteolytic shedding of TNFR1 are thought to be involved in TNFR-associated periodic syndrome (TRAPS) that is characterized by chronic inflammation and fever [80].

The inducible expression of TNFR2 offers yet another interesting way of regulation. The intracellular domains of TNFR2 have a higher affinity to TRAF2, thereby depleting the TRAF2 pool in the cell [77]. Hence, TRAF2 is missing at the TNFR1 complex, NF-κB activation is impeded and apoptosis is favored.

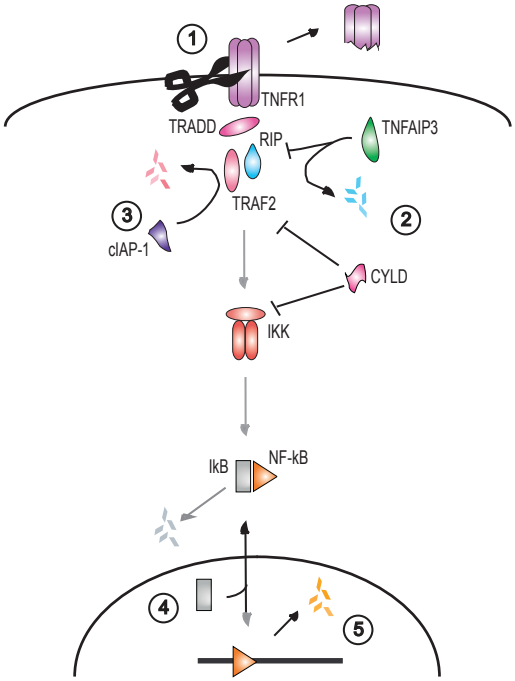

Figure 1.6: TNF-α signaling and NF-κB transcriptional activity are negatively regulated by multiple means. (1) Receptor shedding renders the cell less excitable and releases solube TNFR1 that can scavenge extracellular TNF-α. (2) The de-ubiquitinating enzymes CYLD and TNFAIP3 remove activating ubiquitins from TRAF2 and IKK-γ as well as RIP1, respectively. Additionally, TNFAIP3 possesses ubiquitin ligase activity for tagging RIP1 for degradation. (3) TRAF2 can be scavenged to TNFR2 and be degraded, after being ubiquitinated by cIAP-1. (4) Re-synthesized IκB-α shuttles NF-κB back to the cytosol. (5) Besides, NF-κB gets degraded upon phosphorylation.

1.2 RNA Interference

The amount of protein being made from a gene can be controlled at the level of transcription and translation. The sequences of enhancer and promoter regions of a gene determine the efficacy of transcription. Transcription factors controlled by inducible signaling pathways activate the expression of genes that are not constitutively expressed. But also after transcription, gene expression can be altered. RNA interference (RNAi) is one mechanism of posttranscriptional gene regulation.

RNAi evolved as a defense mechanism against molecular parasites such as viruses and transposons [252, 156]. Discovered in plants and first described as RNAi in *Caenorhabditis elegans* [68, 74], this evolutionarily conserved gene silencing mechanism has proven to be a valuable tool for studying gene function in several species by transiently silencing genes [94].

RNAi is mediated by small double-stranded RNAs and relies on sequence complementarity between the small RNA and its mRNA target [168]. These double-stranded RNAs can either be of endogenous origin or be artificially introduced. Naturally occurring RNAs are microRNAs (miRNAs), endogenously expressed short interfering RNAs (endo-siRNAs), Piwi-interacting RNAs (piRNAs), trans-acting siRNAs (tasiRNAs), small-scan RNAs (scnRNAs) and repeat-associated siRNAs (rasiRNAs) as well as viral non-coding RNAs [50, 184]. The best studied naturally occurring RNAi-mediating RNAs are miRNAs. These non-coding RNAs are involved in posttranscriptional gene regulation in both animals and plants. They are transcribed as pri-miRNAs, possessing a characteristic stem-loop structure, that are cleaved twice - once in the nucleus by Drosha [144, 59, 87, 92, 141], once in the cytoplasm by Dicer [266, 153] - yielding the mature miRNAs [10, 63]. miRNAs mediate either cleavage or translational repression of their complementary mRNAs [242].

Among artificially introduced RNAi reagents are e.g. short interfering (si) RNAs, short hairpin (sh) and long hairpin RNAs as well as long double-stranded (ds) RNAs. The latter three are converted inside the cell into siRNAs by Dicer, a cytoplasmic endonuclease [115, 89, 145]. Dicer cleaves long RNA into short RNA duplexes of about 21 nucleotides having 5' phosphates and 2-nucleotide 3' overhangs, characteristic for small RNAi-mediating RNAs [14, 67]. These short RNA duplexes represent the "mature" RNAi-mediating RNA species.

In order to mediate gene silencing effects, the small RNAs have to be incorporated into the RNA-induced silencing complex (RISC) [91, 73]. For enabling association with this multiprotein complex, the small RNA has to be unwound: the strand with the least thermodynamically stable 5' end becomes incorporated into the multiprotein complex [86].

Single-stranded RNAs interact with RISC complex proteins belonging to the family of Argonaute proteins [222, 154, 155]. Argonaute proteins exist in prokaryotes as well as eukaryotes and catalyze RNA cleavage reactions [6]. In eukaryotes, Argonaute proteins are key components of RNAi processes [223]. In complex with these proteins, the small RNA finds its target by sequence complementarity [160]. As a result, the targeted mRNA becomes either degraded or translationally repressed (Figure 1.7) [151, 190, 161, 69].

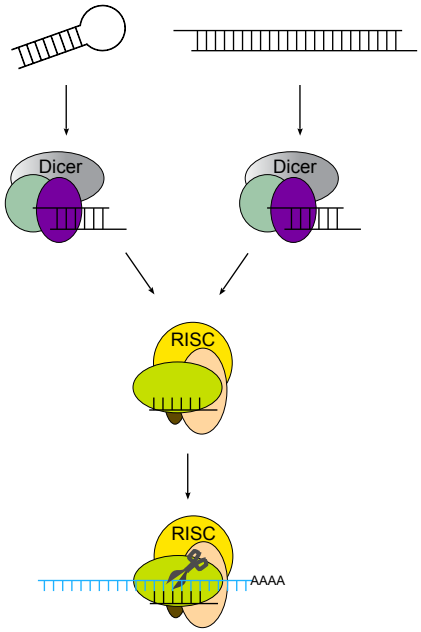

Figure 1.7: Mechanism of RNAi. Short hairpin (sh) RNA-encoding plasmids are transcribed in the nucleus as long RNAs having a characteristic stem-loop structure. Exported into the cytoplasm, the shRNA is converted into small interfering (si) RNAs through cleavage by the RNase III endonuclease Dicer. Similarly, long double stranded (ds) RNAs are cleaved by Dicer into siRNAs. One strand of the siRNA becomes then incorporated into the RNA-induced silencing complex (RISC) guiding the RNAi machinery to the mRNA target by sequence complementarity. As a result, the mRNA becomes degraded.

1.3 Using RNAi to Study Gene Function

Two general approaches are used to infer gene function from loss-of-function phenotypes. Classical forward genetics employ mutagenesis screens in order to create mutant phenotypes. Mutations then have to be mapped to the gene whose loss-of-function caused a phenotype. In contrast, reverse genetics experiments take the gene as starting point assessing whether its loss-of-function yields a phenotype.

Table 1.2: Artificially introduced small non-coding RNAs.

small non-coding RNA	organism	function
double-stranded RNAs (dsRNAs)	bathing of fly cells, feeded to worms	processed to siRNAs: mRNA cleavage
small interfering RNAs (siRNAs)	transfection of mammalian cells	mRNA cleavage
endoribonuclease-prepared short interfering RNAs (esiRNAs)	transfection of mammalian cells	mRNA cleavage
short hairpin RNAs (shRNAs)	transduction/transfection of mammalian cells	matured to siRNAs: mRNA cleavage

RNAi is a powerful tool for reverse genetics experiments. Common RNA species applied in these experiments are dsRNAs, siRNAs, endoribonuclease-prepared short interfering RNA (esiRNAs), shRNAs and long hairpin RNAs (table 1.2). dsRNAs are used to study gene function e.g. in *C. elegans* (applied by feeding or injection), *Drosophila melanogaster* (applied by bathing *ex vivo*) and *Schmidtea mediterranea* (applied by feeding or injection). shRNA-encoding plasmids can be transfected into mammalian cells using viral or non-viral transfection methods. shRNAs are transcribed in the nucleus into pri-miRNA-similar stem loop precursors and mature like miRNAs into "active" siRNAs. siRNAs and esiRNAs are "mature" RNAi-mediating species and are transfected as such into mammalian cells using transfection reagent- or electroporation-based methods. For their use in mammalian cells, siRNAs are chemically modified in order to improve mRNA silencing effects, while avoiding adverse effects such as an interferon response [48, 3, 116, 241].

In genome-wide RNAi screens, each annotated gene in the genome is targeted by an RNAi-mediating reagent. This allows for the systematic investigation of gene function in different biological processes, inferred from their loss-of-function phenotypes. Using the appropriate reporter system for a biological question, the consequences of silencing a gene in any process can be determined. This can be done working in cell culture or even in whole organisms such as worms and flies [132, 62]. Cell-based reporter systems range from assessing cell viability with the help of specific dyes or luciferase reactions and transcriptional activity in low-content screens to monitoring cell morphology in high-content microscopy screens (Figure 1.8) [9, 30, 178, 28].

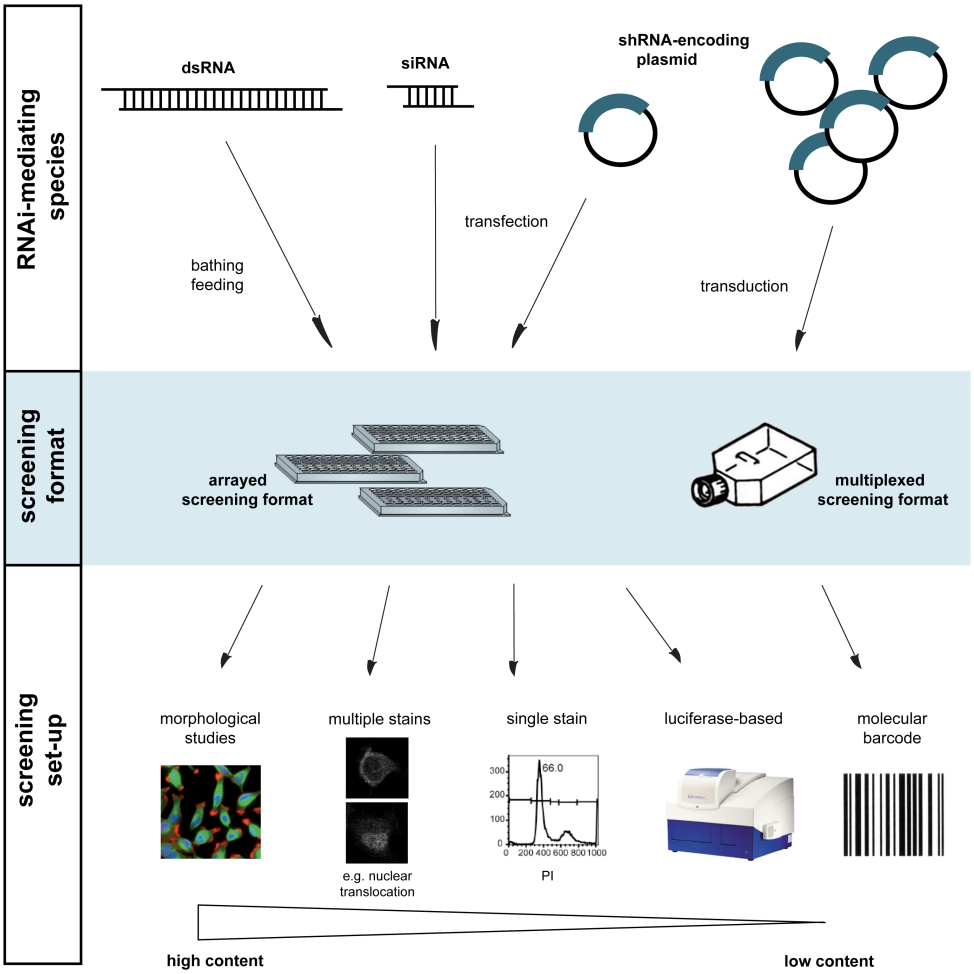

Figure 1.8: Genome-wide RNAi screening approaches. Different RNAi-mediating RNA species are used in research for functional genomics, e.g. double stranded RNAs (dsRNAs), that are fed to worms (via *E. coli* expressing dsRNA) or taken up by fly cells by a process called bathing. Small interfering (si) RNAs and short hairpin (sh) RNA-encoding plasmids are employed for transfection of mammalian cells. The application of barcoded shRNAs permits performing screens in genome-wide pools (multiplexed screens), which are analyzed e.g. by microarray hybridization or DNA sequencing. In contrast, in arrayed screens only one gene is targeted per spot (well). This screening format enables different read-outs, e.g. luciferase-based read-outs looking at cell viability or transcription factor activity. Using clear bottom plates, staining cells with dyes is a possible read-out. Applicable microscopy-based read-outs range from single dye measurements [e.g. studying cell cycle phase by PI staining, measured with the help of an Acumen plate reader or by fluorescence activated cell sorting (FACS)], simple measurements using multiple stains such as nuclear translocation to complex cell morphological studies. As more sophisticated screens generate ever more information, often interrogating multiple features simultaneously, analysis tools need to retrieve, integrate and display more and more parameters.

1.3.1 Cell-based assays employed in RNAi screening

As an example of a screening approach, the dual luciferase assay will be explained. This assay is based on a system that emits visible light at two different wavelengths. One luciferase construct reports whether the biological process of interest is active or not. Another luciferase construct serves as co-reporter to control cell viability and transfection efficiency. The two different reporters can be used in parallel since they convert different substrates and emit light at different wavelengths (Figure 1.9).

For usage as a pathway-specific reporter, a luciferase gene, e.g. the *firefly* luciferase gene, is under the control of regulatory elements relevant to the biological process being studied. For example, if the regulation of one specific gene is to be investigated, the luciferase gene expression is driven by the promoter region of the gene of interest [83]. Likewise, if one specific transcription factor is of interest, transcription factor binding sites can be employed [147]. The reporter has to respond to treatment reflecting the biological process of interest. Accordingly, reporter expression has to be decreased if the studied biological process is interrupted, e.g. by RNAi-mediated gene silencing.

As co-reporter, another luciferase (e.g. the *Renilla* luciferase) construct is used, where the luciferase gene is under the control of a constitutively expressed promoter. Expression of this second reporter is used to normalize the expression of the pathway-specific reporter to.

Data acquired through low-content screening are of low dimensionality such as lists of luminescence counts of two luciferases. In contrast, high-content screening data are complex, usually consisting of microscopic images acquired in different channels. As more sophisticated screens generate ever more information, analysis tools need to retrieve, integrate and display increasing numbers of parameters (e.g. [35]).

1.3.2 RNAi reagents and cell-based screening formats

Different RNAi libraries are available for screening the human genome (or that of model organisms) systematically for effector genes in any biological process of interest. Arrayed libraries are ususally transfected in a miniaturized format (96-, 384- or 1536-well), with either one well per gene, targeted by pooled siRNAs (e.g. [101]), or multiple wells per gene, each of them containing an individual siRNA (e.g. [134]). In contrast, using barcoded shRNA libraries, screens can be performed in genome-wide pools (multiplexed). After selection of the cell population presenting the phenotype of interest, the targeted gene has then to be defined by determining the identity of an shRNA-specific barcode (e.g. [172]).

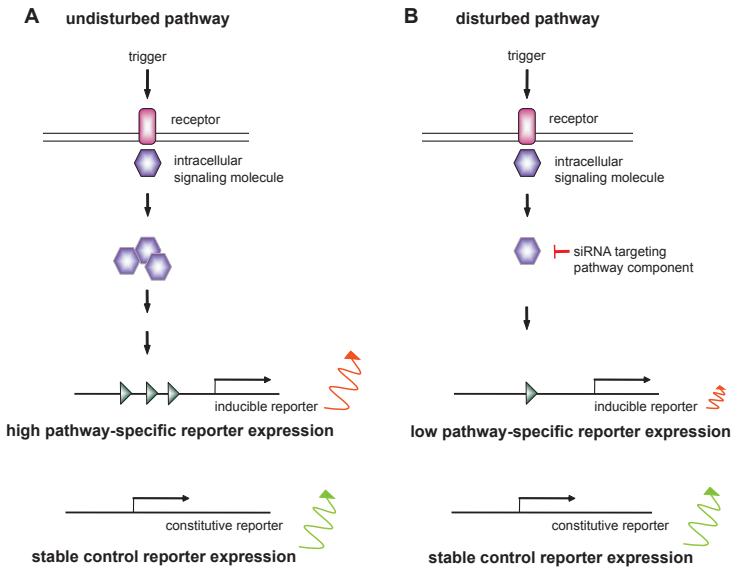

Figure 1.9: Concept of the dual luciferase assay. A constitutively expressed luciferase reporter is used to control cell viability and transfection efficiency. Another luciferase construct reports whether the biological process of interest is active or inactive. Its expression is controlled by regulatory elements relevant to the biological process being studied. A: Triggering of the biological pathway induces pathway-specific reporter expression. B: Pathway-specific reporter expression is decreased when the studied biological process is inhibited by RNAi-mediated gene silencing. Expression of the control reporter stays unchanged.

1.3.3 Assay design

Negative and positive controls are essential for RNAi experiments. These controls are needed to categorize phenotypes observed after siRNA-mediated knockdown of proteins. A negative control consists of an siRNA without cellular target or targeting a protein unrelated to the biological process studied. Negative controls should not influence expression of the pathway-specific reporter allowing to determine "normal" reporter expression level. A positive control consists of an siRNA targeting a known component of the biological process of interest and allows to determine expression levels of the pathway-specific reporter upon disruption of this process. Besides controls, the right assay system has to be chosen for studying the biological process of interest. Measuring cell numbers by ATP levels for example will report cell death, but will not yield any information on cell cycle arrest (unless cell cycle arrest resulted in strongly reduced cell numbers) or morphological abnormalities. Likewise, cloning the promoter region of a gene of interest into a transiently transfected reporter will identify e.g. transcription factors involved in the transcriptional regulation of that gene but cannot cover regulatory mechanisms mediated by chromatin modification. Therefore, the choice of the reporter system will determine the scope of information that

can be acquired by screening.

Figure 1.8 summarizes the different possibilities available for performing RNAi-based screens. The biological question and analysis tools available in the laboratory dictate which library and assay format are best to use. A variety of genome-wide screens has been performed so far, identifying novel players in several different pathways and thus documenting the power of the technique [173].

1.4 Aim of This Thesis

TNF-α is the main mediator of inflammation and a key component of many inflammatory diseases [137]. Even though the TNF-α pathway is relatively well studied, a variety of open questions remain, such as the regulation of IKK activation, of NF-κB transcriptional activity and the termination of the response.

My work aims at finding novel regulators of TNF-α signaling, identified by RNAi screening. As a first step, an assay system was to be established to measure TNF-α-induced NF-κB transcriptional activity in human cells. The assay then had to be adapted to high throughput screening. Subsequently, I intended to perform two genome-wide RNAi screens. This would allow me to identify putative novel regulators of TNF-α signaling by (i) an individual "high-stringency" screening analysis and (ii) a comparative screening analysis, determining hits found in both screens. In the next step, I planned to develop secondary assays to characterize these high confident candidates. The ultimate goal was to define the level of action of chosen candidates in the signaling cascade. Identifying interaction partners would then allow to draw conclusions on mechanistic details of the candidate's function in TNF-α signaling.

Chapter 2

Results

2.1 Genome-wide RNAi Screens for Identifying Novel Regulators of TNF-α Signaling

TNF-α is a potent inflammatory cytokine implicated in the pathology of inflammatory diseases. In order to find novel regulators of TNF-α signaling by genome-wide RNAi screening, I first had to establish a cell-based assay to monitor NF-κB transcriptional activity. This assay had to be suited for the use in miniaturized format that is required for large-scale experiments. After quality control of the established assay, two genome-wide RNAi screens were performed, analyzed and compared to each other. I then determined criteria for hit selection and performed secondary assays to validate candidates.

2.1.1 Design and development of a cell-based assay to study NF-κB transcriptional activity

To perform a cell-based genome-scale RNAi screen for TNF-α signaling, I first identified a cell line that was suited for studying the TNF-α pathway and could be efficiently transfected with siRNAs. Further, siRNA transfection conditions and a cell-based assay to monitor NF-κB transcriptional activity had to be established.

Choice of cell line Human embryonic kidney (HEK) 293T cells have been used successfully in previous studies monitoring TNF-α-induced NF-κB activation (see e.g. [76, 47]). In addition, they could be transfected with siRNAs as well as plasmids very efficiently. To assess their response to TNF-α, HEK293T cells were treated with increasing amounts of TNF-α for different periods of time before cell viability was assessed by measuring ATP levels. Results presented in Figure 2.1 indicate that TNF-α did not induce cell death in HEK293T cells. However, TNF-α induced NF-κB transcriptional activity in these cells

(Figure 2.2), demonstrating that HEK293T cells are a suitable model cell line for studying TNF-α-induced activation of NF-κB.

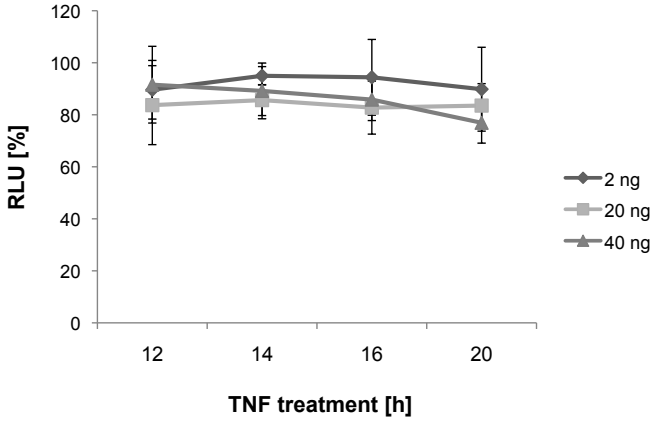

Figure 2.1: TNF-α treatment does not induce cell death in HEK293T cells. HEK293T cells were treated with increasing amounts of TNF-α (ng/ml) for different periods of times (12 - 20 hours (h)) before cell viability was assessed by measuring ATP levels. Measured relative light units (RLU) were normalized to those of untreated cells. RLU describe the strength of ATP-dependent luciferase luminescence. Error bars represent standard deviations of 4 technical replicates. One representative result of 3 independent experiments is shown.

The dual luciferase assay: development of a reporter for monitoring NF-κB transcriptional activity In order to detect NF-κB transcriptional activity a cell-based dual luciferase assay was developed. It is based on a system that emits visible light in two different wavelengths. The dual luciferase assay system is well suited for high throughput screening since it performs reliably also in miniaturized assay format and all necessary processing steps can be supported by automation.

To obtain an NF-κB-dependent reporter with high fold induction upon TNF-α treatment, the *firefly* luciferase gene was fused to an artificial promoter containing eight NF-κB binding sites. Using this "4-4-FL" reporter, I tested whether HEK293T cells responded to TNF-α with induction of NF-κB transcriptional activity. Different amounts of TNF-α, ranging from 2 to 40 ng/ml, were used to stimulate cells for different periods of time. Transfecting different amounts of 4-4-FL (2 - 40 ng/well) showed that induction was highest upon transfection of 2 ng of reporter per well (data not shown). NF-κB reporter expression increased with increasing amounts of TNF-α and increasing stimulation periods (Figure 2.2). Using 2 ng of the reporter and 20 ng/ml TNF-α for 16 hours, the expression of the 4-4-FL NF-κB reporter was induced about 16-fold. The experiment demonstrated

that the 4-4-FL reporter could be used to monitor TNF-α-induced NF-κB activation. In further experiments HEK293T cells were therefore stimulated with 20 ng/ml TNF-α for 16 hours. Under these conditions NF-κB-dependent *firefly* luciferase was highly expressed without further induction of expression after longer incubations.

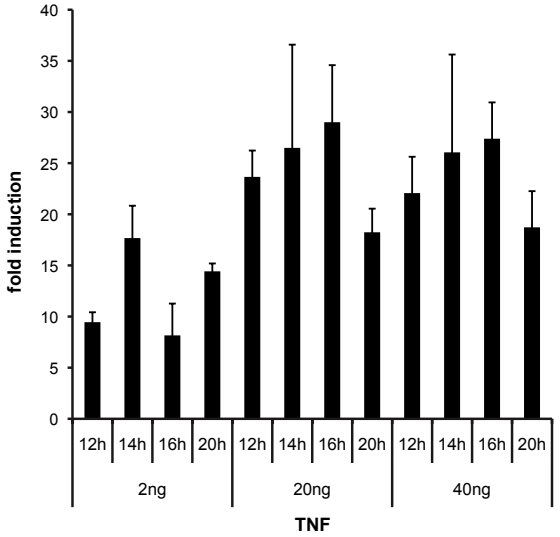

Figure 2.2: TNF-α treatment induces NF-κB transcriptional activity in HEK293T cells. HEK293T cell were transfected with 2 ng 4-4 FL NF-κB reporter per 384-well plate well and treated with different amounts of TNF-α (ng/ml) for different time periods. Fold induction of luciferase expression was calculated in relation to basal (unstimulated) expression. Error bars represent standard deviations of at least 4 technical replicates. One representative result of 3 independent experiments is shown.

The dual luciferase assay: development of a constitutively expressed co-reporter

In luciferase assays based on transient transfection, transfection efficiency of plasmids and cell viability have to be monitored to avoid false positives: besides changes in transcriptional activity, low NF-κB reporter expression could also result from cell death or less effective plasmid transfection. Therefore, a constitutively expressed *Renilla* luciferase reporter was used to control transfection efficiency and cell viability. *Renilla* luciferase converts a different substrate and emits light at another wavelength than *firefly* luciferase enabling the parallel use of these two luciferases.

Two commonly used plasmids encoding *Renilla* luciferase (RL), CMV-RL and TK-RL, driven from constitutively active promoters - CMV and TK, respectively - were tested in HEK293T cells in combination with TNF-α treatment. Neither of them was suitable since *Renilla* luciferase expression from both plasmids was influenced by TNF-α under the

conditions used (Figure 2.3). Whereas CMV-RL expression was strongly induced upon TNF-α treatment, TK-RL expression was decreased by TNF-α to such low levels that the expression would not have been robust enough for a high-throughput assay. As both these promoters are of viral origin and therefore are likely influenced by immune modulatory molecules such as TNF-α [192], a plasmid was cloned containing a constitutively active, non-viral promoter, the human β-actin promoter (act-RL).

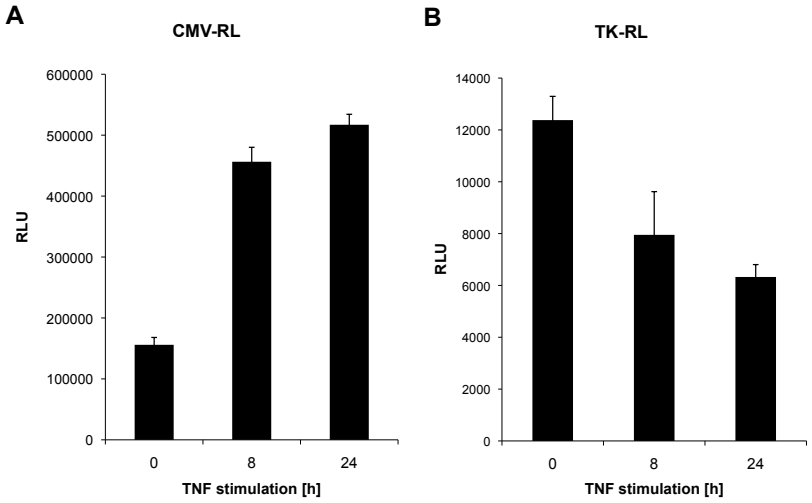

Figure 2.3: Influence of TNF-α stimulation on *Renilla* expression driven by viral promoters. Cells were stimulated for the indicated time periods with 20 ng/ml TNF-α before *Renilla* luciferase expression was determined. A: 2 ng/384-well plate well of CMV-RL were used, yielding a strong luciferase expression. Expression is further increased by TNF-α, rendering the plasmid unsuited for monitoring cell viability defects. One representative result of at least 3 independent experiments is shown. B: 20 ng/384-well plate well of TK-RL were used yielding a much weaker luciferase expression. TK-RL expression was decreased by TNF-α to such low levels that the expression would not be robust enough for a high-throughput assay. A+B: RLU: relative light units representing the strength of luciferase luminescence. Errror bars represent standard deviations of at least 4 technical replicates.

Constitutive expression of the control act-RL reporter was assessed by transfecting HEK293T cells with both reporter plasmids and stimulating these cells two days after transfection with 20 ng/ml TNF-α for 16 hours (Figure 2.4). Even though act-RL expression was reduced by approximately 50% after TNF-α treatment, act-RL expression was high enough to yield stable results under stimulated conditions (in contrast to TK-RL, Figures 2.3 and 2.4). Stimulation by TNF-α was confirmed by induced expression of the 4-4-FL reporter. Subsequent assays showed that TNF-α-induced reduction of act-RL expression was also reduced upon silencing of all TNF-α signaling components tested, except for silencing of TNFR1 (data not shown). Since all TNF-α treated samples (except

for TNFR1 knockdown cells) exhibited similar act-RL expression levels, the reporter was suitable as a reporter for cell viability and transfection efficiency.

By these experiments I determined optimal assay conditions. In further experiments, 2 ng per well 4-4-FL and 20 ng per well act-RL were transfected simultaneously. act-RL expression was used to normalize 4-4-FL expression by dividing *firefly* luciferase luminescence counts by *Renilla* luciferase luminescence counts.

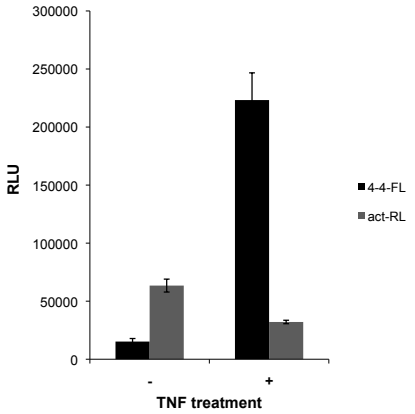

Figure 2.4: Expression levels of NF-κB-dependent 4-4-FL and constitutively expressed act-RL without and with TNF-α treatment (20 ng/ml) for 16 h. RLU: relative light units representing the strength of luciferase luminescence. One representative result of at least 5 independent experiments is shown. Error bars indicate standard deviations of at least 4 technical replicates.

Further aspects to be taken into consideration for assay establishment Firstly, since there are two receptors mediating TNF-α signaling, TNFRSF1A (TNFR1) and TNFRSF1B (TNFR2), I tested which one of these was the major mediator of TNF-α-induced signaling in HEK293T cells. Cells were reverse transfected with relevant siRNAs before being transfected with 4-4-FL and act-RL plasmids on the next day. TNF-α signaling was induced for 16 hours using 20 ng/ml TNF-α. As shown in Figure 2.5A, knockdown of TNFR1 but not of TNFR2 abolished the induction of the NF-κB-dependent *firefly* luciferase. These phenotypes were observed using different individual siRNAs and siRNA pools. Double-knockdown of both TNF-α receptors did not enhance the TNFR1 knockdown phenotype. Thus, TNFR1 but not TNFR2 mediated TNF-α signaling in HEK293T cells. Hence, I used siRNA targeting TNFR1 as a positive control in future assays. Positive and negative siRNA controls are used in RNAi experiments to be able to categorize phenotypes observed after siRNA-mediated knockdown of transcripts. In addition to siTNFR1, siRNA against the TNF-α pathway component RelA was selected as a positive control. Both siRNAs strongly reduced TNF-α-induced 4-4-FL expression (Figure 2.5B). siLRP5

and siControl #1 (siCon) were selected as negative controls (Figure 2.5B). LRP5 is a known component of the Wnt signaling pathway, whereas siCon is a scrambled siRNA without a predicted target. siLRP5 did not significantly alter 4-4-FL expression and was thus well suited as a negative control. Even though siCon showed a mild induction of NF-κB transcriptional activity, it was used as a negative control in a kinase pilot screen (see below).

Secondly, starving cells before cytokine treatment is often used to reduce background signaling activity (e.g. [135, 181, 118]). In order to assess the effect of the absence or presence of serum on the reporter system, the culture medium was exchanged 24 h prior to stimulation and replaced by either complete serum (10%) or reduced serum (0.5%) containing medium. As NF-κB transcriptional activity was similar under both conditions (Figure 2.5C), all luciferase assays were performed in 10% serum containing medium.

Finally, it was technically not feasible to stimulate cells for 16 hours with TNF-α and successively process all plates of a genome-wide screen on one day. Therefore, I had to find a means to uncouple the endpoint of stimulation and the readout. To this end, I tested whether lysed cells could be frozen without loss of the luciferase signal after thawing. Cell lysates were frozen at -80°C and thawed on the next day to perform the luciferase readout. As shown in Figure 2.5D, freezing and thawing did not influence luciferase luminescence, rendering the assay setup feasible for genome-scale experiments.

Validation of the assay: small-scale pilot screen

Before performing a genome-wide RNAi screen I conducted a small-scale pilot screen to assess the quality of the established assay. The pilot screen consisted in three 384-well plates containing 779 known and predicted kinases and 80 cell cycle regulators (Dharmacon Human Protein Kinase Set). The screen was performed in duplicate under the same conditions as a genome-wide screen, including freezing plates after addition of the lysis buffer at -80°C and thawing them on the next day for the luciferase readout. Data was analyzed using the Bioconductor/R package "cellHTS" [29]. First, data consisting in luciferase luminescence reads were log2 transformed and shorth normalized (for details see Material and Methods). After dividing *firefly* by *Renilla* luciferase values, replicates are averaged. The following critical points, reflecting the assay quality, were assessed after analysis:

(i) Plate effects. Spacial effects can affect luminescence reads. As shown in the overview of all plates of the pilot screen in Figure 2.6A, there were no severe plate position effects affecting luciferase counts.

(ii) Reproducibility of replicates. Results of the pilot screen were highly reproducible with an average Spearman rank correlation of replicates of 0.9 (best replicates 0.93, worst

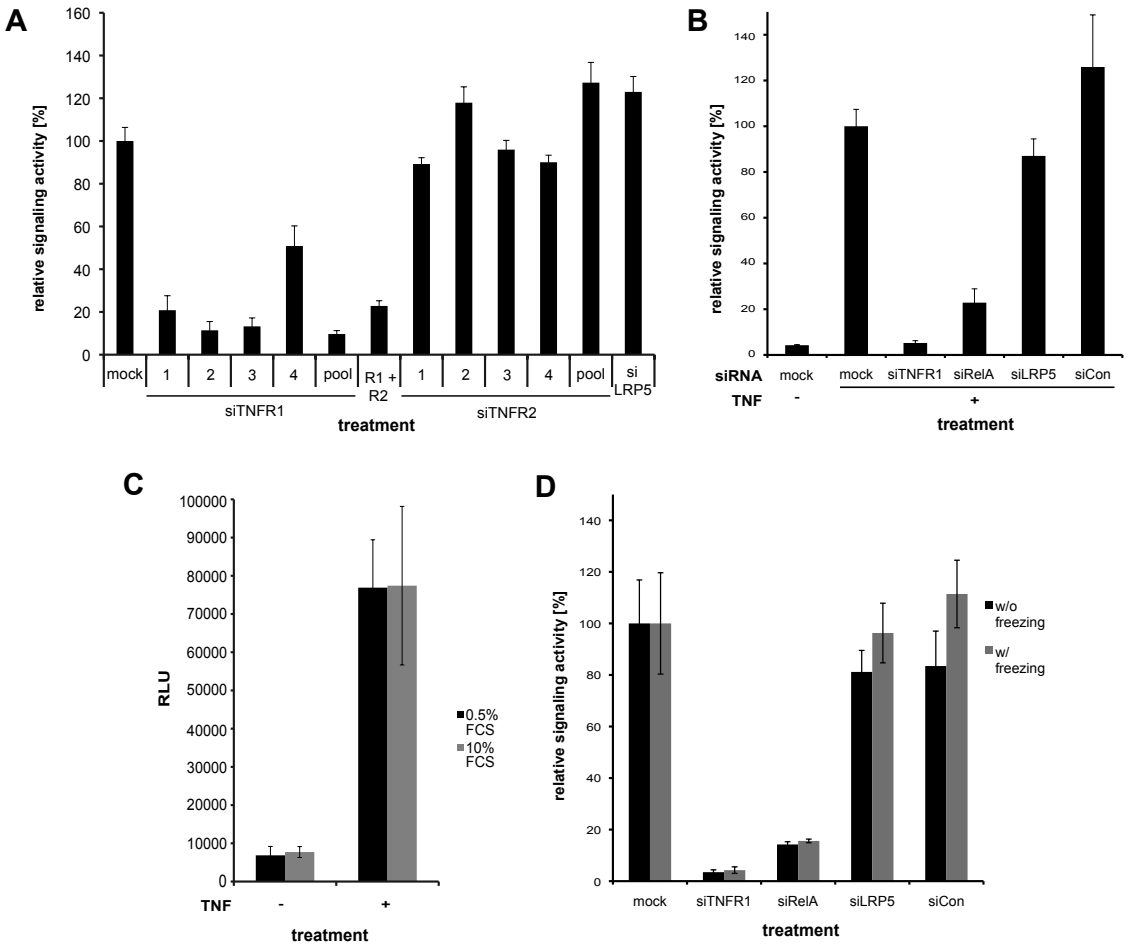

Figure 2.5: Optimizing the NF-κB luciferase assay. A: TNF-α signaling in HEK293T cells was mediated by TNFRSF1A (TNFR1). Knockdown of TNFRSF1B (TNFR2) did not decrease relative signaling pathway activity (compared to mock control). Cells were transfected with four individual siRNAs (1-4) or with pools of four siRNAs (pool, siLRP5). R1+R2: double-knockdown of both receptors (siRNA pools), siLRP5: negative control; siRNA concentration used: 50 nM. One representative result of two independent experiments is shown. B: Phenotypes of the siRNA controls that were used in the RNAi screens. siTNFR1 and siRelA strongly reduced NF-κB reporter activity and served as positive controls. siLRP5 and siCon did not target a known component of the TNF-α pathway and were used as negative controls. Pools of four siRNAs were used. One representative result of at least 3 independent experiments is shown. C: Serum in the culture medium does not affect *firefly* luciferase expression. Cells in either complete serum (10%) or reduced serum (0.5%) containing medium express comparable amounts of *firefly* luciferase. RLU (relative light units) representing strength of *firefly* luciferase luminescence are shown. One representative result of two independent experiments is shown. D: Freezing cell lysates at -80°C and thawing does not affect luciferase luminescence. One representative result of two independent experiments is shown. B+D: Relative signaling pathway activity compared to mock control is shown. mock: medium transfected cells. siRNA concentration used: 50 nM. All error bars represent standard deviations of at least 4 technical replicates.

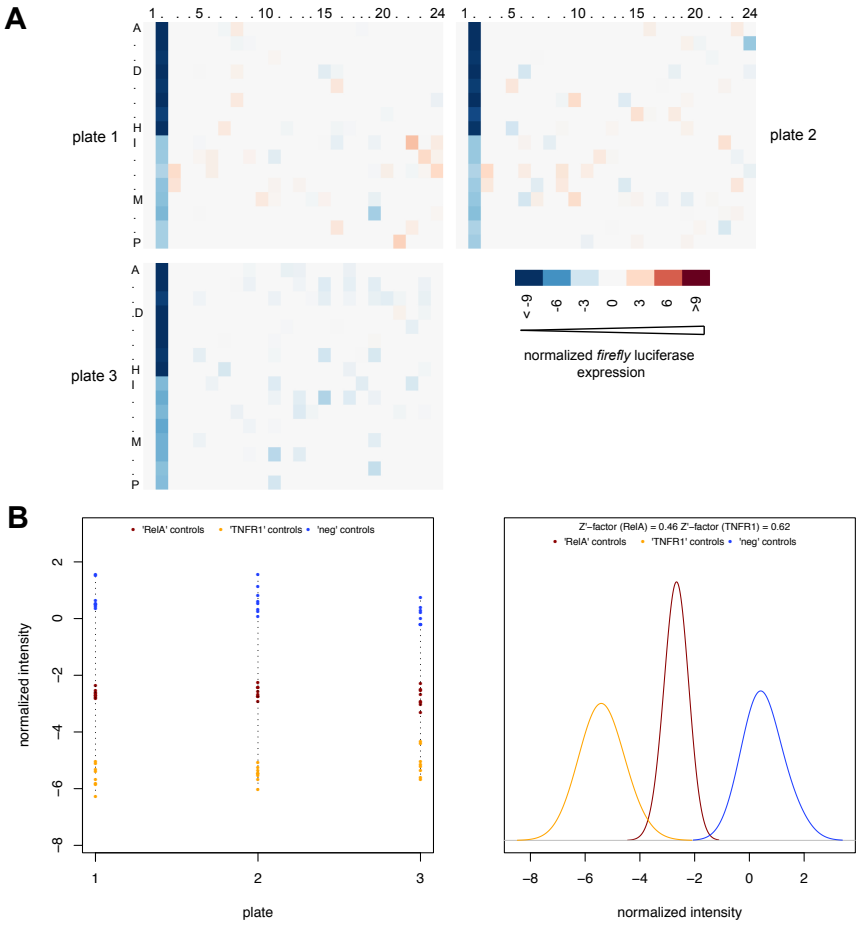

Figure 2.6: Performance of the established luciferase assay in a small scale pilot screen. A: Overview of all plates of the pilot screen. Normalized *firefly* luciferase signals are visualized in heat maps to uncover plate position effects. Blue depicts reduction, red color induction of signaling activity. Wells 2A-H: siTNFR1 (strong positive control), 2I-P: siRelA (intermediate phenotype), 3I-L: siCon, 3M-P: siLRP5 (negative controls). B: Evaluation of positive and negative controls used in the screen. The plot shows the range of log2 transformed values of positive (strong: siTNFR1, weaker phenotype: siRelA) and negative (siLRP5) controls; distributions of negative and positive controls seperated clearly (also reflected in the high Z'-factor of 0.62).

replicates 0.87).

(iii) Performance of the controls. Two different positive controls were used: RelA (NF-κB), whose knockdown resulted in an intermediate phenotype, and TNFR1, whose knockdown decreased *firefly* luciferase expression after TNF-α stimulation to levels comparable to the unstimulated state. siTNFR1 treatment was termed "positive control" in further analysis. Likewise, two different negative controls were used. siCon could not serve as a negative control, since it strongly increased 4-4-FL reporter expression (data not shown). siCon was therefore excluded from further luciferase assays. siLRP5 was termed "negative con-

trol" in further analysis. Positive and negative controls showed clearly distinct phenotypes (Figure 2.6B). The Z'-factor which is a statistical way to express how well the distribution of values for positive and negative controls seperate was calculated to be 0.62. This means that the assay had a very good quality (for details see Material and Methods).

By these means of quality assessment, the established assay was shown to perform well in small-scale pilot screen and could thus be used in genome-wide screens for monitoring TNF-α signaling activity without further modification. Besides, the pilot screen identified several factors implicated in NF-κB signaling such as the MAPKs (mitogen-activated protein kinases) MAP2K3 and MAP2K2 as well as RIPK1 (receptor-interacting protein kinase) as positive regulators.

2.1.2 Genome-wide RNAi screening

I performed two genome-wide RNAi screens to both use their individual data sets to identify novel regulators of TNF-α signaling as well as to compare the results of the two screens to each other. For the first genome-wide RNAi screen I used siRNA library A (as indicated in Materials and Methods). The library targeted almost 22 000 genes and consisted of 68 384-well plates. For the second screen I used the genome-wide siRNA library B (as indicated in Materials and Methods), targeting about 21 000 genes. This library consisted of 56 384-well plates. Both screen were done in duplicate and were analyzed using the Bioconductor/R package cellHTS. The first step of analysis consisted in a logarithmic transformation of the data, followed by normalization. Then *firefly* luciferase counts were divided by *Renilla* luciferase values and replicates were averaged (for details see Materials and Methods). In a second step, the quality of the screens was assessed.

Genome-wide screen using library A

The quality of screen A was assessed by means of plate position effects, reproducibility of replicates and separation of the controls.

(i) Plate effects (Figure 2.7A). The "plate view" representation, an overview of all screening plates, indicated only minor edge effects for most plates, consisting in decreased *firefly* luciferase expression in the first row of the plates. (These rows were excluded from further analysis.) However analysis of the raw data, exemplified in Figure 2.7B, revealed severe plate position effects on many plates of the first batch that was processed. These effects consisted in lower luciferase values in the center of the plate than compared to the edges. These "thawing effects" illustrate that thawing plates for 20 minutes at room temperature was not long enough since the center of the plates was still cold. Less luminescence was detected in the cold center positions probably because catalytic reactions such

as luciferase substrate conversion are temperature-dependent. Plates were thawed longer (30 minutes at 37°C) as soon as this effect was discovered. Plates affected were excluded from analysis.

(ii) Reproducibility of replicates. Results of the screen A showed a lower avarage reproducibility than the pilot screen with an average Spearman rank correlation of replicates of 0.68 (best plates 0.92, worst plates 0.2). However, screening data was reproducible between most replicates, as depicted in Figure 2.8A.

(iii) Performance of the controls (Figure 2.8B and C). As for the pilot screen, siRNAs against TNFR1, giving a strong reduction in TNF-α-dependent 4-4-FL reporter activity, and against RelA, having an intermediate phenotype, were used as positive controls. siLRP5 was used as negative control. The Z'-factor calculated for screen A was 0.5. This Z'-factor indicates that the assay was of good quality [19].

Screen A identified 230 genes whose knockdown strongly reduced TNF-α-induced NF-κB activation (according to criteria specified in 2.1.3).

Genome-wide screen using library B

Likewise, the quality of screen B was assessed.

(i) Plate effects. Figure 2.9B gives an overview of the raw data of all screening plates. There were no thawing effects detectable since plates were thawed 30 minutes at 37°C. However, there were strong edge effects that were also apparent in the overview of all screening plates after normalization (Figure 2.9A): on most plates, either the first or the last (two) row(s) showed an increased luciferase activity. These rows were excluded from further analysis.

(ii) Reproducibility of replicates. The Spearman rank correlation of replicates averaged 0.6 (best plates 0.8, worst plates 0.31) demonstrating a similar reproducibility of screening results as screen A. The reproducibility of replicates is also visualized in Figure 2.10A.

(iii) Performance of the controls. Even though the same controls were used, the Z'-factor was with maximal 0.38 lower than the one in screen A (Figure 2.10B and C). This indicated that the quality of the assay (in terms of separation of the controls) was acceptable, but not good.

Screen B, being of similar quality as screen A, identified 219 genes whose knockdown strongly reduced TNF-α-induced NF-κB activation (according to criteria specified in 2.1.3).

2.1.3 Hit definition and screen comparison

After screening, I was interested in defining so-called hits, namely genes whose knockdown strongly influenced NF-κB reporter activity. To this end, I used a statistical means to

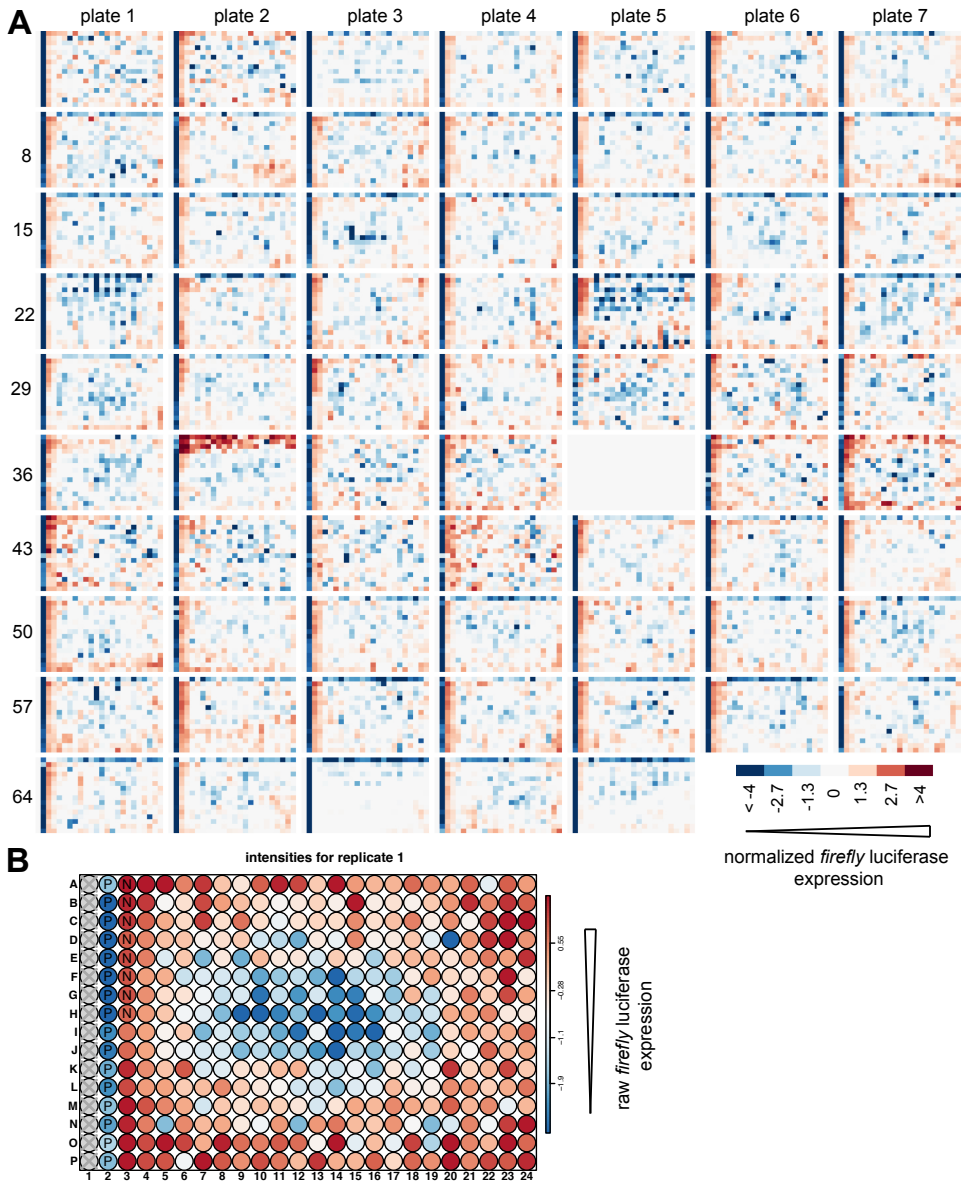

Figure 2.7: Overview of all plates of screen A. A: Color-coded normalized luciferase signal intensities of all plates in screen A (blue equals reduction of the intensity compared to the mean, red means increase of the intensity). This visualization can display plate effects - differences in measured luciferase values resulting from different cell growing conditions according to the position of the well on the plate (edges versus middle). Many plates show mild edge effects consisting in decreased *firefly* luciferase expression in the first row of the plate. The "plate view" also visualizes pipetting errors as depicted in the alternating pattern of luciferase expression in column 2 of plate 33. Besides, an accumulation of wells with low luciferase expression on plate 26 is striking: this plate contained siRNAs targeting genes encoding ribosomal proteins whose silencing strongly decreased viability. Plate 40 is not depicted since both replicates were excluded because of "freezing effects" (see B). B: Unnormalized *firefly* luciferase intensity of one individual plate of the screen. This plate is affected by "freezing effects" (see text), illustrated by lower luciferase values in the center of the plate than compared to the edges. P = positive controls (A-H: siTNFR1, I-P: siRelA), N = negative controls (siLRP5).

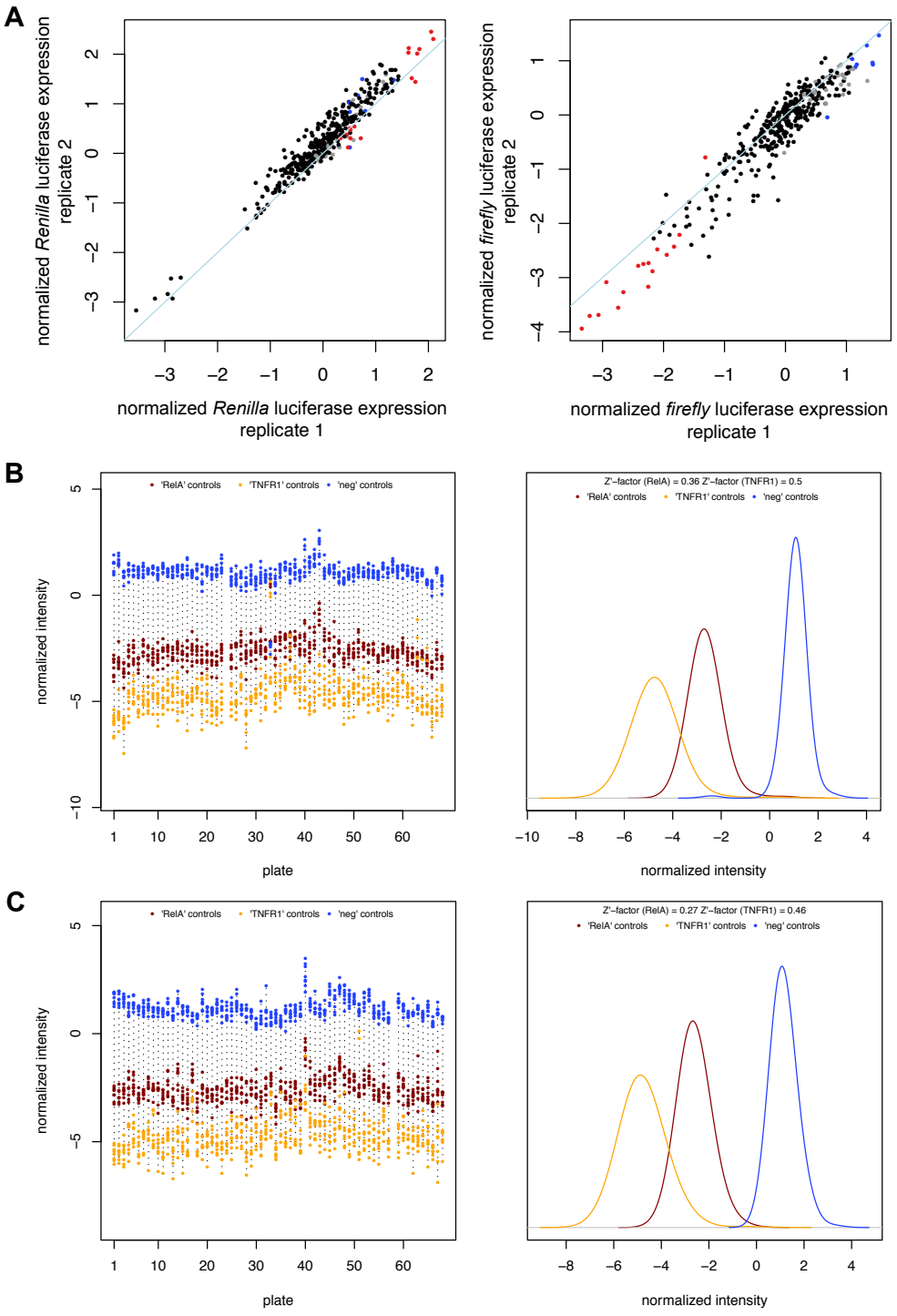

Figure 2.8: Reproducibility of screening results and separation of controls in screen A. A: Scatterplot plotting measurements of the two replicates against each other for channel 1 (*Renilla* luciferase) and channel 2 (*firefly* luciferase). Results of screen A are reproducible, indicated by the distribution of plotted measurements along the diagonal. Red dots depict measurements for positive controls, blue dots for negative controls. B+C: Distribution of normalized luciferase intensities of controls in replicate one and two, respectively. The Z'-factor is a statistical means for expressing the separation of the distribution of luciferase expression values measured for positive (siTNFR1, yellow; siRelA, red) or negative controls (siLRP5, blue). Z'-factors from 0-0.5 depict acceptable, from 0.5-1 very good assays [19].

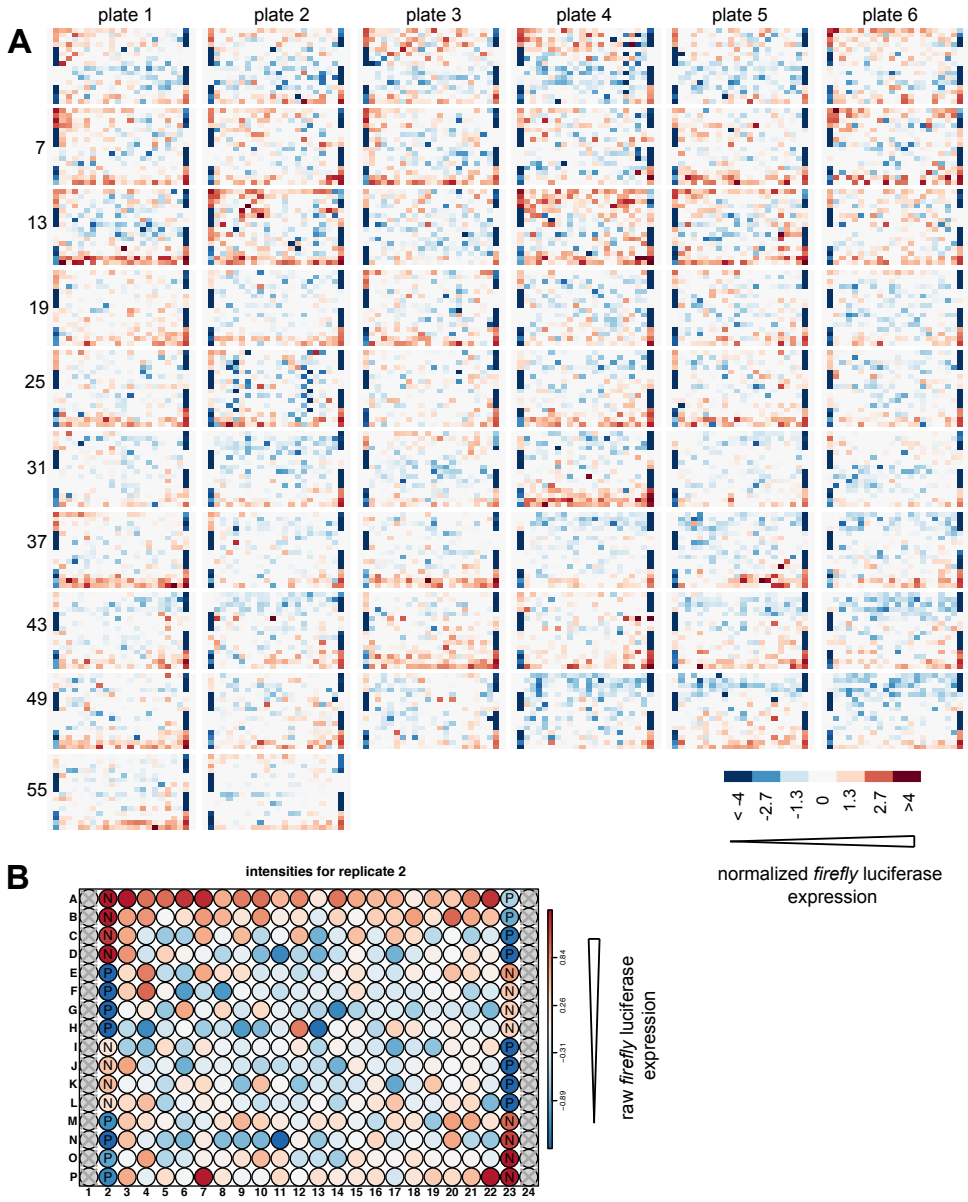

Figure 2.9: Overview of all plates of screen B. A: Color-coded normalized luciferase signal intensities of all plates in screen B (blue equals reduction of the intensity compared to the mean, red means increase of the intensity). This visualization can display plate effects - differences in measured luciferase values resulting from different culture conditions according to the position of the well on the plate (edges versus middle). On most plates of screen B, either the first or the last (two) row(s) showed an increased luciferase activity. B: Unnormalized *firefly* luciferase intensity of one individual plate of the screen. In contrast to screen A, no "freezing effects" were detectable on plates of screen B. P = positive controls (2E-H, 23I-L: siTNFR1; 2M-P, 23A-D: siRelA), N = negative controls (2A-D, 23M-P: siCon; 2I-L, 23E-H: siLRP5).

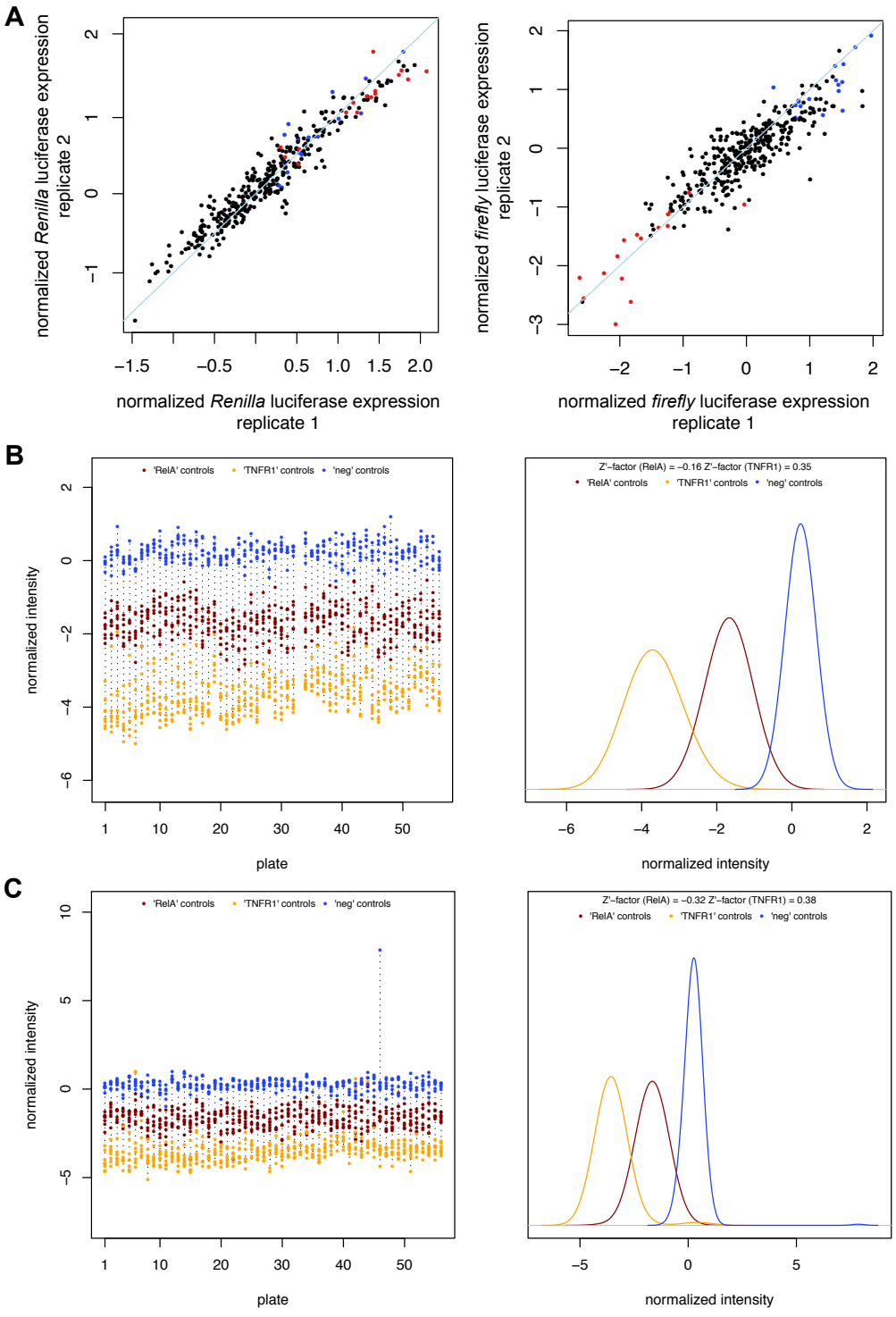

Figure 2.10: Reproducibility of screening results and separation of controls in screen B. A: Scatterplot plotting measurements of the two replicates against each other for channel 1 (*Renilla* luciferase) and channel 2 (*firefly* luciferase). Results of screen B are reproducible, indicated by the distribution of plotted measurements along the diagonal. Red dots depict measurements for positive controls, blue dots for negative controls. B+C: Distribution of normalized luciferase intensities of controls in replicate one and two, respectively. The Z'-factor is a statistical means for expressing the separation of the distribution of luciferase expression values measured for positive (siTNFR1, yellow; siRelA, red) or negative controls (siLRP5, blue). Z'-factors from 0-0.5 depict acceptable, from 0.5-1 very good assays [19].

classify the strength and robustness of a phenotype, the z-score. The z-score expresses how many standard deviation an observation is above or below the mean of all measurements (definition see Materials and Methods). It is used by the software cellHTS to rank all genes covered by the library in its final output. In the analysis of the TNF-α screens, a negative z-score represented a reduction of TNF-α signaling activity, a positive z-score an induction.

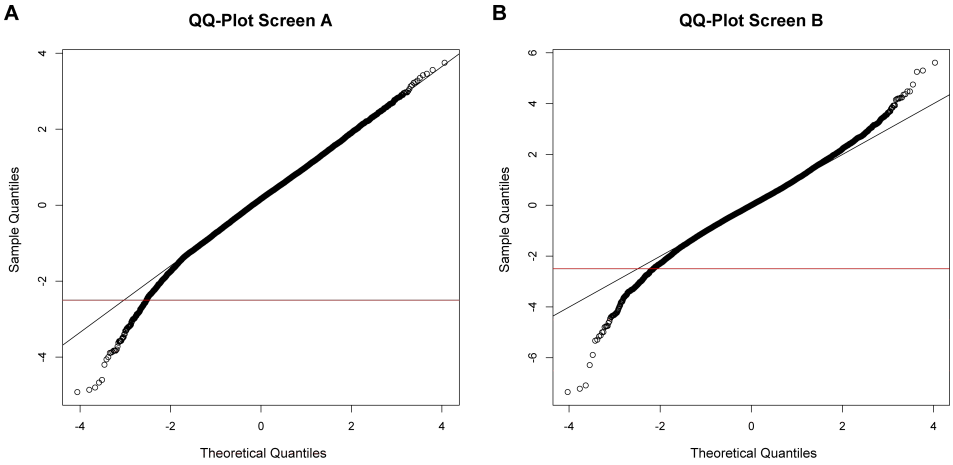

Figure 2.11: Quantile-quantile plots for screening results. Normally distributed quantiles were plotted against actual pathway screening result quantiles. A fit to a normal distribution is represented by the black line. siRNAs in the tail at the negative extreme represent RNAi experiments with significant phenotype. The red line depicts where the z-score cut-off for further analysis was set (z-score $\leq$ -2.5). A: Screen A, B: Screen B.

In a first step, siRNAs were excluded from the hit list of screen A whose phenotypes were most likely not mediated by specific effects on TNF-α signaling but by cytotoxic effects. In order to identify such cytotoxic siRNAs a viability screen using library A had previously been performed in HEK293T cells (Dierk Ingelfinger, unpublished data). These cytotoxic siRNAs of library A were excluded from the hit list of the TNF-α screen A. For library B, similar data were not available. In quantile-quantile (QQ)-plots, normally distributed quantiles are plotted against actual pathway screening result quantiles. A cut-off was determined where z-scores deviated from a normal distribution. For both screen A and B the cut-off was set to a z-score of $\leq$ -2.5, represented by the red lines in Figure 2.11. Two additional filters were applied to further decrease the number of hits, selecting only candidates fulfilling stringent cut-off criteria. In a first filtering step (FL filter), only hits reducing *firefly* luciferase expression at least by 50% (as compared to the mean of all measurements of the experiment) were selected. In a second filtering step (RL filter), siRNAs causing viability defects were excluded by selecting only hits that showed a *Renilla* luciferase expression level of at least 70% as compared to the mean of all measurements of the experiment. Applying these criteria, tables with hits were generated (supplementary

A.1 and A.2). 74 out of 230 initial hits (defined by z-score cut-off) of screen A and 49 out of 219 intial hits of screen B were selected. In addition, candidates were determined that were hits in both screens. For this combined data set, the z-score cut-off was set to $\leq$ -1.25. The loss of stringency (and thereby the increased likeliness of false positives) by this lower threshold is expected to be compensated by a hit selection based on the overlap of two hit lists instead of one. The combined data set did non include data points that were excluded in previous analysis steps in either of the two screens. 177 hits were identified in the overlap of the two screens.

To analyze the overall overlap of the two TNF-α screens, the z-scores of all genes of both screens were plotted against each other. Figure 2.12A shows that most siRNAs in both screens did not show a phenotype (as expected): their z-scores cluster around 0. Strong hits identified in both screens with a negative z-score would appear in the lower left quadrant of the plot. However, there is no accumulation of data points in this quadrant. Only seven genes passed the cut-off that was applied in the individual screening analysis (z-score of $\leq$ -2.5; among them one of the chosen candidates, LILRA2, Figure 2.12B), indicating that screen A and B exhibit only a low overlap.

2.1.4 First candidate selection

From the three different hit lists, candidates with strong phenotypes were selected for further experiments. The most promising candidates were selected by data mining using public online databases, like PubMed, and the Harvester tool [149]. The following criteria were applied in this selection process. Firstly, gene ontology (GO) terms were annotated [81], if available. Candidates were preferred that could be linked to immunity or that were of unknown function. Further, functional domains of the respective proteins were assessed (e.g. using UniProt). Proteins of undefined structure or with domains known to be involved in TNF-α signaling were preferred over those possessing unrelated domains. Additionally, the functions of orthologues in other species were assessed to identify putative evolutionarily conserved proteins. Proteins with potentially conserved function were selected. To summarize, proteins of unknown function or proteins being linked to immune function or NF-κB signaling were particularly interesting. 77 candidates were selected based on this data mining.

2.1.5 Secondary validation of candidate genes

In a process termed "secondary validation" screening phenotypes have to be reconfirmed in order to exclude genes with phenotypes caused by screening artifacts such as plate position

A

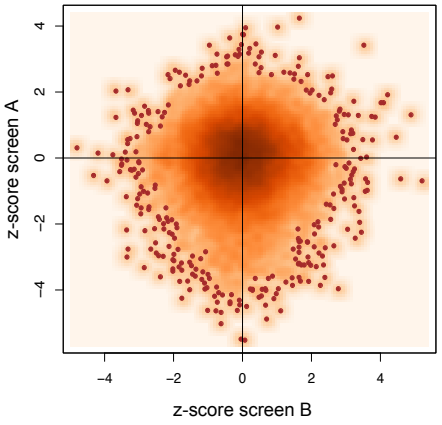

B

Symbol	z-score screen A	z-score screen B	GeneID	RefSeq	description
WDR1	-3	-3,35	9948	NM_005112	WD repeat protein; might be involved in disassembly of actin filaments
EML1	-2,76	-2,66	2009	NM_004434	echinoderm microtubule associated protein like; strong candidate for the Usher syndrome
LILRA2	-2,88	-2,5	11027	NM_006866	leukocyte immunoglobulin-like receptor; integrin
HSMPP8	-2,76	-3,32	54737	NM_017520	M-phase phosphoprotein 8; chromatin binding, cell cycle
ATF7IP	-3,32	-2,85	55729	NM_018179	activating transcription factor 7 interacting protein
ZFPM1	-2,57	-2,52	161882	NM_153813	ZFPM1 zinc finger protein, multitype 1; zinc and DNA binding

Figure 2.12: Comparison of results of screens A and B. A: In this smoothscatter plot the z-scores of each gene in both screens were plotted against each other. The density of measurements (the number of plotted genes) is depicted as a color gradient, with light color depicting low densitiy (little number of genes) and dark color high density (high number of genes) with a distinct z-score. Scattered individual measurements are plotted as dark dots. The two screens showed little overlap in the strongest hits, as indicated by the absent accumulation of points in the left lower quadrant. B: Table listing the seven genes that fulfilled the cut-off criteria applied in the individual screening analysis for both screens.

effects. In secondary validation, the original screening assay was repeated to reproduce screening results. In addition, a different assay - a secondary assay - was employed to confirm the phenotypes using a different readout. Since the dual luciferase assay is based on artificially introduced reporters, a secondary assay was established using an endogenous readout. I used an enzyme-linked immunosorbent assay (ELISA) to detect protein levels of the TNF-α target gene interleukin (IL) 8. Additionally, siRNA-specific but candidate-unspecific artifacts (phenotypes due to effects unrelated to the gene that was supposed to be targeted, such as cytotoxic or off-target effects) were excluded by targeting the same gene with several individual siRNAs. Only if the same phenotype was observed with several siRNAs in both luciferase assay and ELISA, a screening hit was considered to be a confirmed candidate.

Establishing ELISA for IL-8 secretion in HEK293T cells

Since IL-8 is a known target gene of TNF-α [138] and its secretion can easily be measured by ELISA, I assessed whether HEK293T cells secreted IL-8 in a TNF-α- and NF-κB-dependent manner. Cells reverse transfected with siRNAs were stimulated with 20 ng/ml

TNF-α before supernatants were harvested and IL-8 secretion was assessed by ELISA. As illustrated in Figure 2.13, the amount of secreted IL-8 increased with the duration of the TNF-α stimulus. Whereas TNFR1 knockdown abolished IL-8 induction almost completely, there was residual IL-8 secretion upon RelA knockdown. However, IL-8 secretion was strongly dependent on TNF-α signaling. IL-8 secretion measured by ELISA could thus serve as a secondary assay for measuring TNF-α signaling activity.

Supernatants were harvested after 16 hours of stimulation in further assays, as it allowed performing the luciferase assay and the ELISA in parallel and directly comparing the phenotypes in the two different assays.

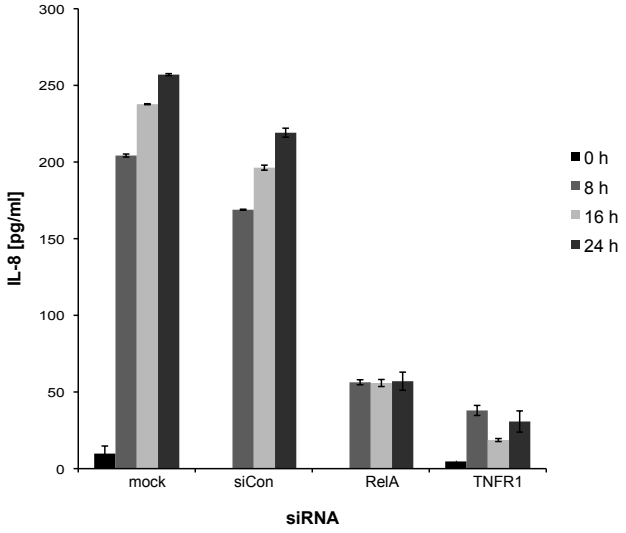

Figure 2.13: HEK293T cells secrete IL-8 upon stimulation with TNF-α. Cells were reverse transfected with negative (medium (mock), siCon) and positive controls (siTNFR1, siRelA). Supernatants were harvested three days after transfection, and at indicated time points prior to that cells were treated with 20 ng/ml TNF-α. IL-8 secretion is shown in pg/ml as assessed by ELISA. siRNA concentration used: 50 nM. One result of two independent experiments is shown. Error bars represent standard deviations of two technical replicates.

Secondary validation in HEK293T and HepG2 cells

In order to validate screening results, phenotypes of the candidates were first confirmed with four individual siRNAs per gene from Dharmacon and a pool of these four siRNAs as well as siRNA pools from Qiagen in HEK293T cells. Silencing effects were assessed both by luciferase assay and by ELISA for IL-8 secretion (supplementary tables A.6 and A.7). After this first round of validation, hits were selected according to the strength and the robustness of their phenotypes. At least two out four individual siRNAs per candidate showed an at

least 20% reduction in TNF-α signaling activity. Subsequently, luciferase assay and ELISA were also established in HepG2 cells (Marie Metzig, MD thesis). These secondary assays were performed in HepG2 cells to test cell type-specific action of candidates (supplementary tables A.8 and A.9). In the end, seven candidates with the most robust phenotypes in both cell lines were chosen for further analysis. The process of secondary validation and candidate selection is summarized in Figure 2.14.

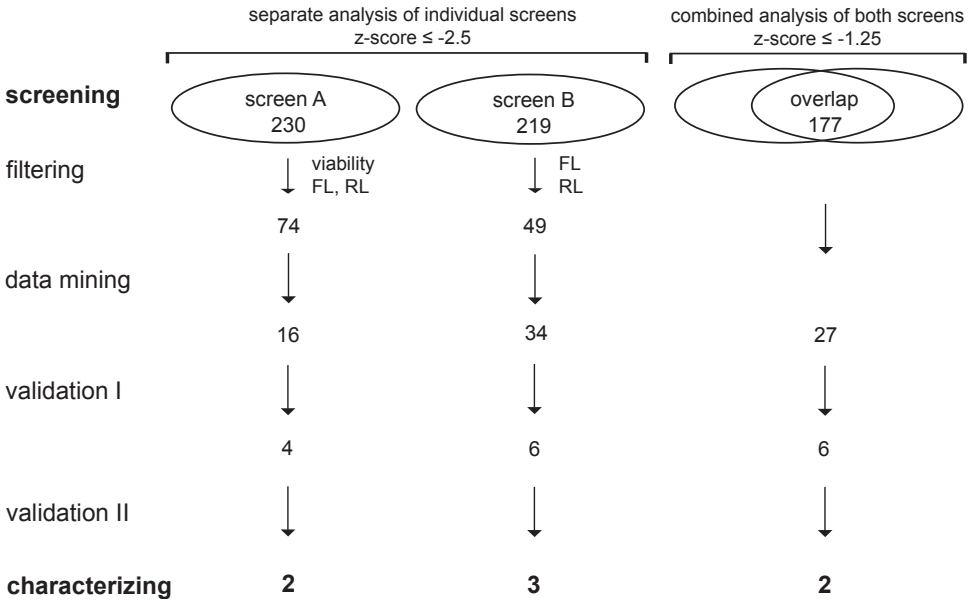

Figure 2.14: Schematic representation of the decision making from the first hit lists to the final candidate list. Genome-wide RNAi screens using two different siRNA libraries yielded three lists of potentially novel regulators of TNF-α signaling. 230 and 219 hits were identified by screens A and B, respectively (based on a z-score cut-off of $\leq$ -2.5), 177 hits were determined by the overlap of the two screens (based on a z-score cut-off of $\leq$ -1.25). By applying stringent filters to the two individual screening hit lists, the number of candidates was minimized to 74 (screen A) and 49 (screen B). These filters consisted in: (i) a viability filter (screen A only), excluding siRNAs (and thus genes) which were shown to be cytotoxic, (ii) FL filter: *firefly* luciferase expression had to average at most 50% of the experiment mean, (iii) RL filter: *Renilla* luciferase expression had to average at least 70% of the experiment mean. Subsequently, 77 candidates were selected by data mining, either showing some relation to immune signaling (e.g. by shared protein domains or interaction partners) or being uncharacterized proteins. The first round of validation consisted in performing the dual-luciferase assay and an IL-8 ELISA in parallel in HEK293T cells, using several individual siRNAs per gene. Thereby, candidates were determined that decreased TNF-α signaling activity in both assays by at least 20 % with at least two different siRNAs. 16 candidates entered the second round of validation in which the same assays and siRNAs were tested in HepG2 cells to exclude cell type-specific phenotypes. Validation resulted in the identification of candidates showing robust phenotypes in two assays with at least two individual siRNAs in two different cell lines.

Phenotypes of the seven selected candidates

Seven candidates were selected in the validation process described above. For more information on these candidates see table 2.1 and the discussion. Figures 2.15 and 2.16 show the phenotypes of siRNAs targeting the candidates with regards to TNF-α signaling in HEK293T and HepG2 cells, respectively. Knockdown of candidates reduced TNF-α signaling activity in luciferase assay and ELISA in both cell lines by at least 20% (except for MEN1 in HepG2 ELISA). In contrast to LILRA2 whose silencing only affected TNF-α signaling activity with statistical significance in the dual luciferase assay in HEK293T cells, the effect of CASP4 silencing exhibited statistical significance under all conditions tested. siGAB3 showed only statistically significant effects in HepG2 cells, whereas the opposite was true for siITGA5. Knockdown of SPP1 and GAB3 decreased TNF-α signaling activity with statistical significance in all assays except for the luciferase assay in HepG2 and HEK293T cells, respectively. Treatment with siMEN1 showed statistically significant effects in the luciferase assay in HepG2 cells as well as the ELISA in HEK293T cells. In addition to effects on TNF-α signaling activity, it was confirmed that knockdown of none of these candidates caused viability defects (Figure 2.17) nor showed pleiotropic phenotypes as assessed by their phenotypes in other genome-wide screens ([106]; Anan Ragab, Dierk Ingelfinger, unpublished observations).

Depletion of candidate mRNAs was ascertained by quantitative (q) real time (RT) PCR (Figure 2.18). Both CASP4 and LILRA2 mRNA levels were strongly reduced to 16 and 15%, respectively, after treatment with specific siRNAs (compared to mRNA levels of siRL treated cells). siITGA5, siGAB3, siUSP2, siSPP1 and siMEN1 reduced levels of corresponding mRNAs by more then 55 %.

In conclusion, I selected 77 hits from the different hit lists generated by genome-wide RNAi screening. Of 77 hits, 7 candidates were determined with the help of two validation rounds. These consisted in performing secondary assays in two different cell lines using several individual siRNAs. Knockdown of the candidates did not affect viability of HEK293T cells. In addition, neither of the candidates was identified by two other genome-wide screens performed in the Boutros laboratory. mRNAs of all candidates were depleted in HEK293T cells upon treatment with corresponding siRNAs.

Table 2.1: Table of seven potential novel regulators of TNF-α signaling. TLR: Toll-like receptor, GRB: growth factor receptor-bound protein, MAPK: mitogen-activated protein kinase, HIV: human immunodeficiency virus.

gene symbol	name	gene function	gene ontology
USP2	ubiquitin specific peptidase 2	deubiquinating enzyme	ubiquitin thiolesterase activity, ubiquitin-dependent protein catabolic process
SPP1	secreted phosphoprotein 1	extracellular matrix protein that can also act intracellularly; involved in may different processes such as immunity and metastasis promotion	cytokine activity, protein binding, cell adhesion, ossification, TLR signaling
GAB3	GRB2-associated binding protein 3	scaffold protein involved in macrophage differentiation	protein binding
MEN1	multiple endocrine neoplasia I	nuclear protein, interacts with NFkB	DNA binding, MAPKKK cascade, histone methylation, negative regulation of cell proliferation, osteoblast development, regulation of transcription
CASP4	caspase 4, apoptosis-related cysteine peptidase	inflammatory caspase	cysteine-type endopeptidase activity, protein binding, induction/regulation of apoptosis
LILRA2	leukocyte immunoglobulin-like receptor, subfamily A, member 2	integrin found on cells of the immune system	antigen binding, receptor activity, immune response, signal transduction
ITGA5	integrin, alpha 5 (fibronectin receptor, alpha polypeptide)	binds SPP1, interacts with HIV proteins	integrin binding, receptor activity, calcium ion binding, cell/leukocyte adhesion, integrin-mediated signaling pathway

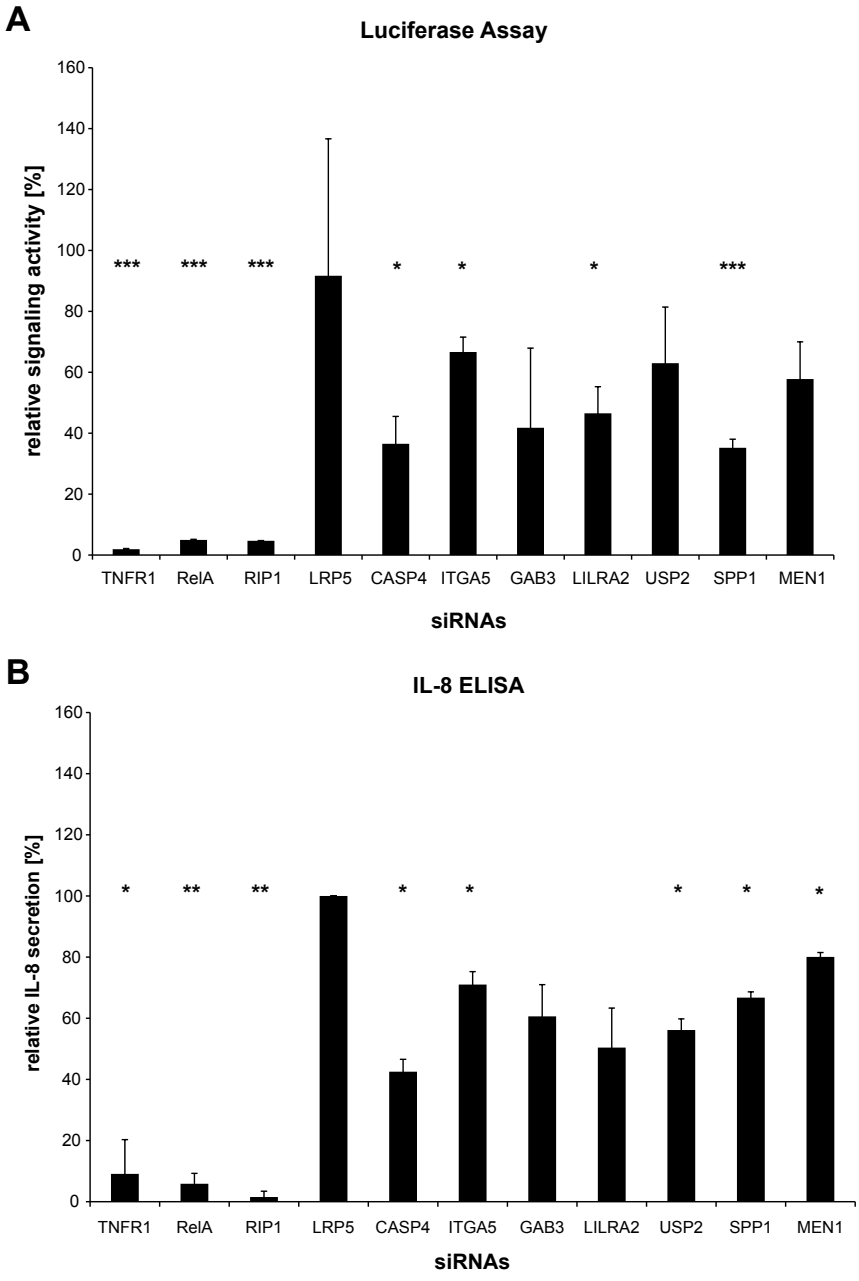

Figure 2.15: Phenoptypes of the seven selected candidates in HEK293T cells using Dharmacon siRNA pools. A: luciferase assay, B: ELISA. Relative signaling activity (i.e. FL/RL compared to mock (medium) transfected cells) and relative IL-8 secretion (percent IL-8 compared to siLRP5 transfected cells) is shown, respectively. siRNA concentration used: 50 nM. Mean values of two independent experiments are shown. Error bars depict standard deviations of the two biological replicates. p-values were calculated using Student's T-test. *: p-value < 0.05, **: p-value < 0.01, ***: p-value < 0.001.

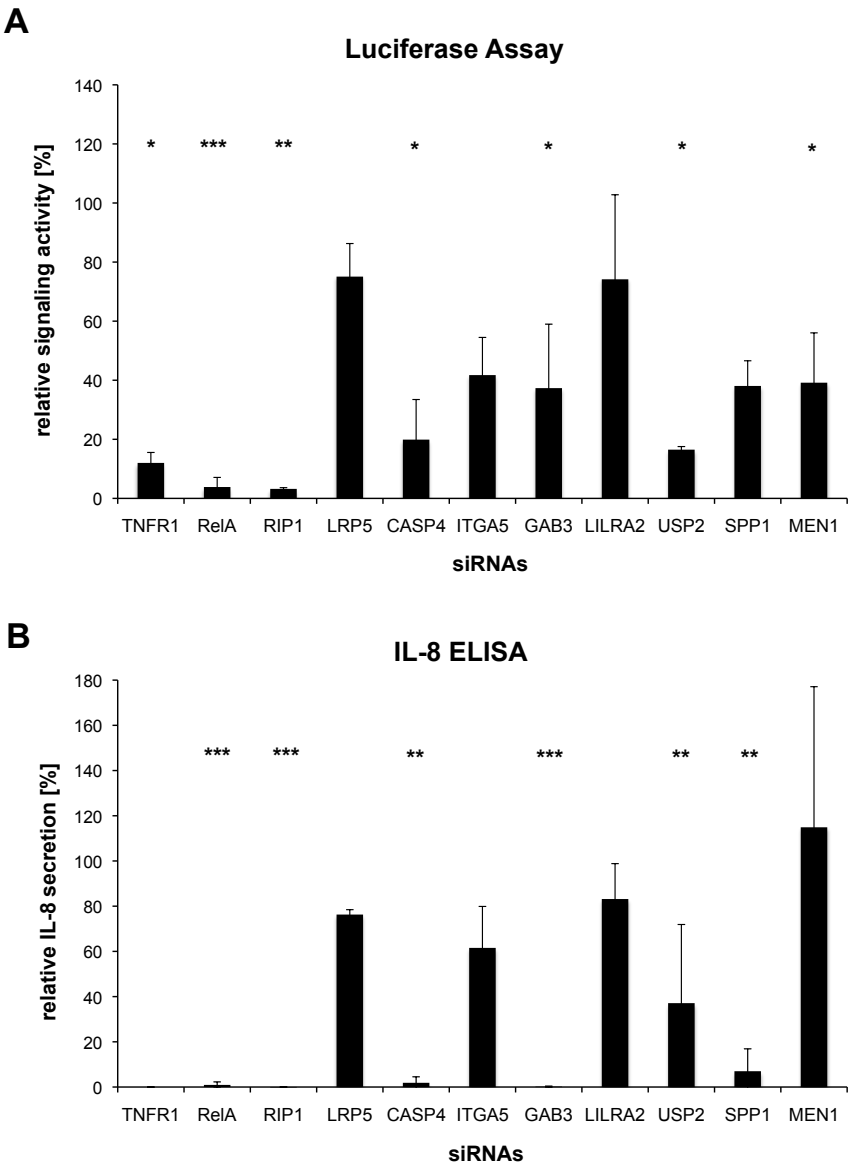

Figure 2.16: Phenoptypes of the seven selected candidates in HepG2 cells using Dharmacon siRNA pools. A: luciferase assay, B: ELISA. Relative signaling activity (i.e. FL/RL compared to mock (medium) transfected cells) and relative IL-8 secretion (percent IL-8 compared to mock transfected cells) is shown, respectively. siRNA concentration used: 50 nM. Mean values of two independent experiments are shown. Error bars depict standard deviations of the two biological replicates. p-values were calculated using Student's T-test. *: p-value < 0.05, **: p-value < 0.01, ***: p-value < 0.001.

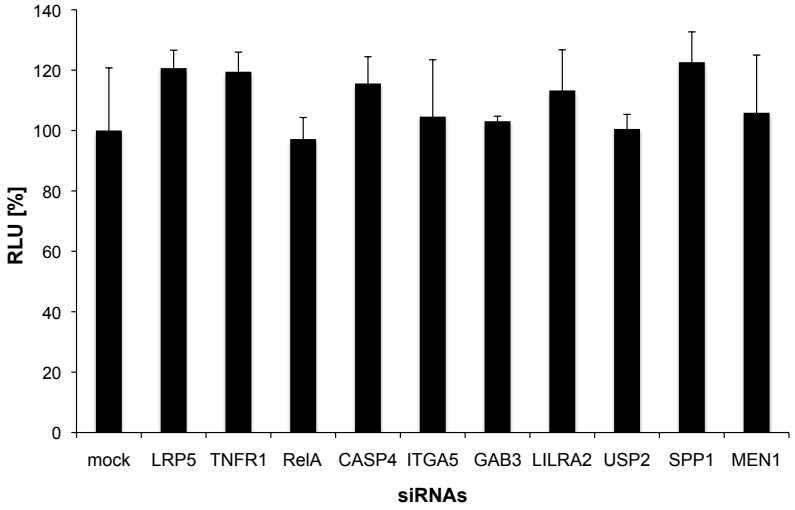

Figure 2.17: Knockdown of the seven selected candidates does not affect cell viability. Measured relative light units (RLU) were normalized to those of mock (medium) transfected cells. RLU describe the strength of ATP-dependent luciferase luminescence. siRNA concentration used: 50 nM. One representative result of two independent experiments is shown. Error bars represent standard deviations of at least 4 technical replicates.

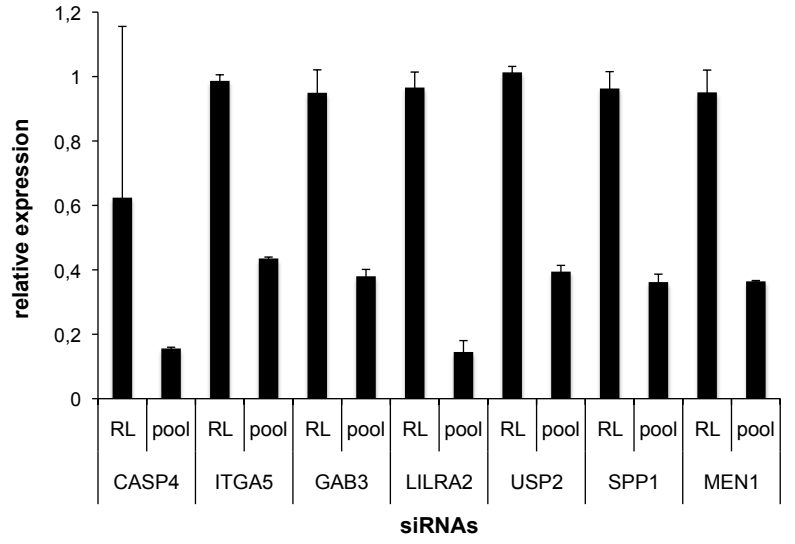

Figure 2.18: Candidate mRNA levels after treatment of HEK293T cells with siRNAs. Relative expression compared to the negative control (RL) is shown. RL: siRNA against *Renilla* luciferase, pool: siRNA pool specific for respective candidate. siRNA concentration used: 50 nM. One representative result of at least 3 independent experiments is shown. Error bars represent standard deviations of two technical replicates.

2.2 SPP1, CASP4, GAB3

I selected three of the seven high-confidence candidates, SPP1, GAB3 and CASP4, for further characterization.

CASP4 CASP4 is a caspase with a caspase recruitment domain (CARD) protein belonging to the family of inflammatory caspases. Overlapping with the CARD domain, CASP4 also possesses a death domain (DD). Both DD and CARD proteins have been described to be components of the TNFR1 complex [24]. There are only few publications on CASP4, one of them showing an involvement in TLR4 signaling [140].

GAB3 GAB3 belongs to a family of adaptor proteins which bind growth factor receptor-bound (GRB) protein 2, a protein that has been shown to interact with TNFR1 [100]. Almost no functional data were available on GAB3.

SPP1 SPP1 is involved in many processes, most of which are dependent on secreted, extracellular SPP1 (e.g. its role in promoting metastasis [97]). However, SPP1 has also been found to act intracellularly [275]. A role in Toll-like receptor (TLR) signaling, which shares homologies with TNF-α signaling, has been described [216].

2.2.1 Knockdown of SPP1, GAB3 and CASP4 interferes with NF-κB transcriptional activity

Knockdown of SPP1, GAB3 and CASP4 interferes with activation of NF-κB as assessed by luciferase assay and ELISA

SPP1, GAB3 and CASP4 were selected for further characterization since their knockdown decreased robustly TNF-α signaling activity as assessed by dual luciferase assay and ELISA. Figure 2.19A summarizes silencing phenotypes of the three candidates in these two assays. In addition to the effect of the siRNA pools, phenotypes of treatment with individual siRNAs are given. In order to compare the strength of the phenotype with knockdown efficiency, mRNA levels of SPP1, GAB3 and CASP4 were determined for each siRNA treatment (Figure 2.19B). A correlation between knockdown efficiency and the phenotypic consequence of siRNA treatment is a strong indicator for the reliability of the observed phenotype.

For CASP4, knockdown efficiencies of siRNAs 3, 4 and the pool corresponded to the strength of the phenotype in both luciferase assay and ELISA. Measuring basal level of CASP4 mRNA in HEK293T cells always yielded variable results (high standard deviations) due to its low expression. For GAB3, knockdown efficiencies of all siRNAs corresponded

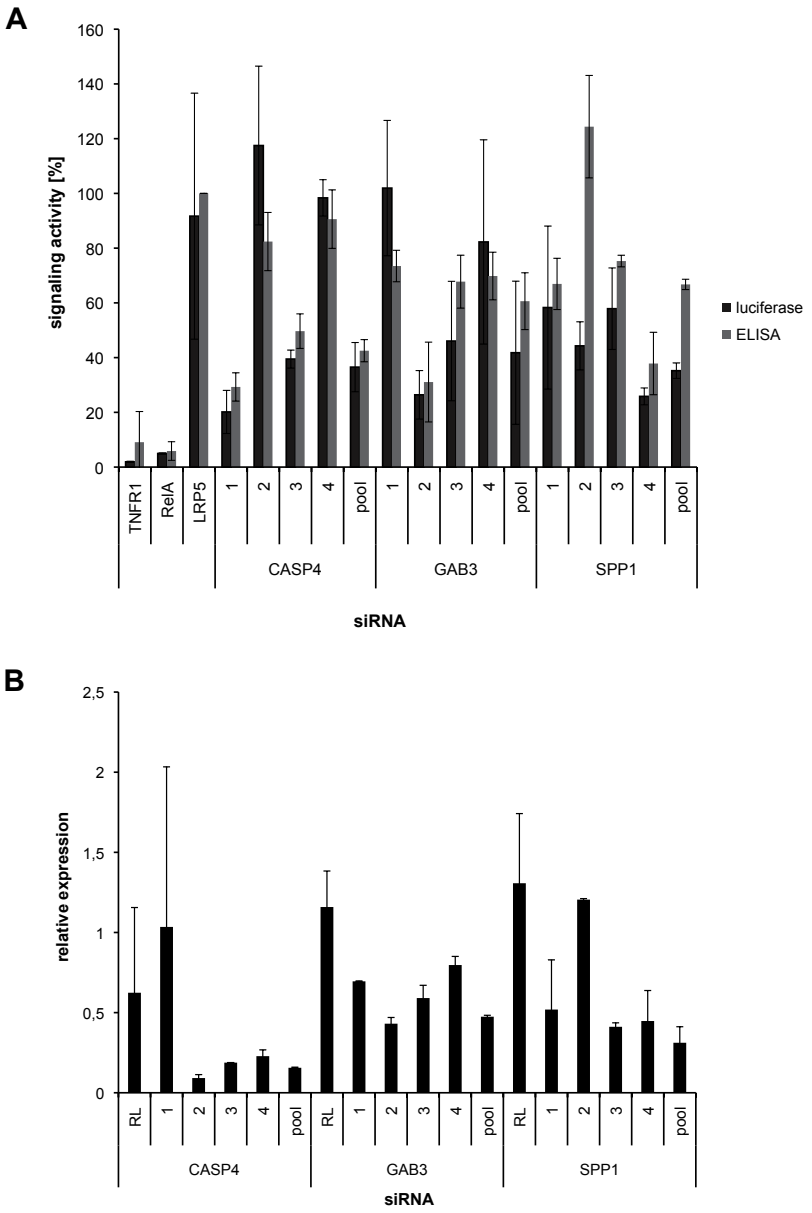

Figure 2.19: Phenotypes of SPP1, GAB3 and CASP4 knockdown in HEK293T cells using individual siRNAs and siRNA pools. HEK293T cells were reverse transfected with siRNAs and the dual luciferase assay and IL-8 ELISA (A) as well as a qRT-PCR assay measuring candidate mRNA levels (B) were performed. A: siRNA-mediated decrease in TNF-α-induced NF-κB activity in the luciferase assay (black bars) and IL-8 ELISA (grey bars). Depicted is relative signaling activity, i.e. FL/RL compared to mock (medium) transfected cells (luciferase assay) or relative IL-8 secretion compared to siLRP5 transfected cells (ELISA). TNFR1, RelA: siRNA pools against TNFRSF1A and RelA, respectively (positive controls), siLRP5: siRNA pool targeting LRP5 (negative control). Mean values of two independent experiments are shown. Error bars depict standard deviations of the two biological replicates. B: siRNA-mediated mRNA depletion. Relative mRNA levels compared to cells transfected with the negative control [*Renilla* luciferase (RL)] are shown. Error bars depict standard deviations of the two technical replicates. Data representative of 3 independent experiments is shown. A + B: 1-4: the four different individual siRNAs targeting the same gene, pool: pool of the four individual siRNAs. siRNA concentration used: 50 nM.

to the strength of the phenotype in validation assays. For SPP1, all siRNAs except for siRNA 2 exhibited similar knockdown efficiencies. The failure of siRNA 2 to deplete SPP1 mRNA is reflected by the corresponding phenotype in the ELISA. Knockdown of all three candidates by one individual siRNA and the siRNA pool reduced TNF-α signaling activity by more than 40%. Except for GAB3, the knockdown of the candidates decreased TNF-α signaling activity with statistical significance with at least 2 individual siRNAs and the pool in both assays (data not shown). Knockdown effects correlated with siRNA-mediated mRNA depletion. Hence, phenotypes observed after treating cells with siRNAs against the three candidates were most probably due to candidate knockdown (and not due to off-target effects).

Knockdown of SPP1, GAB3 and CASP4 interferes with TNF-α target gene expression

To further confirm the influence of candidate knockdown on endogenous TNF-α signaling events, I established an assay to measure endogenous TNF-α target genes. TNF-α induces a wide variety of target genes such as genes encoding cytokines and chemokines, proteins involved in antigen presentation and cell adhesion, anti-apoptotic proteins and others [247]. I assessed the expression of known TNF-α target genes upon stimulation by qRT-PCR and determined the following target genes to be induced in HEK293T cells: TNF-α [211, 51], CCL20/MIP-3α (CC-motif chemokine ligand 20) [139, 238], NFKBIA/IκB-α (nuclear factor of kappa light polypeptide gene enhancer in B-cells inhibitor, alpha) [95, 230, 56], BIRC3/CIAP2 (baculoviral IAP repeat-containing 3) [248] and IL-8. mRNA levels of TNF-α targets were measured to test whether knockdown of the candidates also affected the transcription of endogenous target genes.

To assess the influence of knockdown of SPP1, GAB3 and CASP4 on TNF-α target gene expression, HEK293T cells were reverse transfected with siRNAs against the candidates as well as siRNAs against *Renilla* luciferase as negative, against TNFR1 and RelA as positive controls. After three days of incubation to allow for protein depletion, cells were treated with 20 ng/ml TNF-α for either 0, 2 or 8 hours before RNA was isolated for qRT-PCR analysis. Target gene mRNA levels were normalized to hypoxanthine phosphoribosyltransferase (HPRT) 1 mRNA levels. As depicted in Figure 2.20, SPP1 knockdown decreased TNF-α-dependent expression of IL-8, BIRC3 and TNF-α significantly, but not expression of CCL20 and NFKBIA. BIRC3 expression was only affected after 2 hours of stimulation, whereas IL-8 and TNF-α expression were influenced at both time points. GAB3 knockdown only affected significantly the expression of IL-8 and BIRC3 after 8 and 2 hours of TNF-α treatment, respectively (Figure 2.21). Figure 2.22 shows the effect of CASP4 knockdown

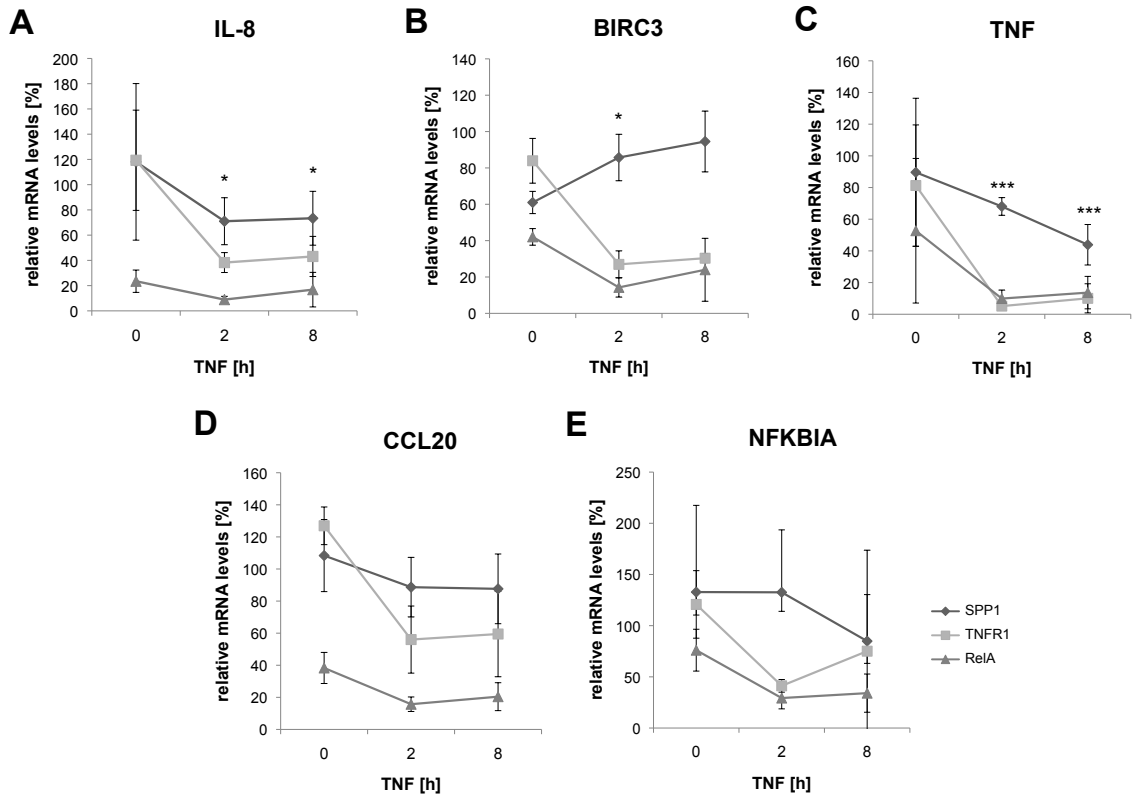

Figure 2.20: Effect of SPP1 knockdown on TNF-α-induced IL-8 (A), BIRC3 (B), TNF-α (C), CCL20 (D) and NFKBIA (E) expression. HEK293T cells were reverse transfected with siRNAs and, three days later, target gene mRNA levels were measured by qRT-PCR after 0, 2 and 8 h of induction using 20 ng/ml TNF-α. Expression levels were normalized to expression in the negative control sample (siRNA against *Renilla* luciferase): for each time point, mRNA expression levels were set to 100% in the control sample and mRNA levels in candidate samples were calculated in relation to the control. TNFR1 and RelA: siRNAs against TNFRSF1A and RelA, respectively (positive controls). siRNA concentration used: 50 nM. Data derived from five independent experiments are shown, error bars indicating the standard deviations of the biological replicates. p-values were calculated using Student's T-test. *: p-value < 0.05, ***: p-value < 0.001.

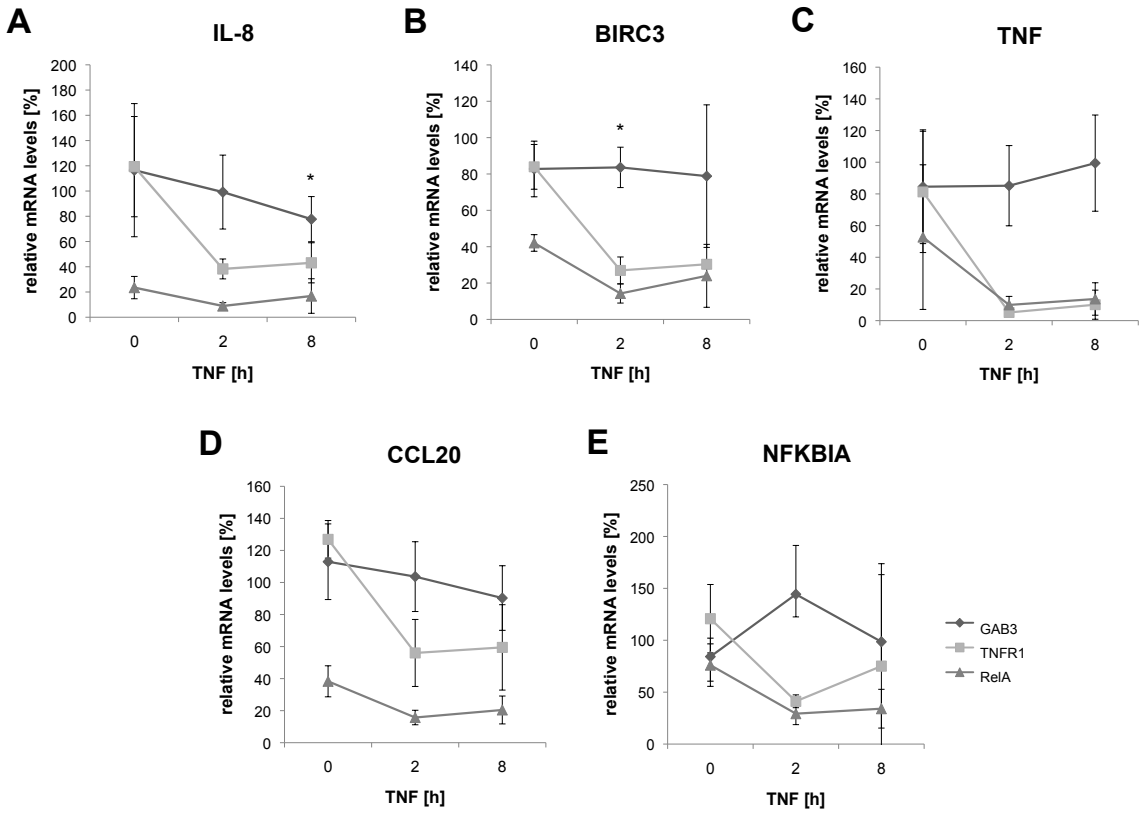

Figure 2.21: Effect of GAB3 knockdown on TNF-α-induced IL-8 (A), BIRC3 (B), TNF-α (C), CCL20 (D) and NFKBIA (E) expression. HEK293T cells were reverse transfected with siRNAs and, three days later, target gene mRNA levels were measured by qRT-PCR after 0, 2 and 8 h of induction using 20 ng/ml TNF-α. Expression levels were normalized to expression in the negative control sample (siRNA against *Renilla* luciferase): for each time point, mRNA expression levels were set to 100% in the control sample and mRNA levels in candidate samples were calculated in relation to the control. TNFR1 and RelA: siRNAs against TNFRSF1A and RelA, respectively (positive controls). siRNA concentration used: 50 nM. Data derived from five independent experiments are shown, error bars indicating the standard deviations of the biological replicates. p-values were calculated using Student's T-test. *: p-value < 0.05.

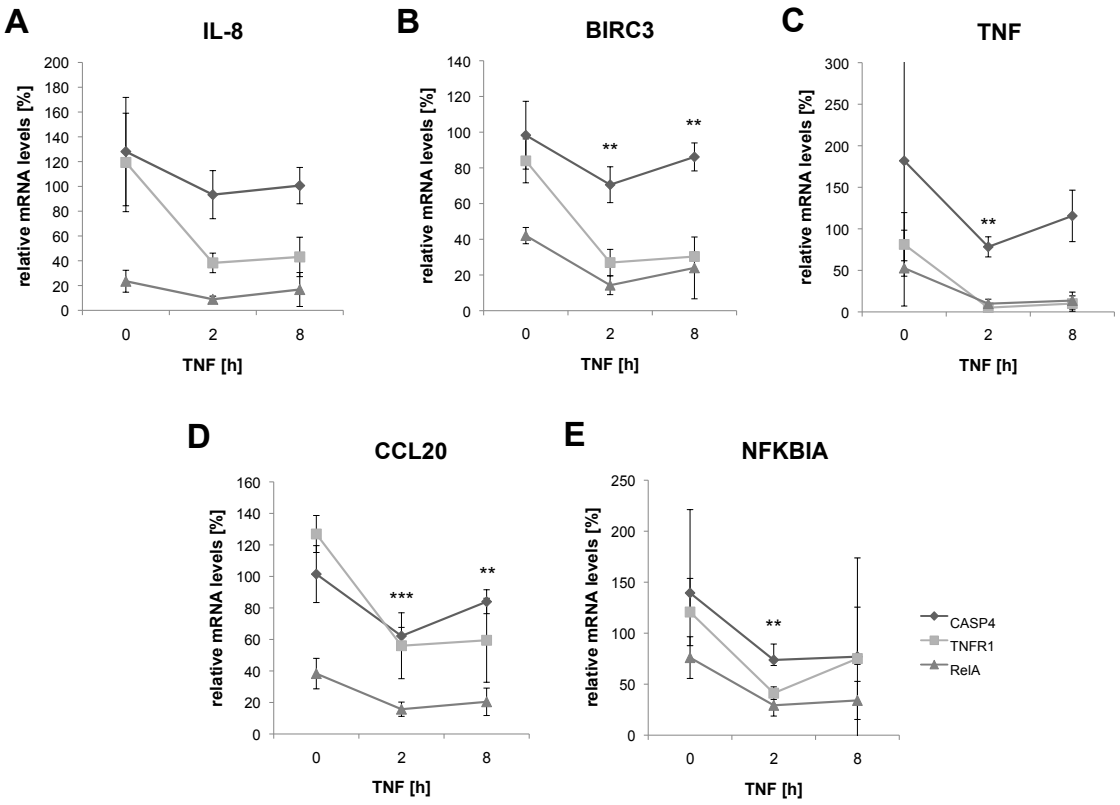

Figure 2.22: Effect of CASP4 knockdown on TNF-α-induced IL-8 (A), BIRC3 (B), TNF-α (C), CCL20 (D) and NFKBIA (E) expression. HEK293T cells were reverse transfected with siRNAs and, three days later, target gene mRNA levels were measured by qRT-PCR after 0, 2 and 8 h of induction using 20 ng/ml TNF-α. Expression levels were normalized to expression in the negative control sample (siRNA against *Renilla* luciferase): for each time point, mRNA expression levels were set to 100% in the control sample and mRNA levels in candidate samples were calculated in relation to the control. TNFR1 and RelA: siRNAs against TNFRSF1A and RelA, respectively (positive controls). siRNA concentration used: 50 nM. Data derived from five independent experiments are shown, error bars indicating the standard deviations of the biological replicates. p-values were calculated using Student's T-test. **: p-value < 0.01, ***: p-value < 0.001.

on TNF-α target gene expression. Except for IL-8, the expression of all measured target genes was statistically significantly reduced upon CASP4 silencing. Whereas BIRC3 and CCL20 expression was affected at both time points, the induction of TNF-α and NFKBIA was influenced only after 2 hours of TNF-α treatment. In summary, knockdown of all candidates showed effects dependent on the target gene and the duration of the stimulus.

Altered target gene expression signature upon knockdown of SPP1, GAB3 and CASP4

I next asked whether the influence of SPP1, GAB3 and CASP4 silencing on TNF-α signaling would also be reflected in an altered target gene expression signature as assessed by expression profiling. To address this question expression profiling was carried out using Illumina microarrays. RNA samples were prepared in the same way as for the qRT-PCR experiments (see 2.2.1). siRNAs against *Renilla* luciferase (RL) served as negative control, siRNAs against TNFR1 and RelA as positive controls. HEK293T cells were either left unstimulated or were treated with 20 ng/ml TNF-α for 2 or 8 hours, before RNA was isolated. Prior to hybridization onto chips by the DKFZ core facility, knockdown of controls (TNFR1, RelA) and of candidates (SPP1, GAB3, CASP4) as well as induction of target genes by TNF-α were validated by qRT-PCR (data not shown). Each condition was represented by biological duplicates. Scanned images of hybridized microarrays were analyzed using the Bioconductor/R packages "beadarray" and "limma" (for details see Materials and Methods).

Two different TNF-α-induced target gene expression signatures were defined: (i) genes altered after 2 hours of TNF-α treatment and (ii) genes altered after 8 hours of TNF-α treatment as compared to unstimulated cells. In order to define a TNF-α-induced gene expression signature, first differentially expressed genes in TNF-α stimulated cells were determined that were treated with the negative contol siRNA. Subsequently, only those genes out of these differentially expressed genes were selected that were previously published to be TNF-α target genes (downloaded from "bioinfo.lifl.fr :: Bioinformatics Software Server" [18]). The expression signature of these genes was then assessed in all samples.

Similarity of gene expression signatures of the differently treated samples is visualized using a Trellis dot plot (Figure 2.23). After 2 hours of stimulation, data points or siSPP1 and siRL treated cells lie closely together, indicating that silencing of SPP1 did not affect TNF-α target gene expression compared to negative control treated cells (Figure 2.23A). GAB3 and CASP4 knockdown cells show a very similar TNF-α target gene expression profile after both 2 and 8 hours of TNF-α treatment which is different from siRL treated cells (Figure 2.23). The expression of many target genes is only slightly influenced by the

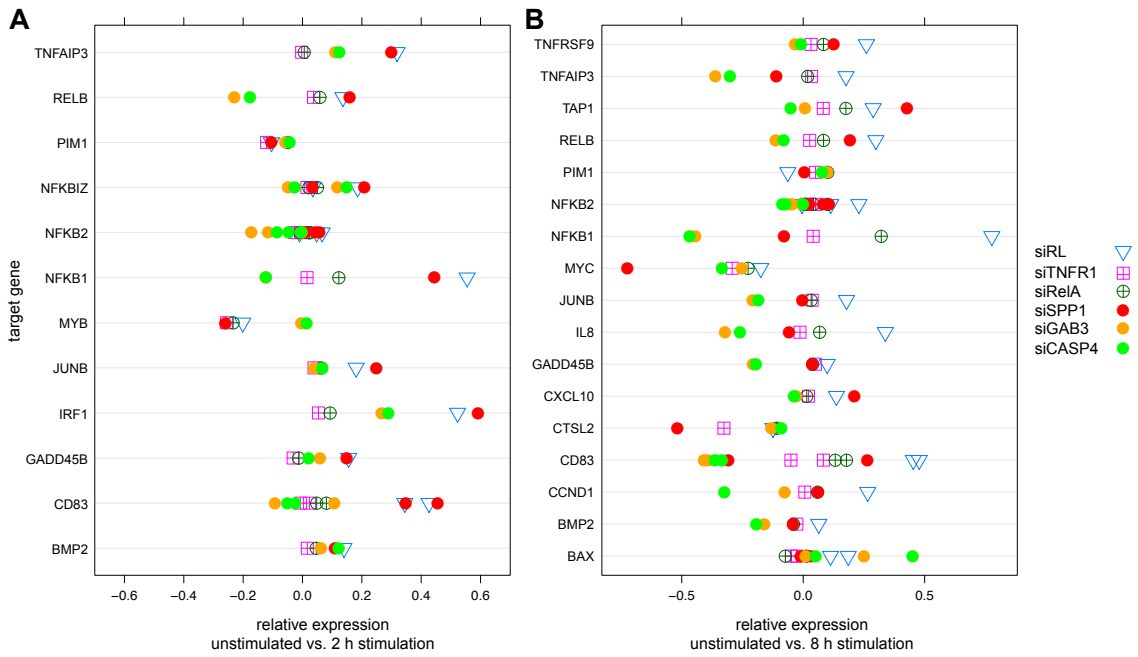

Figure 2.23: Expression of TNF-α target genes in HEK293T cells after 2 hours (A) and 8 hours (B) of TNF-α treatment as compared to unstimulated cells. Data was transformed logarithmically before target genes were plotted versus their relative expression. siRL: siRNA against *Renilla* luciferase (negative control; blue triangle), siTNFR1 and siRelA: siRNA against TNFRSF1A (pink plus sign) and RelA (dark green plus sign), respectively (positive controls). Filled circles represent measurements in cells treated with siSPP1 (red), siGAB3 (yellow) and siCASP4 (green). siRNA concentration used: 50 nM. Summarized data of two biological replicates is shown. Multiple symbols of the same type for one target gene indicates that there was more than one probe for that target gene on the array.

transfection of different siRNAs [TNFRSF9 (8 h), PIM1 (2 and 8 h), NFKB2 (2 and 8 h), MyB (2 h, except for siGAB3 and siCASP4), Myc (8 h, except for siSPP1), BMP2 (2 and 8 h)]. However, clear effects can be seen for the expression of TNFAIP3, NFKB1, IRF1 and CD83 after 2 hours of TNF-α treatment. Whereas siRL and siSPP1 treated cells show a clear induction of expression of these target genes, levels are not or only slightly affected by TNF-α stimulation in the other samples. The remaining, not as strongly induced target genes show the same trend in their expression profiles. Interestingly, expression of RelB is only slightly increased after TNF-α stimulation in siRL and siSPP1 treated cells while it is decreased upon GAB and CASP4 silencing. This expression profile was observed for more genes after 8 hours of stimulation (TNFAIP3, NFKB1, JunB, IL-8, GADD48B, CD83). In general, target gene expression profiles of cells that were transfected with siRNAs targeting the candidates resemble those of positive control treated cells than to negative control treated cells. An exception was the gene expression profile of siSPP1 treated cells after 2

hours of TNF-α treatment. This observation is also visualized in Figure 2.24. Here, similarity of the different microarray samples according to their TNF-α target gene expression signature was assessed using the heatmap.2 function of the R package "gplots", which assessed the euclidian distance between data points. siSPP1 treated cells stimulated for 2 hours cluster with siRL treated cells as their TNF-α target gene expression profile is very similar. TNF-α target gene expression remains largely unaffected by TNF-α treatment in TNFR1 and RelA knockdown cells. In contrast, siGAB3 and siCASP4 treated cells show the opposite phenotype after 8 hours of stimulation with expression of TNF-α target genes being decreased. Strikingly, the observed expression of the target genes does not reflect their published categorization into early response genes, late response genes and genes whose expression peaks in the middle between the first two [104, 236]. In conclusion, knockdown of all candidates affected the TNF-α target gene expression signature as compared to the negative control. siCASP4 and siGAB3 treated cells show similar target gene expression signatures. These signatures are similar to the positive control after 2 hours of stimulation and show decreased target gene expression after 8 hours of TNF-α treatment. Whereas knockdown of SPP1 resulted in a TNF-α target gene expression signature similar to the negative control after 2 hours of stimulation, it caused a phenotype similar to the positive controls after 8 hours.

2.2.2 Epistasis assays map novel regulators in the pathway

Epistasis assays are means to place potential novel regulators into a known pathway. Epistasis experiments can be performed in different ways. For example, overexpression of different known components of TNF-α signaling induces the pathway at different levels of the signaling cascade. If a candidate shows a phenotype, the candidate acts downstream of the overexpressed protein; if silencing does not affect signaling activity, the candidate acts upstream of the overexpressed pathway component. Another means for epistasis analysis is detecting phosphorylation status of IκB-α (inhibitor of κB-α) to determine whether a candidate acts upstream or downstream of the IKK (IκB kinase) that is responsible for IκB-α phosphorylation [270, 218]. If - after knockdown of a potential regulator - IκB-α is still phosphorylated, the novel regulator acts downstream of the activation of the IKK. However, if phosphorylation is lost, IKK activity was not induced upon stimulation with TNF-α. Thus, the regulator plays a role in activating the IKK.

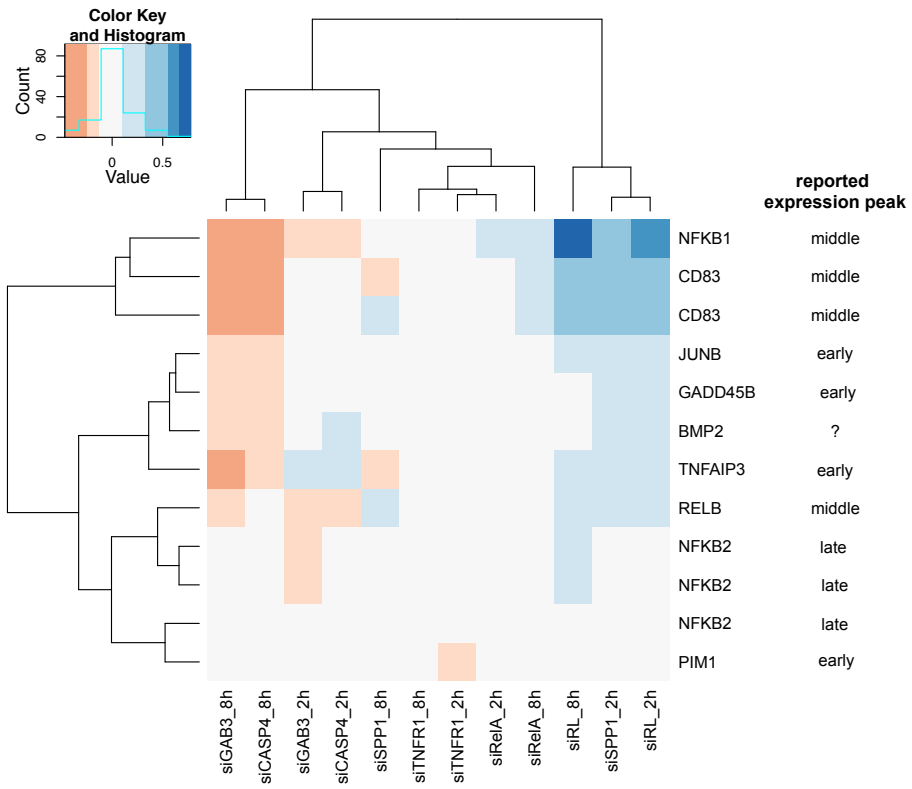

Figure 2.24: TNF-α target gene expression signature of HEK293T cells after 2 hours and 8 hours of TNF-α treatment as compared to unstimulated cells. Data were transformed logarithmically before similarity was assessed by euclidean distance between data points. Rows of the heatmap are different genes; their published categorization into early response genes, late response genes and genes whose expression peaks in the middle between the first two is given in the table. Columns of the heatmap are different samples. Lower expression compared to unstimulated cells is depicted in red, higher expression depicted in blue. siRL: siRNA against *Renilla* luciferase (negative control), siTNFR1 and siRelA: siRNA against TNFRSF1A and RelA, respectively (positive controls). siRNA concentration used: 50 nM. Summarized data of two biological replicates is shown.

Epistasis assays by assessing phospho-IκB-α levels demonstrated candidate action at the level or upstream of the IKK.

Phospho-IκB-α levels were assessed in HeLa cells, since these cells express high levels of IκB-α (Novartis gene expression atlas [182]). HeLa cells were reverse transfected with siRNAs against *Renilla* luciferase (siRL) as negative, against TNFR1 as positive control, or siRNAs against the candidates. After two days of protein depletion, cells were stimulated for either 0, 5, 10 or 20 minutes with 50 ng/ml TNF-α and then were lysed. After protein transfer, immunoblotting for phospho-IκB-α revealed that IκB-α phosphorylation peaked after 5 minutes of TNF-α stimulation in siRL treated cells (Figure 2.25). Phosphorylation represents a signal for IκB-α degradation [227, 13], which could be detected as fast as in 20 minutes after induction of TNF-α signaling. In siTNFR1 treated cells, induction of IκB-α phosphorylation was decreased (Figure 2.25A) or entirely missing (Figure 2.25B). Likewise, knockdown of SPP1 (Figure 2.25A), GAB3 (Figure 2.25B) and CASP4 (Figure 2.25C) abolished induction of IκB-α phosphorylation. In conclusion, all three candidates act at the level or upstream of the activation of the IKK.

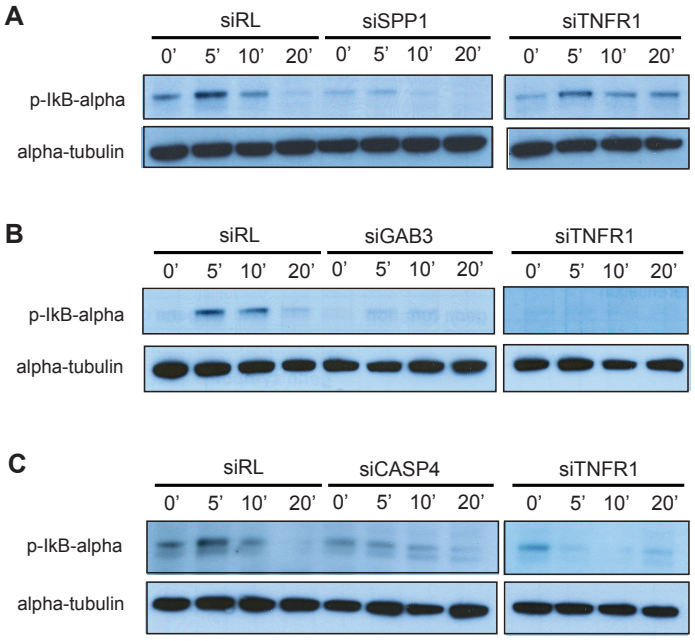

Figure 2.25: Knockdown of (A) SPP1, (B) GAB3 and (C) CASP4 abolishes IκB-α phosphorylation upon TNF-α stimulation in HeLa cells. HeLa cells were transfected with siRNA pools before IκB-α phosphorylation upon TNF-α treatment (50 ng/ml) was assessed by immunoblotting. siRL: siRNA against *Renilla* luciferase (negative control), siTNFR1: siRNA against TNFRSF1A (positive control). siRNA concentration used: 50 nM. As loading control served α-tubulin. Data shown is representative of four independent experiments. p-IκB-α: phospho-IκB-α.

Feedback loops interfere with epistasis assays.

I also intended to place the candidates into the TNF-α pathway by overpressing known pathway components. TNF-α signaling was activated at four different levels: (a) at the receptor by treating cells with TNF-α, (b) directly downstream of the receptor by overexpressing TRADD (TNFR-associated death domain), (c) by overexpressing RIP1 (receptor interacting protein 1) and (d) by overexpressing IKK-β. To avoid a positive feedback loop via NF-κB-induced TNF-α secretion which would impede the epistasis assay design, cells were additionally treated with Enbrel (soluble TNFR1) to scavenge secreted TNF-α. HEK293T cells were reverse transfected with siRNAs before luciferase expression and overexpression plasmids were transfected on the next day. After an incubation for two days to allow for siRNA-mediated protein depletion and plasmid-encoded protein expression, the luciferase assay was performed. Control cells were stimulated with 20 ng/ml TNF-α 16 hours prior to the read out, while cells transfected with overexpression plasmids were treated with 12.5 μg/ml Enbrel.

Figure 2.26 shows the result of the dual luciferase assay. Even when treating cells with Enbrel, transfection of siRNAs targeting TNFR1 decreased relative signaling activity independent of the activating stimulus. However, induction via overexpression of pathway components downstream of the receptor should be independent of the presence or absence of TNFR1. The phenotype of siTNFR1 can be either explained by the presence of a positive feedback loop via activation of TNF-α that was not scavenged potently by Enbrel or alternatively by the necessity of the intracellular part of the TNFR1 for the assembly of the signaling inducing TNFR complex. Therefore, no conclusive results could be obtained from this overexpression experiment.

2.2.3 Knockdown of SPP1, GAB3 and CASP4 does not affect TNFR1 cell surface expression

Besides playing a role in the activation of the IKK, silencing of SPP1, GAB3 and CASP4 could also have an effect on the shuttling of TNFR1 to the plasma membrane. Interruption of this transport could also explain the phenotypes observed after knockdown of SPP1, GAB3 and CASP4.

HeLa cells were used to determine TNFR1 surface expression because they express higher levels of TNFR1 than HEK293T cells [182]. HeLa cells were reverse transfected with siRNAs - against *Renilla* luciferase as negative, against TNFR1 as positive controls, and against the candidates. After two days of protein depletion, cells were detached by scraping. TNFR1 expression on the plasma membrane was detected using a specific antibody labelled with phycoerythrin (PE). As control served an unspecific antibody of the same isotype.

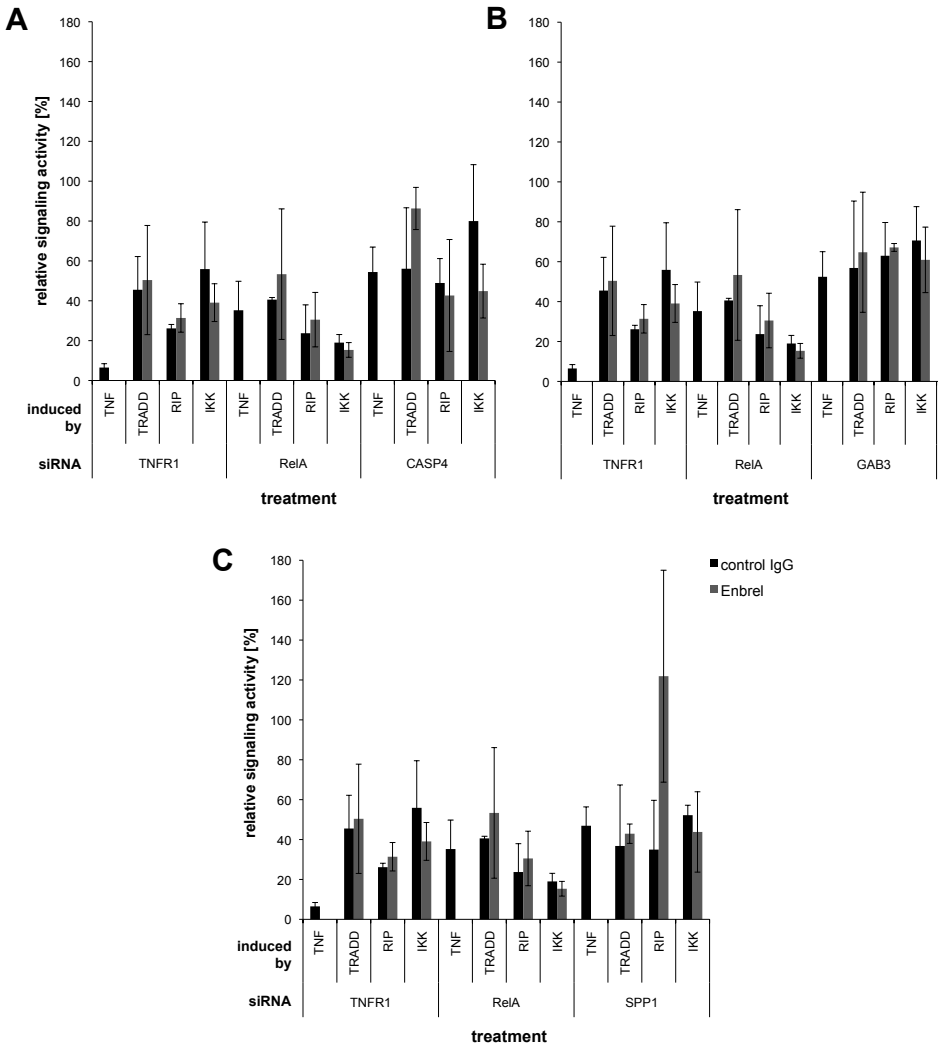

Figure 2.26: Epistasis experiments in HEK293T cells by overexpressing known pathway components. HEK293T cells were reverse transfected with different siRNA pools (day 1) before TNF-α signaling was either induced by overexpression of the known pathway components TRADD (20 ng/384-well plates well), RIP1 (RIP, 2 ng/well) and IKK-β (IKK, 2 ng/well; day 2) or treatment with 20 ng/ml TNF-α (TNF, day 3). The dual luciferase assay was performed, shown is relative signaling activity (i.e. FL/RL compared to mock (H_2O) transfected cells) in control IgG (black bars) or Enbrel (grey bars) treated cells. TNF-α induced reporter activity 14-fold, whereas TRADD overexpression induced 5.5-fold, RIP1 overexpression 6.5-fold and IKK-β overexpression 8.5-fold. siRNA concentration used: 50 nM. Mean values of two independent experiments are shown. Error bars depict standard deviations of the two biological replicates. Effect of CASP4 (A), GAB3 (B) and SPP1 (C) knockdown as compared to the positive controls siTNFR1 and siRelA.

PE staining was assessed by fluorescence activated cell sorting (FACS).

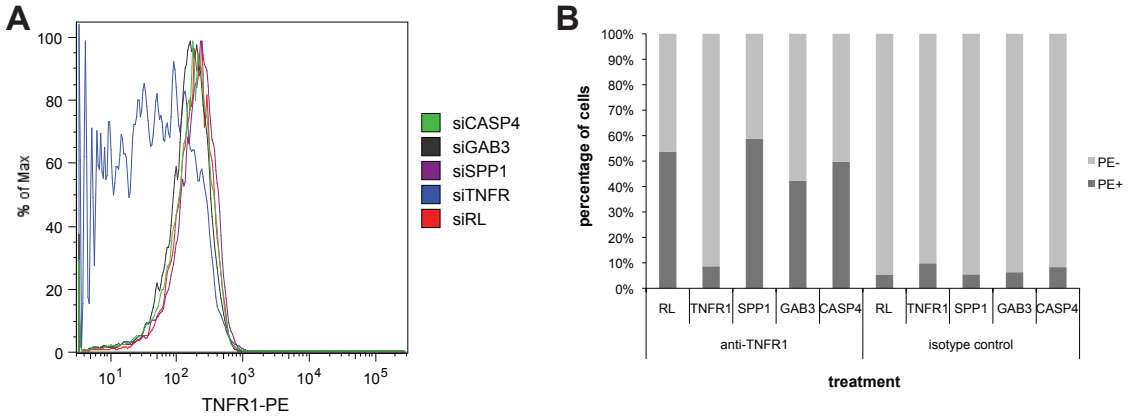

Figure 2.27: Knockdown of SPP1, GAB3 and CASP4 does not affect TNFR1 cell surface expression. HeLa cells were transfected with control and candidate siRNAs and were stained for cell surface TNFR1 after 2 days of incubation. TNFR1 was detected using a specific antibody labelled with phycoerythrin (PE). PE staining was assessed by FACS (fluorescence activated cell sorting). A: Histogram representing the intensity of the TNFR1-PE stain (x-axis) in dependency of cell number (y-axis). An overlay of all samples is shown, with the green curve depicting siCASP4-treated cells, grey being siGAB3-treated cells, violet siSPP1-treated, blue siTNFR1-treated and red siRL-treated cells. Whereas TNFR1 depleted cells exhibited less TNFR1-PE staining, the staining of the other samples was similar. B: Quantification of PE-positive (dark grey) and -negative (light grey) cells as percentage of all analyzed cells. For quantification, two populations, PE-positive and PE-negative, were defined based on siRL-treated cells being stained with the isotype-matched control antibody (isotype control). For each sample the percentage of cells was calculated being in either of the two populations. Control antibody stained cells showed background staining. anti-TNFR1 staining in siTNFR1 cells was decreased to background, while cells treated with siRNAs against the candidates or the negative control exhibited similar staining. A + B: siRL: siRNA pool against *Renilla* luciferase (negative control), siTNFR1: siRNA pool against TNFRSF1A (positive control), siCASP4, siGAB3, siSPP1: siRNA pools against the candidates. siRNA concentration used: 50 nM. Data shown is representative of two independent experiments.

Figure 2.27A shows histograms representing the PE-staining intensity and thus the amount of TNFR1 at the cell surface. The histograms for cells treated with the negative control (siRL, red curve) and siRNAs against the candidates (siCASP4: green curve, siGAB3: grey curve, siSPP1: violet curve) overlap. This indicates that cells in these samples displayed similar amounts of TNFR1 on their cell surface. In contrast, cells treated with siTNFR1 (positive control, blue curve) exhibited diminished TNFR1 cell surface expression. The quantification of PE-positive versus PE-negative cells shown in Figure 2.27B yielded the same result. The staining pattern by the isotype-matched control antibody (isotype control), defined to be background, was unaffected by all siRNAs, including siT-

NFR1. Only depletion of TNFR1 diminished the number of cells being stained for TNFR1 (PE-positive). Thus, knockdown of the candidates SPP1, GAB3 and CASP4 had no influence on TNFR1 cell surface expression. In conclusion, the phenotypes observed upon SPP1, GAB3 and CASP4 silencing were not caused by interrupted shuttling of the TNFR1 to the cell surface but by interruption of the intracellular TNF-α signaling cascade.

2.3 Caspase 4 As a Novel Regulator of TNF-α Signaling

The role of CASP4 in TNF-α signaling was studied in more detail since siRNA-mediated silencing of this candidate was the most efficient and showed the strongest phenotype in the dual luciferase assay, ELISA and the qRT-PCR assay measuring TNF-α target gene expression. In addition knockdown could be validated at the protein level (Figure 2.28).

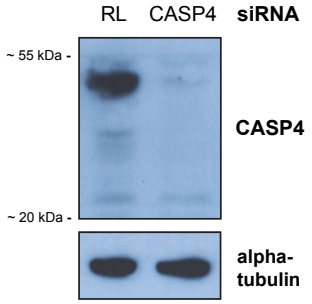

Figure 2.28: CASP4 protein depletion upon siCASP4 treatment. HeLa cells were treated with siRNAs against *Renilla* luciferase (siRL, negative control) and against CASP4 (siCASP4) for two days before CASP4 protein levels were determined by immunoblotting. siRNA concentration used: 50 nM. As loading control served α-tubulin. Data shown is representative of five independent experiments.

2.3.1 CASP4 primarily localizes to the cytoplasm

Epistasis experiments showed that CASP4 acts at the level or upstream of IKK. Since the cytoplasmic TNFR complex I acts upstream of the IKK, it was tested if cellular localization of CASP4 would permit interaction with the TNFR complex. Since HeLa cells express CASP4 more strongly than HEK293T cells [182], endogenous CASP4 protein was visualized in HeLa cells using a specific antibody by confocal microscopy.

CASP4 has been detected at the endoplasmic reticulum (ER) membrane [102, 186], but is annotated in the Human Protein Reference database as primary cytoplasmatic [122]. To determine whether CASP4 localizes to the ER, HeLa cells, seeded onto coverslips, were co-stained with an anti-CASP4 antibody and an antibody detecting the ER marker calnexin [244]. CASP4 partly co-localized with calnexin in HeLa cells, however the major part of the

staining appeared to be cytoplasmatic (Figure 2.29). CASP4 could therefore theoretically interact with the cytoplasmic machinery of TNF-α signal transduction.

In a next step, it was tested whether CASP4 localization changed upon stimulation of HeLa cells with TNF-α. HeLa cells were seeded onto coverslips and starved for 3-4 hours prior to treatment with 50 ng/ml TNF-α. Cells were then stained for CASP4 using a CASP4-specific antibody. No obvious change of CASP4 localization could be detected upon TNF-α stimulation (Figure 2.29). However, the strong ubiquitous cytoplasmic staining could have masked any changes in localization.

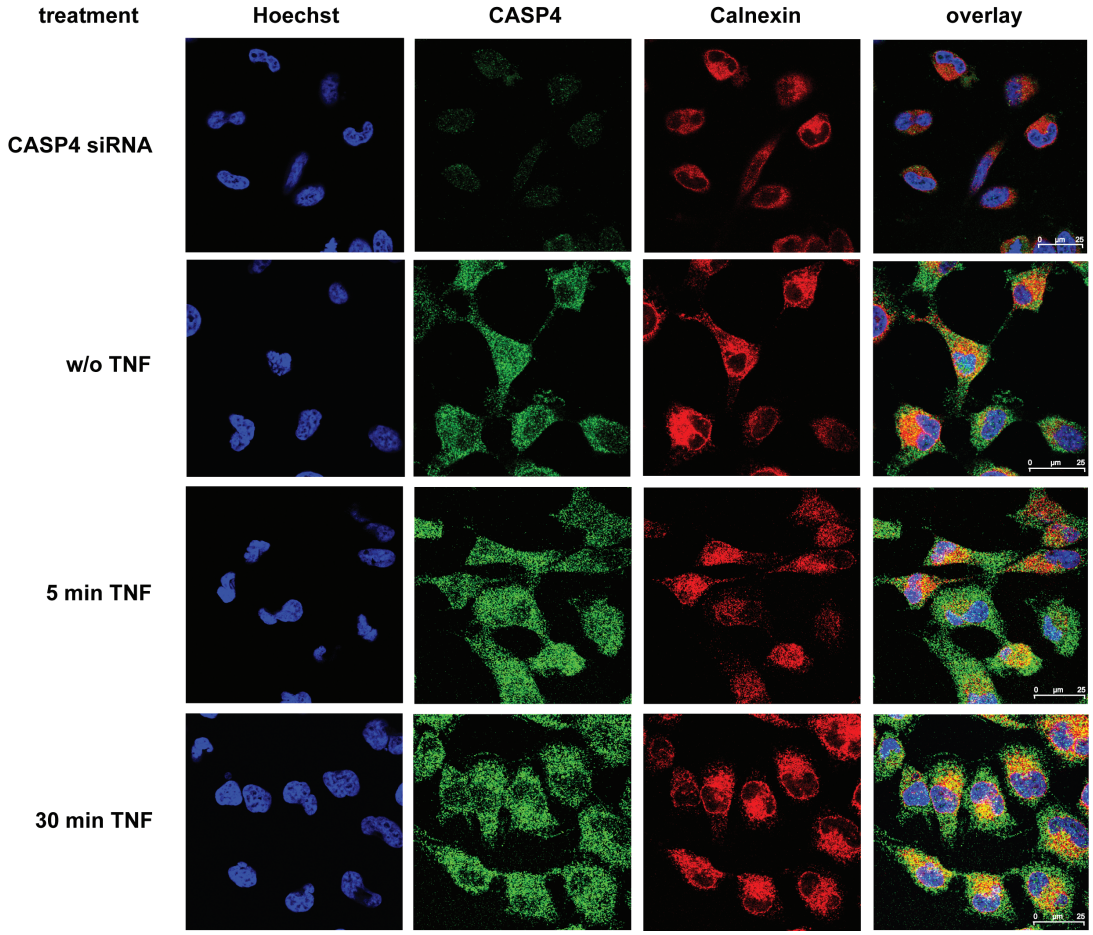

Figure 2.29: Cytoplasmatic localization of CASP4 does not change upon TNF-α treatment as determined by immunofluorescence microscopy. HeLa cells were seeded onto coverslips. Before staining for CASP4 with a CASP4-specific antibody (green) and with an antibody against ER-resident calnexin (red), cells were starved and then treated with 50 ng/ml TNF-α for 0, 5 or 30 minutes. CASP4 staining appeared to be mainly cytoplasmatic (spotty staining) and only partially overlapped with the ER stain. CASP4 cellular localization did not obviously change upon treatment with TNF-α. Almost no CASP4 staining was detectable in siCASP4 treated cells, illustrating the specificity of the CASP4 antibody. Hoechst: DNA stain (blue).

2.3.2 CASP4 is not cleaved after TNF-α stimulation

Caspases are cysteine-aspartate specific proteases that - when enzymatically activated - act by cleavage of target proteins. Caspases are enzymatically activated upon induced aggregation which entails the cleavage of the pre-caspase into two smaller subunits. These subunits then form the catalytically active caspase [200]. Cleavage of CASP4 could thus serve as an indirect indicator of whether CASP4 becomes enzymatically activated upon TNF-α treatment.

To determine CASP4 cleavage by western blotting, HeLa cells were transfected with siRNA - either siRNAs against CASP4 or *Renilla* luciferase as a negative control. After two days of protein depletion, cells were stimulated for either 0, 0.5 or 1 hours with 50 ng/ml TNF-α. After protein transfer, immunoblotting for CASP4 revealed that CASP4 was not cleaved after TNF-α stimulation (Figure 2.30).

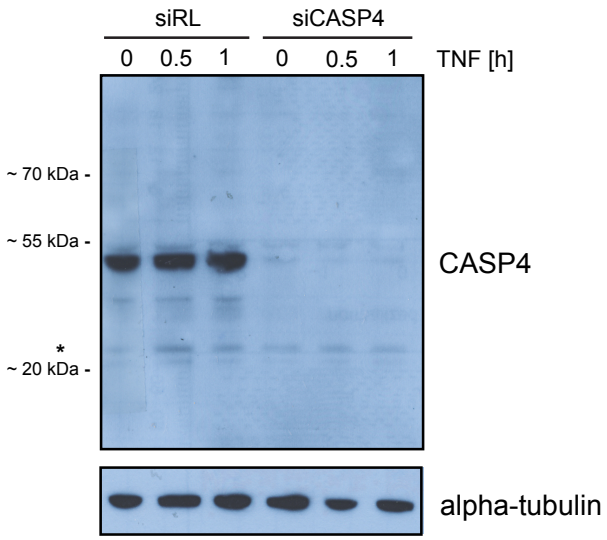

Figure 2.30: CASP4 is not cleaved upon TNF-α treatment in HeLa cells. HeLa cells were reverse transfected with siRNAs against *Renilla* luciferase (RL, negative control) and CASP4 and incubated for 2 days to allow for protein depletion. Cells were starved and then stimulated with 50 ng/ml TNF-α for different time periods before CASP4 protein cleavage was determined by immunoblotting. As loading control served α-tubulin. The asterix indicates a putatively unspecific band, as it is not diminished upon CASP4 depletion.

In summary, I have shown that siRNA-mediated CASP4 depletion specifically interfered with TNF-α signaling, reducing NF-κB transcriptional activity. Epistasis experiments demonstrated that CASP4 acted at the level or upstream of the activiation of the IKK. CASP4 could thus be a component of the TNFR complex. CASP4's cytoplasmic localization would enable interaction with the TNFR complex. However, interaction with a known

TNFR complex component has not been shown so far. Results indicate that CASP4 is not cleaved upon TNF-α treatment (Figure 2.30) and is probably also not enzymatically activated (data not shown). CASP4's function might therefore be different from TNF-α-induced cleavage of a TNF-α pathway component. In conclusion, the presented data strongly implies CASP4 to be a novel regulator of TNF-α-induced signaling at the TNFR1 complex.

Chapter 3

Discussion

Inflammation is essential for an efficient innate immune response and has to be well controlled in order to avoid damage to the host. The severe consequences of exaggerated inflammation is most prominently demonstrated by the effects of septic shock upon challenge with endotoxins, such as LPS [15]. Along these lines, chronic inflammation has been shown to be a key component of many diseases such as autoimmune disorders and cancer [79, 159]. Recently, Mantovani proposed to add inflammation to the hallmarks of cancer that were coined by Hanahan and Weinberg [93, 158].

TNF-α is the major mediator of inflammation. In order to identify novel regulators of TNF-α signaling, I set out to perform genome-wide RNAi screens. I established a cell-based assay that was suited to study TNF-α-induced activation of NF-κB transcriptional activity in miniaturized format. Using this assay, two screens were performed in HEK293T cells. These screens identified several known components as well as putative novel regulators of TNF-α signaling whose phenotypes were validated in secondary assays. Three candidates, SPP1, GAB3 and CASP4, were further characterized.

3.1 RNAi Screening Design and Analysis

I aimed at identifying novel regulators of TNF-α signaling by genome-wide RNAi screens. The nature of the assay is of paramount importance for any RNAi screen and determines how much information can be gained from such a screen. Therefore, I critically evaluated different aspects of the screening setup during assay establishment.

3.1.1 Selection of a suitable cell line for RNAi screening

Since TNF-α signaling is involved in innate immunity, immune cells would have been the most obvious cells to use for my studies. However, using RNAi reagents in immune cells can be problematic since the immune system is equipped to recognize introduced double- and single-stranded (ds/ss) RNAs. Recognition is mediated by different RNA-binding molecules, like Toll-like receptor (TLR) family members, that induce an interferon response [107, 219] and the activation of NF-κB [3]. Whereas reports are contradicting with regards to whether siRNAs trigger these immune mechanisms in non-immune cells [107, 119, 124], it is agreed on the superior sensitivity of immune cells expressing higher levels of the dsRNA and ssRNA detection machinery [124]. Hence, I chose to study immune signaling by RNAi in non-immune cells. TNFR1-mediated signaling can be investigated in non-immune cells, since this receptor is abundantly expressed [247]. I decided to work with HEK293T cells as this cell line is responsive to TNF-α and is widely used to explore proteins' functions in TNF-α signaling [197, 199, 198, 75]. In contrast to immune cells, HEK293T cells are less likely to get immune-activated by transfection with RNAi reagents. Nevertheless, the possibility that RNAi per se could interfere with the assay employed in the screens that I performed cannot be excluded.

3.1.2 Designing a dual luciferase assay for monitoring NF-κB activity

Activity of TNF-α signaling can be assessed by multiple means e.g. by measuring the presence of signaling intermediates like phospho-proteins, nuclear translocation of NF-κB or TNF-α target gene expression. My goal was to identify genes affecting NF-κB transcriptional activity upon TNF-α treatment. Therefore the dual luciferase assay represented a simple and straight forward assay to monitor the activity of the whole pathway. Other strategies would have consisted in microscopic assays suited for genome-wide screening. These assays would have the disadvantage of either not covering the whole pathway (such as staining a signaling intermediate or monitoring NF-κB nuclear translocation) or giving the same information as the dual luciferase assay while demanding a more sophisticated analysis. However, one disadvantage of the dual luciferase assay is its dependance on arti-

ficially introduced reporters.

To report NF-κB transcriptional activity a highly inducible NF-κB-dependent reporter is essential. Many commercially available or published reporters make use of different numbers of NF-κB binding sites (e.g. [203, 75, 250]). Li et al. tested different numbers of NF-κB binding sites for their NF-κB-dependent reporter (1, 2, 6, 12, 24) to obtain a reporter with good signal to noise ratio for their screen [147]. The authors report that 6 NF-κB binding sites in the artificial promoter exhibited the best signal to noise ratio [147]. My strategy to determine assay conditions with an optimal signal to noise ratio was to select a reporter with high expression levels and subsequently optimize fold induction of expression upon TNF-α stimulation by varying the amount of transfected reporter (data not shown). Therefore, I fused an artificial promoter containing 8 NF-κB binding sites to the *firefly* luciferase gene. This reporter yielded high expression levels upon TNF-α treatment, being required for stable results during large-scale experiments such as genome-wide RNAi screens (Figure 2.4).

In addition to the pathway specific reporter, a constitutively expressed luciferase construct is needed to report differences in plasmid transfection efficiency and cell numbers between wells and plates. Commonly used reporters controlled by viral promoters have been shown to be influenced by TNF-α treatment [192]. I decided to use a co-reporter without viral promoter and fused the β-actin promoter upstream of the *Renilla* luciferase coding sequence. The expression of this construct (act-RL) was to some extent negatively influenced by TNF-α. However in contrast to co-reporters under the control of viral promoters, act-RL reporter expression levels were very stable under stimulated conditions, prerequisite to monitor viability effects, while being high enough to give rise to stable results in large-scale experiments (Figure 2.4).

A luciferase-based assay depends on protein synthesis and is therefore not suited to detect fast changes in signaling activity. To obtain stable *firefly* expression levels, TNF-α stimulation for 16 hours was used. Under these conditions I was able to detect phenotypes of varying strength of silenced positive regulators with high sensitivity. However the long stimulation with TNF-α yields such a high expression level of the NF-κB-dependent reporter that expression cannot be further increased by silencing of negative regulators of TNF-α signaling. The established assay is thus not suited for detecting negative regulators (e.g. CYLD (cylindromas) [239]). Besides, as TNF-α signaling is influenced by positive and negative feedback loops, it is to be expected that the NF-κB-dependent *firefly* luciferase expression construct does not only report changes in direct signaling from TNFR1 to NF-κB, but also changes in induced feedback loops. Therefore, secondary assays allowing shorter stimulation periods are needed to distinguish direct and feedback loop effects (see below).

3.1.3 Defining criteria for screening hit selection

Two genome-wide screens using two independent libraries were preformed to identify novel regulators of TNF-α signaling. Performing two screens for the same signaling pathway in the same cell line with different libraries allowed me to evaluate hits from single screens as well as from the overlap of the two screens. RNAi phenotypes identified in both experiments were independent of the RNAi reagent used and thus less likely to be false positives.

For the individual analysis of either screen, a "high stringency strategy" was pursued. First, strongest hits were selected by applying a z-score filter of $\leq$ -2.5. These hits were further filtered by applying viability (screen A hit list only) as well as *firefly* and *Renilla* luciferase expression filters. In addition, in the combined analysis of both screens the stringency of the z-score cut-off was lowered as reliability of hit selection should be provided by the overlap of two independent experiments. I assessed different z-score filters for the number of genes passing the cut-off in the overlap data set. As shown in Figure 3.1A, only very few genes (seven) are identified in the overlap of the two screens when a z-score cut-off of $\leq$ -2.5 is applied. When lowering the cut-off the number of genes in the overlap data set increases (Figure 3.1A). Determining the p-value by Exact Fisher Test to assess whether the observed number of overlapping hits is random or not reveals that for most z-score cut-offs the overlap is statistically significant (Figure 3.1B, dashed line). However, the odds ratio for the observed number of overlapping hits is only higher than 1 (and thus higher than expected) for the z-score cut-offs -2.5 and -1.75 (Figure 3.1B, full line). An obvious z-score cut-off to choose is indicated by the blue line in Figure 3.1B, marking a negative peak for the p-value and at the same time a positive peak for the odds ratio. But when setting the cut-off at -1.75 only 46 genes would be selected, among them no known TNF-α pathway component. I therefore decided to set the z-score cut-off to determine the screening overlap at -1.25, selecting 177 genes (indicated by the red line in Figure 3.1B). These genes include the known TNF-α pathway components IKK-α and IKK-β as well as MAP4K5 (supplementary table A.3).

A comparison of both screens gene by gene revealed only a low overlap (2.12). This low overlap could be due to three general reasons: (i) technical variation, (ii) high false negative rates and (iii) high false positive rates. Technical variation could have been introduced by the use of different siRNA libraries. These libraries contain siRNAs with non-identical sequences which target the same gene. This might yield different silencing efficiencies or off-target effects, resulting in different phenotypes for the same targeted gene. Off-target effects are mediated by siRNAs that silence not only the targeted gene but also gene(s) exhibiting some sequence complementarity to the used siRNA (e.g. [240]). Another cause of technical variation might be plate position effects possibly disguising or mimicking phenotypes of a

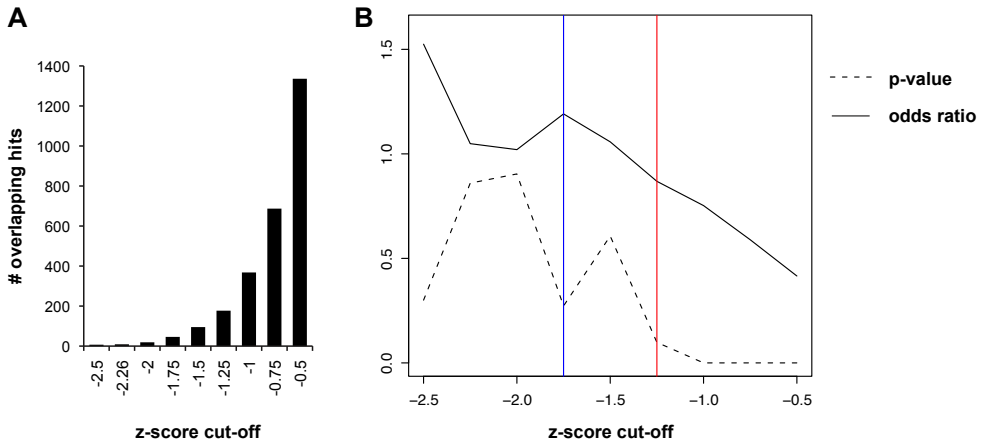

Figure 3.1: Overlap of the two screens at different z-score cut-offs. A: Number of genes identified in the overlap of the two genome-wide screens when setting the cut-off at the indicated z-scores. #: number. B: p-value and odds ratio for the observed number of overlapping hits at the indicated z-score cut-offs as calculated by Exact Fisher Test. Dashed line: p-value, full line: odds ratio. The number of overlapping hits is statistically significant at any threshold except for cut-offs set at z-scores of $\leq$ -2.25, -2 and -1.5. The number of hits is only higher than expected (odds ratio bigger than 1) for the cut-offs set at z-scores of $\leq$ -2.5 and -1.75.

gene in one screen but not the other. Plate effects are screening artifacts that result from the influence of the well position on luciferase expression, for example caused by increased evaporation in wells at the edges of the plate. Since siRNAs targeting a distinct gene most probably have different plate positions in different libraries, the corresponding luciferase reads might be differently affected by these plate position effects. In addition, unstable performance of the assay could contribute to technical variation between the screens. To estimate the variability of the assay, I compared the three plates of screen A with the kinase pilot screen which are identical. When plotting the z-scores of each gene of the pilot kinase screen and the kinase plates of the genome-wide screen against each other, a diagonal is visible, indicating the presence of numerous genes with similar z-scores in both screens (Figure 3.2). Comparing Figure 3.2 to Figure 2.12 illustrates that the overlap between the two genome-wide screens is lower than the overlap between the kinase plates, even though in the latter case two different assays (small scale vs. large scale experiments) are compared. Hence, the use of two different libraries probably contributed more to the technical variation of the two screens than the assay itself.

Other reasons for the low overlap could be high false negative rates in both screens, with different false negatives in both screens, or a high false positive rate in at least one screen, minimizing the overlap [28]. False positives result from screening artifacts or off-target effects, whereas false negatives can be caused by screening artifacts as well as by

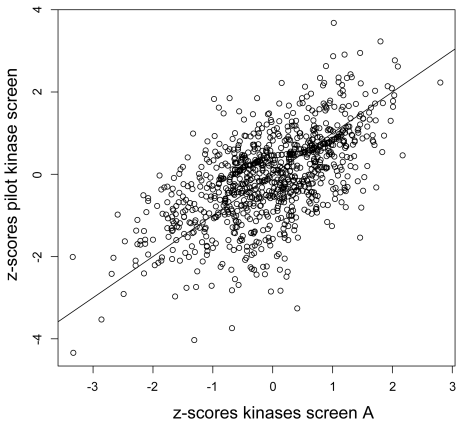

Figure 3.2: Comparison of the pilot kinase screens with the kinase plates of screen A. The z-scores of all genes in the pilot kinase screen and all genes of the first three plates of screen A, which are identical, are plotted against each other. The diagonal indicates perfect reproducibility of z-scores between the two screens. Even though two different assays - a small scale vs. a large scale experiment - are compared, plotted values are distributed along the diagonal, indicating that similar results were obtained by the two screens (pearson correlation coefficient of 0.6).

inefficient gene silencing. I estimated the false positive rate by evaluating the percentage of positively retested candidates in both screens. About 50% of the retested candidates identified in screen A could be confirmed in subsequent retests; for candidates of screen B the rate was about 60%. Comparable false positive rates have been observed for other similar screens (unpublished observations).

In order to assess the false negative rate of the screens in a systematic manner, I determined the fraction of known regulators of inflammation identified by the screens. Two online databases storing information on which proteins that are involved in different signaling pathways were employed to retrieve two gene sets, the "TNF signaling gene set" and the "inflammation gene set". The TNF signaling gene set contained 52 genes of which 49 were covered, the inflammation gene set contained 157 genes of which 155 were targeted by the libraries. 8 genes (16.3 %) of the TNF signaling gene set passed the cut-off of $\leq$ -1.25 that was applied to the combined analysis of both screens in screen A, 6 (12.2 %) in screen B and 2 genes (4.1 %) in the overlap (supplementary table A.4). Of the inflammation gene set 18 genes (11.6 %) passed the z-score cut-off of $\leq$ -1.25 in screen A, 19 (12.3 %) in screen B and 4 genes (2.6 %) in the overlap (supplementary table A.5). The enrichment of known components of inflammatory signaling pathways did not reach statistical significance (as assessed by Exact Fisher Test, data not shown). However, the false negative rate might be overestimated since the gene sets were not filtered for positive regulators.

3.1.4 Comparison to other RNAi screens for TNF-α signaling

TNF-α and NF-κB signaling were also dissected by other groups using RNAi screening in the mammalian system. Table 3.1 lists these published mammalian screens. None of the screens made use of immune cells for studying TNF-α signaling. One study used HEK293T cells like I did [271]. All published screens and the screens presented in this thesis share similar stimulation conditions (varying from 10-50 ng/ml TNF-α for 6-24 hours) and the use of a luciferase reporter to monitor NF-κB transcriptional activity. However, none of the published screens were genome-wide as the two screens presented here.

The first TNF-α screen was published by Brummelkamp et al. [32]. The screen that focused on de-ubiquinating enzymes only identified one negative regulator, CYLD. Another published screening paper described one negative regulator, WIP1 [46]. The authors claimed to have identified 15 phosphatases implicated in TNF-α signaling, but did not provide a list of candidates. I did not identify CYLD nor WIP1 in my screens since the employed assay set-up was not suited to find negative regulators. None of the candidates of other published screens passed the z-score cut-off of $\leq$ -2.5 that I applied in the individual analysis of the screens that I performed.

The difference in the candidate lists between my screens and the published screens can probably be explained by the difference in the screening assays and the reagents used. Different cells, reporters and slightly different stimulation conditions were used in each study. Nevertheless both screens that I performed and most of the published screens identified not only known pathway components but also novel TNF-α pathway regulators according to stringent criteria whose phenotypes could be reconfirmed.

Interestingly, even though published TNF-α screens exhibit only little overlap, another report studying RIP1-dependent necroptosis unexpectedly identified other TNF-α pathway components and one of the candidates presented in this thesis, SPP1, as hits in a genome-wide screen [101]. This supports my hypothesis that SPP1 might be a novel regulator of TNF-α-induced NF-κB activity.

Table 3.1: Published RNAi screens for TNF-α-induced activation of NF-κB.

screen reference	year of publication	coverage	RNAi reagent	cell line	conditions	readout	hit definition	confirmation	# candidates identified
[32]	2003	50 de-ubiquitinating enzymes	self-made siRNA expression vectors, 4 constructs per gene pooled	U2-OS	20 ng/ml TNF, 24 h	pNFkB-luc, pRL-SV40	increase in reporter activity	second stimulus: PMA	1 negative regulator
[271]	2004	8000 genes of multiple annotations	self-made siRNA expression vectors, 2 constructs per gene	HEK293T cells	10 ng/ml TNF, 12-14 h; unstimulated	pNFkB-luc, pRL-SV40	more than 6-fold increase or more than 70% reduction in reporter activity	different individual siRNAs	19 negative regulators, 1 positive regulator
[147]	2006	250 phosphatases	self-made siRNA expression vectors, 2 constructs per gene pooled	primary mouse astrocytes	10 ng/ml TNF, 6 -8 h	NF-κB reporter, constitutive reporter	(1) two standard deviations above/below mean, (2) no statistically significant influence on mutated NF-κB reporter	(1) confirmed expression, (2) confirmation of phenotypes in secondary assay	13 positive, 6 negative regulators
[46]	2009	phosphatase set, Ambion	3 individuals siRNAs per gene	A549 NF-κB-luc reporter cells	50 ng/ml TNF 18 h	NF-κB reporter	more then 1.5-fold increase of reporter activity	different individual siRNAs	15

3.1.5 Various assays are required to place candidates into the pathway

The consequences of TNF-α signaling are strongly dependent on kinetics. Firstly, TNF-α signaling is regulated by feedback loops. For instance, TNF-α induces its own expression thereby amplifying TNF-α signaling activity [211, 51]. Secondly, the expression of some TNF-α target genes - the early response genes - is induced quickly after TNF-α stimulation, whereas expression of other TNF-α target genes - the late response genes - is induced with a delay [104]. Several different factors determine the gene expression program activated by NF-κB. Duration of the stimulating signal and the timing of NF-κB nuclear translocation oscillations are well established to influence target gene expression [104]. Also, the site of NF-κB phosphorylation and thereby its nuclear interaction partners are known to be important (e.g. [82]). Besides, it has been speculated that promoters of some target genes are stably engaged by core factors of the transcription machinery and are therefore more sensitive to activation by NF-κB and hence less sensitive to a partial disruption of the NF-κB activating signaling cascade [183, 21]. These aspects of TNF-α signaling had to be taken into consideration when monitoring NF-κB transcriptional activity after TNF-α stimulation.

In both luciferase assay and ELISA, cells were treated for 16 hours with TNF-α. These assays therefore monitored NF-κB transcriptional activity induced by extended TNF-α signaling. As a consequence, neither assay allowed me to distinguish between phenotypes caused by direct effects on TNF-α signaling or phenotypes caused by disruption of feedback loops. For this reason I employed assays suitable for differentiating between direct and indirect effects. I decided to measure the presence of a signaling intermediate and the induction of TNF-α target genes. Other assays suitable to distinguish between direct effects and feedback loops are for example microscopic nuclear translocation assays or EMSA (electrophoretic mobility shift assay).

I established a western blot to monitor the fast induction of phospho-IκB-α. Using this assay I could show that the knockdown of SPP1, GAB3 and CASP4 abolished phosphorylation of IκB-α after 5 minutes of stimulation (Figure 2.25) und thus that their silencing affected direct signaling to NF-κB.

Another way to assess the effects of short stimulation with TNF-α is measuring induction of target gene expression by qRT-PCR. Expression of TNF-α early and late response genes peaks after approximately 1.5 and 6-8 hours, respectively [104]. Therefore, TNF-α target gene expression was assessed after 2 and 8 hours of induction. The time-dependent effects of TNF-α signaling and hence of its disruption is exemplified by the phenotype of CASP4 knockdown in ELISA and qRT-PCR assay. Whereas CASP4 depletion strongly decreased IL-8 secretion after 16 hours of stimulation (Figure 2.19), IL-8 mRNA levels

were unaffected after 2 and 8 hours of stimulation (Figure 2.22). Since CASP4 silencing showed no direct effect on IL-8 induction, the reduced IL-8 secretion upon CASP4 silencing was probably caused by disruption of TNF-α-induced feedback loops that further induce production of IL-8.

Additionally, I used a global approach to assess target gene expression in candidate knockdown cells after TNF-α stimulation. Data acquired through gene expression profiling support the requirement of the candidates for TNF-α-induced target gene expression. Target gene expression signatures after silencing of GAB3 and CASP4 were strikingly similar (Figure 2.23); in both cases repressed TNF-α target gene expression was observed. A similar phenomenon has been described for IKK-dependent target gene expression in IKK-α/β knockout cells [174]. However, whereas knockdown of GAB3 and CASP4 affected target gene expression at both time points (2 and 8 hours after treatment), SPP1 silencing only showed an effect after 8 hours of TNF-α stimulation (Figure 2.24). Since SPP1 most likely acts in the direct signaling cascade from TNFR1 to NF-κB (Figure 2.25A), it would be interesting to address the question why SPP1 knockdown did not show an immediate effect on target gene expression. A possible explanation might be that SPP1 knockdown affects NF-κB nuclear oscillations as has been observed for other regulators of NF-κB activity [54, 255]. Consequently, a clear phenotype might only be observed at a later time point after stimulation with TNF-α [177]. Interestingly, TNF-α target genes in HEK293T cells could not be grouped according to their expression profiles into early and late response genes as has been reported for other cell lines [104, 236]. This observation indicates that HEK293T cells show different signaling properties, at least with regards to mechanisms regulating NF-κB-induced target gene expression. A disadvantage of microarray experiments is their inferior sensitivity compared to qRT-PCR experiments. For instance, the changes in expression of the target genes observed in the qRT-PCR assays were not high enough to be detected in the microarray experiment.

Taken together, both qRT-PCR as well as microarray-based gene expression profiling revealed different effects of candidate knockdown depending on the target gene and on duration of stimulation. These effects can probably be explained by the different gene regulatory mechanisms for each of the target genes that are influenced in different ways by the knockdown of the three candidates.

3.2 Potential Novel Regulators of TNF-α Signaling Identified by Genome-wide RNAi Screening

I validated the phenotypes of seven hits in depth (Figure 2.14 presents the process of hit selection) whose phenotypes were assessed to be specific as siRNAs targeting these seven hits neither affected HEK293T cell viability (Figure 2.17) nor were identified in unrelated genome-wide RNAi screens that were performed in the laboratory (data not shown): SPP1, GAB3, CASP4, MEN1, USP2, LILRA2 and ITGA5. The latter are two plasma transmembrane proteins. LILRA2 is an integrin expressed by cells of the immune system. ITGA5 serves as a transmembrane receptor for extracellular SPP1, another candidate identified in the screen. Both proteins could thus be involved in the same TNF-α-induced feedback loop to NF-κB.

Another candidate is the de-ubiquitinating enzyme USP2. As ubiquitination plays an important role at different levels of the TNF-α pathway, USP2 is an interesting candidate. Its function in TNF-α signaling has been studied by Marie Metzig (MD thesis). Its expression is most probably needed for the activation of the IKK and can be correlated to different stages of cancer.

MEN1 is a nuclear protein. Inside the nucleus, activated NF-κB relies on the interaction with other proteins to efficiently induce the expression of target genes. MEN1 has already been described to interact with NF-κB [98]. Whereas I identified MEN1 as a positive regulator of TNF-α signaling, Heppner et al. reported MEN1 to negatively regulate NF-κB function [98]. However, studies exploring MEN1's function in NF-κB activation have been based on overexpression [98]. It is thus possible that artificially high amounts of MEN1 inhibit NF-κB action, whereas lower endogenous protein levels are needed for proper interaction of NF-κB with DNA.

The candidates GAB3, SPP1 and CASP4 are described in more detail below, as they were selected for further characterization (Figure 2.19).

Overexpression of none of the candidates resulted in the induction of TNF-α signaling (data not shown). Likewise, none of the phenotypes resulting from candidates knockdown could be rescued (reversed) by the overexpression of corresponding mouse orthologues (data not shown). There could be different reasons as to why the mouse orthologues did not reconstitute TNF-α signaling activity after candidate knockdown. On the one hand, the ability of a mouse protein to substitute its human orthologue is dependent not only on the overall degree of homology between the two proteins but also on the presence of the human structural motif that is important for its role in the pathway. Similarities be-

tween the mouse and human orthologues of the screening candidates might have not been sufficient. On the other hand, overexpression of a protein can lead to artifacts such as protein mislocation or protein misfolding due to protein overproduction which will hinder the overexpressed protein from fulfilling its functions.

3.2.1 GAB3 in TNF-α signaling

GAB3 was identified in both screens (z-scores of -1.86 and -2.41; supplementary table A.3). GAB3 knockdown decreased the expression of IL-8 and BIRC3 in a statistically significant manner (Figure 2.21). GAB3 function in the signaling cascade was determined to be at the level or upstream of the IKK, as assessed by TNF-α-induced IκB-α phosphorylation (Figure 2.25B).

GAB3 was first described in 2002 on the basis of its sequence homology to GAB1 [259]. Together with GAB2, these proteins form the family of "GRB2-associated binding" (GAB) proteins. This family of scaffolding proteins is involved in signaling mediated by growth factor, cytokine and antigen receptors [180, 201]. GAB proteins share a well-conserved N-terminal pleckstrin homology (PH) domain and are related to the *Drosophila* scaffold protein DOS. They contain multiple tyrosine residues that become phosphorylated upon receptor ligation and serve as binding sites for Src homology (SH) 2 domains. An additional binding site for SH3 domains is provided by proline-rich regions. Upon receptor stimulation, GAB family members recruit signaling molecules to the plasma membrane via these SH2 and SH3 binding domains [201].

GAB1 is the best-studied GAB family member. It plays a role in epidermal growth factor receptor (EGFR)-mediated activation of NF-κB in glioblastoma cell lines [123]. Ligation of EGFR has been shown to induce an interaction of GAB1 with the protein tyrosine phosphatase SHP2 that mediates the activation of PI(3)K/AKT. Activated PI(3)K/AKT in turn might activate NF-κB [123]. GAB2 has been shown to be involved in NF-κB signaling as well: Wada et al. have demonstrated that GAB2 interacts with the TNFR superfamily member RANK upon receptor ligation. In osteoclasts, this interaction is necessary for RANK-induced activation of NF-κB [245].

GAB3 expression is lower than GAB1 and GAB2 expression. GAB3 is mostly expressed by cells of the hematopoietic system, lymphocytes and bone marrow-derived macrophages [208]. Based on its expression profile, a function for GAB3 in immunity and hematopoiesis was proposed [259]. However, GAB3 knockout mice do not show obvious defects in hematopoiesis or immune cell function [208].

GAB3 was the only member of this family identified in both screens [siGAB1 was un-

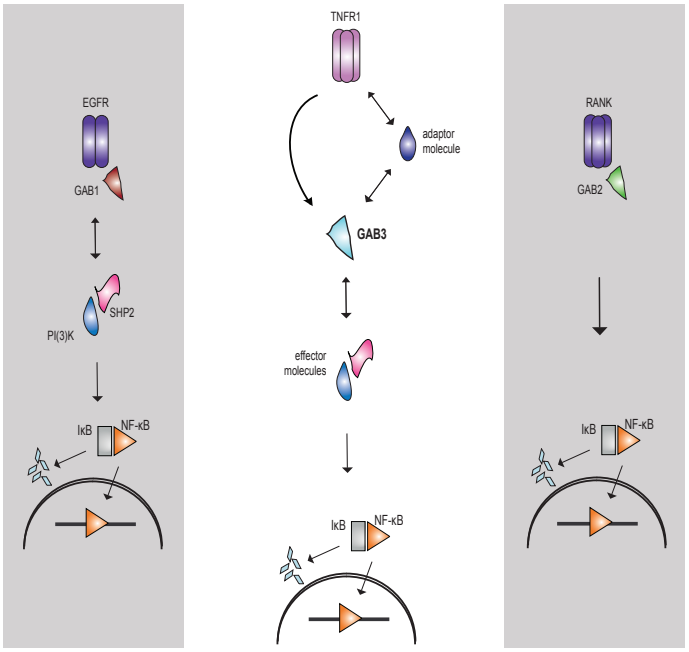

Figure 3.3: Models of GAB3's mode of action in TNF-α signaling. Analogously to GAB1's role in EGFR signaling (left grey panel), GAB3 could interact SHP2 and PI(3)K upon TNF-α stimulation. This interaction could then activate NF-κB via PI(3)K. GAB3 could also mediate NF-κB activation by interacting with SHP2 in a PI(3)K-independent manner. Alternatively, GAB3 could activate PI(3)K by its interaction with GRB2. Besides, GAB3 was shown to interact with the adaptor molecule GRAP2 which could link it to MAPK-mediated activation of NF-κB. Finally, analogously to GAB2's role in RANK signaling (right grey panel), GAB3 could directly interact with TNFR1 to activate NF-κB.

remarkable (z-scores of 0.04 and 1.5), whereas siGAB2 showed a low z-score in only one of the screens (z-scores of 0.16 and -2.29)]. GAB3 interacts constitutively with GRB2 [259], a known interactant of TNFR1, bridging TNFR1 signaling and the Ras signaling cascade [100]. Ras is known to influence NF-κB through the activation of PI(3)K [41]. Upon treatment with macrophage colony-stimulating factor (M-CSF) and IL-3, GAB3 is phosphorylated which enables its interaction with SHP2 and PI(3)K [259]. Whereas PI(3)K can activate NF-κB via protein kinase C [193], SHP2 mediates activation of NF-κB both PI(3)K-dependently [123] and PI(3)K-independently [268]. Further, GAB3 has been described to associate with GRB2-related adaptor protein (GRAP) 2 [26], a scaffold protein involved in MAPK (mitogen-activated protein kinase) signaling [25]. Hence, numerous GAB3 interaction partners may mediate GAB3's interaction with TNFR1 to activate NF-κB. This mode of action would be similar to GAB1-mediated NF-κB activation upon EGFR ligation. Analogous to GAB2's function in RANK signaling, GAB3 could also bind to TNFR1 directly, supporting the recruitment of signaling pathway components. These

two possible modes of action are represented in Figure 3.3.

In order to further analyze the role of GAB3 in TNF-α signaling, it could be tested whether GAB3 becomes phosphorylated after TNF-α treatment, as was described for M-CSF and IL-3. The GAB3 antibodies I have tested so far were not specific enough to reliably detect the protein in cell lysates. Immunoprecipitation experiments could be performed to test the hypothesis that GAB3 associates with TNFR1 either directly or possibly via TNFR1-bound GRB2. These experiments could also assess whether TNF-α treatment induces an interaction between GAB3 and PI(3)K, SHP2 or GRAP2. Further, since the other GAB family members have been shown to be able to interact with GRB2, PI(3)K and SHP2, it would be interesting to test if these two factors influence TNF-α signaling as well, even though they were not identified in my screens.

3.2.2 SPP1 in TNF-α signaling

SPP1 was identified as potential regulator of TNF-α signaling in screen A (z-score -2.84). Its silencing significantly decreased the induction of the TNF-α target genes IL-8, BIRC3 and TNF-α upon stimulation (Figure 2.20).

The cytokine-like SPP1 has first been described to be a secreted protein acting extracellularly but is now known to also fulfill functions intracellularly [33]. The protein is upregulated in several inflammatory diseases, e.g. multiple sclerosis and rheumatoid arthritis [225, 261, 52]. SPP1 is broadly expressed and can be extensively post-translationally modified by phosphorylation, N- and O-glycosylation as well as cleavage [221, 49, 210]. Most reports have focused on extracellular SPP1. In essence, secreted SPP1 binds to integrins and CD44 on cell surfaces, thereby promoting migration and inducing expression of cytokines through NF-κB and MAPK signaling [8, 254, 273, 272]. Secreted SPP1 thus plays roles in inflammation, angiogenesis and tumor metastasis [53]. Its serum levels are elevated in cancer patients and patients suffering from inflammatory diseases [53, 127]. SPP1 knockout mice exhibit a partly immunocompromised phenotype with attenuated responses to e.g. bacterial infection, arthritis and multiple sclerosis [175, 269, 38].

Since extracellular SPP1 is an activator of NF-κB [55, 133] and one of its cell surface receptors, ITGA5 [110], was also identified as required for TNF-α signaling in this study, I suspected a feedback loop via SPP1/ITGA5. However, my results show that SPP1 knockdown diminished TNF-α-induced IκB-α phosphorylation already after 5 minutes of TNF-α stimulation (Figure 2.25). SPP1 seems therefore not to be part of a TNF-α-induced feedback loop. To test whether extracellular SPP1 can rescue the siSPP1 phenotype in TNF-α signaling, I treated SPP1 knockdown cells with recombinant SPP1. The treatment did not reconstitute NF-κB activity (data not shown). However, the used recombinant SPP1 was

not post-translationallly modified, and these modifications could be required for its function. It would be interesting to assess the potential of neutralizing SPP1 antibodies to block TNF-α-induced activation of NF-κB in order to gain further insights into which variant of SPP1, the extra- or the intracelluar one, mediates its function in TNF-α signaling.

Alternative translation yields a SPP1 variant that lacks the secretion signal and thus localizes inside the cell [215, 277]. Little is known about the function of intracellular SPP1. It is expressed in osteoclasts, fibroblasts, macrophages as well as dendritic and T cells where it modulates the cytoskeleton, cell shape and cell migration [277, 231, 215]. SPP1 is also involved in osteogenic differentiation and cell proliferation [273, 276, 274]. The intracellular protein has been shown to localize to distinct spots at the plasma membrane as well as in cell processes, co-localizing with CD44 and ezrin [277, 273]. Interestingly, SPP1 has also been shown to co-localize with the death domain (DD) containing protein MyD88. By immunoprecipitation and microscopy, Shinohara et al. have demonstrated a co-localization with MyD88 upon induction of Toll-like receptor (TLR) 9 in plasmacytoid dendritic cells [216]. However, SPP1 was only required for interferon regulatory factor (IRF) 7-induced production of interferon α but not for NF-κB-induced expression of IL-6 and TNF-α [216].

Recently, CASP8 has been demonstrated to cleave the secreted variant of SPP1 [131]. Cleavage was induced in HeLa cells upon oxidative stress, preluding cell death [131]. In contrast, uncleaved SPP1 inhibited apoptosis induced by oxidative stress, probably by regulating AKT activity [131]. Interestingly, TNF-α treatment did not induce SPP1 cleavage [131]. An intriguing hypothesis is that uncleaved intracellular SPP1 influences NF-κB activation after TNF-α stimulation by controlling activity of AKT [41].

My results indicate that SPP1 acts at the level or upstream of the activation of the IKK since silencing abolished TNF-α-induced phosphorylation of IκB-α (Figure 2.25). Therefore, I assessed whether the intracellular localization of SPP1 would support a function at the TNFR1 complex. While the secreted variant of SPP1 localizes to Golgi and vesicles, the intracellular version has been described to be cytoplasmic [275, 277]. However, staining of endogenous SPP1 detected only to-be-secreted protein that co-localized with Golgi and early endosome markers (data not shown). I was not able to detect any cytoplasmic staining, probably because of the high intensity of the staining in the Golgi and in vesicles. Overexpression of a CFP-tagged SPP1 construct indicated that SPP1 is cytoplasmic, but this observation may be confounded overexpression of the protein (data not shown). The staining pattern of endogenous SPP1 did not change upon TNF-α stimulation (data not shown); neither exocytosis of vesicles nor accumulation at distinct foci was induced.

A conceivable hypothesis on SPP1's action in TNF-α signaling is that SPP1 might interact with DD proteins in the TNFR1 complex, analogously to its TLR-induced inter-

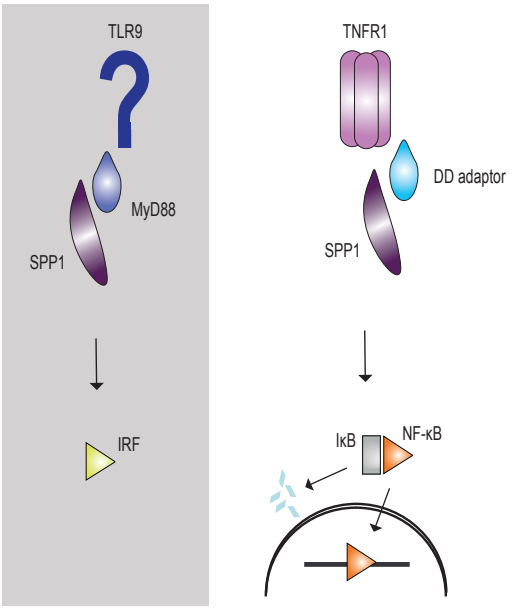

Figure 3.4: Model of SPP1's mode of action in TNF-α signaling. Analogously to its function in Toll-like receptor (TLR) 9 signaling (left grey panel), SPP1 could interact with DD proteins in the TNFR1 complex - TNFR1, TRADD, RIP1 - to facilitate activation of NF-κB.

action with the DD protein MyD88 [216]. This model is represented in Figure 3.4. Even though SPP1 is not involved in NF-κB activation by TLR9 [216], it could be involved in TNFR1-mediated activation of NF-κB, e.g. by interaction with different adaptor and effector proteins. It would be interesting to assess whether SPP1 is able to interact with one of the DD proteins in the TNFR1 complex, namely TNFR1, TRADD and RIP1.

3.2.3 CASP4 as a novel regulator of TNF-α signaling

Caspase 4 (CASP4) was identified in screen B (z-score: -2.53). Its silencing significantly reduced expression of the TNF-α target genes BIRC3, TNF-α, CCL20 and NFKBIA (Figure 2.22). My results indicate that CASP4 acts at the level or upstream of the activation of the IKK since its knockdown interfered with TNF-α-induced phosphorylation of IκB-α (Figure 2.25C).

Caspases are mainly involved in apoptosis induction, however other functions have begun to emerge as well [1]. Upon activation, usually by cleavage of the pro-caspase into two subunits, caspases act as cysteine proteases. CASP4 belongs to the family of inflammatory caspases which are, as the name implies, involved in immune function. In addition to CASP4, two other caspases are members of the family of inflammatory caspases: CASP1 and CASP5 [163]. Both of them did not significantly alter NF-κB reporter activity in either of the screens I have performed. All inflammatory caspases share caspase recruitment

domains (CARD) which are related to the DD. Besides mediating homotypic protein interactions [253], CARD domains further promote interaction with RING, kinase and DD domains [194]. These domains are also found in components of the TNF-α signaling cascade. Accordingly, CARD domain containing proteins are involved in the regulation of NF-κB signaling [24].

CASP1 is the best-studied human inflammatory caspase. It represents the catalytically active component of the inflammasome, an intracellular protein complex activated through pathogen-associated molecular patterns (PAMPs) [164]. Upon activation, CASP1 cleaves pro-IL-1β and pro-IL18 into mature cytokines [164]. Once secreted, these two cytokines are potent mediators of inflammation and activate NF-κB [71, 85]. CASP5, a component of the inflammasome as well, is also involved in pro-IL-1β processing [162].

Interestingly, CASP4 and CASP5 probably arouse by gene duplication of the mouse inflammatory caspase Caspase-11 [164]. Caspase-11 has been implicated in signaling through TLR4 [251] and to be an upstream regulator of mouse Caspase-1, the orthologue of human CASP1 [251]. Besides, mouse inflammatory caspase 12 has been reported to bind to TRAF2 [267], rendering it a potential regulator of TNF-α signaling.

Few functional data are available on CASP4. It has been identified based on its sequence homology to CASP1 [122]. Both caspases share conserved residues in the catalytic site. While CASP4 barely cleaves the CASP1 substrate pro-IL-1β [122], it cleaves and activates CASP1 [72]. CASP4 is expressed in most tissues [122] and its expression has been demonstrated to be induced by interferons [4]. It can be cleaved in an autocatalytical manner or by CASP8 into two subunits of 21 and 10 kDa, respectively [121].

The Induced Proximity Model [200] suggests that caspases are enzymatically activated upon induced aggregation leading to the cleavage of the zymogen. My results indicate that CASP4 is not cleaved upon treatment with TNF-α (Figure 2.30). However, no control for CASP4 cleavage was used since a specific activator of CASP4 is not known. Yet it would be interesting to see whether the pan-caspase-activator citrate would induce cleavage of CASP4 that could be detected by immunoblot [128].

The absent cleavage of CASP4 might be explained by another recent model, which proposes that interaction with other factors induces caspase activation, rather than caspase cleavage [213]. Thus, CASP4 could be catalytically active without being cleaved. I tested whether treatment of HEK293T cells with a CASP4 inhibitor affected NF-κB activation by TNF-α. First experiments indicate that CASP4's catalytical activity is dispensable for its role in TNF-α signaling (data not shown). However, these results have to be interpreted with caution since no positive control for actual CASP4 inhibition was available. An alter-

native to measure CASP4 enzymatic activity after TNF-α treatment could be colorimetric assays where the cleavage of a caspase substrate can be detected via spectrometry. The disadvantage of these assays is yet that there is no really caspase-specific substrate.

Similar to my observations regarding CASP4, CASP8 has been reported to be involved in TNF-α-induced NF-κB activation independent from its caspase activity [42]. How exactly CASP8 mediates NF-κB activation is still elusive. Shikama et al. reported that the death effector domain of CASP8 is required for its role in NF-κB activation [214]. They showed that CASP8 can interact with RIP1 and TRAF2 [214]. Jun at al. in contrast proposed that CASP8 does not bind TRAF2 directly but via its interaction with CASP8AP2 [120]. The authors stated that siRNA-mediated silencing of CASP8 decreased NF-κB reporter activity upon TNF-α treatment in HEK293 cells. I could not confirm these results using the dual luciferase assay in HEK293T cells (data not shown). Likewise, Su et al. reported CASP8 not to be involved in TNF-α-mediated activation of NF-κB in mouse fibroblasts [228]. However, CASP8 was shown to be involved in TLR4- and antigen receptor-induced activation of NF-κB, two signaling pathways that are similar to TNFR1 signaling [228]. Both CASP4 and CASP8 could thus act alike as scaffold proteins. Figure 3.5 presents this conceivable analogous mode of action of CASP4 in TNF-α signaling. Putative interaction partners among TNF-α pathway components for CASP4 could be CARD domain proteins such as IKK-γ as well as RING and DD domain proteins such as TRAF2 and RIP1, respectively [24].

CASP4 has been reported to be an ER (endoplasmatic reticulum)-resident protein [102, 186]. Yet by immunostaining of endogenous CASP4 in HeLa cells I could show that CASP4 mainly localizes to the cytoplasm (Figure 2.29). Cytoplasmic localization of CASP4 would allow interaction with the likewise cytoplasmic TNFR1 complex.

Two reports have demonstrated that CASP4 can interact with TRAF proteins. Lakshmanan et al. have shown that CASP4 played a role in TLR4-mediated activation of NF-κB by interaction with TRAF6 and IRAK1 [140]. Pastorino et al. have reported that CASP4 is involved in TNF-α- and ethanol-induced liver damage [185]. They have shown that TRAF2 is recruited to ER-localized CASP4 in HepG2 cells. However, this interaction was only observed when cells were treated with both TNF-α and ethanol, but not with TNF-α alone [185]. Similarly, I could not detect any interaction of CASP4 and TRAF2 by immunoprecipitation of the two endogenous proteins nor by immunofluorescence microscopy in HeLa cells (data not shown). This was true for untreated as well as TNF-α treated cells. One explanation for these results might be that TNF-α alone may not induce interaction between TRAF2 and CASP4, in agreement with Pastorino and coworkers. Another

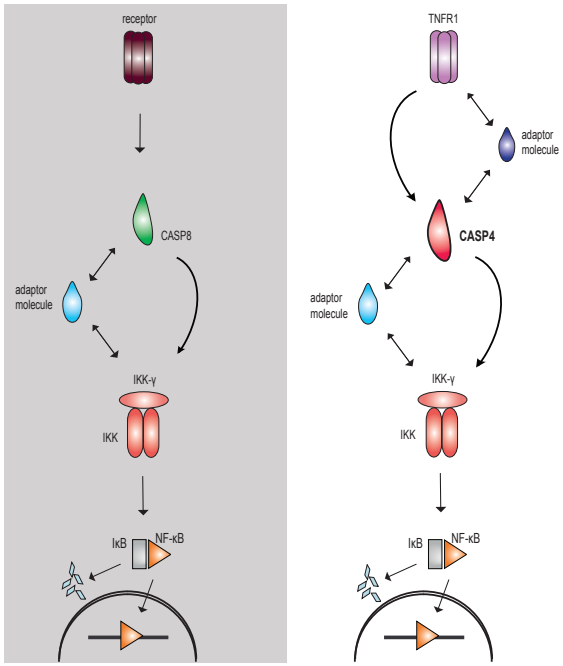

Figure 3.5: Model of CASP4's mode of action in TNF-α signaling. As described for other caspases such as CASP8 (left grey panel), CASP4 could serve as a scaffold protein at the TNFR1 complex. As a CARD domain protein, CASP4 could interact either with DD proteins like TNFR1 and RIP1, TRAF proteins like TRAF5 or other CARD proteins like IKK-γ.

explanation might be that the interaction between CASP4 and TRAF2 is too transient or weak to be detected working with endogenous protein levels. It would be interesting to repeat the immunoprecipitation assays while overexpressing one of the two proteins, although these kind of experiments would have to be interpreted carefully due to possible overexpression artifacts. Similarly, I could not detect an interaction of CASP4 with RIP1 (data not shown). IKK-γ and the other TRAF protein present at the TNFR1 complex, TRAF5, represent plausible targets for future investigations.

3.3 Outlook

Making use of carefully designed assays, RNAi screens represent a powerful technique to identify novel components of signaling pathways. Application of stringent filters to select primary hits and multiple secondary assays are required to determine the most promising candidates for further characterization, as presented here. However, also the caveats of RNAi screens have to considered. As reported here and by others (e.g. [157, 66, 226]), the high false positive and negative rates in high-throughput experiments can be problematic aggravating interpretation of screening results. Better statistical methods to analyze RNAi screening data might help to decrease false positive and negative rates. This is especially important for facilitating the use of RNAi screening data for gaining systems biology perspectives on biological processes. In addition, improved and more standardized screening designs could yield more robust results, enabling a better comparability of screens. Unspecific effects of siRNA transfection procedures or of siRNAs themselves is another challenge that has to be faced. In the near future a worthwhile method to exclude these unspecific effects and to confirm RNAi phenotypes could be knockout cells created by zinc finger nucleases, a technique that has recently been developed [191, 37].

After selection of screening hits and their confirmation, the biggest challenge consists in assessing the biological function of identified novel regulators. By using assays monitoring fast signaling events after TNF-α stimulation I could show that SPP1, GAB3 and CASP4 play a role in the direct signaling cascade from TNFR1 to IKK. Further research has to focus on the functional characterization of these candidates. Rescue experiments using human expression constructs that will not be targeted by siRNAs will be established. These rescues will allow functional studies, e.g. deletion of protein domains to assess their requirement for signaling activity. Additionally, in order to map SPP1, GAB3 and CASP4 into the TNFR1 pathway, interaction partners have to be identified. In parallel to optimizing immunoprecipitation conditions, constructs for Yeast-2-Hybrid screening are currently designed for employing a method other than a candidate approach for identifying interaction partners of SPP1, GAB3 and CASP4. By these means, the exact role of the three novel regulators of TNF-α signaling - SPP1, GAB3 and CASP4 - will be determined.

Chapter 4

Material and Methods

4.1 Material

4.1.1 Cell lines

Cell line	*Cell type*	*supplied with by*
HEK293T	human embryonic kidney cells	C. Niehrs, DKFZ, Heidelberg
HeLa	human cervix carcinoma cells	DKFZ, Heidelberg
HepG2	hepatoma cells	T. Dick, DKFZ, Heidelberg

4.1.2 Chemicals, media, buffers and solutions

Chemicals All chemicals were purchased from Sigma if not stated otherwise (see below).

adenosine triphosphate (ATP)	Roche
bicine	Gerbu
bovine serum albumin (BSA)	Gerbu
ethylenediaminetetraacetic acid (EDTA)	Applichem
H_2SO_4	V. Stadler, DKFZ, Heidelberg
3-(N-Morpholino)propanesulfonic acid (MOPS)	Applichem
NaCl	VWR
sodium dodecyl sulphate (SDS)	Gerbu
TritonX-100	Applichem

Media, buffers and solutions

Human complete medium	Dulbecco's Modified Eagle Medium (DMEM), Invitrogen, #41965062 supplemented with 10% fetal calf serum
Fetal calf serum	Biochrom, #S0115
RPMI 1640 medium	Invitrogen, #31870074
Trypsin-EDTA (1x)	Invitrogen, #25200056
PBS (1x)	137 mM NaCl, 2.7 mM KCl, 10 mM Na_2HPO_4, 2 mM KH_2PO_4; Invitrogen, #P3813
Cryoprotective medium	Fetal calf serum containing 10% dimethylsulfoxide (DMSO)
Trypan Blue	Sigma, #T8154
Cell lysis buffer	1x PBS, 10% Triton, protease inhibitor, phosphatase inhibitors
5x siRNA buffer	Dharmacon/Thermo Fisher Scientific, #B-002000-UB-100
Laemmli buffer	62.5 mM Tris-Cl (pH 6.8), 10% glycerol, 2% SDS, 5% β-Mercaptoethanol, 0.02% Bromophenol Blue, 0.1 M DTT
SDS PAGE running buffer	50 mM Tris Base, 50 mM MOPS, 1.025 mM EDTA, 69.3 mM SDS
Western Blot transfer buffer	0.5 M BisTris, 0.5 M bicine, 0.02 M EDTA
TBS-Tween (TBS-T)	0.137 M NaCl, 0.02 M Tris-HCl (pH 7.8), 0.1 % Tween20
Western Blot blocking buffer	5% milk in TBS-T
Antibody dilution buffer	0.5% milk in TBS-T
Western Blot stripping solution	0.2 M NaOH
ELISA blocking buffer	1% BSA in 1x PBS
ELISA washing buffer	0.05% Tween20 in 1x PBS
ELISA sample buffer	0.1% BSA in 1x PBS
ELISA stopping buffer	2 N H_2SO_4
Immunofluorescence blocking buffer	1% BSA in 1x PBS
SOC	2% tryptone, 0.5% yeast extract, 10 mM $MgCl_2$, 20 mM glucose
buffer G	Promega, #R007A
50x Tris-acetate-EDTA (TAE) buffer	1 M Tris base, 50 mM EDTA, 9 mM NaCl, 25 mM KCl, 17.5% glacial acetic acid
FACS buffer	4% FCS in PBS

4.1.3 siRNAs, plasmids and transfection reagents

Genome-wide knockdown experiments were performed with a synthetic siRNA library, library A, vended by Dharmacon (Human Genome Set (#G-005000), Druggable Set (#G-004650), Human Protein Kinases (#G-003500) and G Protein-Coupled Receptors (#G-003600); Dharmacon/Thermo Fisher Scientific) - covering all unique genes annotated in the human Reference Sequence (RefSeq) collection (National Center for Biotechnology Information) version 5.0 - and a synthetic siRNA library, library B, vended by Qiagen (#1027490, Human Druggable Genome Set Version 3.0 and Human Whole Genome Supplement Set Version 1.0). Libraries sequences were annotated using RefSeq release 27.

Screening results were validated making use of deconvoluted siRNA-pools (siGENOME set of four upgrade, Dharmacon/Thermo Fisher Scientific) and siRNA pools picked from the genome-scale siRNA library from Qiagen. Sequences of the siRNAs that were used in further experiments are listed in table4.1. All these siRNAs were purchased from Dharmacon (Thermo Fisher Scientific). Lyophilized siRNAs were reconstituted in 1x siRNA buffer and further diluted with nuclease-free water to a concentration of 500 nM (Dharmacon siRNAs) or 200 nM (Qiagen siRNAs).

Dharmafect 1 transfection reagent	Dharmacon/Thermo Fisher Scientific, #T-2001-04
TransIT-LT1 Transfection reagent	VWR/Mirrus, #731-0029MIRUMIR2306
4-4-FL	NF-κB dependent *firefly* luciferase expression plasmid, based on "pGL3 promoter" (Promega)
act-RL	*Renilla* luciferase expression plasmid, bearing β-actin promoter, based on "pRL null" (Promega)
CMV-RL	T. Dick, DKFZ, Heidelberg
TK-RL	Promega
pcDNA5	empty vector, Invitrogen
RIP1	Tobias Haas
TRADD	Tobias Haas
IKK-β	Tobias Haas

Table 4.1: siRNA sequences of controls and candidates. NA: not available. (For IDs of all siRNAs used in this work see supplementary table A.10.)

RefSeq	Symbol		siRNA	sequence
NM_001065	TNFRSF1A	1	D-005197-01	CAAAGGAACCUACUUGUACUU
		2	D-005197-02	GAGCUUGAAGGAACUACUAUU
		3	D-005197-03	CACAGAGCCUAGACACUGAUU
		4	D-005197-04	UCCAAGCUCUACUCCAUUGUU
NM_001066	TNFRSF1B	1	D-003934-01	GCACAUGCCGGCUCAGAGAUU
		2	D-003934-02	CAUCAGACGUGGUGUGCAAUU
		3	D-003934-03	UCACUUGCCUGCCGAUAAGUU
		4	D-003934-04	UAAUAGGAGUGGUGAACUGUU
NM_033306	CASP4	1	D-004404-01	GGACUAUAGUGUAGAUGUA
		2	D-004404-02	GAGACUAUGUAAAGAAAGA
		3	D-004404-04	GAGGGAAUCUGCGGAACUG
		4	D-004404-17	UAGAGGAAGUAUUUCGGAA
NM_001081573	GAB3	1	D-015239-01	GAAGAAAGCUACAUCGAAA
		2	D-015239-02	GAGAUGACCCAAACACUAA
		3	D-015239-03	UGUGAUAGCUGGUCAAACU
		4	D-015239-04	CCACCAUUCAGGUAGAUAA
NM_001040058	SPP1	1	D-012558-05	CAUCUUCUGAGGUCAAUUAUU
		2	D-012558-06	UGAACGCGCCUUCUGAUUGUU
		3	D-012558-07	CCGAUGUGAUUGAUAGUCAUU
		4	D-012558-08	GGACUGAGGUCAAAAUCUAUU
NM_002205	ITGA5		D-008003-05	ACACGUUGCUGACUCCAUU
			D-008003-06	GAACGAGUCAGAAUUUCGA
			D-008003-07	CAAACGCUCCCUCCCAUAU
			D-008003-20	UGAAGAUGCCCUACCGAAU
NM_130799	MEN1		D-011082-02	GAUCAUACAUGCGCUGUGA
			D-011082-03	GGAGCUGGCUGUACCUGAA
			D-011082-04	GAUCAUGCCUGGGUAGUGU
			D-011082-17	CGGCAGAAGGUGCGCAUAG
NM_006866	LILRA2		D-019855-01	GCUGAGGAGUACCAUCUAU
			D-019855-02	AAAUCAGCAUCCUGGGUUA
			D-019855-03	CCAGAGAAGCCUACAAGAU
			D-019855-04	CUACAGCCACAAUCACUCA
NM_004205,	USP2		D-006069-01	CCAGCAAGCUCACAACAUUUU
NM_171997			D-006069-02	UCGCUGACGUGUACAGAUUUU
			D-006069-03	GAACCUCGAUCAUCUUCCUUU
			D-006069-04	GCCGACAGAUGUGGAGAAAUU
NM_021975	RelA		D-003533-03	GGAUUGAGGAGAAACGUAAUU
			D-003533-04	CUCAAGAUCUGCCGAGUGAUU
			D-003533-05	GGCUAUAACUCGCCUAGUGUU
			D-003533-18	GAUUGAGGAGAAACGUAA
NM_003804	RIP1		D-004445-03	GAAAGAGUAUUCAAACGAAUU
			D-004445-04	CCACUAGUCUGACGGAUAAUU
			D-004445-05	GAAGCCAACUACCAUCUUUUU
			D-004445-06	GCACAAAUACGAACUUCAAUU
NA	siCon #1		D-001210-01-20	
NM_002335	LRP5		D-003844-01	CCAACGACCUCACCAUUGAUU
			D-003844-02	GCAUGACGCUGGUGGACAAUU
			D-003844-03	CCGACGAGCUCAUGUGUGAUU
			D-003844-04	CGUCAAAGCCAUCGACUAUUU
NA	siRL	NA	P-002070-01-05	AAACATGCAGAAAATGCTG

Cloning of 4-4-FL As a pathway specific reporter, a NF-κB-dependent *firefly* luciferase (FL) expression plasmid was cloned (4-4-FL). The first step of the cloning consisted in annealing and ligating six oligos (table 4.2) containing all together eight times the following NF-κB binding site: GGGGACTTTCC [NF-κB binds the consensus sequence 5'-GGGRN W YYCC-3' (where G stands for purine base, N denotes any base, W is an adenine or thymine, Y denotes a pyrimidine base] [209, 143, 43]). The ends bore XmaI (5' end) and BglII (3' end) restriction sites that were used to ligate it into "pGL3 promoter". Correct cloning was controlled by sequencing the insert from both ends (see Figure 4.1).

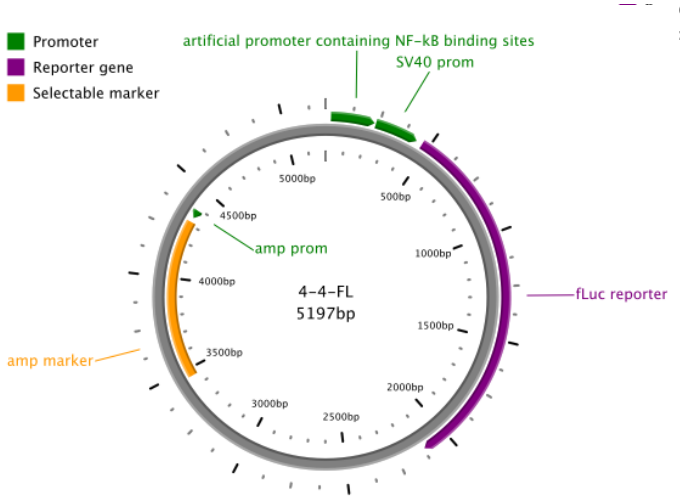

Figure 4.1: Plasmid map of the 4-4-FL NF-κB reporter. fluc: *firefly* luciferase, amp: ampicillin, prom: promoter, SV: Simian Virus.

Cloning of act-RL The β-actin promoter, an approx. 1100 bp sequence in the 5' untranslated region of the β-actin coding sequence, was amplified using PCR primers bearing restriction sites for HindIII (5' end) and SpeI (3' end, table 4.2). These restriction sites were used to insert the promoter sequence into cut "pRL null" being cut with the same restriction enzymes. Correct cloning was controlled by sequencing the inserted promoter sequence from both ends (see Figure 4.2).

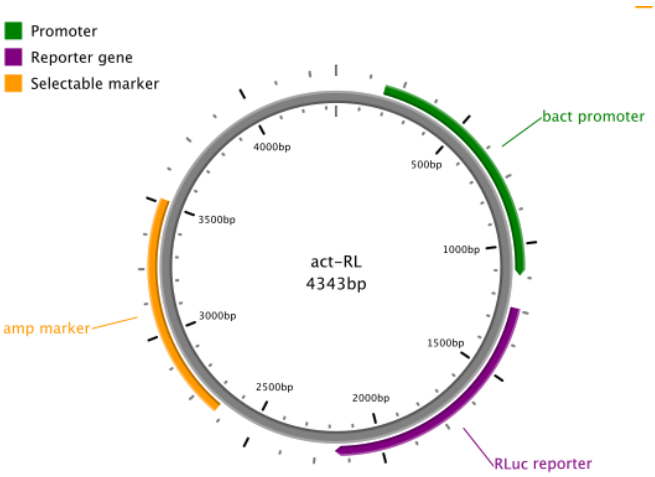

Figure 4.2: Plasmid map of the act-RL co-reporter. amp: ampicillin, bact: β-actin, RLuc: *Renilla* luciferase.

4.1.4 Antibodies

antigen	*company*	*application*	*dilution*
phospho-IκB-α (5A5, mouse)	Cell Signaling, #9246S	immunoblotting	1:2000
α-tubulin (DM1A, mouse)	Sigma, #T9026	immunoblotting	1:10 000
CASP4 (4B9, mouse)	MBL, #M029-3	immunoblotting	1:1000
		immunofluorescence	1:500
TRAF-2 (C192, rabbit)	Cell Signaling, #4724	immunofluorescence	1:100
calnexin (mouse)	M. Weiss (DKFZ)	immunofluorescence	1:100
anti-mouse IgG1 HRP (goat)	Southern Biotech, #1070-05	immunoblotting	1:20 000
anti-mouse HRP (sheep)	GE Healthcare, #NA931	immunoblotting	1:10 000
anti-rabbit Alexa594 (goat)	Invitrogen, #A11012	immunofluorescence	1:1000
anti-mouse Alexa488 (goat)	Invitrogen, #A11001	immunofluorescence	1:1000
Enbrel	P. Krammer (DKFZ)	cell culture	12.5 μg/ml
IgG control	P. Krammer (DKFZ)	cell culture	12.5 μg/ml
TNFRSF1A (MABTNFR1-B1, mouse)	BD Pharmingen, #550514	FACS	1:50
TNFRSF1B (M1) (rat)	BD , #551311	FACS	1:50
mouse and rat isotype controls	H. Walzcak, London	FACS	1:200
F(ab')$_2$ Anti-Mouse IgG (H+L) Biotin (goat)	Southern Biotech, #1032-08	FACS	1:100
Anti-Rat IgG Biotin (goat)	Southern Biotech, #3030-08	FACS	1:200
Streptavidin-PE	BD	FACS	1:200

4.1.5 Enzymes and kits

human CXCL8/IL-8 ELISA	R&D, #DY208
CellTiterGlo	Promega, #G7571
BCA assay	Pierce (Perbio), #23227
QIAprep Spin Miniprep Kit	Qiagen, #27106
Endofree Plasmid Maxi Kit	Qiagen, #12362
ECL Plus	Amersham, #RPN 2131
phosphatase inhibitor	Sigma, Phosphatase Inhibitor Cocktails 1 and 2
Complete Mini Protease Inhibitor	Roche, #11836153001
XmaI	NEB, #R0180S
BglII	NEB, #R0144S
SpeI	NEB, #R0133S
HindIII	NEB, #R0104S
Phusion	NEB, #F-530 S
T4 DNA ligase	NEB, #M0202S
T4 polynucleotide kinase (PNK)	NEB, #M0201S
Lambda Protein Phosphatase	NEB, #P0753S
Taq DNA Ploymerase	Qiagen, #201207
probes master	Roche, #4887301001
superscript III with RT-buffer	Invitrogen, #18080044
RNAse inhibitor	Fermentas, #EO0381

4.1.6 Oligos

Oligos for cloning

Table 4.2 lists the oligos that were used for cloning of the luciferase contructs for the dual luciferase assay. For 4-4-FL cloning, oligos 1a and 1b, 2a and 2b and 3a and 3b were first annealed to each other, before 1 was ligated with 2 and 3. The ligated insert was cut with XmaI (5', oligo 1) and BglII (3', oligo 3). The oligos for act-RL cloning were used as PCR primers.

qPCR primers

Table 4.3 lists all qRT-PCR primers and respective universal probe library (UPL) probes that were used in qRT-PCR assays.

Table 4.2: Oligos for cloning of luciferase contructs.

4-4-FL cloning	
oligo	**sequence**
1a	CCGGGTCAGAGGGGACTTTCCGAGAGGCGTCAG
	AGGGGACTTTCCGAGAGGCGTCAGAGGGGACTTTCCGAGA
1b	TGACGCCTCTCGGAAAGTCCCCTCTGACGCCTCTC
	GGAAAGTCCCCTCTGACGCCTCTCGGAAAGTCCCCTCTGAC
2a	GGCGTCAGAGGGGACTTTCCGAGAGGCGTCAGAG
	GGGACTTTCCGAGAGGCGTCAGAGGGGACT
2b	TCTCGGAAAGTCCCCTCTGACGCCTCTCGGAAAGTC
	CCCTCTGACGCCTCTCGGAAAGTCCCCTC
3a	TTCCGAGAGGCGTCAGAGGGGACTTTCCGA
	GAGGCGTCAGAGGGGACTTTCCGAGAGGCGA
3b	AGATCTCGCCTCTCGGAAAGTCCCCTCTG
	ACGCCTCTCGGAAAGTCCCCTCTGACGCC

act-RL cloning	
oligo	**sequence**
left primer	agtcaagcttgcgagggcagtgcagactttctctatc
right primer	agtcactagtatctcaaggcgaggctcgtgctc

Table 4.3: qRT-PCR primers for references, controls, candidates and target genes.

RefSeq	**Gene Symbol**	**Forward Primer**	**Reverse Primer**	**UPL #**
NM_002046	GAPDH	agccacatcgctcagacac	gcccaatacgaccaaatcc	60
NM_000194	HPRT1	tgaccttgatttattttgcatacc	cgagcaagacgttcagtcct	73
NM_021975	RelA	cgggatggcttctatgagg	ctccaggtcccgcttctt	47
NM_001065	TNFRSF1A	gagaggccatagctgtctgg	gaggggtatattcccaccaac	59
NM_000594	TNF	cagcctcttctccttcctgat	gccagagggctgattagaga	29
NM_000584	IL8	agacagcagagcacacaagc	atggttccttccggtggt	72
NM_004591	CCL20	gctgctttgatgtcagtgct	tcaaagttgcttgctgcttc	39
NM_020529	NFkBIA	gtcaaggagctgcaggagat	gatggccaagtgcaggaa	38
NM_001165	BIRC3	cttgtccttgctggtgcat	aagaagtcgttttcctcctttgt	44
NM_001081573	GAB3	tccagagaagacgaagaaagcta	cgtaagggcaccactgct	25
NM_006866	LILRA2	caaccctacctgctgtctc	gtgttggcctagggatgct	1
NM_002205	ITGA5	caacatctgtgtgcctgacc	ccaggtacacatggttctgc	11
NM_001040058	SPP1	tttcgcagacctgacatcc	ggctgtcccaatcagaagg	61
NM_130799	MEN1	gacccactcaccctctacca	tgtgttcatcccgatagtaggtc	30
NM_033306	CASP4 gamma	gaccaaatatcccccaataaaaa	caaagcttgagggcatctgt	2
NM_004205	USP2	ttcgactcgtccatactcca	tggcactcagtggggact	34

4.1.7 Miscellanous

nuclease-free water	Acros Organics, #327390050
TNF-α	Biosource/Invitrogen, #PHC3015
vecta shield	Biozol, #VEC-H-1000
NuPage precast 10% Bis-Tris non-gradient gels	Invitrogen, #NP0301BOX
PageRuler Prestained Protein ladder plus	Fermentas, #SM1811
ECL detection membrane	GE Healthcare, #RPN2132
Fuji Super RX 100NIF medical X-ray film	Kisker, #RX1318
DH5α	competent *Escherichia coli*, Invitrogen, #18263012
dNTPs	Fermentas, #R0182
oligo dT primer	home-made (see pimer list)
Hoechst	Invitrogen, #H1399
RNase-Free Spray	Steinbrenner, #SL-5454
non-fat dry milk	Biorad, #170-6404
Parafilm	VWR, #291-1219
Stericup-GP, Filtertop + Bottle	Millipore, #SCGPU05RE
Sybr Safe	Invitrogen, #S33102
TrackIt 100 bp DNA ladder	Invitrogen, #10488058
Lysis buffer and substrates for luciferase assays	home-made, confidential recipe

4.2 Methods

4.2.1 Cell culture and cell maintenance

Human embryonic kidney (HEK) 293T cells, human cervix carcinoma cells (HeLa) and hepatoma cells (HepG2) were maintained in complete medium at 37°C in a humidified atmosphere with 5% CO_2. Every 2-3 days, the adherent cell layer was washed with PBS, incubated for approximately 30 seconds (HEK293T) or 4 minutes with 1x trypsin and separated cells were resuspended in complete medium. Cells were diluted 1:5 and 1:10 being seeded in 75 cm^2 cell culture flasks with vented cap (BD Falcon). All cell types were always kept below a maximum confluence of 80-95% and a passage number lower than passage 20.

To preserve cells, cells out of one 75 cm^2 cell culture flask were resuspended in 2 ml ice-cold cryoprotective medium and aliquoted into screw cap cryogenic vials (Corning) (i.e. approximately 4-5 million cells per vial). Vials were placed in isopropanol filled "Mr.

Frosty" (Neolab) and gently cooled down by being placed at -80°C over night prior to being stored in liquid nitrogen. Cells were thawed at 37°C (waterbath Julabo TW12) before being spun down (Centrifuge 5804, Eppendorf) in 9 ml culture medium and seeded in 12 ml in a 75 cm^2 cell culture flask.

For determing cell number when cells were seeded for assays, cells were stained with trypan blue and counted using a standard Neubauer hemocytometer (VWR).

4.2.2 Transfection protocols

siRNA transfections

Generally, siRNAs were transfected into cells using a reverse transfection method, i.e. cells were seeded onto siRNAs mixed with the transfection reagent DharmaFect1. siRNA final concentration was 50 nM for Dharmacon siRNAs and 20 nM for Qiagen siRNAs. Genome-wide screens were done in duplicates. All other experiments in 384-well format were carried out at least in quadruplicates and were repeated at least three times. For experiments with more than two plates, the Biomek FX pipetting robot (Beckman Coulter) was used to distribute siRNAs in the 384-well plates. Transfection reagent, cells, plasmid mix and TNF-α were pipetted using an automated 8-channel liquid dispenser (Multidrop, Thermo Labsystems).

384-well plate format 0.05 μl DharmaFECT1 were gently mixed with 4.95 μl RPMI per well and incubated for 10 min at room temperature before another 10 μl RPMI were added. This mix was then pipetted to 5 μl 500 nM (Dharmacon) or 200 nM (Qiagen) siRNA (in siRNA buffer) followed by another incubation for 30 min at room temperature. $4*10^3$ (HEK293T) or $4.5*10^3$ (HepG2) cells in 30 μl (antibiotics free) culture medium were seeded on top of the siRNAs, plates were shortly spun (Centrifuge 5804, Eppendorf) to collect all liquid at the bottom of the wells and then kept in the incubator (Binder) for three days to allow for protein depletion.

96-well plate format - HEK293T cells Per well (Microtest Tissue Culture Plate 96 well Flat Bottom, Falcon), 0.2 μl DharmaFECT1 were gently mixed with 9.8 μl RPMI and incubated for 10 min at room temperature. This mix was then added to 10 μl 500 nM siRNA (in RPMI) followed by another incubation for 30 min at room temperature. $1.7*10^4$ cells in 80 μl (antibiotics free) culture medium were seeded on top of the siRNAs and kept in the incubator for three days to allow for protein depletion.

24-well plate format - HeLa cells 0.35 μl DharmaFECT1 were gently mixed with 49.65 μl RPMI per well (24-well tissue culture plate, Greiner) and incubated for 10 min at room temperature. This mix was then added to 50 μl 500 nM siRNA (in RPMI) followed by another incubation for 30 min at room temperature. $2*10^4$ cells in 400 μl (antibiotics free) culture medium were seeded on top of the siRNAs, gently mixed to distribute cells equally in the well and kept in the incubator for two days to allow for protein depletion.

6well plate format - HeLa cells Per well, 1.5 μl DharmaFECT1 were gently mixed with 196 μl RPMI in a 1.5 ml tube (Eppendorf) and incubated for 10 min at room temperature. Then 2.5 μl siRNA [20 μM] were added, followed by another incubation for 30 min. The mix was pipetted into the well, $1.3*10^5$ cells in 800 μl were added and gently mixed. Transfected cells were kept in the incubator for two days to allow for protein depletion.

Dual luciferase assay and plasmid transfections

Dual luciferase assay Luciferase assays were performed in 384-well format (white plates, Greiner). TransIT served as transfection reagent. Cells were contained in 50 μl (antibiotics free) culture medium per well, seeded on the day before.

Per well, 0.2 μl TransIT were gently mixed with 4.8 μl RPMI and incubated for 10 min at room temperature before being added to 15 μl RPMI containing the plasmids. For HEK293T cells, in total 50 ng plasmid were transfected: 2 ng of the *Firely* luciferase expression plasmid, 20 ng of the *Renilla* luciferase expression plasmid and 28 ng empty plasmid. For HepG2 cells, 2 ng of the *Firely* luciferase expression plasmid and 55 ng of the *Renilla* luciferase expression plasmid were used. After addition of the transfection reagent, the mix was incubated for another 30 min. Then, the transfection mix was added to the cells, plates were shortly spun (Centrifuge 5804, Eppendorf) to collect all liquid at the bottom of the wells and then kept in the incubator (Binder) for two days to allow for plasmid expression.

16 (HEK293T) or 24 (HepG2) hours prior to the readout, cells were stimulated with 10 μl TNF-α in (antibiotics free) culture medium to yield a final concentration of 20 (HEK293T) or 50 (HepG2) ng/ml.

For the luciferase readout, medium was sucked off wells using a 24-channel wand (V&P scientific) and 20 μl lysis buffer was added. Cells were lysed for 20 min prior to addition of 30 μl of the substrates, first for the *firefly* luciferase and then - after measuring luminescence with a Mithras LB940 plate reader (Berthold Technologies) - for the *Renilla* luciferase. *firefly* luciferase luminescence was measured without filter, *Renilla* luciferase luminescence using a filter at 485 nm. Data was analyzed by dividing the measured *firefly* luciferase

luminescence counts by the *Renilla* luciferase luminescence counts and then avaraging values corresponding to one treatment.

4.2.3 Measuring cell viability using the CellTiterGlo assay

Cell viability was measured in 384-well format (white plates, Greiner) using the CellTiterGlo assay which assesses ATP content in wells of lysed cells for infering cell number. The CellTiterGlo reagent contains a luciferase and its substrate which is converted in a luminescent product ATP-dependently.

Medium was sucked off using a 24-channel wand (V&P scientific) and per well 20 μl of a mix of CellTiterGlo reagent with (serum and antibiotics free) DMEM (1:4) was added. After an incubation for 20 min in the dark, luminescence was measured without filter with a Mithras LB940 plate reader (Berthold Technologies).

4.2.4 ELISA

For ELISA, cells were reverse transfected with siRNAs using the standard protocol (see 4.2.2). ELISAs were carried out in parallel to luciferase assays, but instead of transfecting plasmids, 20 μl (antibiotics free) medium was added per well. After 16 (HEK293T) or 24 (HepG2) hours of incubation with a final concentration of 20 (HEK293T) or 25 (HepG2) ng/ml TNF-α, supernatents were harvested pooling 8 equally treated wells. Interleukin (IL)-8 concentration of supernatents, undiluted or 1:2 diluted in reagent diluent, was assessed using the human CXCL8/IL-8 ELISA kit by following exactly manufacturer's instructions. Measurements were carried out in technical duplicates in 96-well format (MaxiSorp F, Nunc), the standard supplied by the vendor was applied in a range from 0 - 1000 pg/ml. Absorbance was measured with the Mithras LB940 plate reader (Berthold Technologies) having the filter set at 450 nm.

4.2.5 Handling bacteria

Transformation DH5α *E. coli* (50 μl aliquot) were thawed on ice before adding the plasmid to be transformed with: for re-transformations 0.5 μl vector, for first transformations after cloning 5 μl vector were used. After an incubation of approximately 15 min on ice, bacteria were heat-shocked at 42°C for 30 seconds and then placed on ice for 2 min. Then, bacteria were mixed with 500 μl SOC medium and incubated at 37°C for 45-60 min while shaking (Thermomixer!). After spinning down in a benchtop centrifuge (5415D, Eppendorf) for 10 min at 5000 rpm, half of the medium was discarded and bacteria were resupended in the other half. Bacteria (50 - 200 μl) were plated on agar plates containing the appropriate antibiotic for selection which where then placed at 37°C over night.

Colony PCR For verifying that bacteria contained the plasmid with the intended insert, colony PCRs were performed. For this purpose, 10 μl sterile water were pipetted into a PCR tube (Biozym), one bacterial colony was picked with a yellow tip and then mixed with the water. 3 μl of this mix were taken for a PCR.

The general PCR mix contained - besides these 3 μl - 5 μl PCR buffer (coral load, supplied with Qiagen Taq polymerase), 1 μl dNTPs (10 mM), 2 μl each 5' and 3' primers (10 pmol/μl), 2 μl Taq in a total volume of 50 μl (filled up with H_2O).

The general PCR protocol was the following:

one cycle:	5 min at 95°C
then 35 cycles:	1 min at 95°C,
	1 min at ((melting temperature oligos)-2)°C,
	1 min/kb at 72°C
then 1 cycle	72°C for 10 min
and finally cooling down to 4°C.	

PCRs were evaluated on 1% agarose gels in 1x TAE buffer.

4.2.6 Cloning

PCR using Phusion When the proof-reading DNA polymerase "Phusion" was used, the following PCR protocol was used:

one cycle:	30 sec at 98°C
then 35 cycles:	10 sec at 98°C,
	30 sec at ((melting temperature oligos)+3)°C,
	30 sec/kb at 72°C
then 1 cycle	72°C for 10 min
and finally cooling down to 4°C.	

PCRs were evaluated on 1% agarose gels in 1x TAE buffer.

Digest of DNA Restriction digests were done in a final volume of 20 μl (filled up with water). 10 μl of a mini prep (prepared according to manufacturer's instructions) were mixed with 2 μl of the appropriate buffer, 1 μl total enzyme (so 0.5 μl per enzyme if it was a double digest) and - when needed - 2 μl BSA. Digest were done for 1-2 h at 37°C. If needed, enzymes were heat-inactivated at 65°C for 20 min.

Annealing of oligos 10 μl of 2 to-be-annealed oligos (100 μM) were mixed with each other and added to 2.5 μl buffer G, 15 μl $MgCl_2$ (25 nM) and 12.5 μl H_2O in a 1.5 ml tube (Eppendorf). After mixing, the tube was placed in a water bath (Yulebo) heated up to 95°C. After 5 min, the waterbath was switched off, leaving the tube inside to slowly cool down over night.

For ligations, annealed oligos had to be phosphorylated. For this purpose, 15 μl annealed oligos (100 μM) were mixed with 2 μl polynucleotide kinase (PNK) buffer, 2 μl ATP (10 mM) and 1 μl PNK. The mix was incubated for an hour at 37°C before the enzyme was heat-inactivated at 65°C for 20 min.

Ligation of inserts into vectors Inserts were ligated into cut vectors usually at the ratio 1:3 or 1:1, calculated using "Promega Biomath" (http://www.promega.com/biomath). Reaction batches were pipetted in a final volume of 20 μl (filled up with water):

x μl oligo
200 ng vector (cut)
1 μl T4 DNA ligase
2 μl T4 DNA ligase buffer

Ligations were performed over night at 16°C.

4.2.7 RNA extraction, cDNA synthesis and quantitative real time PCR

RNA extraction was done with the help of the RNeasy kit. Usually, RNA was extracted from cells being reverse transfected in 96-well plates according to the standard protocol (see 4.2.2). After two days of transfection, medium was sucked of and 50 μl RLT buffer per well were added. After waiting for 2-3 min at room temperature, the RLT-cell mix was pipetted up and down with small tips (for shearing genomic DNA), transferred into PCR tubes (Biozym) and then frozen over night at -80°C. Thawed on the next day, the content of the PCR tubes corresponding to one row of a 96-well plate were pooled and RNA was extracted according to manufacturer's instructions, performing DNase digest on column. RNA was eluted from the column in 30 μl.

RNA concentration was measured using a nanodrop ND-1000 (Peqlab) and 1 μg of RNA was taken for cDNA synthesis. For this purpose, RNA was mixed with 1 μl of dNTPs (10 mM) as well as of oligo dT primer (0.5 μg/ml) in a volume of 12.25 μl in nuclease free water in a PCR tube and incubated for 5 min at 65°C. After cooling the mix down on ice for approximately 1-2 min, 4 μl of RT buffer, 1 μl DTT, 0.25 μl RNase inhibitor and 0.5 μl superscriptIII were added. Then the tube was incubated at 50°C for 90 min, followed by an

incubation at 70°C for 10 min. Assuming that all RNA was reverse transcribed into cDNA, cDNA concentration usually used for qRT-PCR was 50 ng/μl. (As control, a "minus RT" reaction batch was also pipetted, proceeding in exactly the same way as decribed above, but adding nuclease free water instead of superscriptIII.)

qRT-PCRs were performed in 384-well format (LightCycler 480 Multiwell Plate 384, Roche) using the UPL library from Roche. Two mastermixes were prepared: (A) one containing the probes master and the cDNA, and (B) one containing the 5' and 3' primers and the corresponding probe. For A, 5.5 μl probes master was mixed with 1.1 μl cDNA (50 ng/μl) per 384-well plate well. Since the measurements were made in technical duplicates, the 2.5-fold of the given amounts were used. For B, 0.114 μl probe, 0.436 μl primer mix (20 μM each 5' and 3' primer) and 3.85 μl nuclease free water were mixed. To have sufficient volume for technicel dublicates, the 2.2-fold of the given amounts were used. Mix B was distributed into a 96-well plate (VWR), 9.68 μl per well. Then, 15 μl per well mix A was added and mixed, before 11 μl each were aliquoted into two wells of the qRT-PCR plate and the plate was sealed (LightCycler 480 qPCR seal, Roche). For increasing accuracy, pipetting steps were done using electronic pipettes (Eppendorf Research Pro) and multichannel pipettes (Finnpipette, Thermo Labsystems).

The qRT-PCR program consisted in one cycle first denaturation at 95°C for 10 min, followed by 45 cycles of a three steps program - 10 sec denaturation at 95°C, 20 sec annealing at 55°C, 1 sec elongation at 72°C - and finished with one cycle cooling at 40°C for 20 sec.

Analysis of qPCR data was performed according to [189].

4.2.8 Expression profiling

RNA was extracted using the RNeasy kit as decribed above (4.2.7). RNA quality was assessed by measuring mRNA depletion mediated by respective siRNAs and TNF-α-mediated induction of target genes by qRT-PCT before RNA was handed over to the core facility. RNA was hybridized onto Illumina human Sentrix-8 chips.

4.2.9 Cell lysis, measurement of protein concentration, SDS page and Western Blotting

For immunoblotting experiments HeLa cells were reverse transfected with siRNAs in 24-well format using the standard transfection protocol (see 4.2.2). After two days of siRNA treatment, cells were starved for 3-4 hours by exchanging the culture medium with serum free DMEM. Then, medium was sucked off again and exchanged with culture medium or 50 ng/ml TNF-α containing medium to stimulate cells for either 0, 5, 10 or 20 min (4 wells

per condition). After the stimulation, medium was sucked off, cells were washed with PBS and then trypsinized. Cell pellets were spun down at 5000 rpm for 5 min in a benchtop centrifuge (5415D, Eppendorf) and washed twice with ice cold PBS prior to cell lysis for 30 min in 70 μl lysis buffer containing protease and phosphatase inhibitors. After spinning for 20 min at 13 000 rpm at 4°C, the supernatent was harvested and protein concentration determined using the BCA assay, following manufacturer's instructions. 10 - 20 ng protein were mixed with 5x Laemmli buffer in a total of 20 μl and boiled at 96°C for 5 min. Then, proteins were separated on 10% NuPage Bis-Tris non-gradient gels (Novex, Invitrogen) in 1x MOPS buffer. Gels were run at 100 V until samples had migrated into the gel and then at 200 V (PowerPac Universal, Biorad). After the protein transfer onto nitrocellulose membranes by wet transfer (XCellII Blot Module, Invitrogen) in 2x NuPage transfer buffer, membranes were blocked with 5% non-fat dry milk in TBS-Tween (TBS-T) over night at 4°C. Before adding the phospho-specific antibody in 5% BSA-TBS-T, membranes were washed three times for 10 min with TBS-T; if the first antibody was not a phospho-specific one, membranes were only washed once shortly with TBS-T. Incubation with the first antibody was done over night at 4°C. Before and after the following 1 h incubation with the corresponding secondary antibody (in 0.5% milk-TBS-T), membranes were washed three times for 10 min in TBS-T. Blots were developed by enhanced chemiluminescence following the manufacturer's protocol (Amersham Pharmacia Biotech). To reuse the membrane for incubation with further antibodies, blots were stripped with 0.2 M NaOH for 5 min, then first washed with water and then with TBS-T for 5 min each. Afterwards, membranes were blocked again.

4.2.10 Confocal immunofluorescence microscopy

HeLa cells were reverse transfected with siRNAs in 24-well format using the standard transfection protocol (see 4.2.2 with the exception that cells were seeded onto cover slips (Neolab)). After two days of siRNA treatment, cells were starved for 3-4 hours by exchanging the culture medium with serum free DMEM, followed by another exchange with medium containing 50 ng/ml TNF-α. After stimulation for different periods of time medium was sucked off again, cells were washed and fixed for 20 min at room temperature using 4% Pfa in PBS. After two times washing with PBS, cells were permeabilized with 0.2% Triton-X100 in PBS for 5 min at room temperature, followed by another PBS wash. Cells were blocked for at least an hour prior to incubation with the first antibody over night in a wet chamber at 4°C. For that, cover slips were placed upside down on 20 μl drops of antibody diluted in blocking buffer on parafilm. On the next day, cover slips were washed three times with PBS for 5 min followed by the incubation with the secondary antibody for

an hour at room temperature in a wet chamber at 4°C. After another three PBS washes, cells were stained with Hoechst (1 μg/ml) for 5 min at room temperature and then washed again three times for 5 min in PBS. Cover slips were mounted in vecta shield on objectives (Roth) and sealed with nail polish after drying. Samples were stored at 4°C. Samples were analyzed using a Leica SP5 microscope.

4.2.11 FACS staining

HeLa cells were transfected with siRNAs in 6-well format (see 4.2.2). After two days of incubation to allow for protein depletion, cells were washed once in PBS and then scraped off the wells. Cells were spun down at 1000 rpm for 5 min (Centrifuge 5804, Eppendorf), resuspended in ice cold FACS buffer and transferred into 1.5 ml tubes (Eppendorf). Then cells were spun down in a benchtop centrifuge (5415D, Eppendorf) at 5 000 rpm for 2 min before being resupended in 50 μl FACS buffer containing the primary antibody. Prior to three washes in ice cold FACS buffer, cells were incubated for 30 min on ice. Subsequently, cells were incubated in 50 μl FACS buffer containing the secondary antibody, followed by three washes in FACS buffer. Cells were then stained for 20 min with Streptavidin-PE in FACS buffer before being washed four times in FACS buffer. Cells were resuspended in 80 μl FACS buffer, transferred into a V-bottom 96-well plate (microplate, Greiner) and analyzed using a FACSArray (BD). Settings for detecting HeLa cells were the following:

FSC: 40

SSC: 350

Yellow (PE): 310

4.2.12 Computational analyses

Analysis of RNAi screening data

After RNAi screening, large data sets arise that have to be analyzed systematically. Standardization of values is achieved by excluding intrinsic experimental variations (e.g. due to signal variations of the reporter gene when reading multiple plates). To this end, normalization is performed separately for each plate, replicate and channel. This step comprises a log2 transformation of the measured values in order to obtain a (more) symmetrical data distribution around 0. The screens were then normalized using the method "shorth normalization" (so that the shorth values of all plates are relatively constant). The shorth of x is the shortest interval that covers half of the values in x. The shorth is a more robust estimator of location than the median. After shorth normalization, the ratio of the experimental reporter (*firefly* luciferase) to the invariant coreporter (*Renilla* luciferase) value is determined; this is done to exclude possible artifacts such as cell death affecting both

experimental and invariant reporter genes. To determine the most significant candidate phenotypes of the screen, averaged results from multiple independent assays have to be used. All these steps are implemented into the R/Bioconductor software package "cellHTS" [29]. This software also offers different means for quality assessment of the screening data (e.g. plate views displaying the measured values for each well in a color code so that plate position effects become apparent). cellHTS also computes the Z'-factor which is a statistical way to express how well the distribution of values for positive and negative controls seperate:

$$Z' = 1 - 3\frac{\sigma_{pos} + \sigma_{neg}}{|\mu_{pos} - \mu_{neg}|}$$

where μ are the mean values [of positive (pos) and negative (neg) controls] and σ depicts their standard deviation. The Z'-factor is a commonly used statistical means to assess the quality of an assay, with a Z'-factor of 1-0.5 depicting a very good assay, a Z'-factor of 0.5-0 an acceptable assay and a Z'-factor of <0 depicting a non-acceptable assay [19]. However, the Z'-factor is not really suited to report the quality of a screen as it can only assess whether good positive and negative controls were used.

Analysis by cellHTS yields a list (top table) in which siRNAs are scored and ranked according to the strength of their phenotype, expressed as z-scores. The z-score is a statistical means to expresses how many standard deviation an observation is above or below the mean of all measurements

$$z = \frac{x - \mu}{\sigma}$$

where x depicts the measured value that has to be standardized, μ is the mean of all measurements of the same plate and σ is the standard deviation of this mean. In the analysis of the screens presented here a negative z-score means a reduction in signaling pathway activity, whereas a positive z-score means an increase.

Using online databases for determining screening false negative rates

In order to assess the false negative rate of screens in a systematic manner, the fraction of known regulators of inflammation identified by the screens was determined. Two online databases storing information on which proteins are involved in which signaling pathways were employed. GeneIDs and symbols of genes involved in TNF-α and NF-κB signaling were retrieved from the BioCarta pathways database [17]. This "TNF signaling gene set" contained 82 genes. Additionally, GeneIDs and symbols of genes mediating inflammatory responses were retrieved from the PANTHER database [169, 170]. This "inflammation

gene set" contained 315 genes. The expression of the genes of both lists in HEK293T cells was assessed using sequencing data of total mRNA extracted from HEK293T cells (Dierk Ingelfinger, unpublished data). Genes that were not expressed were excluded from the TNF signaling and inflammation gene sets. After this filtering, the TNF signaling gene set contained 52 genes of which 51 genes were targeted by the overlap of the two libraries (matched by GeneID). Of the remaining 157 genes of the inflammation gene set, 155 genes were targeted by the overlap of the two libraries (matched by GeneID). These genes were tested for their z-scores in screening hit lists.

Analysis of microarray data

Microarray data was read into R using the package "beadarray" [64] . After quality control of the different chips using the package "arrayQualityMetrics" [129], data was normalized using the "vsn" method [113, 114]. Then, two different TNF-α-induced target gene expression signatures were defined: (i) genes altered after 2 hours of TNF-α treatments and (ii) genes altered after 8 hours of TNF-α treatment as compared to unstimulated cells. In order to define a TNF-α-induced gene expression signature, first differentially expressed genes in TNF-α stimulated cells were determined that were treated with the negative contol siRNA. Moderated t-statistics of these differentially expressed genes was calculated using the empirical Bayes [220]. Only those genes were considered in the gene expression signature that passed a false discovery rate (FDR; calculated by the Benjamini and Hochberg method) of maximal 0.1. Subsequently, only those genes out of these significantly differentially expressed genes were selected that were previously published to be TNF-α target genes (downloaded from "bioinfo.lifl.fr :: Bioinformatics Software Server" [18]). The expression signature of these genes was then assessed in all samples. Differential gene expression was assessed using the package "limma" [220]. Expression levels of differentially expressed genes were visualized using a Trellis dot plot. Similarity of gene expression signatures between different samples was assessed using the heatmap.2 function of the "gplots" package.

Appendix A

Supplement

Table A.1: Hit list of screen A. The list was filtered against a list of cytotoxic siRNAs generated in a viability screen. Genes listed here passed a z-score cut-off of $\leq$ -2.5, decreased *firefly* luciferase expression by at least half of the plate median and did not decrease *Renilla* luciferase expression by more than 30%.

Symbol	GeneID	RefSeq	z-score
WDR12	55759	NM_018256	-4.98
SPG7	6687	NM_003119	-4.81
SLC5A1	6523	NM_000343	-4.1
WFS1	7466	NM_006005	-4.1
CHFR	55743	NM_018223	-4.07
WAS	7454	NM_000377	-3.99
SLC4A4	8671	NM_003759	-3.91
SSFA2	6744	NM_006751	-3.88
GEMIN7	79760	NM_024331	-3.71
VAMP3	9341	NM_004781	-3.7
PDE3A	5139	NM_005471	-3.62
SLC8A3	6547	NM_002804	-3.53
TARDBP	23435	NM_007375	-3.5
GJB5	2709	NM_004822	-3.44
WHSC2	7469	NM_005663	-3.42
SLC6A12	6539	NM_002797	-3.39
SLC6A7	6534	NM_002793	-3.37
KNTC1	9735	NM_014708	-3.35
DSCR3	10311	NM_014814	-3.35
EMR2	30817	NM_003590	-3.33
SLC5A2	6524	NM_003041	-3.33
SPP1	6696	NM_000582	-3.29
PIGO	84720	NM_032634	-3.17
PGS1	9489	NM_024419	-3.14
FLJ14466	84876	NM_032482	-3.13
FARSLB	10056	NM_005687	-3.09
RARRES3	5920	NM_004585	-3.05
SSB	6741	NM_003142	-3.05
RIOK2	55781	NM_018343	-3.01
WIT-1	51352	NM_015855	-3
WDR8	49856	NM_017818	-2.96
SPOCK	6695	NM_004598	-2.95
OR1L3	26735	XM_377073	-2.93
KIF4A	24137	NM_012310	-2.92
S100A5	6276	NM_002962	-2.92
PLUNC	51297	NM_016046	-2.91
TBPL2	387332	NM_178431	-2.88
SOX12	6666	NM_006943	-2.87

Symbol	GeneID	RefSeq	z-score
PABPC1	26986	NM_002568	-2.84
SPAG4	6676	NM_003116	-2.83
ZDHHC3	51304	NM_016053	-2.8
SLC9A1	6548	NM_006503	-2.77
STIM1	6786	NM_003156	-2.77
ZNF462	58499	NM_020801	-2.74
LAPTM4A	9741	NM_014713	-2.72
PDE1B	5153	NM_000924	-2.71
CUL3	8452	NM_003590	-2.7
TNIP3	79931	NM_024873	-2.68
USP2	9099	NM_004205	-2.67
TOMM7	54543	NM_016077	-2.67
ABTB2	25841	NM_002492	-2.66
SLC39A10	57181	NM_019895	-2.66
ERN1	2081	NM_001433	-2.64
TMC1	117531	NM_138691	-2.64
CCT4	10575	NM_006430	-2.64
H1FX	8971	NM_006026	-2.64
XPO7	23039	NM_015024	-2.63
GOLPH2	51280	NM_015948	-2.63
MGC14126	84984	NM_032898	-2.62
SLC6A11	6538	NM_002795	-2.6
PTPDC1	138639	NM_152422	-2.59
LRDD	55367	NM_018494	-2.59
SPTLC2	9517	NM_003908	-2.58
LOC389429	0	XM_371847	-2.58
PIGA	5277	NM_002108	-2.57
CAMK1D	57118	NM_020397	-2.55
KLK4	9622	NM_004674	-2.55
GTF2A1	2957	NM_015859	-2.55
FREB	84824	NM_022342	-2.53
AKR1C2	1646	NM_001354	-2.51
AKR1C2	1646	NM_001354	-2.51
CEBPD	1052	NM_001088	-2.51
LOC387882	387882	NM_021649	-2.5
FLJ35696	388341	XM_036729	-2.5

Table A.2: Hit list of screen B. Genes listed here passed a z-score cut-off of $\leq$ -2.5, decreased *firefly* luciferase expression by at least half of the plate median and did not decrease *Renilla* luciferase expression by more than 30 %.

Symbol	GeneID	RefSeq	z-score
PSMD14	10213	NM_005805	-6.59
PSMC1	NA	NM_002802	-5.95
PSMA6	5687	NM_002791	-5.48
PSMD7	5713	NM_002811	-5
HNRPC	NA	NM_004500	-4.96
PSMC4	5704	NM_006503, NM_153001	-4.93
PSMD3	NA	NM_002809	-4.89
SUPT5H	NA	NM_003169	-4.88
DDX48	9775	NM_014740	-4.78
PSMD1	NA	NM_002807	-4.78
PSMA5	5686	NM_002790	-4.47
SP1	6667	NM_138473	-4.39
RELA	5970	NM_021975	-4.32
p44S10	NA	NM_014814	-4.2
CKB	1152	NM_001823	-4.19
PSMA7	5688	NM_002792	-4.16
POLR2E	NA	NM_002695	-4.1
CDCA1	83540	NM_031423, NM_145697	-4.09
PSMC6	NA	NM_002806	-4.03
CCL25	6370	NM_005624	-3.76
CKAP5	9793	NM_001008938, NM_014756	-3.55

Symbol	GeneID	RefSeq	z-score
KIAA0999	23387	NM_025164	-3.4
SMARCD3	6604	NM_001003801, NM_001003802, NM_003078	-3.26
NOP17	55011	NM_017916	-3.25
C14orf68	283600	NM_207117	-3.14
PLXNA4B	91584	NM_181775	-3.12
INS	3630	NM_000207	-3.08
PSMD11	NA	NM_002815	-3.06
RPS14	NA	NM_005617	-3.04
C10orf64	NA	NM_173524	-3.01
PRO1855	NA	NM_018509	-3.01
SEZ6L2	26470	NM_012410, NM_201575	-2.92
POLR2D	NA	NM_004805	-2.92
RAD51L3	5892	NM_002878, NM_133629	-2.91
POLR2F	NA	NM_021974	-2.84
C13orf23	80209	NM_025138, NM_170719	-2.79
WEE1	7465	NM_003390	-2.78
APC	324	NM_000038	-2.75
GPR119	139760	NM_178471	-2.75
KIF2B	84643	NM_032559	-2.73
MS4A4A	51338	NM_024021, NM_148975	-2.72
CLTC	NA	NM_004859	-2.71
MKRN2	23609	NM_014160	-2.67
ITGB4BP	3692	NM_002212, NM_181466, NM_181467, NM_181468, NM_181469	-2.64
FLJ10980	NA	NM_019600	-2.61
NHP2L1	NA	NM_001003796	-2.59
GH2	2689	NM_002059, NM_022556, NM_022557, NM_022558	-2.54
MEN1	4221	NM_000244, NM_130799, NM_130800, NM_130801, NM_130802, NM_130803, NM_130804	-2.53
CASP4	837	NM_001225, NM_033306, NM_033307	-2.53

Table A.3: Hit list resulting from the overlap of screens A and B. Genes are listed that passed a z-score cut-off of $\leq$ -1.25 in both screens.

Symbol	GeneID	RefSeq	z-score A	z-score B
TRIB3	57761	NM_021158	-1.69	-2.95
CHKB	1120	NM_005198	-1.47	-2.55
CHUK	1147	NM_001278	-1.57	-1.77
PLK3	1263	NM_014911	-1.39	-1.65
COL4A3BP	10087	NM_022766	-1.92	-1.35
RHOD	29984	NM_014578	-2.41	-1.6
RHOF	54509	NM_019034	-1.79	-1.39
RANBP2	5903	NM_002194	-2.11	-1.9
GKAP1	80318	NM_025211	-3.3	-1.84
SHFM1	7979	NM_005914	-2.2	-2.83
NPEPPS	9520	NM_006310	-2.69	-1.82
ACTG1	71	NM_001614	-1.77	-1.31
PTGS1	5742	NM_000962	-1.97	-1.3
EIF5	1983	NM_001969	-1.65	-1.75
PSCD2	9266	NM_000124	-1.57	-1.87
SRCAP	10847	NM_006662	-2.17	-1.66
RAB6A	5870	NM_002869	-1.29	-1.63
ACTA2	59	NM_001613	-1.39	-2.91
KIF11	3832	NM_004523	-2.68	-2.13
ACP5	54	NM_001611	-1.35	-1.39
PDCD1	5133	NM_005018	-1.26	-1.25
PPM1F	9647	NM_014634	-2.64	-1.81
MPL	4352	NM_005373	-1.29	-1.39
ITGA10	8515	NM_003637	-1.7	-1.28

Symbol	GeneID	RefSeq	z-score A	z-score B
ITGA5	3678	NM_002205	-2	-1.92
HNF4G	3174	NM_004133	-1.36	-1.48
IL6R	3570	NM_000565	-2.91	-1.3
NTF5	4909	NM_006179	-2.68	-1.78
CHRNA1	1134	NM_002195	-2.15	-2.28
MDM2	4193	NM_002392	-1.63	-1.71
USP21	27005	NM_012475	-1.26	-2.26
HDAC6	10013	NM_006044	-3.37	-1.35
LOC220594	220594	NM_145809	-3.13	-1.3
CHFR	55743	NM_018223	-2.65	-1.33
RAD51	5888	NM_006037	-2.77	-1.87
GFAP	2670	NM_002055	-3.43	-2.02
KRT20	54474	NM_019010	-1.38	-2.1
TNPO1	3842	NM_002270	-1.6	-1.57
NUP153	9972	NM_005124	-1.51	-2.94
APOA2	336	NM_001643	-3.18	-1.77
CNGB1	1258	NM_001297	-1.7	-1.41
CDH3	1001	NM_001793	-3.52	-1.45
CDR1	1038	NM_004065	-3.26	-1.48
IKBKB	3551	XM_032491	-1.27	-2.18
NLK	51701	NM_000875	-2.04	-1.51
MAP4K5	11183	NM_006575	-1.53	-1.27
FLJ13265	79935	NM_024877	-1.52	-1.29
GLTSCR2	29997	NM_015710	-4.25	-1.76
HBZ	3050	NM_005332	-1.85	-1.33
GAB3	139716	NM_080612	-1.86	-2.41
HERPUD1	9709	NM_014685	-1.29	-2.03
HPS6	79803	NM_018173	-1.69	-2.09
MGC7036	196383	NM_145058	-3.28	-1.31
OLIG3	167826	NM_022737	-1.55	-1.59
OTOF	9381	NM_032832	-2.14	-2.55
MED8	112950	NM_052877	-2.3	-1.28
PSMD4	5710	NM_002810	-2.68	-1.51
NKTR	4820	NM_005385	-2.22	-1.54
PIB5PA	27124	NM_014422	-2.26	-2.12
OCLN	4950	NM_173470	-1.28	-1.52
RAB31	11031	NM_006868	-1.85	-1.65
SOST	50964	NM_002879	-1.67	-1.89
PTTG2	10744	NM_006607	-2.18	-3.36
WDR1	9948	NM_005112	-3	-3.35
RIOK2	55781	NM_018343	-1.89	-1.51
PTGES	9536	NM_004878	-2.34	-1.72
WHSC2	7469	NM_005663	-3.99	-1.53
SMARCB1	6598	NM_018663	-2.31	-2.04
BFSP1	631	NM_001195	-1.35	-2.08
ATP5G3	518	NM_001689	-3.16	-1.53
CYP2A13	1553	NM_000766	-1.45	-1.39
ADCY2	108	NM_020546	-1.8	-1.56
EML1	2009	NM_004434	-2.76	-2.66
ITGB4BP	3692	NM_004475	-1.37	-2.64
GRID1	2894	XM_043613	-2.96	-2.43
KLK1	3816	NM_001490	-1.25	-1.96
LAMP1	3916	NM_004486	-1.46	-2.82
LRP4	4038	XM_035037	-1.43	-3.07
NUP88	4927	NM_002532	-2.55	-1.86
PCYT1A	5130	NM_005017	-1.37	-1.37
SLC8A2	6543	NM_002802	-3.08	-1.38
PSMD13	5719	NM_002817	-1.58	-1.74
VCP	7415	NM_007126	-1.7	-1.73
SEMA5A	9037	NM_003966	-1.87	-2.05
LRRFIP2	9209	NM_006309	-3.74	-1.82
G10	8896	NM_003910	-3.11	-1.99
DLGAP2	9228	NM_004745	-3.73	-1.59
KLK4	9622	NM_004674	-1.42	-2.54
DHX34	9704	NM_194428	-1.81	-2.2
NAALADL1	10004	NM_005468	-3.58	-1.37
KIAA0555	9832	NM_014790	-2.58	-1.78
SV2A	9900	NM_014849	-1.56	-1.93
RBM19	9904	NM_016196	-1.49	-1.69

Symbol	GeneID	RefSeq	z-score A	z-score B
AP1M2	10053	NM_005498	-1.44	-1.44
ZAP128	10965	NM_006821	-1.56	-1.81
CKAP4	10970	NM_006825	-2.92	-1.99
POP1	10940	NM_015029	-2.5	-1.28
PRSS21	10942	NM_006799	-2.69	-1.63
LILRA2	11027	NM_006866	-2.88	-2.5
CYP4F8	11283	NM_021004	-1.7	-1.86
LSM6	11157	NM_147200	-1.48	-2.62
SRISNF2L	23132	NM_015106	-2.98	-2.3
POLA2	23649	NM_002689	-1.56	-1.51
ZDHHC8	29801	NM_013373	-2.52	-1.65
VILL	50853	NM_015873	-1.78	-1.98
EXOSC3	51010	NM_016042	-1.25	-1.92
PACAP	51237	NM_018413	-2.34	-1.72
TOMM7	54543	NM_016077	-1.54	-1.57
ARS2	51593	NM_015908	-1.5	-1.7
HSMPP8	54737	NM_017520	-2.76	-3.32
FLJ20584	54991	NM_017891	-1.79	-1.74
LRRC8	56262	NM_019594	-1.43	-1.45
CPXM	56265	NM_019609	-1.26	-1.98
RNF150	57484	XM_291090	-1.81	-1.76
SHD	56961	NM_020209	-1.55	-2.03
CFL1	1072	NM_005507	-1.78	-2.44
ATF7IP	55729	NM_018179	-3.32	-2.85
DSC1	1823	NM_001087	-1.48	-2.71
ANKRD1	27063	NM_014391	-1.57	-1.32
FLJ22318	64777	NM_022762	-1.65	-1.26
SLC2A11	66035	NM_022488	-2.38	-1.28
MGC2744	80755	NM_024955	-1.26	-2.02
MGC13186	84284	NM_032324	-1.44	-1.51
MGC12458	84288	NM_032328	-1.34	-1.55
IMMP2L	83943	NM_032549	-1.76	-2.09
RAB34	83871	NM_031934	-1.4	-1.38
FMNL2	114793	NM_052905	-1.92	-1.31
KIAA1904	114794	XM_056282	-1.26	-2
TSLP	85480	NM_033035	-1.52	-1.48
EGLN2	112398	NM_033106	-1.38	-1.44
MGC35194	93190	NM_152290	-2.62	-1.63
MGC15396	91369	NM_052855	-1.81	-1.48
LOC92162	92162	NM_138455	-1.41	-2.5
ZNF526	116115	NM_133444	-1.39	-2
CACNA2D4	93589	NM_172364	-1.55	-1.56
NY-REN-41	91057	NM_080654	-2.27	-1.68
PEX11G	92960	NM_080662	-2.43	-1.97
MRGPRE	116534	XM_171536	-1.31	-2.45
NOR1	127700	NM_145047	-1.64	-1.71
CST11	140880	NM_080830	-1.62	-1.66
SFRS11	9295	NM_004768	-1.51	-2.22
SMAD2	4087	NM_005901	-1.94	-1.4
ZFPM1	161882	NM_153813	-2.57	-2.52
FAM9B	171483	NM_145653	-1.25	-1.34
DNAJB8	165721	NM_153330	-1.66	-2.08
GGN	199720	NM_152657	-1.44	-1.65
SLC37A2	219855	XM_166184	-2.08	-1.75
FLJ25530	220296	NM_152722	-2.04	-1.6
FLJ36674	284040	NM_173622	-1.92	-2.16
PHGDHL1	337867	NM_177967	-1.36	-1.43
ABCC11	85320	NM_032583	-1.52	-1.58
MGC39606	399668	NM_203306	-1.28	-1.54
RP13-15M17.2	199953	XM_114067	-1.49	-1.4
GTF2A1	2957	NM_015859	-1.68	-1.56
GTF2A2	2958	NM_004492	-1.38	-2.29
FOXA3	3171	NM_004497	-1.42	-1.36
FOXD1	2297	NM_004472	-1.97	-1.52
OR2W5	441932	XM_372254	-2.97	-1.45
OR1L3	26735	XM_377073	-3.08	-2.02
MGC88374	440184	XM_373358	-1.36	-1.62
OR6C75	390323	NM_001005497	-1.8	-1.42
OR11G2	390439	NM_001005503	-2.67	-1.7

Symbol	GeneID	RefSeq	z-score A	z-score B
BAI2	576	NM_001703	-1.79	-1.48
F2RL2	2151	NM_004101	-1.99	-2.29
DEFB4	1673	NM_004942	-3.4	-1.76
ADRA1D	146	NM_000678	-2.48	-1.28
ADRA2A	150	NM_000681	-2.69	-1.28
MC1R	4157	NM_002386	-3.6	-2.38
TAS2R48	259294	NM_032119	-1.27	-1.81
MYT1	4661	NM_004535	-1.45	-1.46
SUPT4H1	6827	NM_003168	-1.49	-1.72
CYB5R2	51700	NM_003757	-1.84	-1.48
CD38	952	NM_003403	-2.08	-1.6
ITPA	3704	NM_033453	-1.56	-2.72
AOF2	23028	NM_015013	-3.36	-2.02
HIF1AN	55662	NM_017902	-1.44	-1.65
MAN2B2	23324	XM_052620	-2.71	-1.47

Table A.4: Genes of the TNF test set that passed the z-score filter or $\leq$ -1.25 in at least one of screens (column "cut-off -1.25"). For comparison, column "cut-off -2.5" highlights whether these genes also passed the cut-off of $\leq$ -2.5 applied in individual screening analysis. no: this gene did not reach the cut-off in any of the screens, yes(A): reached the cut-off in screen A, yes(B): reached the cut-off in screen B, yes (A/B): reached the cut-off in both screens.

Symbol	GeneID	RefSeq	z-score A	z-score B	cut-off -2.5	cut-off -1.25
CHUK	1147	NM_001278	-1.57	-1.77	no	yes (A/B)
IKBKB	3551	XM_032491	-1.27	-2.18	no	yes (A/B)
LMNB1	4001	NM_005573	-4.29	-0.55	yes (A)	yes (A)
PAK1	5058	NM_025194	-2.13	0.09	no	yes (A)
MAP2K3	5606	NM_002756	-1.9	0.49	no	yes (A)
RELA	5970	NM_021975	-0.53	-4.32	yes (B)	yes (B)
TNFRSF1A	7132	NM_001065	0.31	-4.8	yes (B)	yes (B)
TRAF3	7187	NM_004652	-0.53	-1.45	no	yes (B)
IKBKAP	8518	NM_003640	-1.28	0.01	no	yes (A)
TRADD	8717	NM_003789	-1.18	-2.33	no	yes (B)
RIPK1	8737	NM_003804	-3.39	0.53	yes (A)	yes (A)
LMNB2	84823	NM_032737	-1.6	-0.31	no	yes (A)

Table A.5: Genes of the inflammation test set that passed the z-score filter or $\leq$ -1.25 in at least one of screens (column "cut-off -1.25"). For comparison, column "cut-off -2.5" highlights whether these genes also passed the cut-off of $\leq$ -2.5 applied in individual screening analysis. no: this gene did not reach the cut-off in any of the screens, yes(A): reached the cut-off in screen A, yes(B): reached the cut-off in screen B, yes (A/B): reached the cut-off in both screens.

Symbol	GeneID	RefSeq	z-score A	z-score B	cut-off -2.5	cut-off -1.25
ADCY6	112	NM_015270	-1.47	0.48	no	yes (A)
ADRBK2	157	NM_005160	-1.69	0.5	no	yes (A)
AKT1	207	NM_005163	-1.29	-0.51	no	yes (A)
CAMK2D	817	NM_001221	0.75	-1.7	no	yes (B)
COL6A1	1291	NM_001848	1.03	-1.11	no	yes (B)
GNG7	2788	NM_000675	-2.03	-0.3	no	yes (A)
GRK5	2869	NM_005308	0.15	-2.65	yes (B)	yes (B)
			0.25			
HRAS	3265	NM_005343	-2.79	-0.57	yes (A)	yes (A)
IKBKB	3551	XM_032491	-1.27	-2.18	no	yes (A/B)
INPP5D	3635	NM_005541	-1.79	0.26	no	yes (A)
ITGA6	3655	NM_000210	-1.87	-0.53	no	yes (A)
ITPR3	3710	NM_022076	-0.68	-2.92	yes (B)	yes (B)

Symbol	GeneID	RefSeq	z-score A	z-score B	cut-off -2.5	cut-off -1.25
NFATC2	4773	NM_012340	-1.52	1.41	no	yes (A)
NFKBIE	4794	NM_004556	-0.16	-2.13	no	yes (B)
NRAS	4893	NM_002524	-2.59	0.22	yes (A)	yes (A)
PAK1	5058	NM_025194	-2.13	0.09	no	yes (A)
PDPK1	5170	NM_004690	0.94	-1.42	no	yes (B)
PRKACB	5567	NM_002731	0.07	-1.45	no	yes (B)
PRKCA	5578	NM_002737	-1.4	-0.09	no	yes (A)
PRKCI	5584	NM_002740	-0.99	-1.34	no	yes (B)
MAPK1	5594	NM_002745	-0.88	-1.28	no	yes (B)
MAPK3	5595	NM_002746	-1.75	0.47	no	yes (B)
PRKY	5616	NM_002760	-0.54	-1.53	no	yes (B)
PTGS1	5742	NM_000962	-1.97	-1.3	no	yes (A/B)
RELA	5970	NM_021975	-0.53	-4.32	yes (B)	yes (B)
RELB	5971	NM_002200	0.18	-2.29	no	yes (B)
SHC1	6464	NM_003029	0.88	-1.59	no	yes (B)
IKBKE	9641	NM_014002	-2.03	0.01	no	yes (A)
ARPC1B	10095	NM_005720	-1.85	0.32	no	yes (A)
ACTR1A	10121	NM_005736	-0.38	-1.89	no	yes (B)
RHOD	29984	NM_014578	-2.41	-1.6	no	yes (A/B)
RHOF	54509	NM_019034	-1.79	-1.39	no	yes (A/B)
LTB4R2	56413	NM_019839	-3.74	-0.68	yes (A)	yes (A)

Table A.6: Phenotypes of knockdown of all selected hits using dual luciferase assay in HEK293T cells to assess NF-κB transcriptional activity. Mean: Average of at least two biological replicates expressed as relative Iluciferase expression as compared to negative control (mock transfected cells) is given (in %). stdev: standard deviation of these two measurements. p-value: p-values were calculated using Student's T-test. Q-: siRNA pool vended by Qiagen. Other siRNAs are either individual siRNAs or siRNA pools vended by Dharmacon.

GeneID	siRNA	mean	stdev	p-value
6696	Q-SPP1	70.868	24.792	0.119
	SPP1-5	58.297	29.785	0.093
	SPP1-6	44.289	8.787	0.006
	SPP1-7	57.873	14.896	0.029
	SPP1-8	25.837	3.078	0.000
	SPP1-pool	35.214	2.820	0.000
51352	Q-WIT1	38.715	15.413	0.015
	WIT1-1	69.140	14.186	0.046
	WIT1-2	50.575	15.179	0.022
	WIT1-3	51.453	23.181	0.049
	WIT1-4	107.254	71.954	0.450
	WIT1-pool	66.693	29.994	0.128
5606	Q-MAP2K3	75.447	31.209	0.191
	MAP2K3-2	121.069	35.950	0.245
	MAP2K3-4	56.442	12.923	0.010
	MAP2K3-5	60.650	28.935	0.083
	MAP2K3-6	86.900	6.754	0.040
	MAP2K3-pool	61.265	23.207	0.056
29941	Q-PKN3	79.689	34.280	0.245
	PKN3-5	85.419	12.019	0.101
	PKN3-6	76.654	8.994	0.020
	PKN3-7	56.477	16.250	0.018
	PKN3-8	127.733	25.307	0.119
	PKN3-pool	92.270	13.894	0.255
6676	Q-SPAG4	63.576	29.312	0.110
	SPAG4-1	139.887	28.475	0.078
	SPAG4-2	67.960	15.054	0.032
	SPAG4-3	176.226	45.966	0.056
	SPAG4-4	75.112	25.408	0.140
	SPAG4-pool	101.530	29.592	0.475
6694	Q-SPP2	70.604	39.158	0.200

GeneID	siRNA	mean	stdev	p-value
	SPP2-1	78.709	11.650	0.046
	SPP2-2	44.882	4.236	0.000
	SPP2-3	135.838	45.738	0.185
	SPP2-4	103.550	21.147	0.418
	SPP2-pool	76.901	6.348	0.008
6744	Q-SSFA2	70.511	12.245	0.038
	SSFA2-1	107.079	34.960	0.402
	SSFA2-2	64.556	9.537	0.008
	SSFA2-3	80.696	20.616	0.149
	SSFA2-4	141.059	63.303	0.224
	SSFA2-pool	77.800	28.223	0.184
1152	Q-CKB	61.704	14.904	0.034
6370	Q-CCL25	33.652	9.794	0.005
9793	Q-CKAP5	69.666	44.241	0.217
23387	Q-KIAA0999	52.282	33.338	0.090
5685	Q-PSMA4	54.628	1.078	0.000
55209	Q-SETD5-1	72.468	25.272	0.132
	Q-SETD5-2	51.611	28.148	0.068
	Q-SETD5-3	47.936	19.624	0.032
	Q-SETD5-4	46.065	15.687	0.020
55011	Q-NOP17	44.373	20.025	0.030
4089	Q-SMAD4	51.972	15.669	0.025
57761	Q-TRIB3	46.193	24.677	0.046
26470	Q-SEZ6L2	52.455	32.610	0.088
5756	Q-PTK9	74.794	14.632	0.068
	PTK9-5	83.306	21.408	0.193
	PTK9-9	86.698	18.340	0.206
	PTK9-10	82.637	9.656	0.063
	PTK9-12	80.422	12.701	0.081
	PTK9-pool	100.946	26.192	0.482
10298	Q-PAK4	49.315	14.514	0.019
139760	Q-GPR119	81.491	34.626	0.264
84643	Q-KIF2B	55.781	0.236	0.000
51338	Q-MS4A4A	60.904	4.439	0.003
1213	Q-CLTC	66.473	19.073	0.065
2300	Q-FOXL1	70.906	31.171	0.159
3692	Q-ITGB4BP	61.540	29.272	0.102
9381	Q-OTOF	64.605	31.573	0.127
54538	Q-ROBO4	77.640	30.413	0.204
	ROBO4-1	36.306	2.303	0.000
	ROBO4-2	23.168	4.467	0.001
	ROBO4-3	53.546	15.599	0.026
	ROBO4-4	93.475	18.528	0.334
	ROBO4-pool	49.286	7.358	0.005
837	Q-CASP4	87.539	10.838	0.123
	CASP4-1	20.152	7.878	0.002
	CASP4-2	117.491	29.018	0.242
	CASP4-4	39.476	3.287	0.001
	CASP4-17	98.367	6.642	0.381
	CASP4-pool	36.523	8.992	0.005
2689	Q-GH2	64.653	21.971	0.075
6367	Q-CCL22	63.699	18.851	0.056
4221	Q-MEN1	37.498	7.562	0.004
	MEN1-2	88.177	2.422	0.010
	MEN1-3	115.465	6.810	0.042
	MEN1-4	54.650	5.080	0.003
	MEN1-17	25.473	6.957	0.002
	MEN1-pool	96.113	66.421	0.471
4055	Q-LTBR	59.867	5.702	0.005
10970	Q-CKAP4	81.001	46.849	0.312
1263	Q-PLK3	60.737	27.643	0.091
50964	Q-SOST	64.161	25.501	0.093
57484	Q-RNF150	67.113	23.355	0.092
9622	Q-KLK4	89.213	32.854	0.344
3678	Q-ITGA5	72.485	1.144	0.000
	ITGA5-5	74.109	0.748	0.000
	ITGA5-6	106.421	15.769	0.311
	ITGA5-7	75.007	2.041	0.002
	ITGA5-20	45.388	2.876	0.001

GeneID	siRNA	mean	stdev	p-value
	ITGA5-pool	66.664	4.900	0.005
9972	Q-NUP153	51.017	12.686	0.016
11031	Q-RAB31	43.544	4.303	0.001
5903	Q-RANBP2	48.997	7.268	0.005
55662	Q-HIF1AN	37.669	15.517	0.015
4193	Q-MDM2	50.725	15.821	0.024
1072	Q-CFL1	39.900	16.161	0.017
27124	Q-PIB5PA	77.431	40.688	0.257
7415	Q-VCP	51.067	33.491	0.087
	Q-SHFMA	22.655	4.382	0.001
9037	Q-SEMA5A	55.756	17.467	0.035
	SEMA5A-1	105.965	0.005	0.000
	SEMA5A-3	132.431	9.441	0.020
	SEMA5A-4	39.029	3.890	0.001
	SEMA5A-17	92.053	21.015	0.323
	SEMA5A-pool	99.870	0.697	0.409
9904	Q-RBM19	52.408	18.940	0.035
10311	Q-DSCR3	104.366	32.037	0.432
	DSCR3-1	90.055	14.596	0.214
	DSCR3-2	83.911	26.572	0.238
	DSCR3-3	63.212	7.022	0.003
	DSCR3-4	103.975	24.037	0.419
	DSCR3-pool	77.864	16.399	0.084
	Q-RAPGEF3	129.023	84.804	0.338
	RAPGEF3-1	99.504	47.995	0.495
	RAPGEF3-2	126.518	52.829	0.274
	RAPGEF3-3	65.030	20.593	0.054
	RAPGEF3-4	74.959	10.251	0.023
	RAPGEF3-pool	46.386	14.807	0.008
49856	Q-WDR8	121.988	69.330	0.349
	WDR8-1	40.479	13.251	0.012
	WDR8-2	46.640	10.115	0.009
	WDR8-3	59.407	3.008	0.001
	WDR8-4	61.305	5.883	0.006
	WDR8-pool	47.061	3.257	0.001
9099	Q-USP2	85.467	26.404	0.259
	USP2-1	37.534	6.682	0.003
	USP2-2	84.303	8.207	0.057
	USP2-3	58.446	7.068	0.007
	USP2-4	44.179	12.915	0.013
	USP2-pool	62.988	18.439	0.052
55795	Q-FLJ11305	72.893	31.128	0.172
57705	Q-C10orf64	121.445	111.415	0.405
55379	Q-PRO1855	107.056	50.816	0.431
	PRO1855-1	69.813	2.213	0.001
	PRO1855-2	75.242	21.858	0.125
	PRO1855-3	57.864	0.582	0.000
	PRO1855-4	42.069	3.348	0.001
	PRO1855-pool	63.464	0.992	0.000
148753	Q-MGC16664	138.250	114.953	0.342
11326	Q-VSIG4	76.934	31.190	0.203
1823	Q-DSC1	90.540	0.376	0.000
27342	Q-RABGEF1	95.102	33.830	0.428
	RABGEF1-1	42.111	9.714	0.007
	RABGEF1-2	51.937	1.289	0.000
	RABGEF1-3	87.114	3.607	0.019
	RABGEF1-4	74.275	8.506	0.025
	RABGEF1-pool	61.357	1.775	0.001
56204	Q-FLJ10980	126.497	81.382	0.345
56961	Q-SHD	90.429	58.831	0.420
93190	Q-MGC35194	77.701	41.045	0.261
	MGC35194-1	66.358	5.972	0.008
	MGC35194-2	123.609	1.777	0.001
	MGC35194-3	28.887	0.090	0.000
	MGC35194-4	17.210	3.284	0.000
	MGC35194-pool	23.163	1.109	0.000
139716	Q-GAB3	76.352	35.583	0.223
	GAB3-1	101.937	24.732	0.461
	GAB3-2	26.406	8.852	0.004

GeneID	siRNA	mean	stdev	p-value
	GAB3-3	46.055	21.822	0.036
	GAB3-4	82.265	37.303	0.285
	GAB3-pool	41.785	26.155	0.044
9900	Q-SV2A	94.587	59.487	0.455
11027	Q-LILRA2	88.236	22.577	0.269
	LILRA2-1	24.617	8.011	0.003
	LILRA2-2	89.088	31.590	0.337
	LILRA2-3	30.308	8.665	0.004
	LILRA2-4	38.895	8.240	0.004
	LILRA2-pool	46.531	8.739	0.007
116	Q-PACAP	88.872	39.208	0.363
54737	Q-HSMPP8	55.148	12.800	0.019
167826	Q-OLiG3	129.448	70.077	0.306
6598	Q-SMARCB1	74.442	0.835	0.000
9704	Q-DHX34	71.378	14.415	0.053
	DHX34-1	151.152	3.502	0.001
	DHX34-2	79.714	25.708	0.190
	DHX34-3	84.157	32.186	0.279
	DHX34-4	102.954	76.520	0.481
	DHX34-pool	85.093	45.609	0.345
9948	Q-WDR1	50.047	14.773	0.021
9647	PPM1F-1	128.086	18.191	0.028
	PPM1F-2	239.628	74.954	0.044
	PPM1F-3	88.587	15.604	0.199
	PPM1F-4	166.511	35.311	0.043
	PPM1F-pool	133.775	20.777	0.059
	SPTCL2-1	88.849	26.871	0.308
	SPTCL2-2	96.881	43.616	0.465
	SPTCL2-3	149.792	43.352	0.110
	SPTCL2-4	95.335	11.904	0.318
	SPTCL2-pool	117.692	20.306	0.163
	CYB7B1-1	142.499	33.206	0.092
	CYB7B1-2	129.478	37.945	0.187
	CYB7B1-3	113.623	24.727	0.257
	CYB7B1-4	146.678	52.804	0.160
	CYB7B1-pool	127.943	40.888	0.213
6500	SKP1A-5	146.364	55.360	0.171
	SKP1A-8	91.556	17.920	0.286
	SKP1A-9	57.293	15.377	0.017
	SKP1A-10	45.202	13.642	0.006
	SKP1A-pool	42.452	6.878	0.001
30817	EMR2-1	79.731	40.836	0.277
	EMR2-2	142.371	34.725	0.100
	EMR2-3	123.122	43.017	0.261
	EMR2-4	176.632	52.757	0.073
	EMR2-pool	125.607	67.285	0.322

Table A.7: Phenotypes of knockdown of all selected hits using IL-8 ELISA in HEK293T cells to assess NF-κB transcriptional activity. Mean: Average of at least two biological replicates expressed as relative IL-8 secretion as compared to negative control (siLRP5 transfected cells) is given (in %). stdev: standard deviation of these two measurements. p-value: p-values were calculated using Student's T-test. siRNAs are either individual siRNAs or siRNA pools vended by Dharmacon.

GeneID	siRNA	mean	stdev	p-value
6696	SPP1-5	66.929	9.366	0.019
	SPP1-6	124.381	18.723	0.103
	SPP1-7	75.284	2.126	0.002
	SPP1-8	37.846	11.411	0.008
	SPP1-pool	66.747	1.886	0.001
51352	WIT1-1	87.096	3.417	0.017
	WIT1-2	39.630	2.650	0.000
	WIT1-3	44.277	8.190	0.005

GeneID	siRNA	mean	stdev	p-value
	WIT1-4	65.781	9.055	0.017
	WIT1-pool	35.313	7.002	0.003
5756	PTK9-5	97.065	4.151	0.211
	PTK9-9	100.849	16.421	0.474
	PTK9-10	107.094	13.031	0.261
	PTK9-12	107.657	5.293	0.089
	PTK9-pool	111.346	5.173	0.045
54538	ROBO4-1	89.727	20.527	0.276
	ROBO4-2	119.797	4.752	0.014
	ROBO4-3	160.602	26.842	0.043
	ROBO4-4	119.065	11.280	0.070
	ROBO4-pool	189.911	29.674	0.025
837	CASP4-1	29.281	5.155	0.001
	CASP4-2	82.406	10.635	0.072
	CASP4-4	49.671	6.315	0.004
	CASP4-17	90.592	10.680	0.170
	CASP4-pool	42.524	4.049	0.001
4221	MEN1-2	129.168	7.116	0.014
	MEN1-3	79.613	16.833	0.114
	MEN1-4	39.672	23.079	0.033
	MEN1-17	51.088	6.935	0.005
	MEN1-pool	80.070	1.433	0.001
3678	ITGA5-5	77.646	10.890	0.050
	ITGA5-6	80.452	3.302	0.007
	ITGA5-7	53.779	0.707	0.000
	ITGA5-20	112.746	12.499	0.143
	ITGA5-pool	71.023	4.229	0.005
9037	SEMA5A-1	133.543	12.068	0.030
	SEMA5A-3	129.467	0.328	0.000
	SEMA5A-4	95.061	4.221	0.120
	SEMA5A-17	102.601	9.861	0.372
	SEMA5A-pool	100.350	2.982	0.442
49856	WDR8-1	37.309	0.633	0.000
	WDR8-2	47.898	0.478	0.000
	WDR8-3	94.046	13.902	0.303
	WDR8-4	65.350	4.506	0.004
	WDR8-pool	49.030	2.436	0.001
9099	USP2-1	36.173	1.630	0.000
	USP2-2	88.321	9.745	0.116
	USP2-3	92.137	6.606	0.117
	USP2-4	41.375	5.763	0.002
	USP2-pool	56.154	3.647	0.002
55379	PRO1855-1	188.102	5.129	0.001
	PRO1855-2	71.589	10.560	0.031
	PRO1855-3	64.942	9.462	0.017
	PRO1855-4	88.564	12.424	0.161
	PRO1855-pool	126.144	36.512	0.209
27342	RABGEF1-1	115.467	14.494	0.135
	RABGEF1-2	83.041	29.983	0.254
	RABGEF1-3	79.675	21.995	0.161
	RABGEF1-4	62.551	12.341	0.025
	RABGEF1-pool	81.004	9.457	0.052
93190	MGC35194-1	124.075	6.138	0.016
	MGC35194-2	74.675	5.143	0.010
	MGC35194-3	80.524	17.497	0.128
	MGC35194-4	94.587	9.201	0.246
	MGC35194-pool	102.185	5.024	0.301
139716	GAB3-1	73.465	5.750	0.011
	GAB3-2	31.074	14.579	0.011
	GAB3-3	67.764	9.666	0.021
	GAB3-4	69.814	8.702	0.020
	GAB3-pool	60.617	10.379	0.017
11027	LILRA2-1	19.824	9.489	0.003
	LILRA2-2	102.693	5.466	0.279
	LILRA2-3	78.345	2.992	0.005
	LILRA2-4	45.618	4.235	0.002
	LILRA2-pool	50.406	12.938	0.016
9704	DHX34-1	53.258	15.813	0.026
	DHX34-2	67.080	6.766	0.010

GeneID	siRNA	mean	stdev	p-value
	DHX34-3	56.655	14.048	0.024
	DHX34-4	73.473	27.014	0.150
	DHX34-pool	65.556	6.157	0.008
9647	PPM1F-1	85.606	19.124	0.199
	PPM1F-2	90.188	29.275	0.341
	PPM1F-3	64.122	22.405	0.076
	PPM1F-4	96.591	28.843	0.441
	PPM1F-pool	83.793	33.391	0.282
	SPTCL2-1	86.563	0.830	0.001
	SPTCL2-2	104.157	19.868	0.398
	SPTCL2-3	70.394	10.949	0.031
	SPTCL2-4	83.124	29.286	0.250
	SPTCL2-pool	96.976	28.792	0.448
6694	SPP2-1	55.353	8.321	0.008
	SPP2-2	60.741	14.868	0.032
	SPP2-3	54.049	7.701	0.007
	SPP2-4	57.641	11.861	0.019
	SPP2-pool	49.444	11.134	0.012
6744	SSFA2-1	68.411	23.115	0.096
	SSFA2-2	48.624	8.598	0.007
	SSFA2-3	32.968	3.138	0.001
	SSFA2-4	90.060	20.832	0.285
	SSFA2-pool	49.763	8.219	0.007
6676	SPAG4-1	74.207	10.484	0.037
	SPAG4-2	42.272	8.835	0.006
	SPAG4-3	79.181	20.697	0.145
	SPAG4-4	106.136	37.395	0.419
	SPAG4-pool	57.558	17.399	0.037
29941	PKN3-5	87.924	28.041	0.302
	PKN3-6	72.692	15.705	0.067
	PKN3-7	56.812	6.134	0.005
	PKN3-8	44.203	4.872	0.002
	PKN3-pool	47.900	6.419	0.004
10311	DSCR3-1	79.838	11.883	0.069
	DSCR3-2	54.328	11.002	0.014
	DSCR3-3	58.708	3.577	0.002
	DSCR3-4	75.261	28.211	0.170
	DSCR3-pool	65.195	16.577	0.049
5606	MAP2K3-2	59.276	1.418	0.000
	MAP2K3-4	92.985	29.508	0.384
	MAP2K3-5	38.612	6.003	0.002
	MAP2K3-6	44.142	3.111	0.001
	MAP2K3-pool	51.041	5.672	0.003
	CYB7B1-1	112.739	42.347	0.356
	CYB7B1-2	71.645	12.998	0.045
	CYB7B1-3	86.935	42.375	0.353
	CYB7B1-4	66.489	16.472	0.051
	CYB7B1-pool	82.187	22.605	0.191
6500	SKP1A-5	88.114	21.614	0.259
	SKP1A-8	94.825	46.001	0.444
	SKP1A-9	100.879	36.822	0.488
	SKP1A-10	101.277	54.122	0.488
	SKP1A-pool	142.344	42.240	0.146
30817	EMR2-1	58.258	9.017	0.011
	EMR2-2	62.055	11.039	0.020
	EMR2-3	96.843	17.892	0.413
	EMR2-4	81.957	13.075	0.095
	EMR2-pool	71.026	10.671	0.031
	RAPGEF3-1	189.849	85.238	0.137
	RAGGEF3-2	152.268	20.971	0.036
	RAPGEF3-3	81.494	20.950	0.169
	RAPGEF3-4	74.571	12.202	0.049
	RAPGEF3-pool	95.531	39.412	0.444

Table A.8: Phenotypes of knockdown of all selected hits using dual luciferase assay in HepG2 cells to assess NF-κB transcriptional activity. Mean: Average of two biological replicates expressed as relative luciferase expression as compared to negative control (mock transfected cells) is given (in %). stdev: standard deviation of these two measurements. p-value: p-values were calculated using Student's T-test. Q-: siRNA pool vended by Qiagen. For Qiagen siRNAs only one biological replicate was available (given is then the average of four technical replicates.) Other siRNAs are either individual siRNAs or siRNA pools vended by Dharmacon. NA: not available.

GeneID	siRNA	mean	stdev	p-value
5756	Q-PTK9	49.158	NA	NA
	PTK9-5	143.647	2.402	0.001
	PTK9-9	92.498	14.790	0.274
	PTK9-10	151.584	6.849	0.004
	PTK9-12	118.726	20.606	0.164
	PTK9-pool	133.474	33.624	0.147
54538	Q-ROBO4	68.177	NA	NA
	ROBO4-1	56.306	12.869	0.020
	ROBO4-2	34.979	1.496	0.000
	ROBO4-3	116.275	14.621	0.128
	ROBO4-4	131.934	31.192	0.142
	ROBO4-pool	97.572	11.484	0.397
837	Q-CASP4	63.147	NA	NA
	CASP4-1	25.178	2.347	0.000
	CASP4-2	180.619	51.802	0.079
	CASP4-4	43.419	11.492	0.010
	CASP4-17	109.446	0.948	0.002
	CASP4-pool	47.811	11.884	0.012
4221	Q-MEN1	44.307	NA	NA
	MEN1-2	137.628	34.110	0.130
	MEN1-3	119.196	43.534	0.298
	MEN1-4	71.432	5.023	0.008
	MEN1-17	48.470	10.257	0.010
	MEN1-pool	121.732	5.901	0.017
55379	Q-PRO1855	135.969	NA	NA
	PRO1855-1	150.609	41.071	0.112
	PRO1855-2	159.993	35.623	0.070
	PRO1855-3	256.281	93.242	0.071
	PRO1855-4	90.411	13.218	0.206
	PRO1855-pool	200.319	104.195	0.153
27342	Q-RABGEF1	57.859	NA	NA
	RABGEF1-1	51.483	7.856	0.006
	RABGEF1-2	38.426	9.632	0.006
	RABGEF1-3	58.385	4.314	0.003
	RABGEF1-4	77.304	23.468	0.152
	RABGEF1-pool	52.379	10.277	0.011
3678	Q-ITGA5	99.962	NA	NA
	ITGA5-5	90.908	17.882	0.273
	ITGA5-6	119.878	3.759	0.009
	ITGA5-7	46.771	20.390	0.033
	ITGA5-20	111.039	22.792	0.282
	ITGA5-pool	63.035	10.416	0.019
9037	Q-SEMA5A	57.809	NA	NA
	SEMA5A-1	141.663	26.443	0.078
	SEMA5A-3	171.527	22.408	0.023
	SEMA5A-4	197.778	5.622	0.001
	SEMA5A-17	68.240	5.269	0.007
	SEMA5A-pool	181.487	28.167	0.027
93190	Q-MGC35194	49.766	NA	NA
	MGC35194-1	65.499	13.946	0.036
	MGC35194-2	58.979	15.406	0.032
	MGC35194-3	25.678	0.001	0.000
	MGC35194-4	58.107	1.114	0.000
	MGC35194-pool	32.063	5.707	0.002
139716	Q-GAB3	42.772	NA	NA

GeneID	siRNA	mean	stdev	p-value
	GAB3-1	96.073	26.983	0.428
	GAB3-2	31.327	12.311	0.008
	GAB3-3	62.068	32.581	0.121
	GAB3-4	81.974	9.644	0.059
	GAB3-pool	62.958	20.992	0.065
11027	Q-LILRA2	73.566	NA	NA
	LILRA2-1	46.411	3.756	0.001
	LILRA2-2	99.549	25.099	0.491
	LILRA2-3	16.661	1.987	0.000
	LILRA2-4	24.924	4.302	0.001
	LILRA2-pool	28.772	1.663	0.000
9704	Q-DHX34	87.683	NA	NA
	DHX34-1	109.765	36.123	0.370
	DHX34-2	61.148	1.007	0.000
	DHX34-3	61.135	20.383	0.057
	DHX34-4	104.147	34.854	0.441
	DHX34-pool	56.103	18.811	0.040
51352	Q-WIT1	74.959	NA	NA
	WIT1-1	91.110	28.679	0.352
	WIT1-2	59.772	27.111	0.085
	WIT1-3	156.997	18.893	0.025
	WIT1-4	110.247	23.942	0.303
	WIT1-pool	126.265	47.850	0.259
9099	Q-USP2	102.437	NA	NA
	USP2-1	50.697	17.059	0.027
	USP2-2	192.069	138.189	0.223
	USP2-3	48.460	20.977	0.037
	USP2-4	91.023	36.146	0.379
	USP2-pool	70.659	19.688	0.085
49856	Q-WDR8	115.668	NA	NA
	WDR8-1	72.779	50.619	0.263
	WDR8-2	39.626	15.602	0.016
	WDR8-3	58.828	29.055	0.091
	WDR8-4	37.330	6.821	0.003
	WDR8-pool	44.714	4.439	0.002
6696	Q-SPP1	65.752	NA	NA
	SPP1-5	94.741	22.244	0.385
	SPP1-6	34.684	8.669	0.004
	SPP1-7	122.162	18.800	0.119
	SPP1-8	78.461	6.611	0.022
	SPP1-pool	66.182	22.330	0.083

Table A.9: Phenotypes of all selected hits using IL-8 ELISA in HepG2 cells to assess NF-κB transcriptional activity. Mean: Average of two biological replicates expressed as relative IL-8 secretion as compared to negative control (mock transfected cells) is given (in %). stdev: standard deviation of these two measurements. p-value: p-values were calculated using Student's T-test. Q-...: siRNA pool vended by Qiagen. For Qiagen siRNAs only one biological replicate was available (given is then the average of four technical replicates.) Other siRNAs are either individual siRNAs or siRNA pools vended by Dharmacon. NA: not available.

GeneID	siRNA	mean	stdev	p-value
5756	Q-PTK9	36.907	NA	NA
	PTK9-5	274.649	37.173	0.011
	PTK9-9	70.996	6.563	0.012
	PTK9-10	0.182	0.257	0.000
	PTK9-12	47.548	10.410	0.010
	PTK9-pool	28.615	4.470	0.001
54538	Q-ROBO4	87.414	NA	NA
	ROBO4-1	0.000	0.000	NA
	ROBO4-2	143.096	52.719	0.184

GeneID	siRNA	mean	stdev	p-value
	ROBO4-3	162.938	36.553	0.068
	ROBO4-4	217.074	68.372	0.068
	ROBO4-pool	104.773	26.292	0.411
837	Q-CASP4	26.283	NA	NA
	CASP4-1	0.000	0.000	NA
	CASP4-2	247.429	71.703	0.050
	CASP4-4	4.180	3.340	0.000
	CASP4-17	86.343	11.085	0.112
	CASP4-pool	1.869	2.643	0.000
4221	Q-MEN1	53.743	NA	NA
	MEN1-2	0.935	1.322	0.000
	MEN1-3	616.600	246.150	0.049
	MEN1-4	90.571	15.978	0.246
	MEN1-17	98.751	13.662	0.454
	MEN1-pool	114.894	62.204	0.384
55379	Q-PRO1855	145.603	NA	NA
	PRO1855-1	85.327	7.534	0.055
	PRO1855-2	262.726	61.966	0.033
	PRO1855-3	11.682	16.521	0.009
	PRO1855-4	498.486	184.535	0.046
	PRO1855-pool	34.353	6.928	0.003
27342	Q-RABGEF1	100.163	NA	NA
	RABGEF1-1	259.614	35.967	0.012
	RABGEF1-2	142.393	65.609	0.229
	RABGEF1-3	117.733	23.824	0.201
	RABGEF1-4	48.435	24.868	0.050
	RABGEF1-pool	242.487	165.776	0.174
3678	Q-ITGA5	196.927	NA	NA
	ITGA5-5	147.857	83.352	0.251
	ITGA5-6	156.378	114.209	0.279
	ITGA5-7	34.447	25.772	0.035
	ITGA5-20	138.585	108.479	0.332
	ITGA5-pool	61.548	18.337	0.049
9037	Q-SEMA5A	162.275	NA	NA
	SEMA5A-1	243.064	115.188	0.111
	SEMA5A-3	260.767	143.358	0.127
	SEMA5A-4	805.056	599.039	0.119
	SEMA5A-17	106.868	62.370	0.445
	SEMA5A-pool	228.015	122.741	0.139
93190	Q-MGC35194	187.283	NA	NA
	MGC35194-1	177.220	149.952	0.271
	MGC35194-2	142.745	64.838	0.225
	MGC35194-3	450.007	249.880	0.093
	MGC35194-4	603.355	400.298	0.109
	MGC35194-pool	675.482	413.285	0.094
139716	Q-GAB3	72.213	NA	NA
	GAB3-1	73.120	7.121	0.017
	GAB3-2	8.776	2.005	0.000
	GAB3-3	0.000	0.000	NA
	GAB3-4	103.994	26.961	0.427
	GAB3-pool	0.177	0.251	0.000
11027	Q-LILRA2	33.475	NA	NA
	LILRA2-1	21.351	14.062	0.008
	LILRA2-2	172.179	50.673	0.091
	LILRA2-3	147.089	8.922	0.009
	LILRA2-4	57.834	10.736	0.015
	LILRA2-pool	83.162	15.663	0.134
9704	Q-DHX34	38.542	NA	NA
	DHX34-1	32.622	9.406	0.005
	DHX34-2	55.418	21.049	0.048
	DHX34-3	411.867	68.688	0.012
	DHX34-4	260.127	13.636	0.002
	DHX34-pool	246.797	58.420	0.035
51352	Q-WIT1	150.834	NA	NA
	WIT1-1	54.781	7.467	0.007
	WIT1-2	30.223	23.339	0.026
	WIT1-3	144.236	45.744	0.152
	WIT1-4	184.048	19.263	0.013
	WIT1-pool	91.724	39.173	0.397

GeneID	siRNA	mean	stdev	p-value
9099	Q-USP2	88.885	NA	NA
	USP2-1	45.727	28.881	0.059
	USP2-2	498.566	197.601	0.052
	USP2-3	292.184	82.941	0.041
	USP2-4	10.599	14.990	0.007
	USP2-pool	37.105	34.796	0.062
49856	Q-WDR8	221.608	NA	NA
	WDR8-1	362.622	188.160	0.094
	WDR8-2	1.720	2.433	0.000
	WDR8-3	139.814	12.758	0.024
	WDR8-4	591.299	265.796	0.060
	WDR8-pool	168.323	50.920	0.099
6696	Q-SPP1	34.129	NA	NA
	SPP1-5	1.443	2.040	0.000
	SPP1-6	6.992	9.889	0.003
	SPP1-7	154.742	35.594	0.081
	SPP1-8	8.380	11.851	0.004
	SPP1-pool	6.992	9.889	0.003

Table A.10: Table listing IDs of all siRNAs vended by Dharmacon that were used in this work.

Symbol	Dharmacon-ID
CASP4	M-004404-00
CCL22	M-007834-00
CCL25	M-007837-01
CFL1	M-012707-00
CKAP4	M-012755-00
CKAP5	M-006847-00
CKB	M-006706-01
CLTC	M-004001-00
DHX34	M-032233-00
DSC1	M-011995-00
DSCR3	M-012163-00
EMR2	M-005488-00
FLJ10587	M-016480-00
FLJ10980	M-022243-00
FLJ11305	M-020730-00
FOXL1	M-008986-00
GAB3	M-015239-00
GH2	M-011668-00
GPR119	M-005521-00
HIF1AN	M-004073-01
HSMPP8	M-021680-00
ITGA5	M-008003-01
ITGB4BP	M-010096-01
KIAA0999	M-004779-02
KIF2B	M-008345-01
KLK4	M-005915-01
LILRA2	M-019855-00
LTBR	M-008023-01
MAP2K3	M-003509-01
MDM2	M-003279-02
MEN1	M-011082-00
MGC16664	M-018554-00
MGC35194	M-016852-00
MS4A4A	M-017214-00
NOP17	M-020963-00
NUP153	M-005283-00
ORMDL3	M-017002-00
OTOF	M-011942-00
PACAP	M-004433-00
PAK4	M-003615-02
PIB5PA	M-009108-00
PKN3	M-004647-00
PLK3	M-003257-02

Symbol	Dharmacon-ID
PPM1F	M-009544-00
PRO1855	M-010669-00
PSCD2	M-011925-01
PSMA4	M-017211-00
PTK9	M-003168-03
RAB31	M-010065-01
RABGEF1	M-008541-00
RANBP2	M-004746-01
RAPGEF3	M-007676-00
RBM19	M-021123-00
RNF150	M-010713-00
ROBO4	M-015216-00
SEMA5A	M-019490-00
SETD5	M-028069-00
SEZ6L2	M-008062-00
SHD	M-023905-00
SKP1A	M-003323-02
SMAD4	M-003902-01
SMARCB1	M-010536-00
SOST	M-014616-00
SPAG4	M-011397-00
SPP1	M-012558-00
SPP2	M-019720-00
SSFA2	M-015325-00
SV2A	M-007631-00
TRIB3	M-003754-01
TRIM68	M-007007-00
USP2	M-006069-00
VCP	M-008727-01
VSIG4	M-012788-00
WDR1	M-011984-00
WDR8	M-013318-00
WIT1	M-013209-00

List of Figures

1.1 The role of inflammation in health and disease. 2
1.2 Signaling pathways initiated by members of the TNF-α family share similarities. 3
1.3 Schematic presentation of human TNF-α signaling. 5
1.4 Inducers and regulators of NF-κB signaling. 7
1.5 Levels of regulation of TNF-α signaling. 10
1.6 Negative regulation of TNF-α signaling and NF-κB transcriptional activity. 12
1.7 Mechanism of RNAi. 14
1.8 Genome-wide RNAi screening approaches. 16
1.9 Concept of the dual luciferase assay. 18

2.1 TNF-α treatment does not induce cell death in HEK293T cells. 22
2.2 TNF-α treatment induces NF-κB transcriptional activity in HEK293T cells. 23
2.3 Influence of TNF-α stimulation on *Renilla* luciferase expression driven by viral promoters. 24
2.4 Expression levels of NF-κB-dependent 4-4-FL (black bars) and constitutively expressed act-RL (grey bars) without and with TNF-α treatment. . . 25
2.5 Optimizing the NF-κB luciferase assay. 27
2.6 Performance of the established luciferase assay in a small scale pilot screen. 28
2.7 Overview of all plates of screen A. 31
2.8 Reproducibility of screening results and separation of controls in screen A. . 32
2.9 Overview of all plates of screen B. 33
2.10 Reproducibility of screening results and separation of controls in screen B. . 34
2.11 Quantile-quantile plots for screening results. 35
2.12 Comparison of results of screens A and B. 37
2.13 HEK293T cells secrete IL-8 upon stimulation with TNF-α. 38
2.14 Schematic representation of the decision making from the first hit lists to the final candidate list. 39
2.15 Retests in HEK293T cells. 42

2.16 Retests in HepG2 cells. 43
2.17 Knockdown of the seven selected candidates does not affect cell viability. . . 44
2.18 Candidate mRNA levels after treatment of HEK293T cells with siRNAs. . . 44
2.19 Effects in HEK293T cells mediated by siRNAs targeting SPP1, GAB3 and CASP4. 46
2.20 Effect of SPP1 knockdown on TNF-α-induced target gene expression. 48
2.21 Effect of GAB3 knockdown on TNF-α-induced target gene expression. . . . 49
2.22 Effect of CASP4 knockdown on TNF-α-induced target gene expression. . . . 50
2.23 Expression of TNF-α target genes. 52
2.24 TNF-α target gene expression signature. 54
2.25 Knockdown of SPP1, GAB3 and CASP4 abolishes upon TNF-α stimulation in HeLa cells. 55
2.26 Epistasis experiments in HEK293T cells by overexpressing known pathway components. 57
2.27 Knockdown of SPP1, GAB3 and CASP4 does not affect TNFR1 cell surface expression. 58
2.28 CASP4 protein depletion upon siCASP4 treatment. 59
2.29 IF determining the cellular localization of CASP4. 60
2.30 CASP4 is not cleaved upon TNF-α treatment. 61

3.1 Overlap of the two screens at different z-score cut-offs. 67
3.2 Comparison of the pilot kinase screen with the kinase plates of screen A. . . 68
3.3 Models of GAB3's mode of action in TNF-α signaling. 75
3.4 Model of SPP1's mode of action in TNF-α signaling. 78
3.5 Model of CASP4's mode of action in TNF-α signaling. 81

4.1 Plasmid map of the 4-4-FL NF-κB reporter. 87
4.2 Plasmid map of the act-RL co-reporter. 88

List of Tables

1.1 Protein domains important in TNF-α signaling. 6
1.2 Artificially introduced small non-coding RNAs. 15

2.1 Table of seven potential novel regulators of TNF-α signaling. 41

3.1 Published RNAi screens for TNF-α-induced activation of NF-κB. 70

4.1 siRNA sequences of controls and candidates. NA: not available. (For IDs of all siRNAs used in this work see supplementary table A.10.) 86
4.2 Oligos for cloning. 91
4.3 qRT-PCR primers. 91

A.1 Hit list of screen A. 103
A.2 Hit list of screen B. 104
A.3 Overlap of screens A and B. 105
A.4 Overlap between TNF gene set and screening hit list. 108
A.5 Overlap between inflammation gene set and screening hit list. 108
A.6 Phenotypes of knockdown of all selected hits using dual luciferase assay in HEK293T cells to assess NF-κB transcriptional activity. 109
A.7 Phenotypes of knockdown of selected hits using IL-8 ELISA in HEK293T cells to assess NF-κB transcriptional activity. 112
A.8 Phenotypes of knockdown of selected hits using dual luciferase assay in HepG2 cells to assess NF-κB transcriptional activity. 115
A.9 Phenotypes of knockdown of selected hits using IL-8 ELISA in HepG2 cells to assess NF-κB transcriptional activity. 116
A.10 Table listing IDs of all siRNAs vended by Dharmacon. 118

Nomenclature

4-4-FL	NF-κB-dependent *firefly* luciferase expression construct
act-RL	*Renilla* luciferase expression construct where the luciferase gene is under the control of the β-actin promoter
AKT	v-akt murine thymoma viral oncogene homolog
AP	activator protein
ARE	AU-rich element
ATP	adenosine triphosphate
BAG4	Bcl-2-associated athanogen
BAX	BCL2-associated X protein
BCA	bicinchoninic acid
BIRC	baculoviral IAP repeat-containing
BMP	bone morphogenic protein
bp	basepair
BSA	bovine serum albumine
CARD	caspase recruitment domain
CASP	caspase
CASP8AP	caspase 8 associated protein
CCL	CC-motif chemokine ligand
CCND1	cyclin D1
CD	cluster of differentiation
cDNA	complementary DNA
CMV	cytomegalovirus
CPB	cAMP responsive element binding protein (CREB) binding protein
CTSL1	cathepsin L1
CXCL	C-X-C motif chemokine ligand
CYLD	cylindromatosis
DD	death domain
DMEM	*Dulbecco's Modified Eagle Medium*

DMSO	dimethyl sulfoxide
DNA	deoxyribonucleic acid
DOS	daughter of sevenless
dsRNA	double-stranded RNA
DUB	de-ubiquitinating
e.g.	exempli gratia
EDTA	ethylenediaminetetraacetic acid
EGFR	epidermal growth factor receptor
ELISA	enzyme-linked immunosorbent assay
EMSA	electrophoretic mobility shift assay
endo-siRNA	endogenous siRNA
ERK	extracellular signal-regulated kinase
esiRNA	endoribonuclease-prepared short interfering RNA
et al.	et alia
FACS	fluorescence activated cell sorting
FADD	Fas-associated death domain
FCS	fetal calf serum
FL	*Firefly* luciferase
GAB	GRB2-associated binding protein 3
GADD	growth arrest- and DNA damage-inducible gene
GAPDH	glyceraldehyde 3-phosphate dehydrogenase
GO	gene ontology
GRAP	GRB2-related adaptor protein
GRB	growth factor receptor-bound protein
GTP	guanosine triphosphate
h	hour(s)
HAT	histone acetyl transferase
HIV	human immunodeficiency virus
HRP	horseradish peroxidase
HRPT	Hypoxanthine-guanine phosphoribosyltransferase
IκB	inhibitor of κB
i.e.	id est
IAP	inhibitor of apoptosis
IKK	IκB kinase
IL	interleukin
IRAK	interleukin-1 receptor-associated kinase

IRF	interferon regulatory factor
ITGA5	integrin, α 5
JNK	Jun N-terminal kinase
JunB	jun B proto-oncogene
kb	kilobase
LILRA	leukocyte immunoglobulin-like receptor, subfamily A
LPS	lipopolysaccharide
LRP	low-density lipoprotein receptor-related protein
LT	lymphotoxin
M-CSF	macrophage colony-stimulating factor
MAPK	mitogen-activated protein kinase
MEKK	MAPK kinase kinase
MEN	menin
min	minute(s)
miRNA	microRNA
ml	milliliter
MOPS	3-(N-Morpholino)propanesulfonic acid
mRNA	messenger RNA
MYB	v-myb myeloblastosis viral oncogene homolog
MYC	v-myc myelocytomatosis viral oncogene homolog
MyD88	myeloid differentiation primary response gene (88)
NES	nuclear export signal
NF-κB	nuclear factor κB
NFKBIA	nuclear factor of kappa light polypeptide gene enhancer in B-cells inhibitor, alpha; encodes IκB-α
NLR	NOD protein-like receptor
NLS	nuclear localization signal
nM	nanomolar
NO	nitric oxide
NOD	nucleotide oligomerization domain
PAMP	pathogen-associated molecular pattern
PBS	phosphate-buffered saline
PCR	polymerase chain reaction
PE	phycoerythrin
Pfa	paraformaldehyde
PH	pleckstrin homology

PI	propidium iodide
PI(3)K	phosphoinositide-3-kinase
PIM1	pim-1 oncogene
piRNA	Piwi-interacting RNA
PKB/C	protein kinase B/C
PRR	pattern recognition receptor
QQ	quantile-quantile
qRT-PCR	quantitative realtime PCR
RANKL	receptor activator of NF-κB ligand
Ras	rat sarcoma
rasiRNA	repeat-associated siRNAs
RHD	Rel homology domain
RIG	retinoic acid inducible gene
RING	really interesting new gene
RIP	receptor interacting protein
RISC	RNA-induced silencing complex
RL	*Renilla* luciferase
RLU	relative light units, representing the strength of luciferase luminescence
RNA	ribonucleic acid
RNAi	RNA interference
ROS	reactive oxygen species
rpm	revolutions per minute
SCF	Skp-1/Cul/F box
scnRNA	small-scan siRNAs
SDS	sodium dodecyl sulphate
sec	seconds
SH	Src homology
SHP	protein tyrosine phosphatase
shRNA	short-hairpin RNAs
siCon	siControl #1
siRNA	small interfering RNA
SMase	sphingomyelinase
SPP (OPN)	secreted phosphoprotein (Osteopontin)
TAB	TAK1-binding protein
TACE	TNF-αconverting enzyme

TAD	transcription activation domain
TAE	Tris-acetate-EDTA
TAK	transforming growth factor-β-activated kinase
TAP1	transporter 1, ATP-binding cassette, sub-family B
tasiRNA	trans-acting siRNAs
TK	thymidin kinase
TLR	Toll-like receptor
TNF-α	tumor necrosis factor-α
TNFAIP	TNF-α-induced protein
TNFR-C	tumor necrosis factor-α receptor 1 complex I
TNFRSF1A (TNFR1)	TNF receptor superfamily member 1A
TNFRSF1B (TNFR2)	TNF receptor superfamily member 1B
TRADD	TNFR1-associated death domain protein
TRAF	TNFR-associated factor
TRAIL	TNF-related apoptosis-inducing ligand
TRAPS	TNFR-associated periodic syndrome
TTP	tristetraprolin
Ubc	ubiquitin conjugating enzyme
UBD	ubiquitin binding domain
Uev	Ubc-like factor ubiquitin conjugationg enzyme variant
UPL	universal probe library
USP	ubiquitin specific peptidase
UTR	untranslated region
V	volt
vs.	versus
w/	with
w/o	without
WIT	Wilms tumor upstream neighbor

Bibliography

[1] Abraham, M. C. and Shaham, S. Death without caspases, caspases without death. *Trends in Cell Biology*, 14(4):184–193 (2004).

[2] Adam-Klages, S., Adam, D., Wiegmann, K., Struve, S., Kolanus, W., Schneider-Mergener, J., and Kroenke, M. FAN, a novel WD-repeat protein, couples the p55 TNF-receptor to neutral sphingomyelinase. *Cell*, 86(6):937–947 (1996).

[3] Agrawal, S. and Kandimalla, E. R. Role of toll-like receptors in antisense and siRNA [corrected]. *Nature Biotechnology*, 22(12):1533–1537 (2004).

[4] Ahn, E., Pan, G., Vickers, S. M., and McDonald, J. M. IFN-gamma upregulates apoptosis-related molecules and enhances fas-mediated apoptosis in human cholangiocarcinoma. *International Journal of Cancer*, 100(4):445–451 (2002).

[5] Akira, S. Innate immunity to pathogens: diversity in receptors for microbial recognition. *Immunological Reviews*, 227(1):5–8 (2009).

[6] Anantharaman, V., Koonin, E. V., and Aravind, L. Comparative genomics and evolution of proteins involved in RNA metabolism. *Nucl. Acids Res.*, 30(7):1427–1464 (2002).

[7] Anest, V., Hanson, J. L., Cogswell, P. C., Steinbrecher, K. A., Strahl, B. D., and Baldwin, A. S. A nucleosomal function for IkappaB kinase-alpha in NF-kappaB-dependent gene expression. *Nature*, 423(6940):659–663 (2003).

[8] Ashkar, S., Weber, G. F., Panoutsakopoulou, V., Sanchirico, M. E., Jansson, M., Zawaideh, S., Rittling, S. R., Denhardt, D. T., Glimcher, M. J., and Cantor, H. Eta-1 (osteopontin): an early component of type-1 (cell-mediated) immunity. *Science*, 287(5454):860–864 (2000).

[9] Aza-Blanc, P., Cooper, C. L., Wagner, K., Batalov, S., Deveraux, Q. L., and Cooke, M. P. Identification of modulators of TRAIL-induced apoptosis via RNAi-based phenotypic screening. *Molecular Cell*, 12(3):627–637 (2003).

[10] Bartel, D. P. MicroRNAs: genomics, biogenesis, mechanism, and function. *Cell*, 116(2):281–297 (2004).

[11] Barton, G. M. and Kagan, J. C. A cell biological view of toll-like receptor function: regulation through compartmentalization. *Nature Reviews. Immunology*, 9(8):535–542 (2009).

[12] Baud, V. and Karin, M. Signal transduction by tumor necrosis factor and its relatives. *Trends in Cell Biology*, 11(9):372–377 (2001).

[13] Ben-Neriah, Y. Regulatory functions of ubiquitination in the immune system. *Nature Immunology*, 3(1):20–26 (2002).

[14] Bernstein, E., Denli, A. M., and Hannon, G. J. The rest is silence. *RNA*, 7(11):1509–1521 (2001).

[15] Beutler, B., Milsark, I. W., and Cerami, A. C. Passive immunization against cachectin/tumor necrosis factor protects mice from lethal effect of endotoxin. *Science*, 229(4716):869–871 (1985).

[16] Bhoj, V. G. and Chen, Z. J. Ubiquitylation in innate and adaptive immunity. *Nature*, 458(7237):430–437 (2009).

[17] BioCarta. http://www.biocarta.com/genes/index.asp.

[18] bioinfo.lifl.fr. Bioinformatics software server. *http://bioinfo.lifl.fr/NF-KB/.*

[19] Birmingham, A., Selfors, L. M., Forster, T., Wrobel, D., Kennedy, C. J., Shanks, E., Santoyo-Lopez, J., Dunican, D. J., Long, A., Kelleher, D., Smith, Q., Beijersbergen, R. L., Ghazal, P., and Shamu, C. E. Statistical methods for analysis of high-throughput RNA interference screens. *Nature Methods*, 6(8):569–575 (2009).

[20] Black, R. A., Rauch, C. T., Kozlosky, C. J., Peschon, J. J., Slack, J. L., Wolfson, M. F., Castner, B. J., Stocking, K. L., Reddy, P., Srinivasan, S., Nelson, N., Boiani, N., Schooley, K. A., Gerhart, M., Davis, R., Fitzner, J. N., Johnson, R. S., Paxton, R. J., March, C. J., and Cerretti, D. P. A metalloproteinase disintegrin that releases tumour-necrosis factor-alpha from cells. *Nature*, 385(6618):729–733 (1997).

[21] Blackwell, K., Zhang, L., Thomas, G. S., Sun, S., Nakano, H., and Habelhah, H. TRAF2 phosphorylation modulates tumor necrosis factor alpha-induced gene expression and cell resistance to apoptosis. *Molecular and Cellular Biology*, 29(2):303–314 (2009).

[22] Bodmer, J., Schneider, P., and Tschopp, J. The molecular architecture of the TNF superfamily. *Trends in Biochemical Sciences*, 27(1):19–26 (2002).

[23] Bonizzi, G. and Karin, M. The two NF-kappaB activation pathways and their role in innate and adaptive immunity. *Trends in Immunology*, 25(6):280–288 (2004).

[24] Bouchier-Hayes, L. and Martin, S. J. CARD games in apoptosis and immunity. *EMBO Reports*, 3(7):616–621 (2002).

[25] Bourgin, C., Bourette, R., Mouchiroud, G., and Arnaud, S. Expression of mona (monocytic adapter) in myeloid progenitor cells results in increased and prolonged MAP kinase activation upon macrophage colony-stimulating factor stimulation. *FEBS Letters*, 480(2-3):113–117 (2000).

[26] Bourgin, C., Bourette, R. P., Arnaud, S., Liu, Y., Rohrschneider, L. R., and Mouchiroud, G. Induced expression and association of the Mona/Gads adapter and gab3 scaffolding protein during monocyte/macrophage differentiation. *Molecular and Cellular Biology*, 22(11):3744–3756 (2002).

[27] Bourteele, S., Hausser, A., Doeppler, H., Horn-Mueller, J., Roepke, C., Schwarzmann, G., Pfizenmaier, K., and Mueller, G. Tumor necrosis factor induces ceramide oscillations and negatively controls sphingolipid synthases by caspases in apoptotic kym-1 cells. *The Journal of Biological Chemistry*, 273(47):31245–31251 (1998).

[28] Boutros, M. and Ahringer, J. The art and design of genetic screens: RNA interference. *Nature Reviews. Genetics*, 9(7):554–566 (2008).

[29] Boutros, M., Bras, L. P., and Huber, W. Analysis of cell-based RNAi screens. *Genome Biology*, 7(7):R66 (2006).

[30] Boutros, M., Kiger, A. A., Armknecht, S., Kerr, K., Hild, M., Koch, B., Haas, S. A., Paro, R., and Perrimon, N. Genome-wide RNAi analysis of growth and viability in drosophila cells. *Science*, 303(5659):832–835 (2004).

[31] Bradley, J. R. TNF-mediated inflammatory disease. *The Journal of Pathology*, 214(2):149–160 (2008).

[32] Brummelkamp, T. R., Nijman, S. M. B., Dirac, A. M. G., and Bernards, R. Loss of the cylindromatosis tumour suppressor inhibits apoptosis by activating NF-kappaB. *Nature*, 424(6950):797–801 (2003).

[33] Cantor, H. and Shinohara, M. L. Regulation of t-helper-cell lineage development by osteopontin: the inside story. *Nature Reviews. Immunology*, 9(2):137–141 (2009).

[34] Carballo, E., Lai, W. S., and Blackshear, P. J. Feedback inhibition of macrophage tumor necrosis factor-alpha production by tristetraprolin. *Science*, 281(5379):1001–1005 (1998).

[35] Carpenter, A. E., Jones, T. R., Lamprecht, M. R., Clarke, C., Kang, I. H., Friman, O., Guertin, D. A., Chang, J. H., Lindquist, R. A., Moffat, J., Golland, P., and Sabatini, D. M. CellProfiler: image analysis software for identifying and quantifying cell phenotypes. *Genome Biology*, 7(10):R100 (2006).

[36] Carswell, E. A., Old, L. J., Kassel, R. L., Green, S., Fiore, N., and Williamson, B. An endotoxin-induced serum factor that causes necrosis of tumors. *Proceedings of the National Academy of Sciences of the United States of America*, 72(9):3666–3670 (1975).

[37] Cathomen, T. and Joung, J. K. Zinc-finger nucleases: the next generation emerges. *Molecular Therapy: The Journal of the American Society of Gene Therapy*, 16(7):1200–1207 (2008).

[38] Chabas, D., Baranzini, S. E., Mitchell, D., Bernard, C. C., Rittling, S. R., Denhardt, D. T., Sobel, R. A., Lock, C., Karpuj, M., Pedotti, R., Heller, R., Oksenberg, J. R., and Steinman, L. The influence of the proinflammatory cytokine, osteopontin, on autoimmune demyelinating disease. *Science*, 294(5547):1731–1735 (2001).

[39] Chan, F. K., Chun, H. J., Zheng, L., Siegel, R. M., Bui, K. L., and Lenardo, M. J. A domain in TNF receptors that mediates ligand-independent receptor assembly and signaling. *Science*, 288(5475):2351–2354 (2000).

[40] Chandel, N. S., Schumacker, P. T., and Arch, R. H. Reactive oxygen species are downstream products of TRAF-mediated signal transduction. *The Journal of Biological Chemistry*, 276(46):42728–42736 (2001).

[41] Chang, F., Steelman, L. S., Lee, J. T., Shelton, J. G., Navolanic, P. M., Blalock, W. L., Franklin, R. A., and McCubrey, J. A. Signal transduction mediated by the Ras//Raf//MEK//ERK pathway from cytokine receptors to transcription factors: potential targeting for therapeutic intervention. *Leukemia*, 17(7):1263–1293 (2003).

[42] Chaudhary, P. M., Eby, M. T., Jasmin, A., Kumar, A., Liu, L., and Hood, L. Activation of the NF-kappaB pathway by caspase 8 and its homologs. *Oncogene*, 19(39):4451–4460 (2000).

[43] Chen, F. E. and Ghosh, G. Regulation of DNA binding by Rel/NF-kappaB transcription factors: structural views. *Oncogene*, 18(49):6845–6852 (1999).

[44] Chen, L. and Greene, W. C. Shaping the nuclear action of NF-kappaB. *Nature Reviews. Molecular Cell Biology*, 5(5):392–401 (2004).

[45] Chen, Z. J. Ubiquitin signalling in the NF-kappaB pathway. *Nature Cell Biology*, 7(8):758–765 (2005).

[46] Chew, J., Biswas, S., Shreeram, S., Humaidi, M., Wong, E. T., Dhillion, M. K., Teo, H., Hazra, A., Fang, C. C., Lopez-Collazo, E., Bulavin, D. V., and Tergaonkar, V. WIP1 phosphatase is a negative regulator of NF-kappaB signalling. *Nature Cell Biology*, 11(5):659–666 (2009).

[47] Chhabra, R., Adlakha, Y. K., Hariharan, M., Scaria, V., and Saini, N. Upregulation of miR-23a approximately 27a approximately 24-2 cluster induces Caspase-Dependent and -Independent apoptosis in human embryonic kidney cells. *PLoS ONE*, 4(6):e5848 (2009).

[48] Chiu, Y. and Rana, T. M. RNAi in human cells: basic structural and functional features of small interfering RNA. *Molecular Cell*, 10(3):549–561 (2002).

[49] Christensen, B., Nielsen, M. S., Haselmann, K. F., Petersen, T. E., and Sorensen, E. S. Post-translationally modified residues of native human osteopontin are located in clusters: identification of 36 phosphorylation and five o-glycosylation sites and their biological implications. *The Biochemical Journal*, 390(Pt 1):285–292 (2005).

[50] Chu, C. and Rana, T. M. Small RNAs: regulators and guardians of the genome. *Journal of Cellular Physiology*, 213(2):412–419 (2007).

[51] Collart, M. A., Baeuerle, P., and Vassalli, P. Regulation of tumor necrosis factor alpha transcription in macrophages: involvement of four kappa b-like motifs and of constitutive and inducible forms of NF-kappa b. *Molecular and Cellular Biology*, 10(4):1498–1506 (1990).

[52] Comabella, M., Pericot, I., Goertsches, R., Nos, C., Castillo, M., Navarro, J. B., Rio, J., and Montalban, X. Plasma osteopontin levels in multiple sclerosis. *Journal of Neuroimmunology*, 158(1-2):231–239 (2005).

[53] Cook, A. C., Tuck, A. B., McCarthy, S., Turner, J. G., Irby, R. B., Bloom, G. C., Yeatman, T. J., and Chambers, A. F. Osteopontin induces multiple changes in gene expression that reflect the six "hallmarks of cancer" in a model of breast cancer progression. *Molecular Carcinogenesis*, 43(4):225–236 (2005).

[54] Covert, M. W., Leung, T. H., Gaston, J. E., and Baltimore, D. Achieving stability of Lipopolysaccharide-Induced NF-kappaB activation. *Science*, 309(5742):1854–1857 (2005).

[55] Das, R., Mahabeleshwar, G. H., and Kundu, G. C. Osteopontin stimulates cell motility and nuclear factor kappaB-mediated secretion of urokinase type plasminogen activator through phosphatidylinositol 3-kinase/Akt signaling pathways in breast cancer cells. *The Journal of Biological Chemistry*, 278(31):28593–28606 (2003).

[56] de Martin, R., Vanhove, B., Cheng, Q., Hofer, E., Csizmadia, V., Winkler, H., and Bach, F. H. Cytokine-inducible expression in endothelial cells of an i kappa b alpha-like gene is regulated by NF kappa b. *The EMBO Journal*, 12(7):2773–2779 (1993).

[57] Delhase, M., Hayakawa, M., Chen, Y., and Karin, M. Positive and negative regulation of IkappaB kinase activity through IKKbeta subunit phosphorylation. *Science*, 284(5412):309–313 (1999).

[58] Deng, L. Activation of the IkappaB kinase complex by TRAF6 requires a dimeric Ubiquitin-Conjugating enzyme complex and a unique polyubiquitin chain. *Cell*, 103(2):351–361 (2000).

[59] Denli, A. M., Tops, B. B. J., Plasterk, R. H. A., Ketting, R. F., and Hannon, G. J. Processing of primary microRNAs by the microprocessor complex. *Nature*, 432(7014):231–235 (2004).

[60] Devin, A., Cook, A., Lin, Y., Rodriguez, Y., Kelliher, M., and Liu, Z. The distinct roles of TRAF2 and RIP in IKK activation by TNF-R1: TRAF2 recruits IKK to TNF-R1 while RIP mediates IKK activation. *Immunity*, 12(4):419–429 (2000).

[61] DiDonato, J. A., Hayakawa, M., Rothwarf, D. M., Zandi, E., and Karin, M. A cytokine-responsive IkappaB kinase that activates the transcription factor NF-kappaB. *Nature*, 388(6642):548–554 (1997).

[62] Dietzl, G., Chen, D., Schnorrer, F., Su, K., Barinova, Y., Fellner, M., Gasser, B., Kinsey, K., Oppel, S., Scheiblauer, S., Couto, A., Marra, V., Keleman, K., and Dickson, B. J. A genome-wide transgenic RNAi library for conditional gene inactivation in drosophila. *Nature*, 448(7150):151–156 (2007).

[63] Du, T. and Zamore, P. D. microPrimer: the biogenesis and function of microRNA. *Development*, 132(21):4645–4652 (2005).

[64] Dunning, M. J., Smith, M. L., Ritchie, M. E., and Tavare, S. beadarray: R classes and methods for illumina bead-based data. *Bioinformatics*, 23(16):2183–2184 (2007).

[65] Ea, C., Deng, L., Xia, Z., Pineda, G., and Chen, Z. J. Activation of IKK by TNFalpha requires site-specific ubiquitination of RIP1 and polyubiquitin binding by NEMO. *Molecular Cell*, 22(2):245–257 (2006).

[66] Echeverri, C. J., Beachy, P. A., Baum, B., Boutros, M., Buchholz, F., Chanda, S. K., Downward, J., Ellenberg, J., Fraser, A. G., Hacohen, N., Hahn, W. C., Jackson, A. L., Kiger, A., Linsley, P. S., Lum, L., Ma, Y., Mathey-Prevot, B., Root, D. E., Sabatini, D. M., Taipale, J., Perrimon, N., and Bernards, R. Minimizing the risk of reporting false positives in large-scale RNAi screens. *Nature Methods*, 3(10):777–779 (2006).

[67] Elbashir, S. M., Martinez, J., Patkaniowska, A., Lendeckel, W., and Tuschl, T. Functional anatomy of siRNAs for mediating efficient RNAi in drosophila melanogaster embryo lysate. *The EMBO Journal*, 20(23):6877–6888 (2001).

[68] English, J. J., Mueller, E., and Baulcombe, D. C. Suppression of virus accumulation in transgenic plants exhibiting silencing of nuclear genes. *The Plant Cell*, 8(2):179–188 (1996).

[69] Eulalio, A., Huntzinger, E., and Izaurralde, E. Getting to the root of miRNA-mediated gene silencing. *Cell*, 132(1):9–14 (2008).

[70] Ewald, S. E., Lee, B. L., Lau, L., Wickliffe, K. E., Shi, G., Chapman, H. A., and Barton, G. M. The ectodomain of toll-like receptor 9 is cleaved to generate a functional receptor. *Nature*, 456(7222):658–662 (2008).

[71] Fantuzzi, G. Lessons from interleukin-deficient mice: the interleukin-1 system. *Acta Physiologica Scandinavica*, 173(1):5–9 (2001).

[72] Faucheu, C., Diu, A., Chan, A. W., Blanchet, A. M., Miossec, C., Herve, F., Collard-Dutilleul, V., Gu, Y., Aldape, R. A., and Lippke, J. A. A novel human protease similar to the interleukin-1 beta converting enzyme induces apoptosis in transfected cells. *The EMBO Journal*, 14(9):1914–1922 (1995).

[73] Filipowicz, W. RNAi: the nuts and bolts of the RISC machine. *Cell*, 122(1):17–20 (2005).

[74] Fire, A., Xu, S., Montgomery, M. K., Kostas, S. A., Driver, S. E., and Mello, C. C. Potent and specific genetic interference by double-stranded RNA in caenorhabditis elegans. *Nature*, 391(6669):806–811 (1998).

[75] Fitzgerald, K. A., Palsson-McDermott, E. M., Bowie, A. G., Jefferies, C. A., Mansell, A. S., Brady, G., Brint, E., Dunne, A., Gray, P., Harte, M. T., McMurray, D., Smith, D. E., Sims, J. E., Bird, T. A., and O'Neill, L. A. Mal (MyD88-adapter-like) is required for toll-like receptor-4 signal transduction. *Nature*, 413(6851):78–83 (2001).

[76] Fontalba, A., Gutierrez, O., and Fernandez-Luna, J. L. NLRP2, an inhibitor of the NF-kappaB pathway, is transcriptionally activated by NF-kappaB and exhibits a nonfunctional allelic variant. *Journal of Immunology*, 179(12):8519–8524 (2007).

[77] Fotin-Mleczek, M., Henkler, F., Samel, D., Reichwein, M., Hausser, A., Parmryd, I., Scheurich, P., Schmid, J. A., and Wajant, H. Apoptotic crosstalk of TNF receptors: TNF-R2-induces depletion of TRAF2 and IAP proteins and accelerates TNF-R1-dependent activation of caspase-8. *Journal of Cell Science*, 115(Pt 13):2757–2770 (2002).

[78] Fukushima, T., Matsuzawa, S., Kress, C. L., Bruey, J. M., Krajewska, M., Lefebvre, S., Zapata, J. M., Ronai, Z., and Reed, J. C. Ubiquitin-conjugating enzyme ubc13 is a critical component of TNF receptor-associated factor (TRAF)-mediated inflammatory responses. *Proceedings of the National Academy of Sciences of the United States of America*, 104(15):6371–6376 (2007).

[79] Galli, S. J., Tsai, M., and Piliponsky, A. M. The development of allergic inflammation. *Nature*, 454(7203):445–454 (2008).

[80] Galon, J., Aksentijevich, I., McDermott, M. F., O'Shea, J. J., and Kastner, D. L. TNFRSF1A mutations and autoinflammatory syndromes. *Current Opinion in Immunology*, 12(4):479–486 (2000).

[81] Gene Ontology Consortium. Creating the gene ontology resource: design and implementation. *Genome Research*, 11(8):1425–1433 (2001).

[82] Geng, H., Wittwer, T., Dittrich-Breiholz, O., Kracht, M., and Schmitz, M. L. Phosphorylation of NF-kappaB p65 at ser468 controls its COMMD1-dependent ubiquitination and target gene-specific proteasomal elimination. *EMBO Reports*, 10(4):381–386 (2009).

[83] Gesellchen, V., Kuttenkeuler, D., Steckel, M., Pelte, N., and Boutros, M. An RNA interference screen identifies inhibitor of apoptosis protein 2 as a regulator of innate immune signalling in drosophila. *EMBO Reports*, 6(10):979–984 (2005).

[84] Ghosh, S. and Hayden, M. S. New regulators of NF-kappaB in inflammation. *Nature Reviews. Immunology*, 8(11):837–848 (2008).

[85] Gracie, J. A., Robertson, S. E., and McInnes, I. B. Interleukin-18. *Journal of Leukocyte Biology*, 73(2):213–224 (2003).

[86] Gregory, R. I., Chendrimada, T. P., Cooch, N., and Shiekhattar, R. Human RISC couples microRNA biogenesis and posttranscriptional gene silencing. *Cell*, 123(4):631–640 (2005).

[87] Gregory, R. I., Yan, K., Amuthan, G., Chendrimada, T., Doratotaj, B., Cooch, N., and Shiekhattar, R. The microprocessor complex mediates the genesis of microRNAs. *Nature*, 432(7014):235–240 (2004).

[88] Grell, M., Wajant, H., Zimmermann, G., and Scheurich, P. The type 1 receptor (CD120a) is the high-affinity receptor for soluble tumor necrosis factor. *Proceedings of the National Academy of Sciences of the United States of America*, 95(2):570–575 (1998).

[89] Grishok, A., Pasquinelli, A. E., Conte, D., Li, N., Parrish, S., Ha, I., Baillie, D. L., Fire, A., Ruvkun, G., and Mello, C. C. Genes and mechanisms related to RNA interference regulate expression of the small temporal RNAs that control c. elegans developmental timing. *Cell*, 106(1):23–34 (2001).

[90] Haecker, H. and Karin, M. Regulation and function of IKK and IKK-related kinases. *Science's STKE: Signal Transduction Knowledge Environment*, 2006(357):re13 (2006).

[91] Hammond, S. M., Bernstein, E., Beach, D., and Hannon, G. J. An RNA-directed nuclease mediates post-transcriptional gene silencing in drosophila cells. *Nature*, 404(6775):293–296 (2000).

[92] Han, J., Lee, Y., Yeom, K., Kim, Y., Jin, H., and Kim, V. N. The Drosha-DGCR8 complex in primary microRNA processing. *Genes & Development*, 18(24):3016–3027 (2004).

[93] Hanahan, D. and Weinberg, R. A. The hallmarks of cancer. *Cell*, 100(1):57–70 (2000).

[94] Harborth, J., Elbashir, S. M., Bechert, K., Tuschl, T., and Weber, K. Identification of essential genes in cultured mammalian cells using small interfering RNAs. *Journal of Cell Science*, 114(Pt 24):4557–4565 (2001).

[95] Haskill, S., Beg, A. A., Tompkins, S. M., Morris, J. S., Yurochko, A. D., Sampson-Johannes, A., Mondal, K., Ralph, P., and Baldwin, A. S. Characterization of an immediate-early gene induced in adherent monocytes that encodes i kappa b-like activity. *Cell*, 65(7):1281–1289 (1991).

[96] Hayden, M. S. and Ghosh, S. Shared principles in NF-kappaB signaling. *Cell*, 132(3):344–362 (2008).

[97] He, B., Mirza, M., and Weber, G. F. An osteopontin splice variant induces anchorage independence in human breast cancer cells. *Oncogene*, 25(15):2192–2202 (2006).

[98] Heppner, C., Bilimoria, K. Y., Agarwal, S. K., Kester, M., Whitty, L. J., Guru, S. C., Chandrasekharappa, S. C., Collins, F. S., Spiegel, A. M., Marx, S. J., and Burns, A. L. The tumor suppressor protein menin interacts with NF-kappaB proteins and inhibits NF-kappaB-mediated transactivation. *Oncogene*, 20(36):4917–4925 (2001).

[99] Higuchi, M. and Aggarwal, B. B. TNF induces internalization of the p60 receptor and shedding of the p80 receptor. *Journal of Immunology (Baltimore, Md.: 1950)*, 152(7):3550–3558 (1994).

[100] Hildt, E. and Oess, S. Identification of grb2 as a novel binding partner of tumor necrosis factor (TNF) receptor i. *The Journal of Experimental Medicine*, 189(11):1707–1714 (1999).

[101] Hitomi, J., Christofferson, D., Ng, A., Yao, J., Degterev, A., Xavier, R., and Yuan, J. Identification of a molecular signaling network that regulates a cellular necrotic cell death pathway. *Cell*, 135(7):1311–1323 (2008).

[102] Hitomi, J., Katayama, T., Eguchi, Y., Kudo, T., Taniguchi, M., Koyama, Y., Manabe, T., Yamagishi, S., Bando, Y., Imaizumi, K., Tsujimoto, Y., and Tohyama, M. Involvement of caspase-4 in endoplasmic reticulum stress-induced apoptosis and abeta-induced cell death. *The Journal of Cell Biology*, 165(3):347–356 (2004).

[103] Hoeflich, K. P., Luo, J., Rubie, E. A., Tsao, M. S., Jin, O., and Woodgett, J. R. Requirement for glycogen synthase kinase-3beta in cell survival and NF-kappaB activation. *Nature*, 406(6791):86–90 (2000).

[104] Hoffmann, A., Levchenko, A., Scott, M. L., and Baltimore, D. The IkappaB-NF-kappaB signaling module: temporal control and selective gene activation. *Science*, 298(5596):1241–1245 (2002).

[105] Hoffmann, A., Natoli, G., and Ghosh, G. Transcriptional regulation via the NF-kappaB signaling module. *Oncogene*, 25(51):6706–6716 (2006).

[106] Horn, T., Arziman, Z., Berger, J., and Boutros, M. GenomeRNAi: a database for cell-based RNAi phenotypes. *Nucleic Acids Research*, 35(Database issue):D492–497 (2007).

[107] Hornung, V., Guenthner-Biller, M., Bourquin, C., Ablasser, A., Schlee, M., Uematsu, S., Noronha, A., Manoharan, M., Akira, S., de Fougerolles, A., Endres, S., and Hartmann, G. Sequence-specific potent induction of IFN-alpha by short interfering RNA in plasmacytoid dendritic cells through TLR7. *Nature Medicine*, 11(3):263–270 (2005).

[108] Hsu, H., Huang, J., Shu, H. B., Baichwal, V., and Goeddel, D. V. TNF-dependent recruitment of the protein kinase RIP to the TNF receptor-1 signaling complex. *Immunity*, 4(4):387–396 (1996).

[109] Hsu, H., Shu, H. B., Pan, M. G., and Goeddel, D. V. TRADD-TRAF2 and TRADD-FADD interactions define two distinct TNF receptor 1 signal transduction pathways. *Cell*, 84(2):299–308 (1996).

[110] Hu, D. D., Lin, E. C., Kovach, N. L., Hoyer, J. R., and Smith, J. W. A biochemical characterization of the binding of osteopontin to integrins alpha v beta 1 and alpha v beta 5. *The Journal of Biological Chemistry*, 270(44):26232–26238 (1995).

[111] Huang, H. K., Joazeiro, C. A., Bonfoco, E., Kamada, S., Leverson, J. D., and Hunter, T. The inhibitor of apoptosis, cIAP2, functions as a ubiquitin-protein ligase and promotes in vitro monoubiquitination of caspases 3 and 7. *The Journal of Biological Chemistry*, 275(35):26661–26664 (2000).

[112] Huang, T. T., Kudo, N., Yoshida, M., and Miyamoto, S. A nuclear export signal in the n-terminal regulatory domain of IkappaBalpha controls cytoplasmic localization of inactive NF-kappaB/IkappaBalpha complexes. *Proceedings of the National Academy of Sciences of the United States of America*, 97(3):1014–1019 (2000).

[113] Huber, W., von Heydebreck, A., Sueltmann, H., Poustka, A., and Vingron, M. Variance stabilization applied to microarray data calibration and to the quantification of differential expression. *Bioinformatics*, 18 Suppl 1:S96–104 (2002).

[114] Huber, W., von Heydebreck, A., Sueltmann, H., Poustka, A., and Vingron, M. Parameter estimation for the calibration and variance stabilization of microarray data. *Statistical Applications in Genetics and Molecular Biology*, 2:Article3 (2003).

[115] Hutvagner, G., McLachlan, J., Pasquinelli, A. E., Balint, E., Tuschl, T., and Zamore, P. D. A cellular function for the RNA-interference enzyme dicer in the maturation of the let-7 small temporal RNA. *Science*, 293(5531):834–838 (2001).

[116] Jackson, A. L., Burchard, J., Leake, D., Reynolds, A., Schelter, J., Guo, J., Johnson, J. M., Lim, L., Karpilow, J., Nichols, K., Marshall, W., Khvorova, A., and Linsley, P. S. Position-specific chemical modification of siRNAs reduces "off-target" transcript silencing. *RNA*, 12(7):1197–1205 (2006).

[117] Jiang, Y., Woronicz, J. D., Liu, W., and Goeddel, D. V. Prevention of constitutive TNF receptor 1 signaling by silencer of death domains. *Science (New York, N.Y.)*, 283(5401):543–546 (1999).

[118] John, T., Mueller, R. D., Oberholzer, A., Zreiqat, H., Kohl, B., Ertel, W., Hostmann, A., Tschoeke, S. K., and Schulze-Tanzil, G. Interleukin-10 modulates pro-apoptotic effects of TNF-alpha in human articular chondrocytes in vitro. *Cytokine*, 40(3):226–234 (2007).

[119] Judge, A. D., Sood, V., Shaw, J. R., Fang, D., McClintock, K., and MacLachlan, I. Sequence-dependent stimulation of the mammalian innate immune response by synthetic siRNA. *Nature Biotechnology*, 23(4):457–462 (2005).

[120] Jun, J., Chung, C., Lee, H., Pyo, J., Lee, K. N., Kim, N., Kim, Y. S., Yoo, H., Lee, T., Kim, E., and Jung, Y. Role of FLASH in caspase-8-mediated activation of NF-kappaB: dominant-negative function of FLASH mutant in NF-kappaB signaling pathway. *Oncogene*, 24(4):688–696 (2005).

[121] Kamada, S., Washida, M., Hasegawa, J., Kusano, H., Funahashi, Y., and Tsujimoto, Y. Involvement of caspase-4(-like) protease in fas-mediated apoptotic pathway. *Oncogene*, 15(3):285–290 (1997).

[122] Kamens, J., Paskind, M., Hugunin, M., Talanian, R. V., Allen, H., Banach, D., Bump, N., Hackett, M., Johnston, C. G., and Li, P. Identification and characterization of ICH-2, a novel member of the interleukin-1 beta-converting enzyme family of cysteine proteases. *The Journal of Biological Chemistry*, 270(25):15250–15256 (1995).

[123] Kapoor, G. S., Zhan, Y., Johnson, G. R., and O'Rourke, D. M. Distinct domains in the SHP-2 phosphatase differentially regulate epidermal growth factor receptor/NF-kappaB activation through gab1 in glioblastoma cells. *Molecular and Cellular Biology*, 24(2):823–836 (2004).

[124] Kariko, K., Bhuyan, P., Capodici, J., and Weissman, D. Small interfering RNAs mediate sequence-independent gene suppression and induce immune activation by signaling through toll-like receptor 3. *Journal of Immunology*, 172(11):6545–6549 (2004).

[125] Karin, M. and Gallagher, E. TNFR signaling: ubiquitin-conjugated TRAFfic signals control stop-and-go for MAPK signaling complexes. *Immunological Reviews*, 228(1):225–240 (2009).

[126] Karin, M. and Greten, F. R. NF-kappaB: linking inflammation and immunity to cancer development and progression. *Nature Reviews. Immunology*, 5(10):749–759 (2005).

[127] Kariuki, S. N., Moore, J. G., Kirou, K. A., Crow, M. K., Utset, T. O., and Niewold, T. B. Age- and gender-specific modulation of serum osteopontin and interferon-alpha by osteopontin genotype in systemic lupus erythematosus. *Genes and Immunity*, 10(5):487–494 (2009).

[128] Karki, P., Dahal, G. R., and Park, I. Both dimerization and interdomain processing are essential for caspase-4 activation. *Biochemical and Biophysical Research Communications*, 356(4):1056–1061 (2007).

[129] Kauffmann, A., Gentleman, R., and Huber, W. arrayQualityMetrics–a bioconductor package for quality assessment of microarray data. *Bioinformatics*, 25(3):415–416 (2009).

[130] Kelliher, M. A., Grimm, S., Ishida, Y., Kuo, F., Stanger, B. Z., and Leder, P. The death domain kinase RIP mediates the TNF-induced NF-kappaB signal. *Immunity*, 8(3):297–303 (1998).

[131] Kim, H., Lee, H., Jun, J., Oh, Y., Choi, S., Kim, H., Chung, C., Kim, I., Park, I., Chae, H., Kim, H., and Jung, Y. Intracellular cleavage of osteopontin by caspase-8 modulates hypoxia/reoxygenation cell death through p53. *Proceedings of the National Academy of Sciences of the United States of America* (2009).

[132] Kittler, R., Putz, G., Pelletier, L., Poser, I., Heninger, A., Drechsel, D., Fischer, S., Konstantinova, I., Habermann, B., Grabner, H., Yaspo, M., Himmelbauer, H., Korn, B., Neugebauer, K., Pisabarro, M. T., and Buchholz, F. An endoribonuclease-prepared siRNA screen in human cells identifies genes essential for cell division. *Nature*, 432(7020):1036–1040 (2004).

[133] Klein, S., de Fougerolles, A. R., Blaikie, P., Khan, L., Pepe, A., Green, C. D., Koteliansky, V., and Giancotti, F. G. Alpha 5 beta 1 integrin activates an NF-kappa b-dependent program of gene expression important for angiogenesis and inflammation. *Molecular and Cellular Biology*, 22(16):5912–5922 (2002).

[134] Koenig, R., Zhou, Y., Elleder, D., Diamond, T. L., Bonamy, G. M. C., Irelan, J. T., Chiang, C., Tu, B. P., Jesus, P. D. D., Lilley, C. E., Seidel, S., Opaluch, A. M., Caldwell, J. S., Weitzman, M. D., Kuhen, K. L., Bandyopadhyay, S., Ideker, T., Orth, A. P., Miraglia, L. J., Bushman, F. D., Young, J. A., and Chanda, S. K. Global analysis of host-pathogen interactions that regulate early-stage HIV-1 replication. *Cell*, 135(1):49–60 (2008).

[135] Kohase, M., Henriksen-DeStefano, D., May, L. T., Vilcek, J., and Sehgal, P. B. Induction of beta 2-interferon by tumor necrosis factor: a homeostatic mechanism in the control of cell proliferation. *Cell*, 45(5):659–666 (1986).

[136] Kovalenko, A., Chable-Bessia, C., Cantarella, G., Israel, A., Wallach, D., and Courtois, G. The tumour suppressor CYLD negatively regulates NF-kappaB signalling by deubiquitination. *Nature*, 424(6950):801–805 (2003).

[137] Kuek, A., Hazleman, B. L., and Ostoer, A. J. K. Immune-mediated inflammatory diseases (IMIDs) and biologic therapy: a medical revolution. *Postgraduate Medical Journal*, 83(978):251–260 (2007).

[138] Kunsch, C. and Rosen, C. A. NF-kappa b subunit-specific regulation of the interleukin-8 promoter. *Molecular and Cellular Biology*, 13(10):6137–6146 (1993).

[139] Kwon, J. H., Keates, S., Bassani, L., Mayer, L. F., and Keates, A. C. Colonic epithelial cells are a major site of macrophage inflammatory protein 3alpha (MIP-3alpha) production in normal colon and inflammatory bowel disease. *Gut*, 51(6):818–826 (2002).

[140] Lakshmanan, U. and Porter, A. G. Caspase-4 interacts with TNF receptor-associated factor 6 and mediates lipopolysaccharide-induced NF-kappaB-dependent production of IL-8 and CC chemokine ligand 4 (macrophage-inflammatory protein-1). *Journal of Immunology*, 179(12):8480–8490 (2007).

[141] Landthaler, M., Yalcin, A., and Tuschl, T. The human DiGeorge syndrome critical region gene 8 and its d. melanogaster homolog are required for miRNA biogenesis. *Current Biology: CB*, 14(23):2162–2167 (2004).

[142] Lawrence, T., Bebien, M., Liu, G. Y., Nizet, V., and Karin, M. IKKalpha limits macrophage NF-kappaB activation and contributes to the resolution of inflammation. *Nature*, 434(7037):1138–1143 (2005).

[143] Le Bail, O., Schmidt-Ullrich, R., and Israel, A. Promoter analysis of the gene encoding the i kappa B-alpha/MAD3 inhibitor of NF-kappa b: positive regulation by members of the rel/NF-kappa b family. *The EMBO Journal*, 12(13):5043–5049 (1993).

[144] Lee, Y., Ahn, C., Han, J., Choi, H., Kim, J., Yim, J., Lee, J., Provost, P., Radmark, O., Kim, S., and Kim, V. N. The nuclear RNase III drosha initiates microRNA processing. *Nature*, 425(6956):415–419 (2003).

[145] Lee, Y. S., Nakahara, K., Pham, J. W., Kim, K., He, Z., Sontheimer, E. J., and Carthew, R. W. Distinct roles for drosophila dicer-1 and dicer-2 in the siRNA/miRNA silencing pathways. *Cell*, 117(1):69–81 (2004).

[146] Legler, D. F., Micheau, O., Doucey, M., Tschopp, J., and Bron, C. Recruitment of TNF receptor 1 to lipid rafts is essential for TNFalpha-mediated NF-kappaB activation. *Immunity*, 18(5):655–664 (2003).

[147] Li, S., Wang, L., Berman, M. A., Zhang, Y., and Dorf, M. E. RNAi screen in mouse astrocytes identifies phosphatases that regulate NF-kappaB signaling. *Molecular Cell*, 24(4):497–509 (2006).

[148] Li, X., Yang, Y., and Ashwell, J. D. TNF-RII and c-IAP1 mediate ubiquitination and degradation of TRAF2. *Nature*, 416(6878):345–347 (2002).

[149] Liebel, U., Kindler, B., and Pepperkok, R. 'Harvester': a fast meta search engine of human protein resources. *Bioinformatics*, 20(12):1962–1963 (2004).

[150] Ling, L., Cao, Z., and Goeddel, D. V. NF-kappaB-inducing kinase activates IKK-alpha by phosphorylation of ser-176. *Proceedings of the National Academy of Sciences of the United States of America*, 95(7):3792–3797 (1998).

[151] Liu, J., Carmell, M. A., Rivas, F. V., Marsden, C. G., Thomson, J. M., Song, J., Hammond, S. M., Joshua-Tor, L., and Hannon, G. J. Argonaute2 is the catalytic engine of mammalian RNAi. *Science*, 305(5689):1437–1441 (2004).

[152] Locksley, R. M., Killeen, N., and Lenardo, M. J. The TNF and TNF receptor superfamilies: integrating mammalian biology. *Cell*, 104(4):487–501 (2001).

[153] Lund, E., Guettinger, S., Calado, A., Dahlberg, J. E., and Kutay, U. Nuclear export of microRNA precursors. *Science*, 303(5654):95–98 (2004).

[154] Ma, J., Ye, K., and Patel, D. J. Structural basis for overhang-specific small interfering RNA recognition by the PAZ domain. *Nature*, 429(6989):318–322 (2004).

[155] Ma, J., Yuan, Y., Meister, G., Pei, Y., Tuschl, T., and Patel, D. J. Structural basis for 5'-end-specific recognition of guide RNA by the a. fulgidus piwi protein. *Nature*, 434(7033):666–670 (2005).

[156] Mallory, A. C. and Vaucheret, H. Functions of microRNAs and related small RNAs in plants. *Nature Genetics*, 38 Suppl:S31–36 (2006).

[157] Malo, N., Hanley, J. A., Cerquozzi, S., Pelletier, J., and Nadon, R. Statistical practice in high-throughput screening data analysis. *Nature Biotechnology*, 24(2):167–175 (2006).

[158] Mantovani, A. Cancer: Inflaming metastasis. *Nature*, 457(7225):36–37 (2009).

[159] Mantovani, A., Allavena, P., Sica, A., and Balkwill, F. Cancer-related inflammation. *Nature*, 454(7203):436–444 (2008).

[160] Martinez, J., Patkaniowska, A., Urlaub, H., Luehrmann, R., and Tuschl, T. Single-stranded antisense siRNAs guide target RNA cleavage in RNAi. *Cell*, 110(5):563–574 (2002).

[161] Martinez, J. and Tuschl, T. RISC is a 5' phosphomonoester-producing RNA endonuclease. *Genes & Development*, 18(9):975–980 (2004).

[162] Martinon, F., Burns, K., and Tschopp, J. The inflammasome: a molecular platform triggering activation of inflammatory caspases and processing of proIL-beta. *Molecular Cell*, 10(2):417–426 (2002).

[163] Martinon, F. and Tschopp, J. Inflammatory caspases: linking an intracellular innate immune system to autoinflammatory diseases. *Cell*, 117(5):561–574 (2004).

[164] Martinon, F. and Tschopp, J. Inflammatory caspases and inflammasomes: master switches of inflammation. *Cell Death and Differentiation*, 14(1):10–22 (2007).

[165] Matsuzawa, A., Tseng, P., Vallabhapurapu, S., Luo, J., Zhang, W., Wang, H., Vignali, D. A. A., Gallagher, E., and Karin, M. Essential cytoplasmic translocation of a cytokine receptor-assembled signaling complex. *Science*, 321(5889):663–668 (2008).

[166] Matzinger, P. The danger model: A renewed sense of self. *Science*, 296(5566):301–305 (2002).

[167] Medzhitov, R. Origin and physiological roles of inflammation. *Nature*, 454(7203):428–435 (2008).

[168] Meister, G. and Tuschl, T. Mechanisms of gene silencing by double-stranded RNA. *Nature*, 431(7006):343–349 (2004).

[169] Mi, H., Lazareva-Ulitsky, B., Loo, R., Kejariwal, A., Vandergriff, J., Rabkin, S., Guo, N., Muruganujan, A., Doremieux, O., Campbell, M. J., Kitano, H., and Thomas, P. D. The PANTHER database of protein families, subfamilies, functions and pathways. *Nucleic Acids Research*, 33(Database issue):D284–288 (2005).

[170] Mi, H. and Thomas, P. PANTHER pathway: an ontology-based pathway database coupled with data analysis tools. *Methods in Molecular Biology*, 563:123–140 (2009).

[171] Micheau, O. and Tschopp, J. Induction of TNF receptor i-mediated apoptosis via two sequential signaling complexes. *Cell*, 114(2):181–190 (2003).

[172] Moffat, J., Grueneberg, D. A., Yang, X., Kim, S. Y., Kloepfer, A. M., Hinkle, G., Piqani, B., Eisenhaure, T. M., Luo, B., Grenier, J. K., Carpenter, A. E., Foo, S. Y., Stewart, S. A., Stockwell, B. R., Hacohen, N., Hahn, W. C., Lander, E. S., Sabatini, D. M., and Root, D. E. A lentiviral RNAi library for human and mouse genes applied to an arrayed viral high-content screen. *Cell*, 124(6):1283–1298 (2006).

[173] Moffat, J. and Sabatini, D. M. Building mammalian signalling pathways with RNAi screens. *Nature Reviews. Molecular Cell Biology*, 7(3):177–187 (2006).

[174] Molestina, R. E. and Sinai, A. P. Host and parasite-derived IKK activities direct distinct temporal phases of NF-kappaB activation and target gene expression following toxoplasma gondii infection. *Journal of Cell Science*, 118(Pt 24):5785–5796 (2005). PMID: 16339966.

[175] Nau, G. J., Liaw, L., Chupp, G. L., Berman, J. S., Hogan, B. L., and Young, R. A. Attenuated host resistance against mycobacterium bovis BCG infection in mice lacking osteopontin. *Infection and Immunity*, 67(8):4223–4230 (1999).

[176] Naumann, M. and Scheidereit, C. Activation of NF-kappa b in vivo is regulated by multiple phosphorylations. *The EMBO Journal*, 13(19):4597–4607 (1994).

[177] Nelson, D. E., Ihekwaba, A. E. C., Elliott, M., Johnson, J. R., Gibney, C. A., Foreman, B. E., Nelson, G., See, V., Horton, C. A., Spiller, D. G., Edwards, S. W., McDowell, H. P., Unitt, J. F., Sullivan, E., Grimley, R., Benson, N., Broomhead, D., Kell, D. B., and White, M. R. H. Oscillations in NF-kappaB signaling control the dynamics of gene expression. *Science*, 306(5696):704–708 (2004).

[178] Neumann, B., Held, M., Liebel, U., Erfle, H., Rogers, P., Pepperkok, R., and Ellenberg, J. High-throughput RNAi screening by time-lapse imaging of live human cells. *Nature Methods*, 3(5):385–390 (2006).

[179] Neumann, M., Grieshammer, T., Chuvpilo, S., Kneitz, B., Lohoff, M., Schimpl, A., Franza, B. R., and Serfling, E. RelA/p65 is a molecular target for the immunosuppressive action of protein kinase a. *The EMBO Journal*, 14(9):1991–2004 (1995).

[180] Nishida, K., Yoshida, Y., Itoh, M., Fukada, T., Ohtani, T., Shirogane, T., Atsumi, T., Takahashi-Tezuka, M., Ishihara, K., Hibi, M., and Hirano, T. Gab-family adapter proteins act downstream of cytokine and growth factor receptors and t- and b-cell antigen receptors. *Blood*, 93(6):1809–1816 (1999).

[181] Noble, K. E., Wickremasinghe, R. G., DeCornet, C., Panayiotidis, P., and Yong, K. L. Monocytes stimulate expression of the bcl-2 family member, a1, in endothelial cells and confer protection against apoptosis. *Journal of Immunology*, 162(3):1376–1383 (1999).

[182] Novartis. Novartis gene expression atlas. *http://biogps.gnf.org/#goto=welcome*.

[183] Nowak, D. E., Tian, B., Jamaluddin, M., Boldogh, I., Vergara, L. A., Choudhary, S., and Brasier, A. R. RelA ser276 phosphorylation is required for activation of a subset of NF-kappaB-dependent genes by recruiting cyclin-dependent kinase 9/cyclin t1 complexes. *Molecular and Cellular Biology*, 28(11):3623–3638 (2008).

[184] Okamura, K. and Lai, E. C. Endogenous small interfering RNAs in animals. *Nature Reviews. Molecular Cell Biology*, 9(9):673–678 (2008).

[185] Pastorino, J. G. and Shulga, N. Tumor necrosis factor-alpha can provoke cleavage and activation of sterol regulatory element-binding protein in ethanol-exposed cells via a caspase-dependent pathway that is cholesterol insensitive. *The Journal of Biological Chemistry*, 283(37):25638–25649 (2008).

[186] Pelletier, N., Casamayor-Palleja, M., Luca, K. D., Mondiere, P., Saltel, F., Jurdic, P., Bella, C., Genestier, L., and Defrance, T. The endoplasmic reticulum is a key component of the plasma cell death pathway. *Journal of Immunology*, 176(3):1340–1347 (2006).

[187] Perkins, N. D. Post-translational modifications regulating the activity and function of the nuclear factor kappa b pathway. *Oncogene*, 25(51):6717–6730 (2006).

[188] Perkins, N. D. Integrating cell-signalling pathways with NF-kappaB and IKK function. *Nature Reviews. Molecular Cell Biology*, 8(1):49–62 (2007).

[189] Pfaffl, M. W. A new mathematical model for relative quantification in real-time RT-PCR. *Nucleic Acids Research*, 29(9):e45 (2001).

[190] Pillai, R. S., Artus, C. G., and Filipowicz, W. Tethering of human ago proteins to mRNA mimics the miRNA-mediated repression of protein synthesis. *RNA (New York, N.Y.)*, 10(10):1518–1525 (2004).

[191] Porteus, M. H. and Carroll, D. Gene targeting using zinc finger nucleases. *Nature Biotechnology*, 23(8):967–973 (2005).

[192] Ramanathan, M., Hasko, G., and Leibovich, S. J. Analysis of signal transduction pathways in macrophages using expression vectors with CMV promoters: a cautionary tale. *Inflammation*, 29(2-3):94–102 (2005).

[193] Reddy, S. A., Huang, J. H., and Liao, W. S. Phosphatidylinositol 3-kinase as a mediator of TNF-induced NF-kappa b activation. *Journal of Immunology*, 164(3):1355–1363 (2000).

[194] Reed, J. C., Doctor, K. S., and Godzik, A. The domains of apoptosis: a genomics perspective. *Science's STKE: Signal Transduction Knowledge Environment*, 2004(239):re9 (2004).

[195] Rodriguez, M. S., Thompson, J., Hay, R. T., and Dargemont, C. Nuclear retention of IkappaBalpha protects it from signal-induced degradation and inhibits nuclear factor kappaB transcriptional activation. *The Journal of Biological Chemistry*, 274(13):9108–9115 (1999).

[196] Rothe, M., Pan, M. G., Henzel, W. J., Ayres, T. M., and Goeddel, D. V. The TNFR2-TRAF signaling complex contains two novel proteins related to baculoviral inhibitor of apoptosis proteins. *Cell*, 83(7):1243–1252 (1995).

[197] Rothe, M., Sarma, V., Dixit, V., and Goeddel, D. TRAF2-mediated activation of NF-kappa b by TNF receptor 2 and CD40. *Science*, 269(5229):1424–1427 (1995).

[198] Saccani, S., Marazzi, I., Beg, A. A., and Natoli, G. Degradation of promoter-bound p65/RelA is essential for the prompt termination of the nuclear factor kappaB response. *J. Exp. Med.*, 200(1):107–113 (2004).

[199] Saleh, M., Vaillancourt, J. P., Graham, R. K., Huyck, M., Srinivasula, S. M., Alnemri, E. S., Steinberg, M. H., Nolan, V., Baldwin, C. T., Hotchkiss, R. S., Buchman, T. G., Zehnbauer, B. A., Hayden, M. R., Farrer, L. A., Roy, S., and Nicholson, D. W. Differential modulation of endotoxin responsiveness by human caspase-12 polymorphisms. *Nature*, 429(6987):75–79 (2004).

[200] Salvesen, G. S. and Dixit, V. M. Caspase activation: the induced-proximity model. *Proceedings of the National Academy of Sciences of the United States of America*, 96(20):10964–10967 (1999).

[201] Sarmay, G., Angyal, A., Kertesz, A., Maus, M., and Medgyesi, D. The multiple function of grb2 associated binder (Gab) adaptor/scaffolding protein in immune cell signaling. *Immunology Letters*, 104(1-2):76–82 (2006).

[202] Sato, S., Sanjo, H., Takeda, K., Ninomiya-Tsuji, J., Yamamoto, M., Kawai, T., Matsumoto, K., Takeuchi, O., and Akira, S. Essential function for the kinase TAK1 in innate and adaptive immune responses. *Nature Immunology*, 6(11):1087–1095 (2005).

[203] Schindler, U. and Baichwal, V. R. Three NF-kappa b binding sites in the human e-selectin gene required for maximal tumor necrosis factor alpha-induced expression. *Mol. Cell. Biol.*, 14(9):5820–5831 (1994).

[204] Schneider-Brachert, W., Tchikov, V., Neumeyer, J., Jakob, M., Winoto-Morbach, S., Held-Feindt, J., Heinrich, M., Merkel, O., Ehrenschwender, M., Adam, D., Mentlein, R., Kabelitz, D., and Schuetze, S. Compartmentalization of TNF receptor 1 signaling: internalized TNF receptosomes as death signaling vesicles. *Immunity*, 21(3):415–428 (2004).

[205] Schuetze, S., Machleidt, T., Adam, D., Schwandner, R., Wiegmann, K., Kruse, M. L., Heinrich, M., Wickel, M., and Kroenke, M. Inhibition of receptor internalization by monodansylcadaverine selectively blocks p55 tumor necrosis factor receptor death domain signaling. *The Journal of Biological Chemistry*, 274(15):10203–10212 (1999).

[206] Schuetze, S., Tchikov, V., and Schneider-Brachert, W. Regulation of TNFR1 and CD95 signalling by receptor compartmentalization. *Nature Reviews. Molecular Cell Biology*, 9(8):655–662 (2008).

[207] Schulze-Osthoff, K., Ferrari, D., Los, M., Wesselborg, S., and Peter, M. E. Apoptosis signaling by death receptors. *European Journal of Biochemistry / FEBS*, 254(3):439–459 (1998).

[208] Seiffert, M., Custodio, J. M., Wolf, I., Harkey, M., Liu, Y., Blattman, J. N., Greenberg, P. D., and Rohrschneider, L. R. Gab3-deficient mice exhibit normal development and hematopoiesis and are immunocompetent. *Molecular and Cellular Biology*, 23(7):2415–2424 (2003).

[209] Sen, R. and Baltimore, D. Inducibility of kappa immunoglobulin enhancer-binding protein nf-kappa b by a posttranslational mechanism. *Cell*, 47(6):921–928 (1986).

[210] Senger, D. R., Perruzzi, C. A., Papadopoulos-Sergiou, A., and de Water, L. V. Adhesive properties of osteopontin: regulation by a naturally occurring thrombin-cleavage in close proximity to the GRGDS cell-binding domain. *Molecular Biology of the Cell*, 5(5):565–574 (1994).

[211] Shakhov, A. N., Collart, M. A., Vassalli, P., Nedospasov, S. A., and Jongeneel, C. V. Kappa b-type enhancers are involved in lipopolysaccharide-mediated transcriptional activation of the tumor necrosis factor alpha gene in primary macrophages. *The Journal of Experimental Medicine*, 171(1):35–47 (1990).

[212] Shaulian, E. and Karin, M. AP-1 as a regulator of cell life and death. *Nature Cell Biology*, 4(5):E131–136 (2002).

[213] Shi, Y. Caspase activation: revisiting the induced proximity model. *Cell*, 117(7):855–858 (2004).

[214] Shikama, Y., Yamada, M., and Miyashita, T. Caspase-8 and caspase-10 activate NF-kappaB through RIP, NIK and IKKalpha kinases. *European Journal of Immunology*, 33(7):1998–2006 (2003).

[215] Shinohara, M. L., Kim, J., Garcia, V. A., and Cantor, H. Engagement of the type i interferon receptor on dendritic cells inhibits t helper 17 cell development: role of intracellular osteopontin. *Immunity*, 29(1):68–78 (2008).

[216] Shinohara, M. L., Lu, L., Bu, J., Werneck, M. B. F., Kobayashi, K. S., Glimcher, L. H., and Cantor, H. Osteopontin expression is essential for interferon-alpha production by plasmacytoid dendritic cells. *Nature Immunology*, 7(5):498–506 (2006).

[217] Shu, H. B., Takeuchi, M., and Goeddel, D. V. The tumor necrosis factor receptor 2 signal transducers TRAF2 and c-IAP1 are components of the tumor necrosis factor receptor 1 signaling complex. *Proceedings of the National Academy of Sciences of the United States of America*, 93(24):13973–13978 (1996).

[218] Sizemore, N., Lerner, N., Dombrowski, N., Sakurai, H., and Stark, G. R. Distinct roles of the ikappa b kinase alpha and beta subunits in liberating nuclear factor kappa b (NF-kappa

b) from ikappa b and in phosphorylating the p65 subunit of NF-kappa b. *The Journal of Biological Chemistry*, 277(6):3863–3869 (2002).

[219] Sledz, C. A., Holko, M., de Veer, M. J., Silverman, R. H., and Williams, B. R. G. Activation of the interferon system by short-interfering RNAs. *Nature Cell Biology*, 5(9):834–839 (2003).

[220] Smyth, G. K. Linear models and empirical bayes methods for assessing differential expression in microarray experiments. *Statistical Applications in Genetics and Molecular Biology*, 3:Article3 (2004).

[221] Sodek, J., Silva, A. P. B. D., and Zohar, R. Osteopontin and mucosal protection. *Journal of Dental Research*, 85(5):404–415 (2006).

[222] Song, J., Liu, J., Tolia, N. H., Schneiderman, J., Smith, S. K., Martienssen, R. A., Hannon, G. J., and Joshua-Tor, L. The crystal structure of the argonaute2 PAZ domain reveals an RNA binding motif in RNAi effector complexes. *Nature Structural Biology*, 10(12):1026–1032 (2003).

[223] Song, J., Smith, S. K., Hannon, G. J., and Joshua-Tor, L. Crystal structure of argonaute and its implications for RISC slicer activity. *Science*, 305(5689):1434–1437 (2004).

[224] Stanger, B. Z., Leder, P., Lee, T. H., Kim, E., and Seed, B. RIP: a novel protein containing a death domain that interacts with Fas/APO-1 (CD95) in yeast and causes cell death. *Cell*, 81(4):513–523 (1995).

[225] Steinman, L., Martin, R., Bernard, C., Conlon, P., and Oksenberg, J. R. Multiple sclerosis: deeper understanding of its pathogenesis reveals new targets for therapy. *Annual Review of Neuroscience*, 25:491–505 (2002).

[226] Stone, D. J., Marine, S., Majercak, J., Ray, W. J., Espeseth, A., Simon, A., and Ferrer, M. High-throughput screening by RNA interference: control of two distinct types of variance. *Cell Cycle*, 6(8):898–901 (2007).

[227] Strack, P., Caligiuri, M., Pelletier, M., Boisclair, M., Theodoras, A., Beer-Romero, P., Glass, S., Parsons, T., Copeland, R. A., Auger, K. R., Benfield, P., Brizuela, L., and Rolfe, M. SCF(beta-TRCP) and phosphorylation dependent ubiquitinationof i kappa b alpha catalyzed by ubc3 and ubc4. *Oncogene*, 19(31):3529–3536 (2000).

[228] Su, H., Bidere, N., Zheng, L., Cubre, A., Sakai, K., Dale, J., Salmena, L., Hakem, R., Straus, S., and Lenardo, M. Requirement for caspase-8 in NF-kappaB activation by antigen receptor. *Science*, 307(5714):1465–1468 (2005).

[229] Sun, S. Deubiquitylation and regulation of the immune response. *Nature Reviews. Immunology*, 8(7):501–511 (2008).

[230] Sun, S. C., Ganchi, P. A., Ballard, D. W., and Greene, W. C. NF-kappa b controls expression of inhibitor i kappa b alpha: evidence for an inducible autoregulatory pathway. *Science (New York, N.Y.)*, 259(5103):1912–1915 (1993).

[231] Suzuki, K., Zhu, B., Rittling, S. R., Denhardt, D. T., Goldberg, H. A., McCulloch, C. A. G., and Sodek, J. Colocalization of intracellular osteopontin with CD44 is associated with migration, cell fusion, and resorption in osteoclasts. *Journal of Bone and Mineral Research*, 17(8):1486–1497 (2002).

[232] Tada, K., Okazaki, T., Sakon, S., Kobarai, T., Kurosawa, K., Yamaoka, S., Hashimoto, H., Mak, T. W., Yagita, H., Okumura, K., Yeh, W. C., and Nakano, H. Critical roles of TRAF2 and TRAF5 in tumor necrosis factor-induced NF-kappa b activation and protection from cell death. *The Journal of Biological Chemistry*, 276(39):36530–36534 (2001).

[233] Tang, P., M-C, H., and Klostergaard, J. Human pro-tumor necrosis factor is a homotrimer. *Biochemistry*, 35(25):8216–8225 (1996).

[234] Tartaglia, L. A., Ayres, T. M., Wong, G. H., and Goeddel, D. V. A novel domain within the 55 kd TNF receptor signals cell death. *Cell*, 74(5):845–853 (1993).

[235] Taylor, G. A., Carballo, E., Lee, D. M., Lai, W. S., Thompson, M. J., Patel, D. D., Schenkman, D. I., Gilkeson, G. S., Broxmeyer, H. E., Haynes, B. F., and Blackshear, P. J. A pathogenetic role for TNF alpha in the syndrome of cachexia, arthritis, and autoimmunity resulting from tristetraprolin (TTP) deficiency. *Immunity*, 4(5):445–454 (1996).

[236] Tian, B., Nowak, D. E., and Brasier, A. R. A TNF-induced gene expression program under oscillatory NF-kappaB control. *BMC Genomics*, 6:137 (2005). PMID: 16191192.

[237] Ting, A. T., Pimentel-Muinos, F. X., and Seed, B. RIP mediates tumor necrosis factor receptor 1 activation of NF-kappaB but not Fas/APO-1-initiated apoptosis. *The EMBO Journal*, 15(22):6189–6196 (1996).

[238] Tomimori, K., Uema, E., Teruya, H., Ishikawa, C., Okudaira, T., Senba, M., Yamamoto, K., Matsuyama, T., Kinjo, F., Fujita, J., and Mori, N. Helicobacter pylori induces CCL20 expression. *Infection and Immunity*, 75(11):5223–5232 (2007).

[239] Trompouki, E., Hatzivassiliou, E., Tsichritzis, T., Farmer, H., Ashworth, A., and Mosialos, G. CYLD is a deubiquitinating enzyme that negatively regulates NF-kappaB activation by TNFR family members. *Nature*, 424(6950):793–796 (2003).

[240] Tschuch, C., Schulz, A., Pscherer, A., Werft, W., Benner, A., Hotz-Wagenblatt, A., Barrionuevo, L. S., Lichter, P., and Mertens, D. Off-target effects of siRNA specific for GFP. *BMC Molecular Biology*, 9:60 (2008).

[241] Ui-Tei, K., Naito, Y., Zenno, S., Nishi, K., Yamato, K., Takahashi, F., Juni, A., and Saigo, K. Functional dissection of siRNA sequence by systematic DNA substitution: modified siRNA with a DNA seed arm is a powerful tool for mammalian gene silencing with significantly reduced off-target effect. *Nucleic Acids Research*, 36(7):2136–2151 (2008).

[242] Valencia-Sanchez, M. A., Liu, J., Hannon, G. J., and Parker, R. Control of translation and mRNA degradation by miRNAs and siRNAs. *Genes & Development*, 20(5):515–524 (2006).

[243] Vallabhapurapu, S. and Karin, M. Regulation and function of NF-kappaB transcription factors in the immune system. *Annual Review of Immunology*, 27:693–733 (2009).

[244] Wada, I., Rindress, D., Cameron, P. H., Ou, W. J., Doherty, J. J., Louvard, D., Bell, A. W., Dignard, D., Thomas, D. Y., and Bergeron, J. J. SSR alpha and associated calnexin are major calcium binding proteins of the endoplasmic reticulum membrane. *The Journal of Biological Chemistry*, 266(29):19599–19610 (1991).

[245] Wada, T., Nakashima, T., Oliveira-dos-Santos, A. J., Gasser, J., Hara, H., Schett, G., and Penninger, J. M. The molecular scaffold gab2 is a crucial component of RANK signaling and osteoclastogenesis. *Nature Medicine*, 11(4):394–399 (2005).

[246] Wajant, H., Henkler, F., and Scheurich, P. The TNF-receptor-associated factor family: scaffold molecules for cytokine receptors, kinases and their regulators. *Cellular Signalling*, 13(6):389–400 (2001).

[247] Wajant, H., Pfizenmaier, K., and Scheurich, P. Tumor necrosis factor signaling. *Cell Death and Differentiation*, 10(1):45–65 (2003).

[248] Wang, C., Mayo, M. W., Korneluk, R. G., Goeddel, D. V., and Baldwin, A. S. NF-B antiapoptosis: Induction of TRAF1 and TRAF2 and c-IAP1 and c-IAP2 to suppress caspase-8 activation. *Science*, 281(5383):1680–1683 (1998).

[249] Wang, D., Westerheide, S. D., Hanson, J. L., and Baldwin, A. S. Tumor necrosis factor alpha-induced phosphorylation of RelA/p65 on ser529 is controlled by casein kinase II. *The Journal of Biological Chemistry*, 275(42):32592–32597 (2000).

[250] Wang, L., Manji, G. A., Grenier, J. M., Al-Garawi, A., Merriam, S., Lora, J. M., Geddes, B. J., Briskin, M., DiStefano, P. S., and Bertin, J. PYPAF7, a novel PYRIN-containing apaf1-like protein that regulates activation of NF-kappaB and caspase-1-dependent cytokine processing. *Journal of Biological Chemistry*, 277(33):29874–29880 (2002).

[251] Wang, S., Miura, M., Jung, Y. K., Zhu, H., Li, E., and Yuan, J. Murine caspase-11, an ICE-interacting protease, is essential for the activation of ICE. *Cell*, 92(4):501–509 (1998).

[252] Waterhouse, P. M., Wang, M. B., and Lough, T. Gene silencing as an adaptive defence against viruses. *Nature*, 411(6839):834–842 (2001).

[253] Weber, C. H. and Vincenz, C. The death domain superfamily: a tale of two interfaces? *Trends in Biochemical Sciences*, 26(8):475–481 (2001).

[254] Weber, G. F. and Ashkar, S. Molecular mechanisms of tumor dissemination in primary and metastatic brain cancers. *Brain Research Bulletin*, 53(4):421–424 (2000).

[255] Werner, S. L., Kearns, J. D., Zadorozhnaya, V., Lynch, C., O'Dea, E., Boldin, M. P., Ma, A., Baltimore, D., and Hoffmann, A. Encoding NF-kappaB temporal control in response to TNF: distinct roles for the negative regulators IkappaBalpha and a20. *Genes & Development*, 22(15):2093–2101 (2008). PMID: 18676814.

[256] Wertz, I. E., O'Rourke, K. M., Zhou, H., Eby, M., Aravind, L., Seshagiri, S., Wu, P., Wiesmann, C., Baker, R., Boone, D. L., Ma, A., Koonin, E. V., and Dixit, V. M. De-ubiquitination and ubiquitin ligase domains of a20 downregulate NF-kappaB signalling. *Nature*, 430(7000):694–699 (2004).

[257] Whiteside, S. T. and Israel, A. I kappa b proteins: structure, function and regulation. *Seminars in Cancer Biology*, 8(2):75–82 (1997).

[258] Wilson, N. S., Dixit, V., and Ashkenazi, A. Death receptor signal transducers: nodes of coordination in immune signaling networks. *Nature Immunology*, 10(4):348–355 (2009).

[259] Wolf, I., Jenkins, B. J., Liu, Y., Seiffert, M., Custodio, J. M., Young, P., and Rohrschneider, L. R. Gab3, a new DOS/Gab family member, facilitates macrophage differentiation. *Molecular and Cellular Biology*, 22(1):231–244 (2002).

[260] Wu, C., Conze, D. B., Li, T., Srinivasula, S. M., and Ashwell, J. D. Sensing of lys 63-linked polyubiquitination by NEMO is a key event in NF-kappaB activation [corrected]. *Nature Cell Biology*, 8(4):398–406 (2006).

[261] Xu, G., Nie, H., Li, N., Zheng, W., Zhang, D., Feng, G., Ni, L., Xu, R., Hong, J., and Zhang, J. Z. Role of osteopontin in amplification and perpetuation of rheumatoid synovitis. *The Journal of Clinical Investigation*, 115(4):1060–1067 (2005).

[262] Yamamoto, M., Okamoto, T., Takeda, K., Sato, S., Sanjo, H., Uematsu, S., Saitoh, T., Yamamoto, N., Sakurai, H., Ishii, K. J., Yamaoka, S., Kawai, T., Matsuura, Y., Takeuchi, O., and Akira, S. Key function for the ubc13 e2 ubiquitin-conjugating enzyme in immune receptor signaling. *Nature Immunology*, 7(9):962–970 (2006).

[263] Yamamoto, Y., Verma, U. N., Prajapati, S., Kwak, Y., and Gaynor, R. B. Histone h3 phosphorylation by IKK-alpha is critical for cytokine-induced gene expression. *Nature*, 423(6940):655–659 (2003).

[264] Yang, J., Lin, Y., Guo, Z., Cheng, J., Huang, J., Deng, L., Liao, W., Chen, Z., Liu, Z., and Su, B. The essential role of MEKK3 in TNF-induced NF-kappaB activation. *Nature Immunology*, 2(7):620–624 (2001).

[265] Yang, Y., Fang, S., Jensen, J. P., Weissman, A. M., and Ashwell, J. D. Ubiquitin protein ligase activity of IAPs and their degradation in proteasomes in response to apoptotic stimuli. *Science*, 288(5467):874–877 (2000).

[266] Yi, R., Qin, Y., Macara, I. G., and Cullen, B. R. Exportin-5 mediates the nuclear export of pre-microRNAs and short hairpin RNAs. *Genes & Development*, 17(24):3011–3016 (2003).

[267] Yoneda, T., Imaizumi, K., Oono, K., Yui, D., Gomi, F., Katayama, T., and Tohyama, M. Activation of caspase-12, an endoplastic reticulum (ER) resident caspase, through tumor necrosis factor receptor-associated factor 2-dependent mechanism in response to the ER stress. *The Journal of Biological Chemistry*, 276(17):13935–13940 (2001).

[268] You, M., Flick, L. M., Yu, D., and Feng, G. S. Modulation of the nuclear factor kappa b pathway by shp-2 tyrosine phosphatase in mediating the induction of interleukin (IL)-6 by IL-1 or tumor necrosis factor. *The Journal of Experimental Medicine*, 193(1):101–110 (2001).

[269] Yumoto, K., Ishijima, M., Rittling, S. R., Tsuji, K., Tsuchiya, Y., Kon, S., Nifuji, A., Uede, T., Denhardt, D. T., and Noda, M. Osteopontin deficiency protects joints against destruction in anti-type II collagen antibody-induced arthritis in mice. *Proceedings of the National Academy of Sciences of the United States of America*, 99(7):4556–4561 (2002).

[270] Zandi, E., Rothwarf, D. M., Delhase, M., Hayakawa, M., and Karin, M. The IkappaB kinase complex (IKK) contains two kinase subunits, IKKalpha and IKKbeta, necessary for IkappaB phosphorylation and NF-kappaB activation. *Cell*, 91(2):243–252 (1997).

[271] Zheng, L., Liu, J., Batalov, S., Zhou, D., Orth, A., Ding, S., and Schultz, P. G. An approach to genomewide screens of expressed small interfering RNAs in mammalian cells. *Proceedings of the National Academy of Sciences of the United States of America*, 101(1):135–140 (2004).

[272] Zheng, W., Li, R., Pan, H., He, D., Xu, R., Guo, T. B., Guo, Y., and Zhang, J. Z. Role of osteopontin in induction of monocyte chemoattractant protein 1 and macrophage inflammatory protein 1beta through the NF-kappaB and MAPK pathways in rheumatoid arthritis. *Arthritis and Rheumatism*, 60(7):1957–1965 (2009).

[273] Zhu, B., Suzuki, K., Goldberg, H. A., Rittling, S. R., Denhardt, D. T., McCulloch, C. A. G., and Sodek, J. Osteopontin modulates CD44-dependent chemotaxis of peritoneal macrophages through g-protein-coupled receptors: evidence of a role for an intracellular form of osteopontin. *Journal of Cellular Physiology*, 198(1):155–167 (2004).

[274] Zohar, R., Cheifetz, S., McCulloch, C. A., and Sodek, J. Analysis of intracellular osteopontin as a marker of osteoblastic cell differentiation and mesenchymal cell migration. *European Journal of Oral Sciences*, 106 Suppl 1:401–407 (1998).

[275] Zohar, R., Lee, W., Arora, P., Cheifetz, S., McCulloch, C., and Sodek, J. Single cell analysis of intracellular osteopontin in osteogenic cultures of fetal rat calvarial cells. *Journal of Cellular Physiology*, 170(1):88–100 (1997).

[276] Zohar, R., McCulloch, C. A., Sampath, K., and Sodek, J. Flow cytometric analysis of recombinant human osteogenic protein-1 (BMP-7) responsive subpopulations from fetal rat calvaria based on intracellular osteopontin content. *Matrix Biology: Journal of the International Society for Matrix Biology*, 16(6):295–306 (1998).

[277] Zohar, R., Suzuki, N., Suzuki, K., Arora, P., Glogauer, M., McCulloch, C. A., and Sodek, J. Intracellular osteopontin is an integral component of the CD44-ERM complex involved in cell migration. *Journal of Cellular Physiology*, 184(1):118–130 (2000).